Pool-Type LMFBR Plant
1000 MWe Phase A-Extension-1 Design

EPRI

Keywords:
Breeder Reactor
Pool-Type Reactor
Nuclear Power Plant
LMFBR

MASTER

MASTER

EPRI NP-882
Volume 2B
Project 620-20
Interim Report
September 1978

Prepared by
General Electric Company
Sunnyvale, California

DISTRIBUTION OF THIS DOCUMENT IS UNLIMITED

ELECTRIC POWER RESEARCH INSTITUTE

DISCLAIMER

This report was prepared as an account of work sponsored by an agency of the United States Government. Neither the United States Government nor any agency thereof, nor any of their employees, makes any warranty, express or implied, or assumes any legal liability or responsibility for the accuracy, completeness, or usefulness of any information, apparatus, product, or process disclosed, or represents that its use would not infringe privately owned rights. Reference herein to any specific commercial product, process, or service by trade name, trademark, manufacturer, or otherwise does not necessarily constitute or imply its endorsement, recommendation, or favoring by the United States Government or any agency thereof. The views and opinions of authors expressed herein do not necessarily state or reflect those of the United States Government or any agency thereof.

DISCLAIMER

Portions of this document may be illegible in electronic image products. Images are produced from the best available original document.

Pool-Type LMFBR Plant
1000 MWe Phase A-Extension-1 Design

PART II: REACTOR ASSEMBLY — STRUCTURES
Sections 7–11

NP-882, Volume 2B
Research Project 620-20

Interim Report, September 1978

Prepared by

GENERAL ELECTRIC COMPANY
Advanced Reactor Systems Department
310 DeGuigne Drive
Sunnyvale, California 94086

Project Manager
S. M. Davies

Prepared for

Electric Power Research Institute
3412 Hillview Avenue
Palo Alto, California 94304

EPRI Project Manager
J. G. Duffy
Nuclear Power Division

DISTRIBUTION OF THIS DOCUMENT IS UNLIMITED

LEGAL NOTICE

This report was prepared by General Electric Company and Bechtel National, Inc. as an account of work sponsored by the Electric Power Research Institute, Inc. (EPRI). Neither EPRI, members of EPRI, General Electric Company, Bechtel, nor any person acting on behalf of any of them: (a) makes any warranty or representation, express or implied, with respect to the accuracy, completeness, or usefulness of the information contained in this report, or that the use of any information, apparatus, method, or process disclosed in this report may not infringe privately owned rights; or (b) assumes any liabilities with respect to the use of, or for damages resulting from the use of, any information, apparatus, method, or process disclosed in this report.

PREFACE

This report describes Phase A Extension 1 work performed between February 8 and July 31, 1978 on the design of a large pool-type LMFBR power plant. The work is the result of a team effort by Bechtel Corporation and General Electric Company which was sponsored and guided by the Electric Power Research Institute (EPRI). The objective of the work was to refine certain areas of design and bring them into better focus than had been provided by Phase A work performed between April 4 and December 30, 1977.

The Phase A effort produced an initial description of the overall plant, structures and systems. During Phase A, General Electric developed the overall nuclear steam supply system (NSSS) conceptual design. It defined specific design approaches for selected NSSS components and subsystems after analyzing various design alternatives. Bechtel assumed responsibility for the intermedaite sodium piping arrangement , the access area above the reactor deck and the Balance of Plant (BOP). The resulting integrated plant design provided the necessary seismic data for both the NSSS and BOP.

The special expertise of several subcontractors was used during Phase A; Byron-Jackson provided a preliminary design of the primary sodium pump, Foster-Wheeler provided a preliminary design of the intermediate heat exchanger (IHX), and CBI Nuclear reviewed the reactor deck design and developed a construction sequence for the overall reactor assembly.

The Phase A effort by General Electric; Bechtel and the subcontractors was funded at a level of nearly 1.7 million dollars. Additionaly, General Electric contributed a company-funded effort and both General Electric and Bechtel utilized their backgrounds of prior work on pool-type LMFBRs and extensive interaction with foreign LMFBR organizations. The results of the Phase A work was published by EPRI in April 1978 in report number NP-646, "Pool-Type LMFBR Plant, 1000 MWe Phase A Design".

During Phase A Extension 1, funded at a level of approximately 1.4 million dollars, specific areas established during Phase A received further development and evaluation. These specific areas included the reactor deck, the reactor assembly, the heat transfer system components, the reactor auxiliary systems, and the instrumentation and control systems. Several subcontractors were also used during Phase A Extension 1; Foster-Wheeler designed an alternate IHX, CBI Nuclear evaluated an alternate deck support scheme and further developed the reactor assembly construction sequence, and United Nuclear Industries provided conceptual designs for removable radiation shielding in the deck.

This report of the Phase A Extension 1 work is logically divided into eight parts, which have the general title "Pool-Type LMFBR, 1000 MWe Phase A – Extension 1 Design":

Part I	Executive Summary
Part II	Reactor Assembly – Structures
Part III	Reactor Assembly – Deck
Part IV	Reactor Assembly – Fabrication
Part V	Heat Transport System Components
Part VI	Reactor Auxiliary Systems
Part VII	Instrumentation and Control
Part VIII	Balance Of Plant

The report is physically divided into six volumes as follows:

Volume 1	Part I
Volume 2	Part II
Volume 3	Part III and Part IV
Volume 4	Part V
Volume 5	Part VI and Part VII
Volume 6	Part VIII

A Table of Contents for all volumes is included at the end of every volume.

POOL-TYPE LMFBR PLANT

1000 MWe PHASE A - EXTENSION 1 DESIGN

Contents

VOLUME 1: Part I: EXECUTIVE SUMMARY

1. Introduction
2. Results and Conclusions
3. Nuclear Steam Supply System
4. Balance of Plant

VOLUME 2: Part II: REACTOR ASSEMBLY - STRUCTURES

1. Introduction and Summary
2. General Arrangement
3. Thermal Barriers
4. Alternate Support for Primary Vessel
5. Seismic Analysis - Alternate Vessel Support
6. Pump-to-Plenum Piping and Seals
7. Upper Internals Structure
8. Internal Shielding
9. Rotating Plug Size Study
10. Rotating Plug Thermal Analysis
11. Rotating Plug Seals

Appendix IIA - Engineering Study of the Design, Fabrication, Construction and Testing of a Pool-Type LMFBR - Alternate Vessel Support

VOLUME 3: Part III: REACTOR ASSEMBLY - DECK

1. Introduction and Summary
2. Design
3. Insulation
4. Penetrations
5. Removable Shielding
6. Inspection
7. Thermal Stress Analysis of Shortened Support Skirt

Appendix IIIA - Design Concepts for Removable Radiation Shielding for the 1000 MWe Pool-Type LMFBR

Appendix IIIB - EPRI Guidelines for LMFBR Pool Design

VOLUME 3: (Cont'd.)

Part IV: REACTOR ASSEMBLY - FABRICATION

1. Introduction and Summary

Appendix IVA - Phase A Extension Engineering Study of the Design, Fabrication, Construction and Testing of a Pool-Type LMFBR - Reference Vessel Support

VOLUME 4:

Part V: HEAT TRANSPORT SYSTEMS COMPONENTS

1. Introduction and Summary
2. Intermediate Heat Exchanger Design
3. IHX Seismic Analysis
4. Primary Pump Valve
5. Primary Pump Seismic Analysis
6. Operation With Components Out Of Service
7. Plant Duty Cycle
8. Plant Transients
9. Reactor Outlet Plenum Thermal Hydraulics

Appendix VA - Preliminary Design of an Alternate Bent-Tube IHX for the 1000 MWe Pool Reactor

VOLUME 5:

Part VI: REACTOR AUXILIARY SYSTEMS

1. Introduction and Summary
2. Primary Sodium Purification and Sampling Systems
3. Auxiliary Cooling Systems
4. Cover Gas Pressure Control

Part VII: INSTRUMENTATION AND CONTROL

1. Introduction and Summary
2. In-Vessel Instrumentation
3. Deck Cabling and Cabinets
4. Failed Fuel Detection
5. Post-Scram Sodium Pump Control
6. Plant Control

VOLUME 6

Part VIII: BALANCE OF PLANT

1. Introduction and Summary
2. Reactor Head Compartment Layout
3. Primary Heat Transport System Component Removal Study
4. Intermediate Heat Transport System Piping Enclosure Study

VOLUME 6:
(Cont'd.)

5. Pool Reactor Assembly Support Interface
6. Decay Heat Removal Systems Layout and Performance Study
7. Cover Gas System
8. Pool Reactor Assembly Erection and Schedule

POOL-TYPE LMFBR PLANT

1000 MWe PHASE A - EXTENSION 1 DESIGN

Volume 2

Contents

Part II: Reactor Assembly - Structures

Section		Page
1	Introduction and Summary	II-1-1
2	General Arrangement	II-2-i
3	Thermal Barriers	II-3-i
4	Alternate Support for Primary Vessel	II-4-i
5	Seismic Analysis - Alternate Vessel Support	II-5-i
6	Pump-to-Plenum Piping and Seals	II-6-i
7	Upper Internals Structure	II-7-i
8	Internal Shielding	II-8-i
9	Rotating Plug Size Study	II-9-i
10	Rotating Plug Thermal Analysis	II-10-i
11	Rotating Plug Seals	II-11-i
Appendix IIA -	Engineering Study of the Design, Fabrication, Construction and Testing of a Pool-Type LMFBR - Alternate Vessel Support	IIA-i

A table of contents for the entire report appears at the end of each volume.

PART II: REACTOR ASSEMBLY - STRUCTURES

SECTION 7: UPPER INTERNALS STRUCTURE

CONTENTS

		Page
II-7.1	INTRODUCTION AND SUMMARY	II-7-1
II-7.2	CONCLUSIONS AND RECOMMENDATIONS	II-7-5
II-7.3	DISCUSSION	II-7-9
	7.3.1 Functional Requirements and Design Condition	II-7-9
	7.3.2 Instrumentation Considerations and Requirements	II-7-15
	7.3.3 Thermal Hydraulic Considerations	II-7-16
	7.3.4 Materials Considerations and Requirements	II-7-21
	7.3.5 Design Approaches	II-7-29
	REFERENCES	II-7-67

TABLES

		Page
3.1-1	Principal Functional Requirements for the Upper Internals Structure	II-7-11
3.1-2	UIS Operation Conditions	II-7-14
3.4.3-1	Estimated Maximum Allowable Metal Surface ΔT Values for a 10^9 Cycle, 1 Hz Design Life	II-7-24

FIGURES

		Page
3.5.1-1	Sectional Elevation of the Upper Internals Structure: Low Baffle Concept	II-7-45
3.5.1-2	Control Rod Shroud Tube Module	II-7-47
3.5.1-3	Control Rod Shroud Tube: Cross Sectional Views	II-7-49
3.5.1-4	Plan View of Upper Internals Structure: Location Grid	II-7-51
3.5.1-5	Plan View of Upper Internals Structure: Intermediate Support Plate and Baffle Plate Pattern	II-7-53
3.5.1-6	Plan View of Upper Internals Structure: Top Support Shell	II-7-55
3.5.2-1	Upper Internals Structure Elevation, High Baffle Design	II-7-57
3.5.2-2	Upper Internals Structure Details, High Baffle Design	II-7-59
3.5.2-3	Mixing Chamber Layout, High Baffle Design	II-7-61
3.5.2-4	Instrumentation Module Plan, High Baffle Design	II-7-63
3.5.2-5	Instrumentation Module Detail, High Baffle Design	II-7-65
3.5.2-6	Grid Plate, High Baffle Design	II-7-66

II-7.1

INTRODUCTION AND SUMMARY

In a LMFBR there are a variety of functions that must be performed in the region directly above the reactor core. These functions require that structure be located in this region. Because of the size of the core and the distance from the top of the core to the nearest support point the dimensions of this structure become substantial. Additionally, the core effluent is characterized by high absolute temperature and rapidly changing temperatures that can cause severe thermal loading on structures in its path. Previous efforts by GE[1] were directed toward defining a design for this component that would be applicable to a commercial sized loop type LMFBR. The concept proposed at that time was similar to the CRBR design. It satisfied the design condition and made use of the design experience gained in CRBR relative to the thermal hydraulic performance and fabrication methods required. There was no work done on this structure during the Phase A Pool Study as it was assumed that the previous design would be applicable to the pool type reactor.

The purpose of the present work is to reevaluate what that led to the Phase II reference design for the Upper Internals Structure (UIS) and to propose designs compatible with the current understanding of the design requirements and operating conditions. This involves taking a fresh look at the functional requirements for the UIS, the environment in which it must operate, and design approaches that ultimately produce acceptable designs.

This study has been directed toward providing a better understanding of the problems associated with the design of an Upper Internals Structure (UIS) for a commercial sized LMFBR and investigating design approaches applicable to the UIS for a pool type reactor. The starting point was the design adopted by GE during Phase II[1] for the loop type plant. The functional requirements, the operating conditions, and the degree to which the Phase II reference design satisfies the design requirements have been reevaluated. It became obvious early in the study that there were two areas in which the extent of our information and knowledge were limited and these areas subsequently received the bulk of the effort. The

first area was the impact of the operating conditions on the materials requirements for the UIS and the selection of a reference material for certain portions of the structure. The second was the definition of the thermal hydraulic requirements and determination of the extent to which the UIS satisfies these requirements.

Materials selection was complicated by the demanding UIS service conditions. The UIS will be exposed to a complex and cyclic temperature spectrum at elevated temperatures, in a liquid sodium environment, and under irradiation conditions. These conditions result in thermal striping (high cycle, steady state fatigue) and low cycle creep and fatigue damage and have been shown to preclude the use of conventional SS-316 construction. From the materials alternates considered, Inconel Alloy 718 was selected as providing the best chance of satisfying the prescribed operating conditions. However, the anticipated service conditions are such that they challenge the capabilities of any commercially available alloy, including I-718. The current work has shown that it may be necessary to integrate the reactor core and the UIS designs to tailor the UIS service conditions to a well characterized alloy. Additionally, regardless of the material selected, there is likely to be a great deal of development effort required to substantiate its use.

The UIS will be required to promote mixing within the hot pool during transient events and during steady state operations. An extensive review has been conducted of past and current mixing test to provide information necessary to define the requirements for the UIS and the degree to which the UIS satisfies these requirements. It was found that the available tests results apply primarily to mixing regions with low aspect ratios and could not be readily extended to the pool configurations with their much larger diameter to depth ratios. Further, and for the same reason, it was found that currently available analytical tools are difficult to employ with pool geometries although some progress is being made in this area. While 3-D codes are being developed that should apply to the pool there is still much work to be done in this area as well as with model flow tests. The current design efforts have proceeded on the basis of information gleaned from the only available information. It is recognized that there is still a great deal of work to be done in this area and that even simple, inexpensive mixing tests with the correct geometry would provide a great deal of information.

Two approaches to the design of a UIS are being pursued by GE consistent with our current understanding of the problem. Features are being incorporated to promote mixing; locally to eliminate the thermal striping potential, and generally to protect

downstream components during high rate temperature transients. Construction methods are being investigated that are responsive to the fabrication requirements for I-718. Both mechanical and welded configurations are being employed.

CONCLUSIONS AND RECOMMENDATIONS

The present work has been directed toward understanding the problems attendant to the design of an Upper Internals Structure (UIS) for a LMFBR. As a result of these studies it has been found that there are a number of uncertainties that will require resolution before the design can be completed. These uncertainties occur both in the requirements and in the service conditions for the UIS and in the performance of the design relative to its intended functions. However, even in view of these uncertainties the present work has allowed us to reach a number of encouraging conclusions and make recommendations for follow on work.

The UIS is a component that interfaces with many other components within the reactor assembly. Principal among these are the reactor core, the closure, the control rod drives, the IHX's, and the above core instrumentation. Most of these are not sufficiently well defined to know their exact influence on the UIS. Conversely, the UIS will have an impact on the design of these reactor internal components, therefore, there must be much feedback and iteration as the integrated reactor design progresses. To allow the present work to proceed, it has been necessary to make various assumptions. The most critical of these have been made relative to the core assembly-to-assembly outlet temperatures. Past core design work and comparison with other existing and more extensively analyzed core designs (CDFR) have been used to substantiate the values used in this work, but it was found that in many instances the resulting environment did not permit the use of SS-316 structures. This led to the adoption of alternate material. Unfortunately, assumptions also had to be made as to the acceptability of the alternate material (I-718). Other critical assumptions lie in the area of the thermal hydraulic performance of the structure. It has been assumed that the UIS will (possibly with minor modifications) promote sufficient hot pool mixing to adequately protect downstream components from thermal shock subsequent to reactor transients. Also, it has been assumed that the designs proposed will isolate the thermal striping effects from components beyond the UIS. Both of these assumptions will require extensive flow testing and analytical work to validate.

The principal conclusions reached as a result of Phase A, Extension efforts are as follows.

- The design of a UIS for a commercial size LMFBR is a feasible task. Two potential concepts are proposed to illustrate this point.

- Some mitigation of currently assumed core assembly-to-assembly ΔT's may be required to achieve a full 40 year life for the UIS.

- Of the currently available materials, I-718 is believed to be the best choice of alloys in terms of potential weld, forming, and fabrication requirements for portions of the UIS where SS-316 has been found unacceptable.

- Instrumentation sensors will be required at virtually every fuel assembly exit and possibly many blanket assembly exits.

- Protection of downstream components during transients can be provided through careful design of the UIS, possibly coupled with primary pump speed control (see Part VII, Section 5).

- The UIS can be made to reduce thermal striping effects to acceptable levels for downstream components.

- Our knowledge of mixing phenonema in the hot pool and analytical tools for predicting this mixing is limited and insufficient.

- Materials limitations will likely limit the operating temperature of an LMFBR to 1050°F for 40 year life components used on the UIS.

The principal recommendations offered as a result of the present efforts are as follows.

- Pursue the design of the UIS consistent with currently available information and in conjunction with data being developed.

- Perform core design necessary to define the core geometry and the sub-assembly outlet temperatures and flow rates during steady state and transient conditions.

- Determine the need for flow control devices on the reactor sub-assemblies to balance the temperatures across the core exit plane.

- Pursue the acquisition of data on I-718 to validate the use of this material in the UIS. Follow ASME Code development and provide input relative to coding I-718.

- Pursue the development of test data and hydrodynamic computer codes necessary to understand the thermal hydraulic performance of the UIS in conjunction with the outlet plenum and outlet plenum components in a pool reactor.

- In conjunction with the core design efforts, reevaluate the need for and/or the extent of the backup holddown functions in the UIS.

- In conjunction with the core design efforts and plant control and safety considerations, optimize the design and extent of the above core instrumentation.

- Determine the need to inspect the gap between the UIS and the reactor core prior to refueling operations. Determine the implication that this has on the UIS and on the closure in terms of the capability to raise the UIS for this inspection.

- Determine the need for and the implication of inspectability and removability requirements on the UIS.

II-7.3

DISCUSSION

7.3.1
FUNCTIONAL REQUIREMENTS AND DESIGN CONDITIONS

The principal functional requirements for the Upper Internals Structure (UIS) have been presented in the Volume II, Paragraph 4.3.3 of the Phase II PLBR Report (GEFR 00099) and are summarized in Table 3.1-1. Of these requirements, the ones that have the most significant impact on the design of the UIS are those related to thermal hydraulics, backup holddown and above core instrumentation. Additionally, the operating environment can give rise to thermal conditions that preclude the use of conventional materials for much of the structure. These considerations are discussed in subsequent paragraphs and have been the primary concerns in the Phase A Extension effort. It will be seen from these following discussions that there are still many questions relative to the UIS requirements, the operating condition, and the design that require resolution for LMFBR's. The current work has served to illustrate that there is a strong interdependence among these items, and that perturbations in one area can potentially cause changes in another. This effect is further complicated by the facts that our information is in many cases incomplete and that tools for analysis and testing are not presently available.

The most pressing question relative to the UIS design is the materials issue which is discussed in Section 7.3.4 below. The problem we face results from anticipated jet temperature differences across the core exit plane that give rise to steady state thermal fatigue in structures at this location. It does not appear as if this thermal environment, as we currently understand it, will permit the use of conventional stainless steel construction. This has, of course, been recognized in the past and the solution has thought to lie in the use of a special material such as Inconel Alloy 718 in which there were large design margins possible.

Currently this thinking is being revised and the margins have been reduced for various reasons. This situation is that design curves presently finding their way into the ASME Code for I-718 are either marginal or do not allow the use

of this material under the design conditions. The materials question is presently being reviewed by experts throughout this country and abroad and its resolution is not likely to occur in the near term. To complicate the picture, there are no acceptable alternates to I-718. The GE design position is that ultimately the materials uncertainties will be resolved and in the interim it is assumed that I-718 will be shown to be acceptable. This position allows the design work to proceed so that the other problem areas can be addressed.

The second area of concern to the UIS designers is the thermal hydraulic performance of this component. There are several thermal hydraulic functions that the UIS must perform. It must provide a substantial degree of mixing of the subassembly outlet flow both within the structure and in the hot pool sodium. This mixing must be achieved in a manner that prevents turbulent pool surface being formed that could cause cover gas entrainment into the sodium. The structure must also mitigate the thermal shock following reactor scrams and isolate the steady state thermal striping from downstream components within the hot pool. Control rod drive lines, which pass through the UIS, must be protected from radial flows that can potentially induce mechanical vibration that result in reactivity noise.

The question of instrumentation support and location is also dependent to some extent upon the mixing achieved by the UIS. The potential exists for reducing the quantity of instruments above the core if the flow distribution can be understood and controlled. For example, failed fuel detection devices could be minimized if detailed knowledge of the flow paths from each reactor assembly could be reliably predicted. As reflected in the discussion in Section 7.3.2 below it has been assumed that some degree of certainty can be obtained in the mixing patterns. However, as discussed, in Section 7.3.3, the capability to accurately predict these flow patterns and temperature distributions in the outlet plenum will take a great deal of effort to develop.

The most significant structural requirements for the UIS are for backup holddown of reactor assemblies in the event of a loss of primary holddown and resistance to motion during seismic events. Both of these requirements are safety related. The backup holddown would prevent an excessive increase in core reactivity that could result from an ejected assembly dropping back into the core. The seismic requirements must limit the lateral motion of the shroud tubes so that control rod scram is not precluded.

Table 3.1-1

PRINCIPAL FUNCTIONAL REQUIREMENTS FOR
THE UPPER INTERNALS STRUCTURE

Provide mixing of the effluent from the reactor assemblies during normal operation such that temperature oscillations are reduced throughout the outlet plenum and the coolant is mixed and isothermal by the time it reaches the plenum outlet.
Mitigate the effects on the outlet plenum components of the rapid changes in coolant flow rate and temperature which occur during reactor transients (scrams). Mitigate the effects of coolant stratification that might occur during transients.
Provide support, positioning, and routing capability for the above-core instrumentation. (See Part VII, Section 2.)
Provide secondary axial hold-down capability for the reactor assemblies in the event of a failure of the primary hold-down. Limit the potential for axial travel of individual reactor assemblies such that prescribed limits for reactivity changes are not exceeded.
Provide alignment of the control rod drive line shrouds and the above-core instrumentation dry wells with the reactor assemblies.
Protect the control rod drive lines and the dry wells from vibration that could result from cross flow in the outlet plenum.
Provide restraint during the seismic events to limit the motion of the UIS relative to the core to prescribed limits.
Provide radiological shielding for all UIS penetrations in the reactor closure such that dose rates in the head access area do not exceed prescribed limits.
Provide seals for the UIS closure head penetration such that leakage of cover gas is maintained below specified maximum values.

In past work, the backup holddown requirement was arbitrarily assumed to apply simultaneously to the entire array of core assemblies. The primary holddown in the current design is developed individually for each assembly and there are no failure modes that could involve the entire core at any one time. Hence, for the present work, the worst loss of holddown malfunction is assumed to involve only those assemblies contained in á single inlet module.

The current Phase A design work, as discussed in Paragraph 3.5 below, has proceeded under the assumption that the functional requirements will be essentially the same as defined for the Phase II (Loop) work except as modified by the EPRI Phase A Pool Reactor Guidelines. There was, however, one liberty taken with respect to the Phase A Guidelines that has resulted in a significent simplification in the two UIS design concepts. The EPRI Guideline core is a heterogeneous type with 24 control rods spaced on an irregular pitch. GE has assumed that the control rods may be relocated such that they fall on a uniform triangular pitch (CR pitch equals 3 times the reactor assembly pitch). The effect of this on the Guideline core layout is to move the middle ring of controls outboard by one reactor assembly ring. To compensate for the reduced worth caused by locating control assemblies next to a ring of blankets, there were six additional control assemblies added to the middle ring which brings the total for the core to 30. The resulting simplifications on the UIS design is that it allows the designer to utilize regularly spaced and uniformly sized modular components to accomplish the instrumentation support and backup holddown functions. This latitude is invaluable in the design stage as it allows features and devices to be considered without concern over whether or not they will be accommodated in all of the possible configurations in an irregular pattern. A further advantage will be realized when the detailed structural analysis is performed on the "uniform grid" UIS. The use of an irregular control rod pattern is not thought to be precluded by the present designs although considerable effort may be required to demonstrate this point.

The operating conditions for the Phase A UIS are essentially the same as specified during Phase II. These are summarized in Table 3.1-2. The significant conditions relative to the UIS are:

a) During normal reactor operation the lower part of the UIS will be subjected to radial temperature gradients produced by the core subassemblies having different temperature effluents.

b) The lower part of the structure is also subjected to the high cycle thermal fluctuations (thermal striping) from adjacent sub-assembly effluent temperature differences.

c) During off-normal operation, various thermal transients arise such as a control rod "scram." These give rise to severe thermal shocks particularly at the lower end of the structure. This manifests itself in a localized effect of a through wall temperature difference, and also a gross effect of an overall radial temperature gradient which may be a reversal of the normal operating conditions.

It should be pointed out that because of limited core design work there is little basis for some of the values presented in Table 3.1-2. In particular, those temperatures associated with reactor assembly temperature rises are subject to change as work is done in this area. Also, the use of flow control devices on the blanket assemblies could greatly improve ΔT values and the UIS environment if employed.

Table 3.1.2

UIS OPERATING CONDITION

Reactor Inlet Temperature	595°F
Reactor Outlet Temperature	
Maximum fuel assembly (2σ)	1015°F
Average fuel assembly	940°F
Bulk mean sodium	875°F
UIS Design Temperature	1025°F
UIS Operating Temperature	970°F

Design Life

Forty years in sodium at the design temperature.

Availability is $\approx$ 80%

Neutron Fluence (Total) $\approx 10^{21}$ n/cm^2.

Environmental Conditions	Max. Temperature Difference ΔT°F			No. of Cycles	Frequency	Rate °F/sec
	Striping	Thru Wall[1]	Radial			
Steady State	270(Fluid)[2]			10^9	1 Hz[3]	-
	-	140	300[4]	-	-	
Transient (Control Rod Scram)		300	280[4]	500	Random	-30

1. Estimated based upon assumed mixing and assembly-to-assembly temperature differences.
2. Based on predicted maximum assembly-to-assembly temperature differences for the reference core.
3. Based upon ANL flow tests (Part V, Section 9).
4. Estimated temperature difference across core.

7.3.2
INSTRUMENTATION CONSIDERATIONS AND REQUIREMENTS

In-vessel instrumentation considerations and requirements are described in Part VII, Section 2. The discussion herein is confined to instrumentation which must be located in the close proximity of the reactor core exit. Sensors required for the Plant Control System or Reactor Protection are mandatory and must conform with Class 1E requirements. A large part of the instrumentation is required for monitoring the individual fuel and blanket assemblies or groups of these assemblies. These sensors, although not mandatory, do provide information needed to verify and improve the design of the core assembly. These sensors also provide information that may be useful in locating a faulty fuel assembly. Table 2-4, Sheet No. 1 of Part VII, Section 2 identifies the sensors located near the reactor discharge and lists some of their requirements.

The following is a list of general requirements that apply to most in-vessel sensors:

- Sensors required for plant operation and control must be replaceable with little if any, loss of plant availability.

- Electrical connectors that need to be disconnected during refueling must be accessible for manual servicing.

- Dry well penetrations and their containment boundaries must not allow air to come in contact with the sodium or cover gas during the 40 year life of the plant.

- Wet well penetrations must have double seal electrical connectors. Their penetrations must also have special flanges to interface with an inerted transfer cask when replacing the sensors.

Both the Plant Control System and Reactor Protection System require reliable measurements of the average sodium temperature at the discharge of the reactor. Wet well thermocouples provide better response time, but they are more difficult to replace. For this reason we propose to use 16 dual thermocouples located in the dry wells that are equally distributed and terminate above sixteen sectors of the core.

Redundant, diverse sensors are required to determine whether the fission product leakage from the fuel assemblies are less than the upper limit approved by the NRC. It is also desirable to determine which fuel assembly or assemblies are the bad leakers. To meet these requirements we propose to use sodium analyzers and cover gas analyzers to monitor the fission product concentration in the sodium

and cover gas, respectively. The cover gas system will determine the fission gas concentration in the cover gas but it will not locate the failed fuel assembly or assemblies. To provide the equivalent performance of the CRBRP delayed neutron detection system (minimum detectable exposed fuel surface of 1.3 sq. cm with a signal to background ratio of 0.33) it is necessary to have eight or more sample streams, one for each 1/8 of the core discharge area. Each sample stream must have a contribution from each fuel assembly assigned to its sector. To meet these requirements we propose to have four sodium sample systems. Each system covers one quadrant of the reactor discharge with a multiport collector as described in Part VII, Section 4.

Some acoustic sensors will be provided to detect abnormal microphonics such as unusual vibrations and loose parts. These detectors can also be used to detect local boiling. We propose to install 16 acoustic sensors in dry wells which are equally distributed and terminate around the periphery of the reactor discharge.

The reactor protection and monitoring system requires diverse measurements of reactor discharge temperature and sodium flow through the reactor. Flow can be determined indirectly by measuring the reactor inlet pressure and the primary pump speed. It can also be measured directly with electromagnetic velocity probes. We propose to provide one dry well probe for each fuel and blanket assembly. Each drywell will contain a dual thermocouple and possibly an electromagnetic probe which can be connected to measure either relative flow or sodium temperature variation. Selected thermocouples will be connected to the reactor protection system. The velocity sensors will not be connected to the reactor protection system until their reliability and accuracy has proven to be acceptable.

7.3.3 THERMAL HYDRAULIC CONSIDERATIONS

Normal Operations

The UIS has the potential of providing a means to control the core exit flow during both steady state and transient situations. During periods of steady state operation this component may be used to effect mixing of core effluent such that the sodium reaching the IHX inlets or other outlet plenum components is near isothermal. During periods in which the core effluent is rapidly changing in temperature (scram transients) the UIS may be the only outlet plenum component available to slow the transient and minimize damage incurred by the IHX. The primary thermal hydraulic functions to be considered in the UIS design are as follows. It is anticipated

that the UIS will be capable of performing these functions by the application of flow baffles, fluid risers or chimneys, and other fluid diversion or mixing devices coupled with a judicial control of pump speed during the transient events.

At steady state reactor operation the following thermohydraulic phenomena must be considered by the designer:

(a) Thermal Cycling (Striping)

Temperature fluctuations are caused by the impingement of different temperature sodium streams exiting the core. These fluctuations will be particularly severe at the core exit plane. Also, very low flow regimes in the plenum may result in local natural convection currents tending to temperature oscillations.

(b) Gas Entrainment

High sodium velocities near the free surface cause cover gas entrainment into the primary sodium system.

(c) Flow Induced Vibration

Internal structures in high vortex shedding regions will be subjected to flow induced vibration.

(d) Instrumentation Location

If installation of certain instrumentation just above the low flow core assemblies is contemplated, the flow in this area must be fully characterized in order to be certain that the instruments read the correct data.

The principal transient to be considered is a reactor scram which may be followed by a main pump trip. In this event cold sodium is discharging into outlet plenum sodium ($\Delta T \sim 280°$). Stratification and inadequate flow distribution may result in poor mixing leading to thermal shock at the IHX inlet port locations.

State of the Art Technique

The flow/temperature field in the outlet plenum is complex and difficult to predict. This problem has been attacked both analytically and experimentally. In the U.S. most of the effort in this area has been directed toward a loop reactor design. This information is only partially applicable to the larger (higher aspect ratio) plenum of a pool plant. Most of the experimental work is done with water or air. In general these experiments adequately simulate sodium flow and it is expected that in sodium temperature gradients will be less steep than the other fluid tests.

The foreign data available consists of work done in the U.K. They have concentrated on small scale model tests of their pool reactors.

The following is a brief description of the recent experimental work and available computer codes.

Experimental Work. Extensive tests were performed to model LMFBR reactor outlet plena, specifically the FFTF and the CRBRP loop configurations. The main objective of these experiments was to determine the outlet nozzle temperature in a down transient in which stratification occurred and to compare them with computer model predictions. The main finding was that indeed, the cold sodium stratifies and consequently the mixing is minimized leading to steeper temperature gradients. These tests are discussed in Part V, Section 9.

A substantial amount of experimental tests have been performed in the U.K. Their water tests consist of flow visualization in which free surface and buoyancy effects can be seen with the aid of either dye or bubble injection. Since they leave the primary pump running on a scram, they are not so much concerned about the mixing in the outlet plenum. Most of the tests address the gas entrainment and the striping phenomena. They employ small model air rigs equipped with hot wire anemometry to investigate temperature and flow oscillations.

Analytical Work. Several 2-D and 3-D computer codes have been developed to analyze the thermohydraulics of the outer plenum as described in Part V, Section 9. The codes are still being developed and improved. Some experimental verification is available.

Mixing in the Hot Pool

Steady State Mixing. The different temperature streams of sodium exiting the core can be mixed directly above the core outlet and the striping problem confined just to this region. A mixing chamber such as is employed in the CRBRP design might fulfill this requirement.

Another method of controlling the striping phenomenon is to construct a low baffle just above the core and extend it radially to cover the main core region. This design forces the hot and cold streams out into the open pool in which the turbulent action reduces the temperature difference to an acceptable level. This

concept is used in the French design and GE/NPC are investigating a similar concept in a joint study. In a preliminary experimental modeling of their design (which includes the shield upstands) the British found that a low baffle caused a large free surface disturbance.

This concept has great potential provided no downstream structures are subjected to large ΔT oscillations.

Transient Mixing. One of the possible advantages of the pool reactor is the large volume of hot pool sodium available for mixing, especially when large flow rates are maintained during and after a scram.

On a scram with pump trip it has been shown experimentally that buoyancy effects take over and stratification occurs. In model tests it has been shown that if the plenum outlet is below the UIS outlet it will "see" a gradual change in temperature rather than a step change. In this case most of the sodium volume below the UIS outlet is involved in the mixing. The implication for the pool design is that the IHX inlet should be within the mixing zone and the mixing zone should include as large a volume of sodium as possible.

Because of the large pool area however, the flow pattern in the upper plenum may not be similar in nature to the flow in a loop reactor. Thus, there is a large uncertainty in applying results from the "loop" mixing tests to the "pool" situation. The current pool design features a large pool flow area. Even at 100% core flow a typical sodium velocity in the middle of the pool is less than 0.5 ft/sec. If cold sodium enters the plenum, after a scram without pump trips, it will sink down due to buoyancy at the speed of about 5 ft/sec dominating the flow field. Thus, regardless of pump flow rates, the flow and temperature distribution in a large pool may be dominated by buoyancy.

Generally, it is the objective of the designer to maximize the mixing effect at the minimum flow rate, achieving a less steep temperature change. Such an optimum flow rate, if it exists, must be known if the plant is to be designed for it. All these considerations lead us to the following questions:

- What portion of the total pool volume "participates" in the mixing process?
- How does this mixing portion vary with the incoming flow rate?
- What is the UIS role in the mixing process?

The first question is directly related to finding which flow patterns exists in a large pool configuration. The second question addresses the effect of buoyancy on the mixing process at various core flow rates. The UIS may contain features with the sole purpose of discharging the core outlet flow at a high elevation in order to enhance mixing. The elimination of these features could simplify significantly the design of structures above the core. Therefore, their effect on the mixing must be determined for the pool configuration.

At the present time the answers to the foregoing questions are unknown. The only means by which we may get closer to an answer is by obtaining experimental data, or by using validated computer codes.

Future Work

The mixing is only one aspect of the overall thermal hydraulics in the outlet plenum which has to be investigated further. Most of the phenomena described before are difficult to predict with the current analytical capabilities. Future work should be concentrated on experimental work and supplementing it with analytical prediction.

Experimental Work. Near term (2-3 years) experimental programs will probably have to be to be limited to small scale water tests. These tests are relatively less expensive to set up and they render very useful information about the basic phenomena. These tests should meet the following requirements:

1. Pool with high aspect (4:1) ratio geometry.

2. Three-dimensional simulation - preferable 360° presentation of the outlet plenum.

3. Flow visualization capabilities.

4. Free surface.

5. Variable inlet flow and temperature (or density) to study the mixing and buoyancy effects.

6. Geometrical flexibility, to study the effect of various geometrical configurations (such as chimney, baffles, IHX inlet location) on the mixing and the free surface.

7. Inlet temperature distribution to study temperature oscillations and thermal striping.

Long term (3 years) experimental programs should include large scale tests possibly using sodium. These tests will answer the questions about the validity of small scale data and the adequacy of applying water data to sodium prototypical conditions.

Analytical Work. Because of practical considerations and computer limitations there is a need for a simplified as well as for more complex (2, 3 dimensional) models. All models require experimental validations and should be checked periodically with test data to ensure that possible modifications have not created significant distortions of the predicted flow and temperature fields.

Detailed flow and temperature distribution can be calculated from a multi-dimensional code. A 2-D (or axisymmetrical) code is then recommended wherever possible, since it is substantially more economical to run than a 3-D code. A 2-D code such as VARR II can be used for parametric studies to optimize UIS design and pump operations. When a two-dimensional version of the three-dimensional codes is available it might be more advantageous to use it instead of VARR II.

There are regions in the hot pool where the thermal hydraulics is definitely three-dimensional in nature. The COMMIX-1 code (or the PNL-3D when it becomes available) can be used for the 3-D analysis. Such a code should be used selectively as it is expensive to operate. It should be used to check the adequacy of the 2-D analysis.

7.3.4
MATERIALS CONSIDERATIONS AND REQUIREMENTS

UIS surfaces will be subjected to thermal striping conditions. Key parameters pertinent to UIS materials selection are thus: (1) the high cycle fatigue strength, (2) the mean coefficient of thermal expansion, and (3) the thermal conductivity at the anticipated service conditions. Together they define the maximum metal surface ΔT that can be tolerated for the 40-year reactor life without nucleation of surface cracks. The maximum anticipated ΔT within the sodium and above adjacent assemblies within the reactor core will be about 270°F. Non-adjacent assemblies may have somewhat higher ΔT, perhaps on the order of 340°F. Using a factor of 0.8 to correlate the temperature differential in sodium to that actually realized at the metal surface, a maximum metal surface ΔT of about 216°F may be experienced. In this manner, a fatigue strength consistent with a metal surface ΔT of about 220°F can be established as the alloy requirement necessary to meet the 40-year (1.26×10^9 cycles at 1 Hz), non-inspectable design life.

Adequate materials performance at the low cycle end of the S-N curve is equally important. To demonstrate this point, consider usage analysis for reactor scram events for a Type 316 stainless steel UIS. For Type 316 plates approximately 0.5 inch thick a total damage factor of 1.0 to 1.5 is calculated for thermal transients anticipated for the UIS. This damage is due primarily to creep and neglects the contribution of thermal striping to the usage factor. Type 316 stainless steel is insufficent based solely on thermal shock considerations except in very thin (≈0.1 inch) sections. The low cycle fatigue strength and creep/fatigue interaction properties are thus key materials selection parameters.

For thermal transient and seismic considerations, fracture toughness parameters will be important. Fracture toughness is in general inversely proportional to the high cycle fatigue strength. And, thus, the unstable crack growth data would be required for Linear Elastic Fracture Mechanics (LEFM) structural integrity analysis. There is limited variation in crack growth data for the primary candidate alloys, and thus, this parameter presents little basis for alloy selection.

Major materials related activities conducted during the current Phase include: (1) a visit to HEDL in Richland, Washington to discuss the mechanical properties and in-sodium performance of proposed candidate alloys, (2) a visit to INEL near Idaho Falls, Idaho to discuss the development program for the candidate Alloy 718, (3) visits to GE (AEG) in Evendale, Ohio to discuss aspects of the acquisition and utilization of mechanical properties data in high temperature design and to become familiar with the fabrication and welding characteristics of Alloy 718, (4) a meeting on candidate alloys for the UIS, jointly held by GE (ARSD) and UK-NPC technical teams at GE (ARSD) in Sunnyvale, California, and (5) participation on the DOE sponsored task force on thermal striping in LMFBRs.

Proposed Candidate Alloys and Alloy Selection

A survey of alternative materials for the UIS has been conducted. The survey centered on four commercially available and well documented alloys: (1) Type 316 Stainless Steel, (2) Inconel 625, (3) Nimonic PE16, and (4) Inconel 718. The four viable candidates were initially compared in terms of the physical properties and mechanical properties (including tensile strength, fatigue strength, toughness, creep rupture, and creep fatigue interaction). Based on the available properties data, the following candidate alloys were selected in order of preference:

#1 Alloy 718
#2 Nimonic PE16
#3 Alloy 625
#4 Type 316 Stainless Steel

In discussions helds at a joint GE/NPC meeting, the candidate alloy list was further narrowed by consideration of additional requirements, such as long time thermal stability, sodium compatibility, irradiation effects, weldability, and fabricability. Confidence associated with the nature of the available data base was also factored into the selection process. As a result, it was decided to drop the Alloys PE 16 and 625 from further consideration. Alloy PE16 was dropped because: (1) there are very limited data for this alloy relevant to UIS design, (2) although there are no significant fabrication problems for the alloy, there are no data to indicate a fabrication advantage over Alloy 718. Alloy 625 was dropped on the basis of (1) a limited data base, and (2) thermal aging instability. This alloy has been shown to exhibit limited room temperature ductility as a result of long time thermal aging[2] at service temperature.

Type 316 stainless steel does not meet the most stringent requirements of the UIS. However, the alloy will have application within the UIS design. Therefore, an effort to fully document the fatigue performance of Type 316 stainless steel is being assessed from the existing US and UK data. Both sodium and air data will be compared in the analysis. A similar analysis for the available US data on Alloy 718 is also being performed. Limited in-sodium fatigue data exists for Alloy 718.

It is suggested that the NILO series of alloys be considered for follow-on, future UIS design. This nickel alloy series can be tailored to yield a very low thermal expansion coefficient, and thus, be quite tolerant of temperature perturbations, such as thermal striping events. However, these alloys currently exhibit: (1) limited elevated temprature strength, and (2) a time/temperature dependent expansion coefficient. The alloys may be application limited to temperatures less than 930°F. An extensive development program would be required to qualify a NILO series alloy for future UIS application.

Elevated Temperature Design Limit for the Candidate Alloy

The maximum temperature to which the UIS is exposed is estimated to be 1015°F for the saturated steam cycle. The design temperature of the UIS will then be approximately 1025°F.

The mean service temperature will have a dramatic impact on Alloy 718 suitability. Alloy 718 has been included in the Code Case 1592 for bolting application. That application is authorized for temperatures up to 1050°F. This upper limit is

primarily based on concern for overaging. The final aging temperature for the conventional heat treatment is 1150°F. It is standard code practice in the US to use a precipitation strengthened alloy at temperatures not exceeding the final aging temperature minus 100°F. It would be very difficult to extend the application range for Alloy 718 above the present 1050°F limit.

Other factors which support establishment of an upper temperature limit for I-718 include:

(i) rapid drop off in tensile strength and yield strength and a dip in ductility at about 1200°F,

(ii) transition in creep mode at about 1150°F,

(iii) transition in the elevated temperature fracture mode (intergranular fracture) around 1200°F,

(iv) transition in the room temperature fracture mode (intergranular fracture) for specimens thermal aged for long times at temperatures in excess of 1100°F, and

(v) potential sodium incompatibility at about 1200°F.

Design Considerations

Thermal striping is a major consideration in UIS design. The maximum metal surface ΔT that Alloys 718 and 316 can endure without nucleating surface cracks in the anticipated 1Hz, 10^9 cycle service life of the UIS are compared in Table 3.4.3-1. Values are estimated on the basis of the "best guess" S-N design curves. The US assessment does not account for potential properties enhancement as a result of the relatively inert service environment (Na). The UK assessment takes into account anticipated, but not demonstrated, in-sodium properties enhancement.

Table 3.4.3-1

Estimated Maximum Allowable Metal Surface ΔT Values
For a 10^9 Cycle, 1 Hz Design Life*

Alloy	US Estimated ΔT_{max}	UK Estimated ΔT_{max}
Type 316 Stainless Steel	40°F	115°F
Alloy 718	240 °F w/o Mean Stress Penalty 175 °F with Maximum Mean Stress Penalty	290°F w/o Mean Stress Penalty

*Estimates are made on the basis of an average thermal expansion coefficent for the subject alloys.

The British estimates of Table 3.4.3-1 include a factor of two enhancement in fatigue strength at the high cycle end of the S-N curve due to the in-sodium service environment. UK data support this factor for austenitic stainless steel, and a similar enhancement is anticipated for Alloy 718. This factor-of-two allowance made to establish the design curve, explains in part why the UK estimated values values are larger than the US estimates. The US estimate is based on air data for both alloys.(3)

In terms of thermal striping considerations only, Allow 718 appears very close to meeting the 40-year, non-inspectable life requirement of the UIS. Air data indicate that the metal surface allowable ΔT_{max} of approximately 230°F will be met, if mean stress effects are minimized. If in-sodium S-N properties enhancement is demonstrated, Alloy 718 would more readily meet the 220°F ΔT_{max} requirement.

The alloy 718 allowable ΔT of 240°F does not take into account the mean stress effects. To demonstrate the significance of mean stress effects, assume an alternating stress of 29 Ksi at 1 Hz (thermal striping) and a sustained mean stress of 65 Ksi for the UIS. This alternating stress of 29 Ksi would result from a surface ΔT of 220°F. This value of mean stress is approximately half of the expected yield strength of the alloy and is a reasonable estimate. Using the standard Walker Equation for mean stress correction, this fatigue spectrum is equivalent to a fully-reversed cycle (R=-1, A=00) stress amplitude of 52 Ksi. Consulting the existing Code fatigue correlation for Alloy 718, (2) the expected endurance limit for Alloy 718 is 62.7 Ksi. The expected endurance limit is thus only 1.2 times greater than the anticipated fatigue conditions. The 52 Ksi stress amplitude intercepts the design (S_a) fatigue curve at approximately 10^5 cycles. Under these assumed conditions, the 10^9 cycle life requirement would not be met by Alloy 718.

The fatigue endurance limit for Alloy 718 is inversely proportional to grain size and thus, this parameter will affect life prediction. An accurate assessment of Alloy 718 suitability for the UIS in terms of the thermal striping phenomenon must take into consideration mean stress and grain size effects.

In evaluating UIS service conditions with respect to the design S-N fatigue curve for a given alloy, one is determining the pseudo-stress limit at (or below) which an acceptable amount of fatigue damage can be tolerated by the alloy. One also must consider the growth of flaws which may already be present. Flaws exist in all commercial alloys irrespective of fabrication, heat treatment, and/or inspection history. Crack growth does occur under alternating stress conditions, and this must be yet another consideration in the design of the UIS. Using the basic Griffith relation for stress intensity at the tip of a sharp crack and considering the R =0 (A = 0) fatigue cycle for the 65 Ksi mean stress/29 Ksi alternating stress condition assumed for the UIS, a stress amplitude of 74 Ksi results. Using the standard Griffith relation, a stress intensity of 13 Ksi$\sqrt{in}$ is calculated. The calculation assumes the presence of a .010" deep semi-circular crack, present within the fabricated Alloy 718. The assumed flaw size of .010" has been estimated on the basis of state-of-the-art fabrication and inspection experience. The calculated stress intensity of 13 Ksi $\sqrt{in}$ is likely greater than the lower threshold limit which can be estimated to be about 9 Ksi $\sqrt{in}$ for I-718. This means that growth of existing surface flaws could occur as a result of thermal striping, and this is inconsistent with a 40-year, non-inspectable life requirement for the UIS. A mean stress is assumed in this calcuation. The importance of mean stress considerations is again demonstrated.

Two preceding examples suggest caution in utilization of Alloy 718 for the UIS. There exists the potential for overextension of the alloy. The design goal of a 40-year, non-inspectable life may be realized through proper integration of reactor core/UIS design coupled with thorough materials characterization.

If a material cannot meet the 40-year, non-inspectable service life requirement, then the UIS must have an established inspection interval. This would dramatically impact the reference design. The inspection interval for the type 316 stainless steel UIS using existing US fatigue design data has been estimated to be approximately two years. This would be the case for the most severe thermal striping anticipated. From an economic standpoint, this is probably unacceptable.

The importance of establishing elevated temperature design properties for the primary candidate alloy is crucial to UIS design. There is current activity toward acceptance of Alloy 718 for high temperature use in an ASME Code Case for non-welded, non-pressure boundary applications [refer to DOE, Development Requirement Specification (DRS) 31.1.02, Rev 6, dated October 1977]. The Code Case may be available as early as 1980. It is recommended that GE assume an active role in the evolvement

of design curves for this alloy.

Welding and Fabricaiton Considerations

At GE (AEG) Evendale, extensive use is made of Alloy 718 in the aircraft gas turbine industry. The experience base with this alloy is ~10-12 years. The material is used in rotating as well as in stationary parts. The material is fabricated by conventional machining, forming, and by EDM. Complicated weldments are employed, and a total of about 5000 inches of welds are required for each engine. Some of the Alloy 718 components, including weldments, are exposed to high temperatures (1200°F) and rapid transients (1100°F/10 sec). Design and fabrication is in accordance with GE specification, and the material is procured to GE specificaiton from commercial suppliers. It is estimated that GE uses about two million pounds of Alloy 718 per year. This alloy is available from a variety of domestic sources.

Alloy 718 is somewhat more difficult to machine than SS-316 but does not present any particular problems (the machinability indices for Alloy 718, SS-316 and mild steel are 10, 50 & 100, respectively). The material may be conventionally machined in the annealed condition with final machining, where necessary, performed after heat treatment. EDM machining is also used. Distortion and shrinkage have not been a problem during heat treatment. The material is shaped by forming in some applications. There are no special sequences of operation, procedure, or heat treatments used in machining and forming this material. Field fabrication with heat treatment in field furnaces (air environment) is considered possible.

Alloy 718 weldments are used extensively in the aerospace industry. TIG welding, both manual and automatic, is the most commonly used type although some use is made of EB and MIG. Two or three passes are required for most of the welds which are about 0.1 inch thick. Welding is done with the metal in the annealed condition and followed by a solution heat treatment and aging. Production welds are 100% RT inspected. There are very few heavy section welds (up to 1/2" thick), and they are generally done by EB methods. Components size is important here because EB welding must be done in a vacuum. In welds on the order of 1/2 inch thick (not performed by EB techniques) approximately 20 passes are required.

Microcracking of Alloy 718 in the heat affected zone (HAZ) is typical, even with electron beam welding, which produces the best HAZ structure. The microcracking generally occurs on the austenite grain boundaries. Laves phases and Ni_3Cb also produce microcracking in large ingots (greater than ~24" diameter) due to interdendritic segregation ("freckels"). These microcracking mechanisms may both be more of a problem with large, thick welded plates.

The low temperature annealing treatment (1750°F) and aging at 1325°F produce the best weld and base metal creep and fatigue properties; however, where optimum properties are not required of the weld, the weld may be aged only rather than annealed and aged.

US experience concerning the welding and fabrication of Alloy 718 is good. HEDL and INEL researchers involved in the national mechanical properties program expresses optimism in the ability to machine, fabricated and weld this alloy. Welding, fabrication and forming operations are equipment/technique limited and not materials limited.

Full Validation of Alloy 718

The following items are considered necessary to fully validate Alloy 718 for the UIS:

(i) In-sodium high cycle (deflection controlled) fatigue data to quantify the influence of the sodium environment on fatigue strength

--priority one is to demonstrate fatigue strength enhancement

--priority two is to quantify the results with respect to air data for design purposes.

(ii) In-sodium crack growth data to establish a correlation for LEFM structural integrity analysis.

(iii) Striping tests based on UK (AEA) studies, using the mixing tee approach to determine the failure mechanism and fracture characteristics of thermal striping.

(iv) Fatigue tests to quantify the actual mean stress penalty for Alloy 718 and to evaluate the influence of grain size on the thermal striping resistance of Alloy 718.

(v) Alloy specifications and heat treatment limitations sufficient to assure the required thermal striping resistance.

(vi) In reactor exposures to evaluate the irradiation influence on the pertinent mechanical properties

--current HEDL programs in the US are concentrating on this effort and may meet the data requirements.

(vii) Sodium compatibility tests at the design temperature.

(viii) Creep fatigue interaction data to characterize the alloy, as required.

(ix) Long-term thermal aging data to confirm alloy stability

--current programs at ORNL INEL and HEDL may meet this data requirement.

Conclusions

A. Key materials parameters pertinent to the upper internals structure design include: (1) high cycle fatigue, (2) mean coefficient of thermal expansion, (3) thermal conductivity, (4) low cycle creep/fatigue interaction, (5) fatigue crack growth, (6) static crack growth, and (7) fracture toughness. Due to the thermal striping phenomenon, suitablity of any commerially available alloy may be challenged.

B. Of the viable candidate alloys, alloy 718 offers the optimum properties balance for a reference design.

C. A design concept resulting in a maximum operating temperature limit of 1050°F or less is recommended based on materials considerations. For extended sodium service at temperatures greater than 1050°F, overaging, surface grain boundary degradation, and other factors limit component life.

D. On the basis of existing data, calculations demonstrate that caution must be used in utilization of Alloy 718 in UIS design. The potential for overextension of the alloy exists due to the thermal striping phenomenon. The design goal of a 40-year, non-inspectable life may be realized through materials characterization.

E. Due to the correlation between design curves and design concept, it is recommended that GE assume an active role in the evolvement of the ASME Code Case for non-pressure boundary applications.

F. The high cycle fatigue endurance of Alloy 718 must be well characterized in terms of grain size, mean stress, temperature and environment. These are the key variables which will establish the S-N design curve.

G. Inconel Alloy 718 is considered a viable material candidate for the UIS in terms of potential weld, forming and fabrication requirements. It has been extensively used in critical application by the aircraft industry. This use has been for structural components subjected to high mechanical stresses and thermal environments similar to those expected in an LMFBR.

H. Some development work is required to fully validate Alloy 718. Key items are presented in the text.

7.3.5
DESIGN APPROACHES

In the present work, GE has pursued two approaches for the design of a UIS for a commercial sized pool type reactor. The motivation at this point is to attempt to identify features that will satisfy the design considerations and requirements discussed in Sections 3.1 through 3.4 above and lend themselves to the special fabrication requirements of the reference material. Of particular concern is the manner in which mechanical and welded joints are utilized. Also of concern is the degree to which the UIS functional requirements (including design life) are

satisfied and the reliability that one may place upon the design. The present work has served to illustrate that there are still a great many questions relative to the design conditions and the expected performance of the UIS under these conditions that are still to be resolved. The most important of these are the local core exit thermal hydraulics which determines the thermal environment and materials application for the UIS and the outlet plenum thermal hydraulics which is presumedly strongly influenced by the UIS design. Because of these uncertainties, and because of on-going parallel work at NPC on two additional designs, there has been no attempt at present to select a reference concept. It is anticipated that there will be sufficient information generated relative to the mechanical designs by late 1978 to make a preliminary selection from among the four alternates for a preferred concept that stands the best chance of satisfying the design conditions as they become understood.

The four basic concepts of the UIS that have been identified for the joint study by GE and NPC engineering teams are as listed below:

- The mixing chamber concept where flow mixing is performed in a plenum at the bottom of the structure and transferred to a higher elevation and ultimately the inner pool.
- The "low baffle" concept which essentially deflects the core flow radially outward into the inner pool at a low elevation. The flow baffle is positioned at an elevation of the order of three feet above the core.
- The "high baffle" concept which is used in conjunction with a perforated cylindrical baffle. The number, size, and distribution of holes in the cylinder govern the mixing and degree of turbulence in the inner pool.
- The "high baffle" concept, without a cylindrical skirt; this is essentially the PFR configuration.

The latter two concepts are being studied by engineers at NPC/Risley. Any promising additional concepts that may evolve during the initial phase of the study will also be open to investigation. The two designs being considered by GE differ in the manner in which the core effluent is routed from the core exit to the outlet plenum and also in construction methods. In the first concept (Low Baffle Design) this effluent is discharged from the UIS at a relatively low elevation in the pool. The second approach (High Baffle Design) uses a baffle located near the hot pool free surface to direct the effluent radially outboard at a high elevation in the pool after passing through a mixing region within the UIS.

Both of these designs proceeded on the assumption that I-718 will be the reference material in order to withstand the severe thermal environment. This alloy has

been identified as being the best available alloy having a substantial, existing, data base. Unfortunately, because of its higher mechanical properties, it is generally more difficult to fabricate than the austenitic stainless steels. For this reason it is desirable to limit its use to parts of the structure suffering the severest environment.

In the current design work, the methods of assembling the UIS were of primary concern and both welded and mechanical attachments have been considered. Welded assemblies have obvious advantages from design and construction viewpoints. They provide a positive attachment, allow minimum cross-sectional thickness to be used (which is desirable in areas subjected to thermal shock) and do not suffer fretting. The problems associated with the welding of Inconel-718 are due to the complex metallurgical phases which arise in the weld and the heat affected zone. In order to restore the desired properties of these regions, it is necessary to perform post-weld heat treatment. This will be difficult with large complex structures such as the UIS. Additionally, existing fabrication experience with this alloy suggests that any weld must be a fully inspectable butt weld which is accessible for weld repair operations during the fabrication stage. Mechanical fasteners avoid the welding disadvantages outlined above, but exhibit a propensity to vibrate and produce "fretting" at the joints. Invariably mechanical fasteners increase cross-section thicknesses and increase the complexity and number of parts subjected to vibration. The type of mechanical fastener or joint which relies on a degree of pre-strain is unsuitable for application in the UIS. Such a fastener would exhibit creep relaxation at a rate dependent on the amount of pre-strain, and would ultimately become loose and subject to fretting. The preferred type of mechanical fastener would have to be designed in a manner that minimized clearances, possibly utilizing tapered contact faces to take up any clearance.

A factor which must be considered at transition joints between Inconel-718 and 316 Stainless Steel is the differential expansion of the materials. This can give rise to induced strain or increased clearance dependent on the design of the fastener.

The method for attaching the UIS to the reactor closure has not been addressed in the current work in lieu of efforts on the more critical regions directly above the core. Likewise, the seismic restraint for the lower end of the UIS has not been considered at this point. A potential concept for the seismic restraint is shown on the Low Baffle design which could be extended to the High Baffle design. Its features were sized for the previous "Chimney" UIS design developed during

Phase II. The weights of both of the Phase A Extension UIS concepts will be less than for the Phase II UIS concept and it is thought that seismic restraint will not be a problem. The use of cylinders extending to the closure provide a higher stiffness for the structure than the Phase II column which further improves the seismic situation. Preliminary seismic analysis is in progress and results of this analysis will be used to determine the need for and the size of restraint members. Likewise, while considered very important and having a significant impact on the UIS design, the questions of removability and inspectability of the UIS have not, as yet, been addressed in detail in the current work. In addition to potential inspection requirements (not yet established) for the UIS's structural integrity following some period of operation there is potentially a need to inspect the gap between the UIS and the top of the core prior to refueling operations. The need for this inspection and its design implications have also not , as yet, been formally addressed.

For the two GE designs discussed in the following paragraphs, an informal set of quidelines was adopted by the designers. These rules are consistent with the design requirements and materials limitations but are certainly subject to modification as the design progresses. Currently they are:

- Inconel-718 material is utilized for structural components below the flow baffle.
- The use of welded joints are limited to assemblies which can be post-weld heat treated. The assemblies must be fully inspectable and accessible for any weld repair which may be necessary during the fabrication stage.
- Bi-metallic welds may be employed between Inconel-718 and stainless steel 316 tube with the above constraints applicable to welded joints.
- Mechanical fasteners are utilized where it is not possible to fulfill the above criteria.
- Mechanical fasteners which do not rely on pre-strain to effect a joint are to be employed to eliminate the problems of creep relaxation and ratchetting during the reactor operation.
- Cross-section thicknesses of components are minimized where possible. Although it is possible to tolerate heavier sections (of the order of 1.25") in I-718 parts which are subjected to the thermal transients, the problems associated with welding would likely be larger for those sections.
- Mechanical vibration of the structure produced by general turbulence at the bottom end indicate deployment of a stiff structure having a high natural frequency. This conflicts with the requirements to limit thermal stresses which are minimized by increasing the structures flexibility. Mechanical joints subject to vibration must be designed to have minimal or no clearance to minimize their potential to fret.

- The structure must be capable of withstanding the impact loading of a subassembly support module in the event of a failure of the hydraulic holddown. The magnitude of the impact is dependent upon the distance the module is allowed to move vertically, i.e., the gap between the core and the UIS.

- The structure must be constrained against relative movement with respect to the core during a seismic event, commensurate with its continued ability to allow unimpaired insertion of the control rods.

- The structure must conform to the requirements and condition discussed in Section 3.1 through 3.4. Specifically, the design must be consistent with EPRI guidelines and core geometry. (Note that a slight modification in the control rod pattern was assumed as mentioned in Section 3.1.)

Low Baffle Design

In this approach, shown in Figure 3.5.1.1, the core effluent is deflected radially outwards into the inner pool at a low elevation (of the order of 3'-6") above the core. This creates a highly turbulent region directly above the core sub-assemblies which may ameliorate the degree of temperature fluctuations experienced by the structural material. The degree of amelioration needs to be established by thermal-hydraulic flow modeling. The high velocity radial outflow from the lower part of the structure, creates substantial mixing in the inner pool, which in conjunction with the large bulk of sodium, mitigates the thermal transients experienced by other primary circuit components, notably the IHX inlet ducts. The effects of thermal striping and thermal shock are in theory confined to structure directly below the baffle.

Control rod shroud tubes are used to protect the control rod drive lines from flow induced vibrations and to support some of the instrumentation. These are supported radially at three axial planes within the UIS and axially by a domed shell. The remaining instrumentation is supported by instrument shroud tubes which are similar to the lower half of the control rod shroud tubes. These tubes are supported at the intermediate support plate level where they terminate. All of the tubes are connected together into a matrix on a constant triangular pitch of 18·135" which is three times the pitch of the core-assemblies.

All of the tubes provide secondary holddown for core sub-assemblies. Ultimately any secondary holddown forces are transmitted to the top support shell (dome). Such forces would only occur in the event of loss of hydraulic balance to either a single core sub-assembly or to a group of seven sub-assemblies.

Four additional tubes are connected to the array of shroud tubes. These carry 6" diameter circular keys which are actuated by mechanisms up in the rotating plug region. The keys locate into the core support barrel and prevent translation of the two structures with respect to each other during a seismic event.

For the purposes of description the UIS concept is separated into the following components:

- Control Rod Shroud Tube module
- Instrument Shroud Tube module
- Seismic Keys
- Bottom Location Grid
- Flow Baffle
- Intermediate Support Plate
- Top Support Shell
- Outer Cylinder
- Instrumentation

Control Rod Shroud Tubes. The control rod shroud tubes (CRST), shown in Figure 3.5.1.2 and 3.5.1.3 are located co-incident with control rod positions in the core. This sub-assembly is fabricated from Inconel 718 and Stainless Steel 316 tubes and forgings as shown. Inconel 718 is used for the portion of the assembly subject to the severest conditions. A matrix of individual diamond shaped Inconel 718 plates, each supported from the tubes, form the flow baffle. Below the baffle plate level the assembly has a double wall tube. This is to encapsulate instrumentation tubes servicing six fuel or blanket sub-assemblies surrounding the control rod and to protect them from the turbulent flow environment. Two smaller diameter tubes supported from the CRST by webs at the bottom end and by the baffle plates provide support and protection to instrument tubes servicing two additional fuel blanket assemblies.

Thirty of these modules are required . Their positions are marked 'C' in plan view Figure 3.5.1.4. The diameter of the CRST could be larger than shown in Figure 3.5.1.2 if found necessary to position the instrument guide tubes above the core sub-assemblies. This would, however, result in a higher degree of flow entrainment and turbulance within the bottom end of th CRST which is undesirable for the control rod drivelines. The chosen diameters allow the thermocouple guide tubes

to be placed above the edge of the sub-assembly flow jet without entraining too much of the effluent. It will be necessary to vent the CRST below the baffle plate level to prevent entrained flow from going to a higher elevation.

Instrument Shroud Tubes. The instrument shroud tube assemblies complete the array in the lower half of the structure. These assemblies are similar to the lower half of the CRSTs. Their function is the provision of support and location to the remaining fuel and blanket assembly instrumentation in the core and the completion of the flow baffle. Fifty-five of these are necessary to fully instrument and provide backup holddown for the fuel and blanket assemblies. The detailed difference between this assembly and a CRST assembly has not been studied. For example, the guidance of instrumentation tubes down to a fuel or a blanket sub-assembly located below the center line of this module is as yet undefined but should not present any major difficulties.

Seismic Location Keys. Four 6" diameter seismic location keys are positioned as shown in Figure 3.5.1.4. The design of these has been deferred until results of the seismic analysis are available. The size of the key shown is equivalent in cross sectional area to the four rectangular keys used for the reference design described in the Phase A report. The keys are located in four guide tubes constructed of Inconel 718 and Stainless Steel 316 tubes and forgings. The lateral support for the tubes is provided by the intermediate support plate and by webs which connnect into and form part of the bottom location grid. The keys are inserted into location bores in the core former by actuating mechanisms located in the closure plug.

Bottom Location Grid. It is necessary to connect modules together at an elevation close to the top of the core to locate them with respect to the core sub-assemblies and also to stablize them against and minimize the displacements resulting from a seismic event. Figure 3.5.1.5 shows the tubes connected together by webs which are part of the forgings on the bottom end of the shroud tube modules. The webs terminate in bosses which are pinned together as shown in Figure 3.5.1.4. Accurate machining with close tolerances will be necessary to ensure that a tight fitting joint is achieved. The pins are lock welded into blind holes to ensure that they cannot drop into the core. The pins are hollow to allow sodium to pass through them to reduce the skin stresses produced by thermal shock. Several alternative grid patterns have been considered. The one shown attempts to balance the conflicting requirements of obtaining flexibility to reduce the radial thermal stresses commensurate with stiffness against the flow induced vibration forces.

Flow Baffle. The flow baffle is comprised of a number of individual plates, each fabricated into the shroud tube module. The plates do not provide any lateral support to the shroud tubes with respect to flow induced vibration. It is not necessary to provide an impervious flow barrier provided that the bulk of the core effluent is deflected radially outward at this level. The amount of leakage flow between plates is dependent upon the gap between them. The gap size that can be tolerated will have to be determined from the flow models or from the thermal hydraulic computer codes. A first approximation gap size of 1/4" has been chosen based purely on intuitive judgement.

The plates are butt welded to the outer wall of the lower part of the shroud tube from which they are supported. Additional support is also provided by the bottom grid via the two smaller diameter tubes which are welded between the grid and baffle. The baffle plates are constructed from either I-718 forgings or from I-718 plates.

Intermediate Support Plate. The intermediate support plate's function is to provide lateral support to the control rod shroud tubes at an axial position that elevates their natural vibration frequency above the range of the flow induced forcing frequency. The plate is located in a region above the flow baffle and therefore will not be subjected to thermal striping and shock. This enables stainless steel 316 to be used for its fabrication. Figure 3.5.1.5 shows a plan view of the plate. The control rod shroud tubes pass through the plate and are connected to it by mechanical fasteners. The fasteners employed will be of a type which does not suffer from creep relaxation at high temperature, e.g. bayonet type fasteners. The instrument shroud tubes terminate at this level and are connected to the plate in similar manner to the CRST's.

Top Support Shell. This component is the structural member that takes the dead weight of the UIS and the reaction loads resulting from core effluent pressure forces and impact loads from a loss of hydraulic balance in the core sub-assembly holddown system. The shell is located in the cover gas region. It will be virtually isothermal during reactor operation and, therefore, insensitive to pool transients. The mild environment allows the shell to be fabricated from stainless steel 316. The spherical or torispherical shape is designed to minimize the deflection of the structure subjected to the above forces commensurate with the maintenance of thin sections to minimize weight. The section thickness of the shell will be of the order of 1".

The control rod shroud tubes are connected to the shell by either mechanical fasteners or by butt welding the tubes to penetration inserts in the shell. The latter solution is preferred for the following reasons:

- The weld will be away from the vicinity of I-718, therefore post weld heat treatment will not be necessary.
- There is access to make a butt welded joint using an orbital or bore welding technique, and for inspection of the welds.
- Welded joints have superior vibrational characteristics to mechanical fasteners.

Figure 3.5.1.6 shows a plan view of the shell. In addition to the control rod shroud tube penetrations, there are twelve (12) ports through which the thermocouple guide tubes pass.

Outer Cylinders. The 12 ft.-1 in. diameter top cylinder will form the connection between the UIS and the intermediate rotating plug, but the design of this has not yet been established. A cylinder is preferred to column supports because it offers greater torsional resistance against the turbulent flow forces. The mild environment allows stainless steel 316 to be used for its fabrication. The cylinder and top support shell are welded together via 'T' section forged ring.

The conical shell between the intermediate and top support plates is a continuation of the top cylinder and has a similar function. This will be welded between the plates. Stainless steel 316 can be used in the mild environment at this level.

The 15 ft. diameter cylindrical shell suspended from the intermediate support plate may not be necessary. In theory, it functions as a cylindrical baffle against pool sodium re-entering the structure above the horizontal baffle plates. Thermal hydraulic flow models and computer codes will determine the necessity for this. The thermal environment will also determine whether Inconel 718 or Stainless Steel 316 can be used. The shell is not connected to the baffle plates and it will probably require some means of increasing its stiffness.

Instrumentation. One instrumentation dry well, 5/8 inch OD is provided at each fuel assembly and each blanket assembly exit. These dry wells are located flush with the bottom of the UIS and approximately 1 inch above the assembly outlet nozzle. Additionally, the following devices will be provided as required and as discussed in Section 3.2 above:

- 16 5/8 inch dry wells for bulk temperature measurements near the UIS discharge ports.
- 16 acoustic monitors located in 5/8 inch dry wells in the lower regions of the UIS.
- 8 sodium sampling (wet wells) tubes in the lower regions of the mixing chamber.

All instrumentation dry wells and wet wells will be guided by and fastened to either a CRST or an instrument shroud tube module. Below the flow baffle plates the instrument tubes wet and dry wells will be protected from the turbulent core effluent by double walled shroud tubes. They will be routed away from the shroud tubes above the intermediate support plate and collected into twelve groups. The instrument tube bundles pass through ports in the top support shell and into penetrations in the rotating plug.

Fabrication. Particular attention has been directed toward designing this concept to facilitate fabrication because of the materials concerns expressed in Section 3.4 above. The fabrication sequence envisaged will be comprised of the following:

- Construct and assemble the control rod shroud tube module.

  --fabricate the forgings

  --weld the tubes and forgings together

  --heat treat the assembly

  --inspect the welds

  --repair any defective weld

  --re-heat treat assembly

  --re-inspect welds

- Construct and assemble the instrument shroud tubes in a similar manner.
- Fabricate the intermediate and top support plates and the outer cylinder.
- Sequentially join the two types of assembly to the intermediate support plate, using mechanical fasteners.
- Pin and lock weld the webs at the bottom of the assemblies together, to form the bottom location grid.
- Install instrumentation tubing.

- Attach the top support shell to the control rod shroud tubes, by orbital butt welded joints.
- Attach the top outer cylinder to the top support shell by butt welding.
- Attach the conical shell between the intermediate and top support plates in segments, by circumferential and longitudinal but welds.
- Attach the lower cylinder to the intermediate support plate in segments, by butt welds.
- Attach the structure to the rotating plug.

High Baffle Design

In this approach, shown in Figure 3.5.2-1, the UIS consists of two separate 8 feet high chambers. The lower chamber is used to promote mixing of the core effluent after it exits the reactor assemblies during normal operation. This mixing reduces the temperature differences that lead to thermal striping and assures that the coolant is as near the isothermal bulk mean temperature as possible when it leaves the lower chamber. The thermal striping is thus confined to the lower chamber. From the lower chamber the sodium passes axially into the upper chamber where it is directed radially outboard, through ports, by a solid flow baffle.

The core exit plane functions of the UIS are accomplished by cylinders located on two superimposed grids. The first grid is on a triangular pitch equal to three times the reactor assembly pitch. It contains cylinders that are tied together by welded ligaments. The cylinders are used to protect the control rod drive shafts and support some of the instrumentation. The bulk of the reactor assembly instrumentation is supported by cylinders that are assembled in four-cylinder modules and extend through the control rod grid. The resulting composite grid is triangular and on an approximately 10.46 inch pitch. All of the cylinders serve as backup holddown structures.

The axial support for all of the cylinders is achieved by the domed structure at the top of the UIS. This dome also ultimately provides the back up holddown restraint. An intermediate grid plate, that also serves as the top surface of the lower chamber, provides seismic restraint and elevates the fundamental frequency of the cylinder above the driving frequency that would result from eddy shedding.

For the purpose of discussion this UIS concept is separated into the following components as shown on Figure 3.5.2-1 : mixing chamber, grid plate, baffle plate,

instrumentation module, outer cylinder and, support dome.

Mixing Chamber. The mixing chamber arrangement is shown on Figures 3.5.2-1 and 3.5.2-3. It is the lower most portion of the UIS and located directly above the reactor core assemblies. It is approximately 8 feet long and its diameter (15 feet) is such that it encompasses the outermost row of blanket assemblies so that all of the core effluent, except the minimal shield assembly coolant, is directed into the chamber. Within the outer cylinder and spaced on a 18.135 inch triangular pitch grid pattern are 85 vertical tubes. The grid consists of a series of diamonds that are randomly orientated to preclude preferential stiffness. These tubes are interconnected at their lower end with ligaments and the resulting grid is tied to the outer cylinder through ligaments. Thirty of these tubes serve as shroud tubes for the control rod drive lines. The remaining 55 tubes fill in the grid pattern and provide holddown and instrumentation support for single reactor assemblies.

The lower 18 inches of each tube is fabricated from a cylindrical forging that contains the weld preparations for the ligament attachments and internal features necessary for instrumentation support or control rod guidance. Since all of the ligaments are located at multiples of 60°, it will be possible to design the forgings such that only two configurations (because of the different diameters) are required. The top of the forgings are welded to 5.75 inch OD tubes that make up the remainder of the 8 feet mixing chamber length. All of the parts within the mixing chamber are fabricated from I-718 and assembled by welding.

The overall dimensions of the mixing chamber have been established so that this total structure may be given the required post welding heat treatments. All of the welds have been located in accessible locations and post heat treatment NDT and weld repair will be feasible. The attachments of subsequent portions of the UIS is accomplished via mechanical devices which will be located in regions where the thermal environment is less severe.

Mixing in the mixing chamber is promoted by generating a large amount of random cross flow in the lower regions. The core effluent at most locations is directed into the bottom of one of the many cylinders above the core and exits these cylinders, horizontally, through slots. These slots can be sized and positioned to optimize the mixing as determined by subsequent thermal hydraulic analysis and mixing studies. The potential also exists for locating most of the mixing and, hence, the thermal striping effects in regions wehre they are isolated from critical

welds and will have a minimum affect on the structure. This mixing may, for example, be localized in a plane above the lower grid.

Instrumentation Module. This assembly is shown on Figure 3.5.2-4 and 3.5.2-5. Its primary purpose is to provide support for the bulk of the above core instrumentation, however, backup holddown and above core mixing functions are also served. Except for some peripheral locations, the instrumentation modules are fabricated from four parallel cylinders arranged in a Y configuration and connected at the lower end by ligaments. The lower 44 inches of the tubes are fabricated from 9 inch OD forgings which are welded to 5.75 inch tubes to give the required length of approximately 8 feet. The forgings are all identical. They contain the structure required at four locations to support the instrumentation and the welding stub for the connecting ligaments. Both the forging and the tubes are I-718.

The instrumentation module will require post welding heat treatment and its overall dimensions (approximately 30" x 30" x 8' long) are compatiable with this requirement. All welds are accessible for post heat treatment NDT and weld repair if required.

The modules will be supported at their upper end from the support dome. Mechanically joined extensions are required to the basic modules to obtain the necessary length. Lateral seismic and flow induced vibration support will be provided at two elevations by the baffle plate and the grid plate. The lower end of the module is located approximately an inch above the top of the core when assembled with the mixing chamber. It is sized and spaced such that it occupies the spaces in the mixing chamber grid 'diamonds'. In conjunction with the mixing chamber tubes, it forms a pattern of tubes above the core on a 10.47" pitch. This arrangement allows the holddown loads for each reactor assembly to be shared by three cylinders so that the cross section of any one cylinder need not be excessively large and makes possible the long unsupported axial lengths.

Grid Plate. The grid plate forms the upper boundary of the mixing chamber and provides the anti-vibration and seismic support for the many tubes that pass through its plane. The sodium from the mixing chamber passes through the plate via the 4.0 inch diameter holes as shown in Figure 3.5.2-6. Mechanical threaded and locked-welded fasteners are provided at each tube location to secure the tubes to the plate and form the conecting component for the tube extensions. The plate and the fasteners are all fabricated from I-718. The grid plate is connected to the outer

15 feet diameter cylinder with mechanical fasteners as discussed below.

Baffle Plate. The baffle plate is similar in construction to the grid plate except that it does not have the holes that allow sodium flow across its plane. It is located about 2 feet below the sodium free surface. The tubes that pass through the grid plate also pass through the baffle and identical mechanical connectors are used at both locations. In addition to its lateral support function, it is used to divert the sodium radially outboard to the outlet plenum. The baffle plate is fabricated from I-718.

Outer Cylinders. Two 15 feet in diameter cylinders are employed to attach the mixing chambers to the structures above. The lower cylinder is fabricated from I-718 and forms the outer boundary of the upper chamber which is the transfer region for sodium between the mixing chamber and the reactor outlet plenum. Sodium exits the upper chamber through ports in the cylinder wall. The ports will ultimately be sized and located to enhance mixing in the hot pool. The upper cylinder is potentially SS-316 as it is located in a relatively mild thermal environment. This cylinder will ultimately form the connection between the UIS and the closure plug, but the design of this interface has not yet been established. The outer cylinders are connected together with a pin and clamp arrangement as shown on Figure 3.5.2-2. The pins are installed through the clamps and the two cylinder flanges in blind holes lock welded in place. They are used to take the shear loads between cylinders. Axial loads are taken by the clamps which would be installed in sections over the cylinder flanges.

Structural Dome. This component is the structural member that takes the axial loads due to the dead weight of the UIS and the loads resulting from loss of hydraulic balance in the reactor assembly holddown system. It is located at the top of the UIS and within the cover gas region of the reactor as shown in Figure 3.5.2-1. Being located within the cover gas, it will be virtually isothermal during reactor operation and insensitive to the hot pool transients. This relatively mild thermal environment allows the dome to be fabricated from SS-316. Except for the control rod shrouds, all of the tubes passing through the UIS will terminate at the dome elevation.

Instrumentation. One instrumentation dry well, 5/8 inch OD is provided at each fuel assembly and each blanket assembly exit. These dry wells are located flush

with the bottom of the UIS and approximately 1 inch above the assembly outlet nozzle. Additionally the following devices are provided as required and discussed in Section 3.2 above:

- 16 5/8 inch dry wells for bulk temperature measurements near the UIS discharge ports.
- 16 acoustic monitors located in 5/8 inch dry wells in the lower regions of the UIS.
- 8 sodium sampling (wet wells) tubes in the lower regions of the mixing chamber.

All instrumentation dry wells and wet wells will pass through either the instrumentation module tubes or the mixing chamber tubes (exclusive of the control rod shrouds). They will exit these tubes above the support dome where they will be collected and grouped for transfer through the rotating plugs.

Fabrication. Particular attention has been directed toward designing this concept to facilitate fabrication because of the materials concerns expressed in Section 3.4 above. Basically the fabrication sequence as presently envisioned will consist of the steps listed below.

- Construct and assemble the mixing chamber module.

  --fabricate the forgings

  --weld the forgings to the lower extension tubes

  --fabricate and weld the outer cylinder

  --assemble and weld the tubes into a grid and weld the grid to the cylinder

  --heat treat this assembly

- Fabricate the instrumentation modules, the outer cylinders, the tube upper extension, the grid and baffle plates, and the support dome.
- Install the instrumentation modules in the mixing chamber.
- Install the grid plate and the mechanical connectors for the tubes.
- Install the upper tube extensions and the lower outer cylinder. Mechanically attach the outer cylinder to the mixing chamber cylinder.
- Assemble the next layer of extension tubes and outer cylinder as above.
- Install the structural dome and weld it to the outer cylinder.
- Attach to the closure assembly.

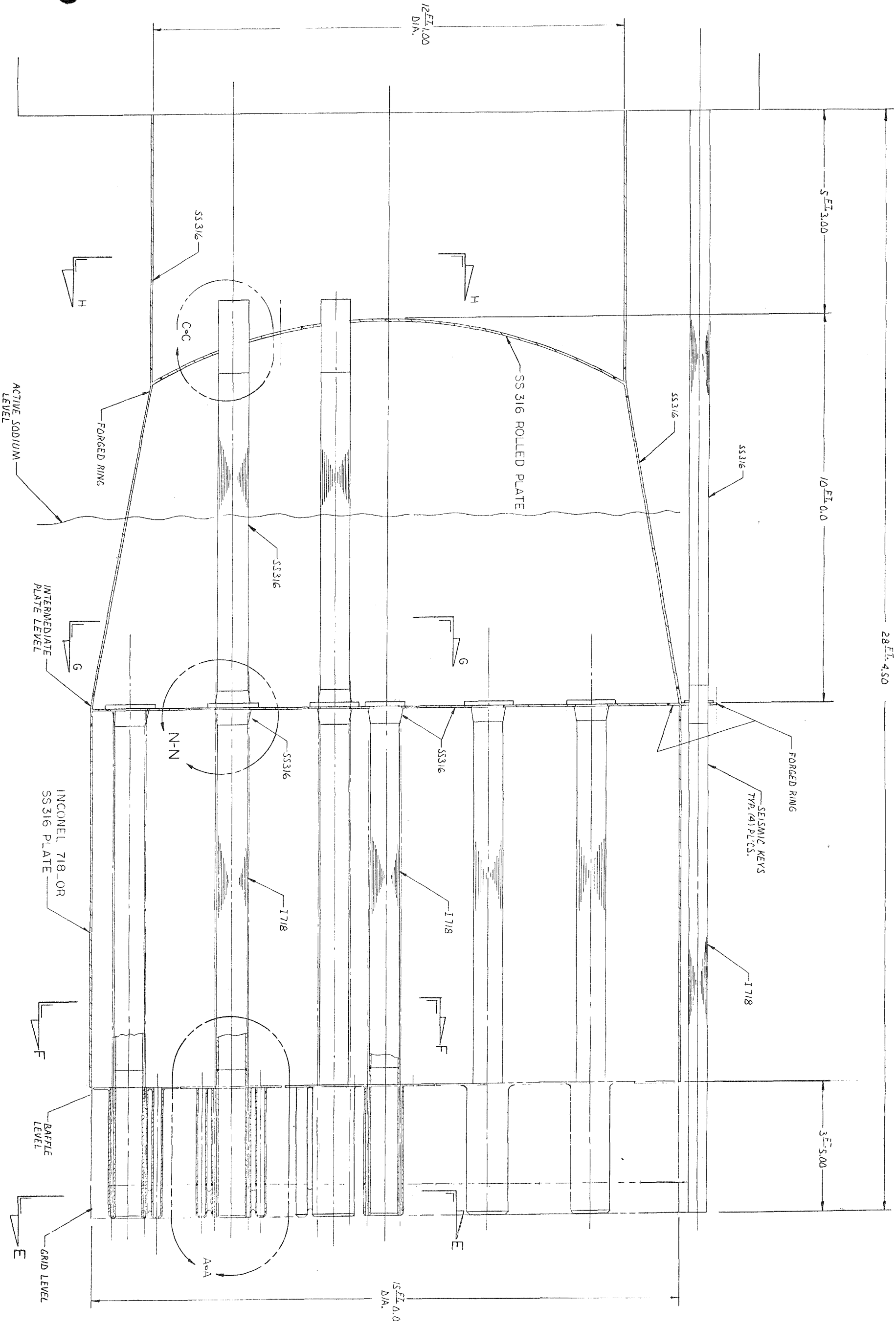

SECTION **J-J**

LOW BAFFLE SCHEME

SECTIONAL ELEVATION OF
UPPER INTERNAL STRUCTURE

Figure 3.5.1.1 Sectional Elevation Of Upper Internals Structure: Low Baffle Concept

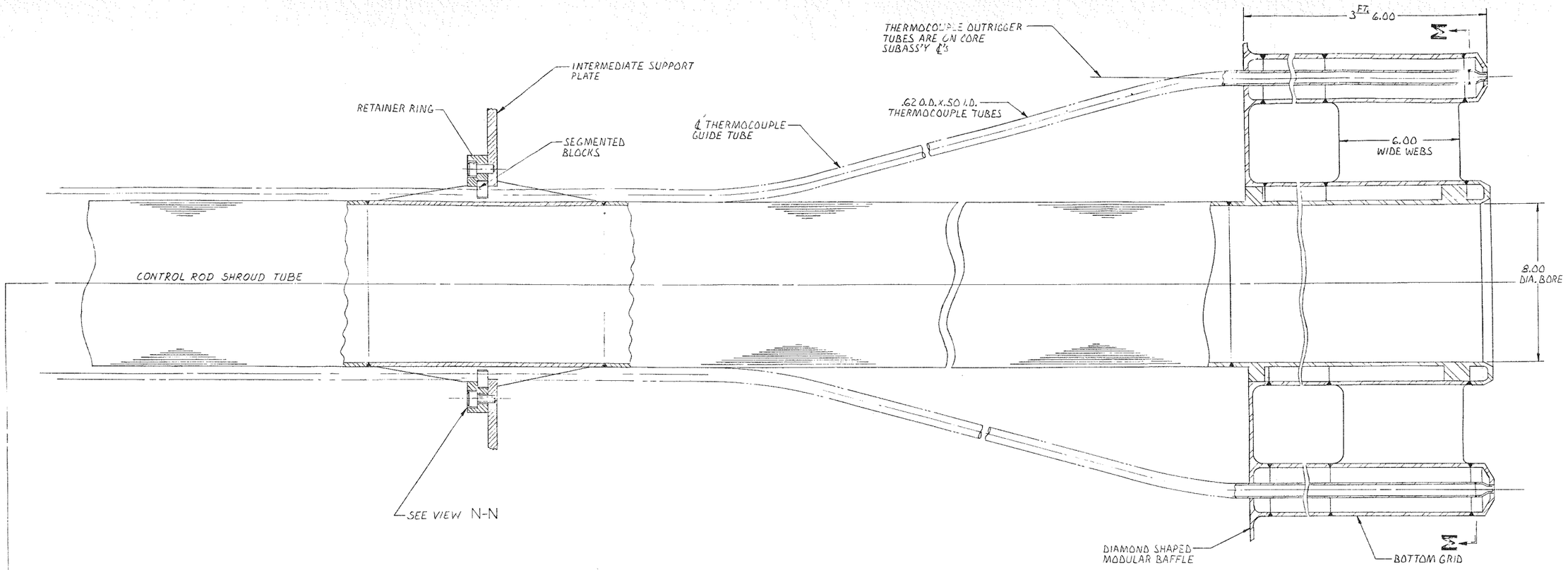

VIEW A-A

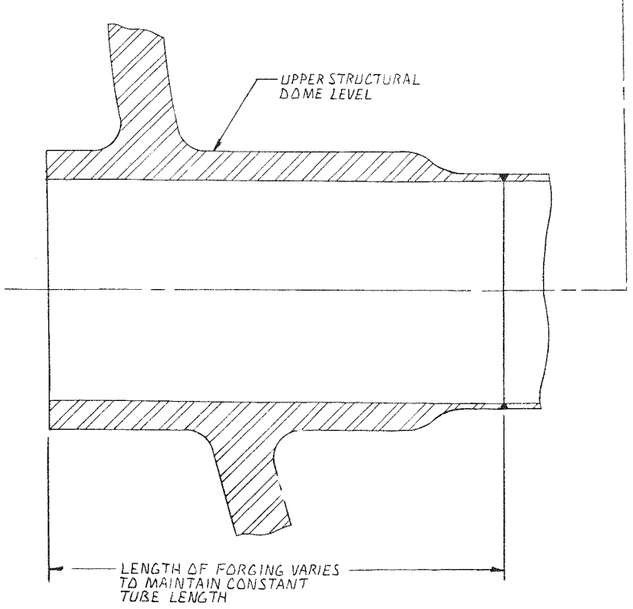

VIEW C-C

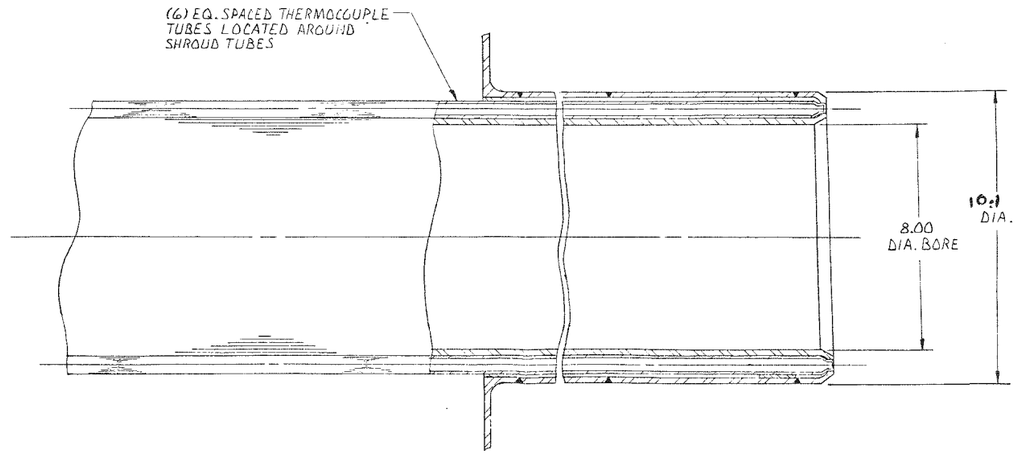

VIEW D-D

CONTROL ROD SHROUD TUBE MODULE

Figure 3.5.1.2 Control Rod Shroud Tube Module

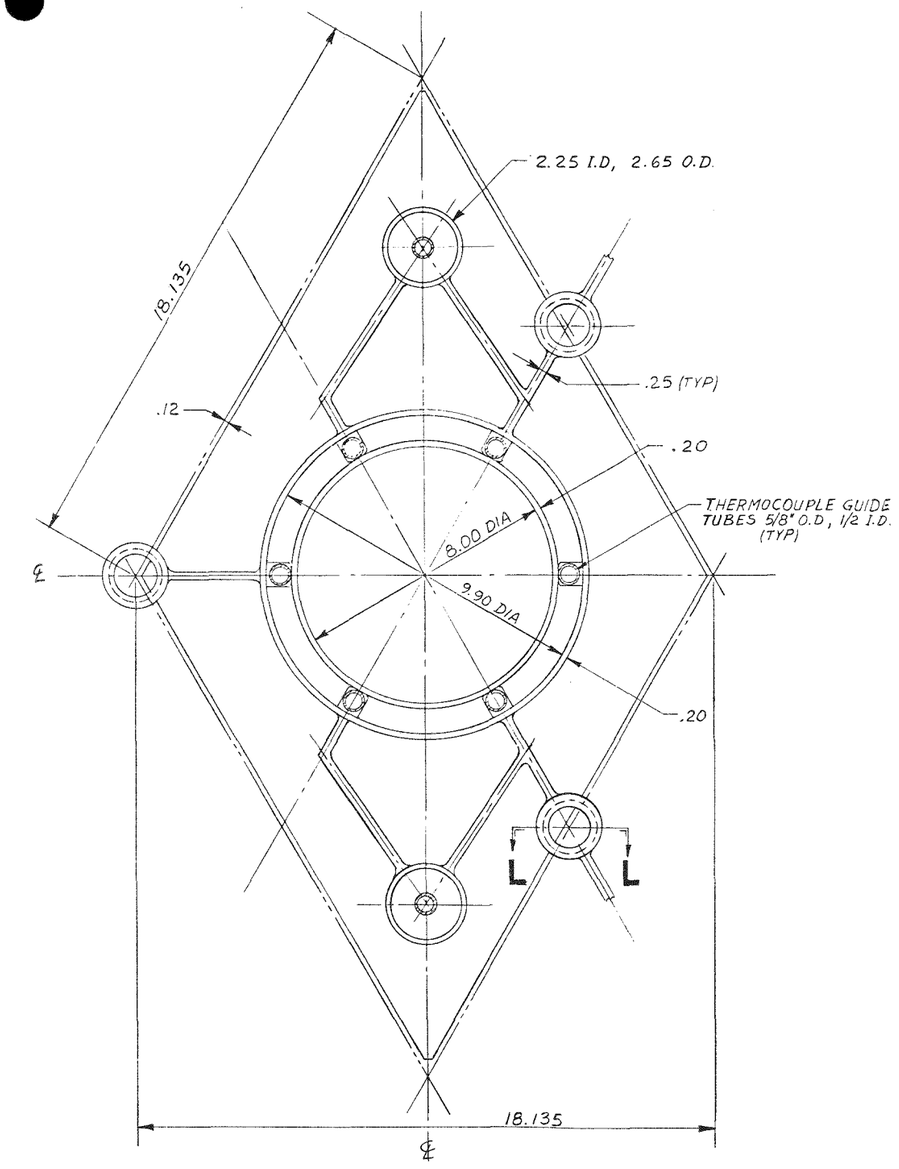

VIEW **M-M**

BAFFLE PLATE BOTTOM VIEW

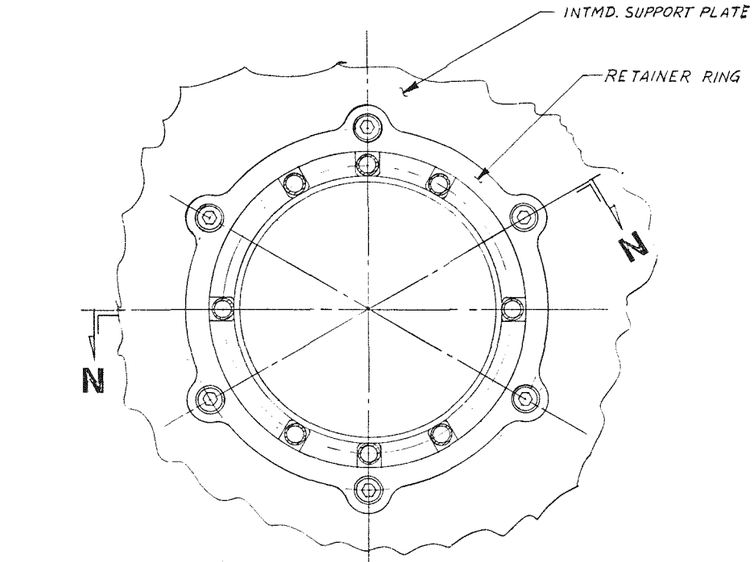

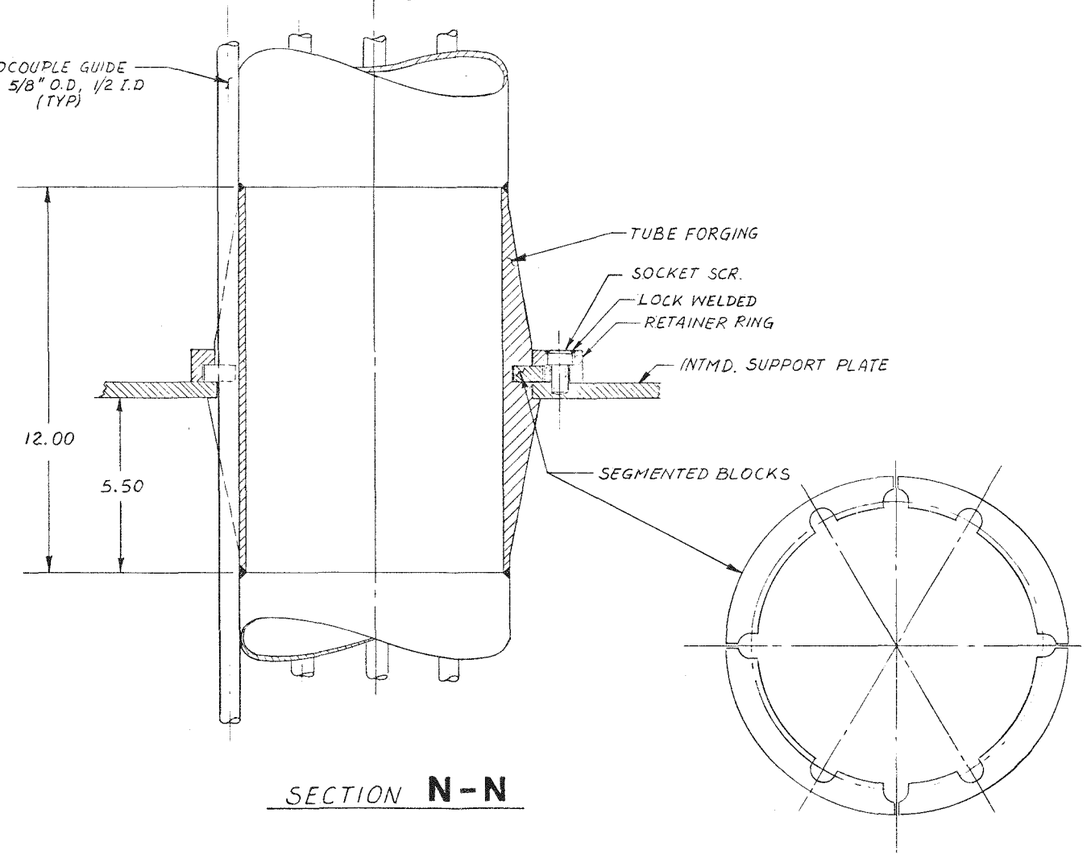

SECTION **N-N**

Figure 3.5.1.3 Control Rod Shroud Tube: Cross Sectional Views

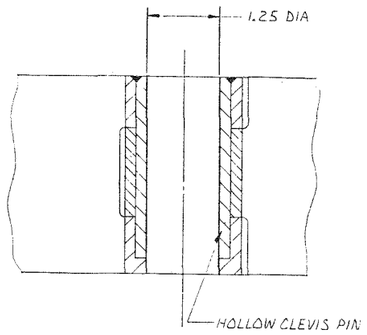

SECTION L-L

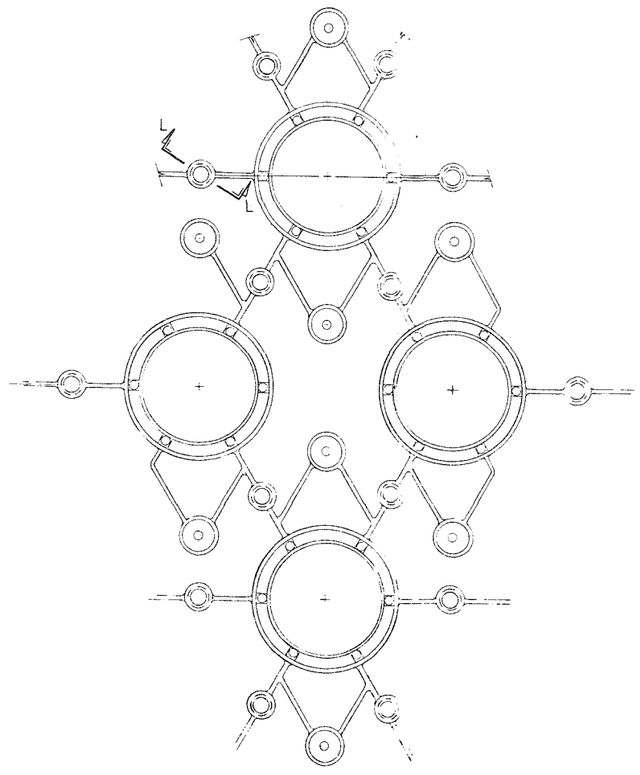

ENLARGED VIEW K-K

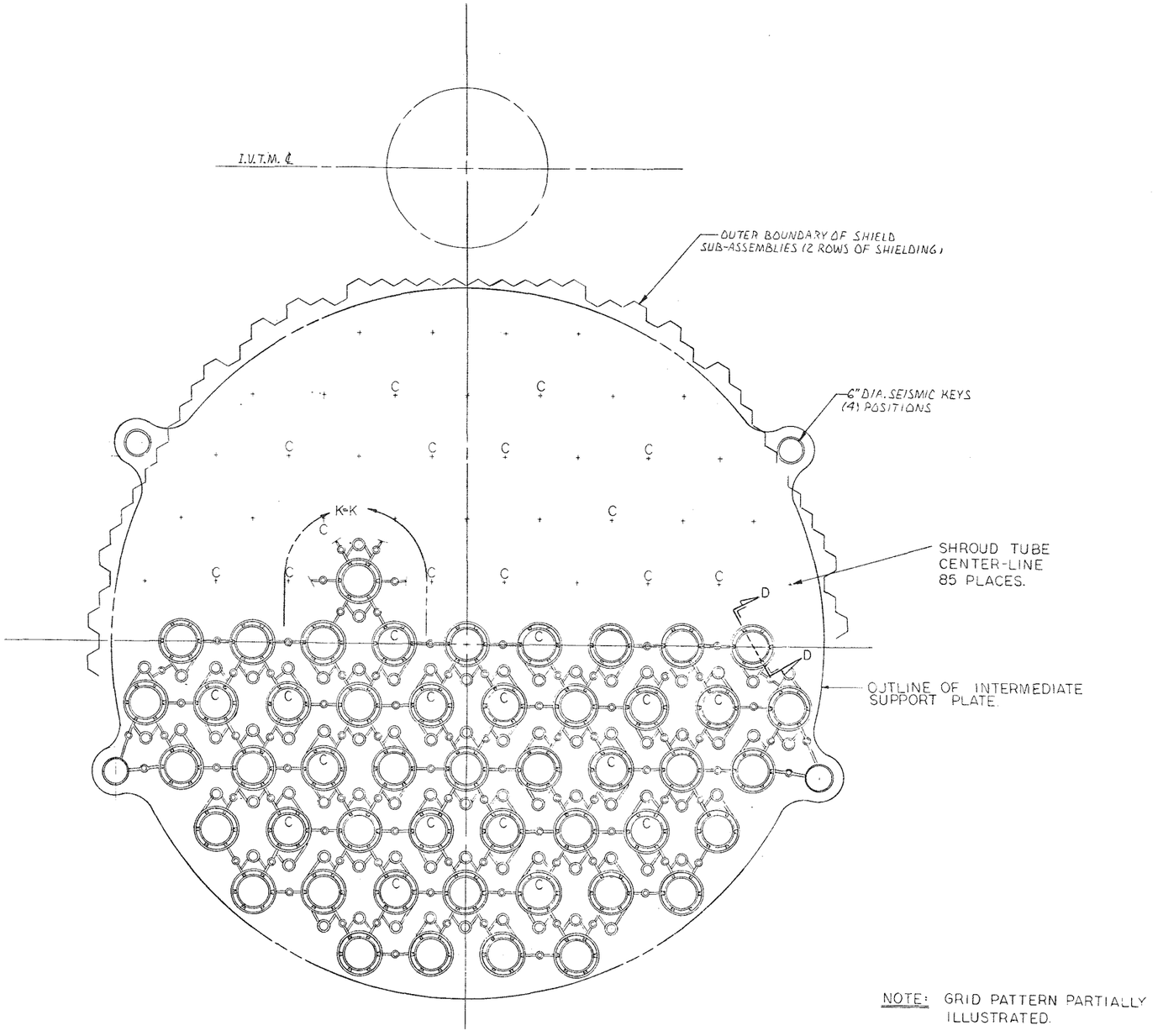

NOTE: GRID PATTERN PARTIALLY ILLUSTRATED.

SECTION E-E
PROPOSED GRID PATTERN

C=CONTROL ROD SHROUD TUBE

Figure 3.5.1.4 Plan View Of Upper Internals Structure: Location Grid

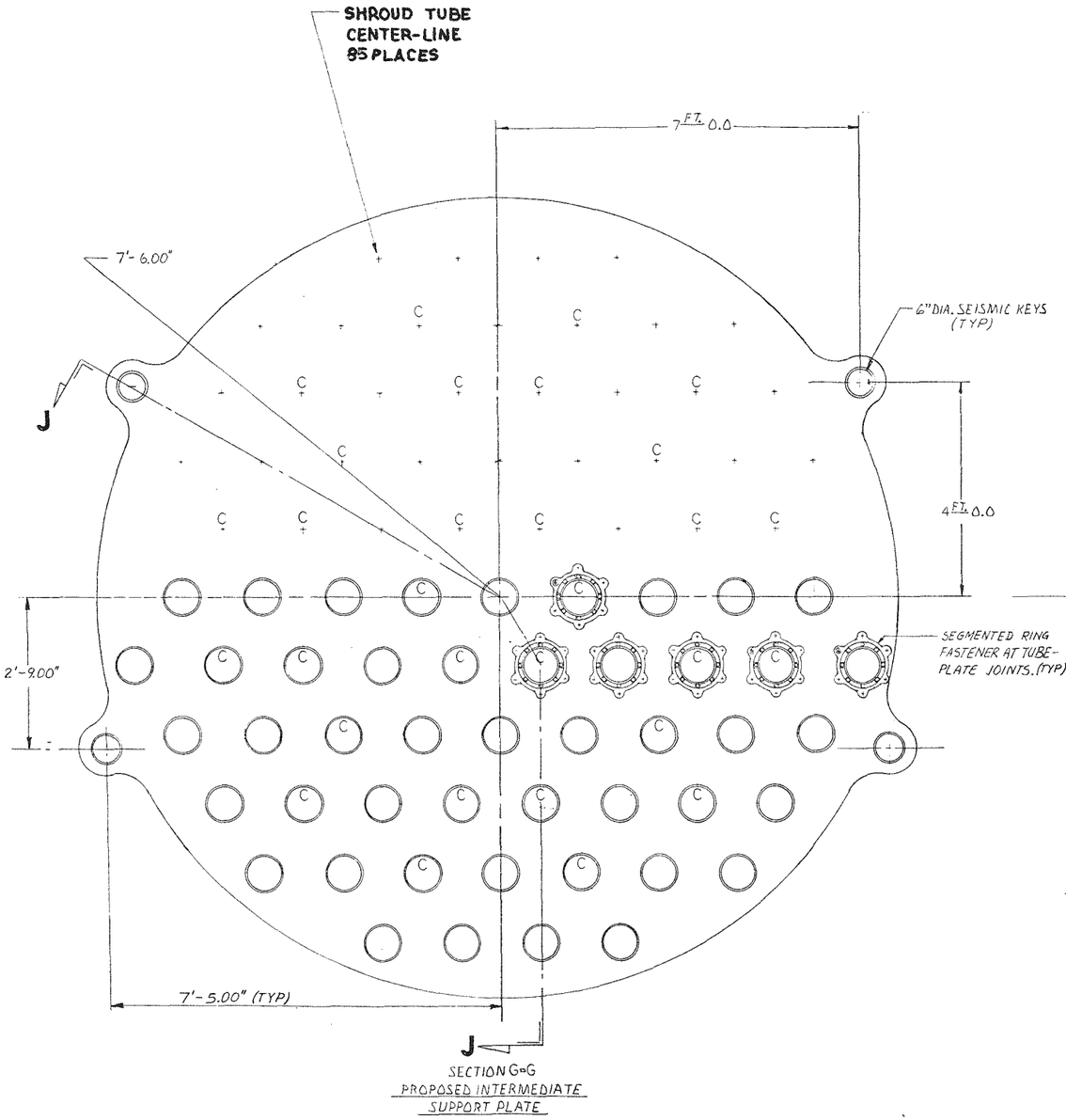

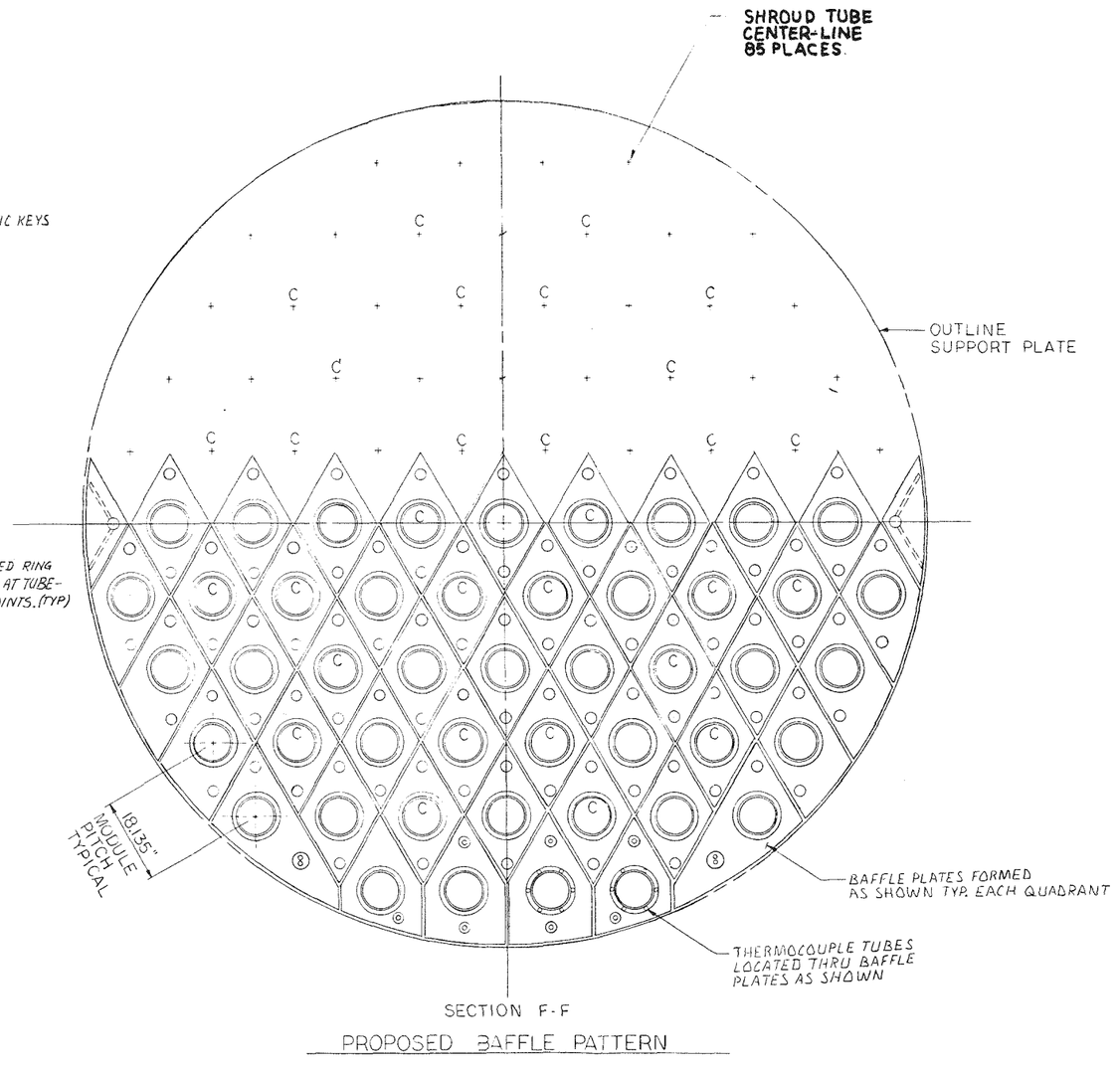

NOTE: BAFFLE PATTERN AND SUPPORT PLATE PARTIALLY ILLUSTRATE

Figure 3.5.1.5 Plan View Of Upper Internals Structure: Intermediate Support Plate And Baffle Plate Pattern

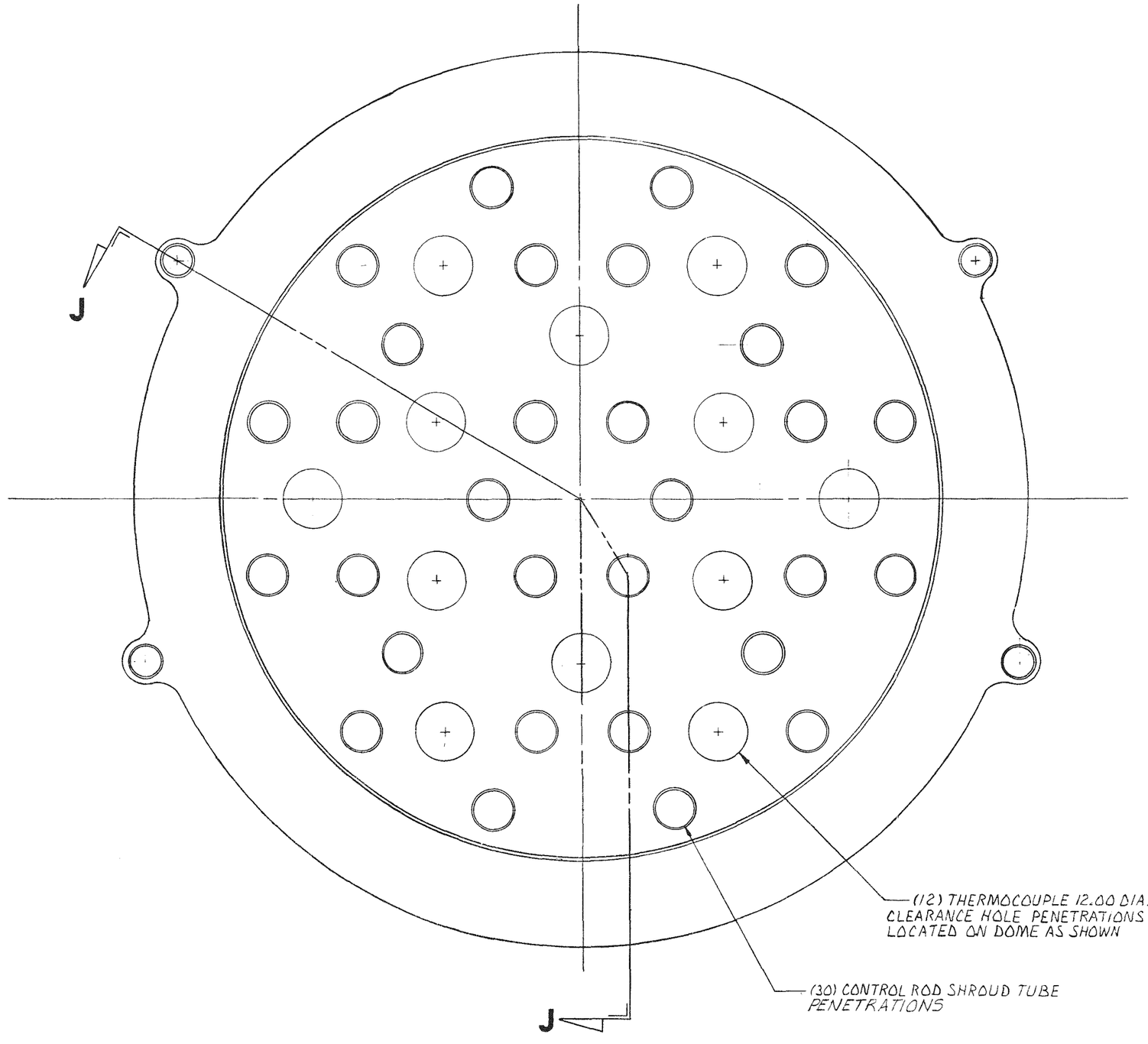

Figure 3.5.1.6 Plan View Of Upper Internal Structure: Top Support Shell

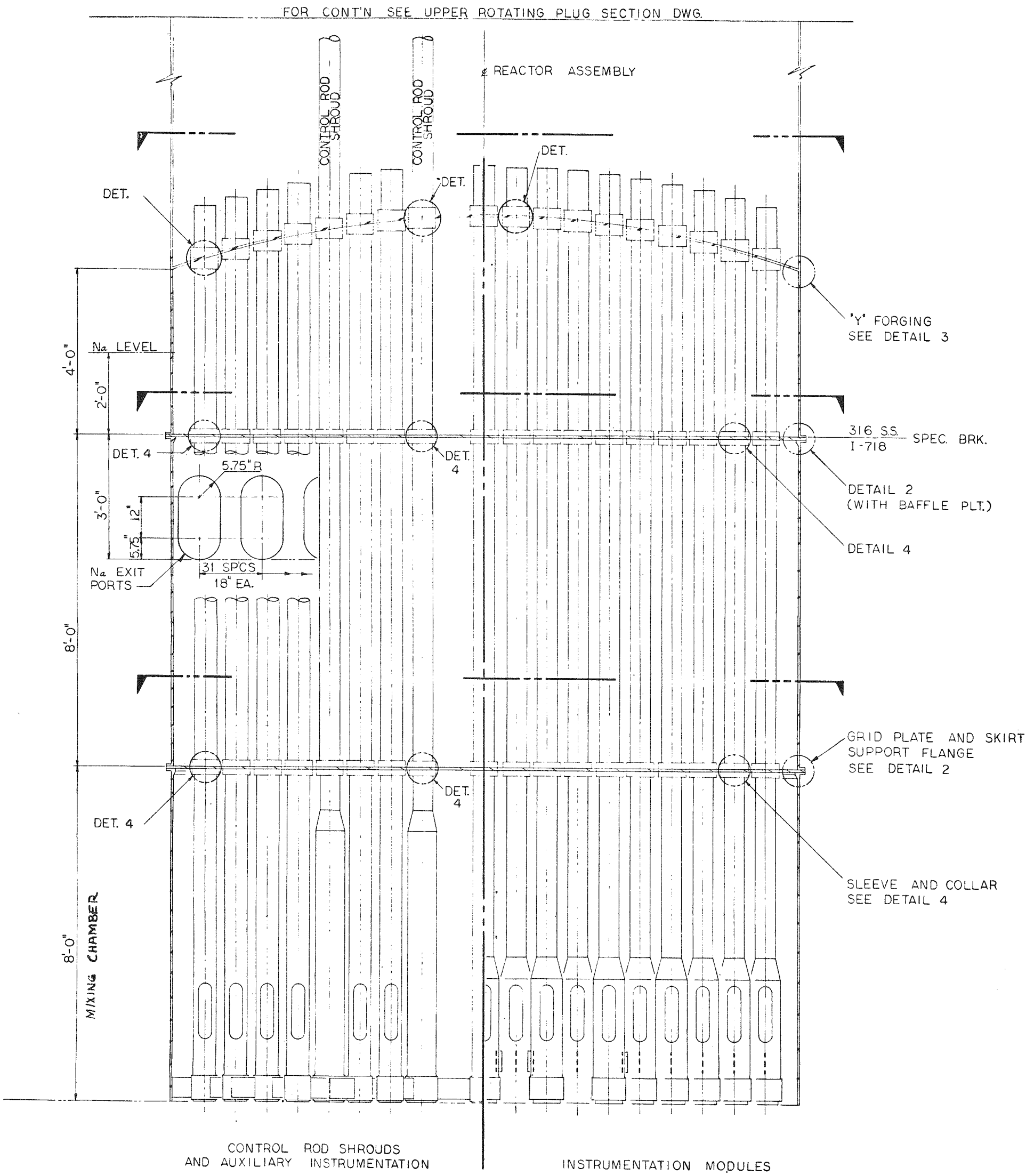

SECTION B-B

UPPER INTERNAL STRUCTURE

SCALE: 1" = 1'-0"

Figure 3.5.2-1 Upper Internals Structure Elevation, High Baffle Design

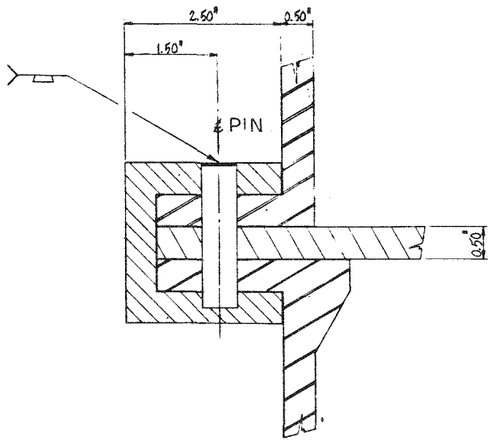

DETAIL 2

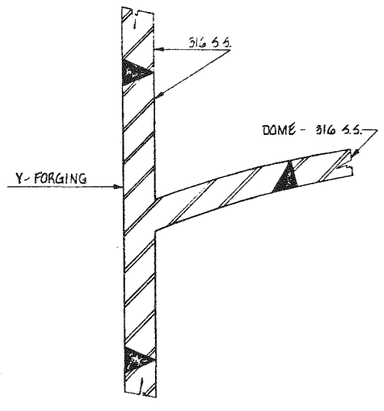

DETAIL 3

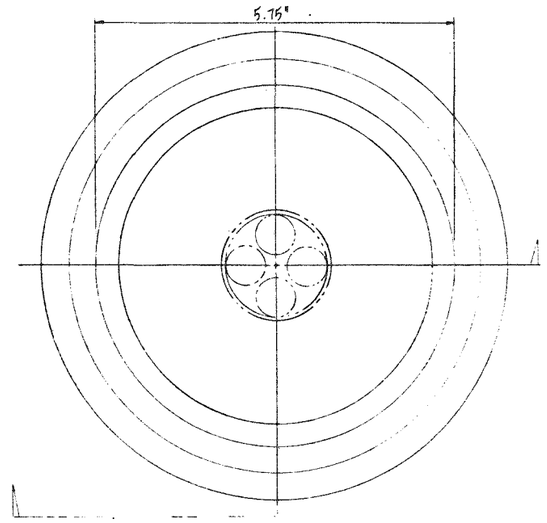

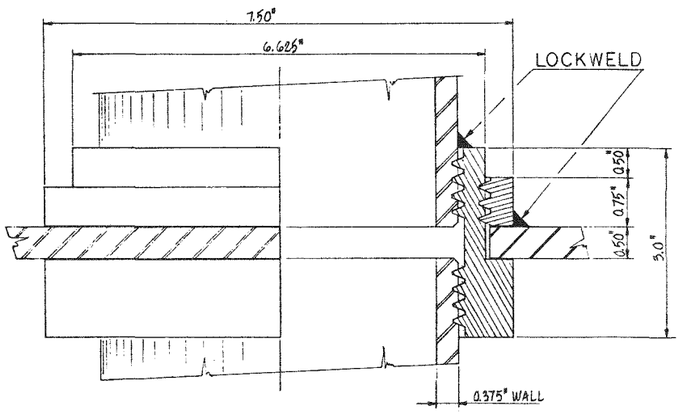

DETAIL 4
INSTRUMENT CYLINDER
SLEEVE & COLLAR ARR'GT
150 - REQ'D

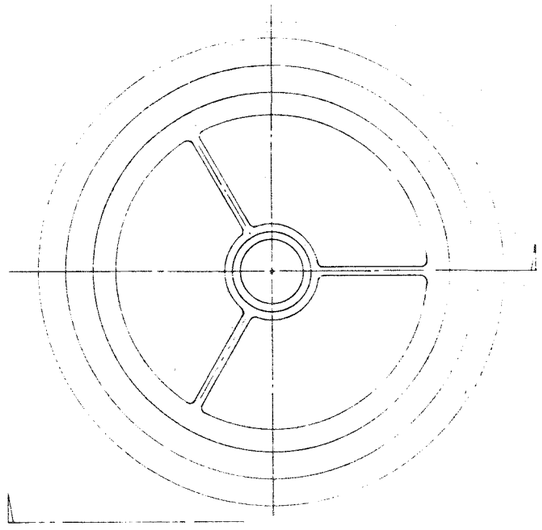

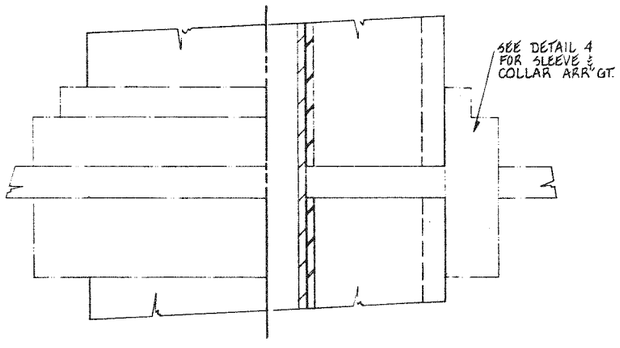

DETAIL 6
CONTROL ROD ASSEMBLY
INSTRUMENT CYLINDER

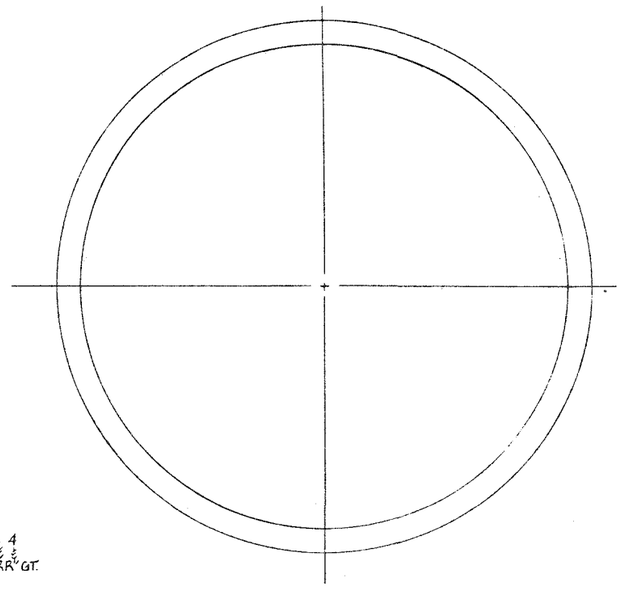

Figure 3.5.2-2 Upper Internals Structure Details, High Baffle Design

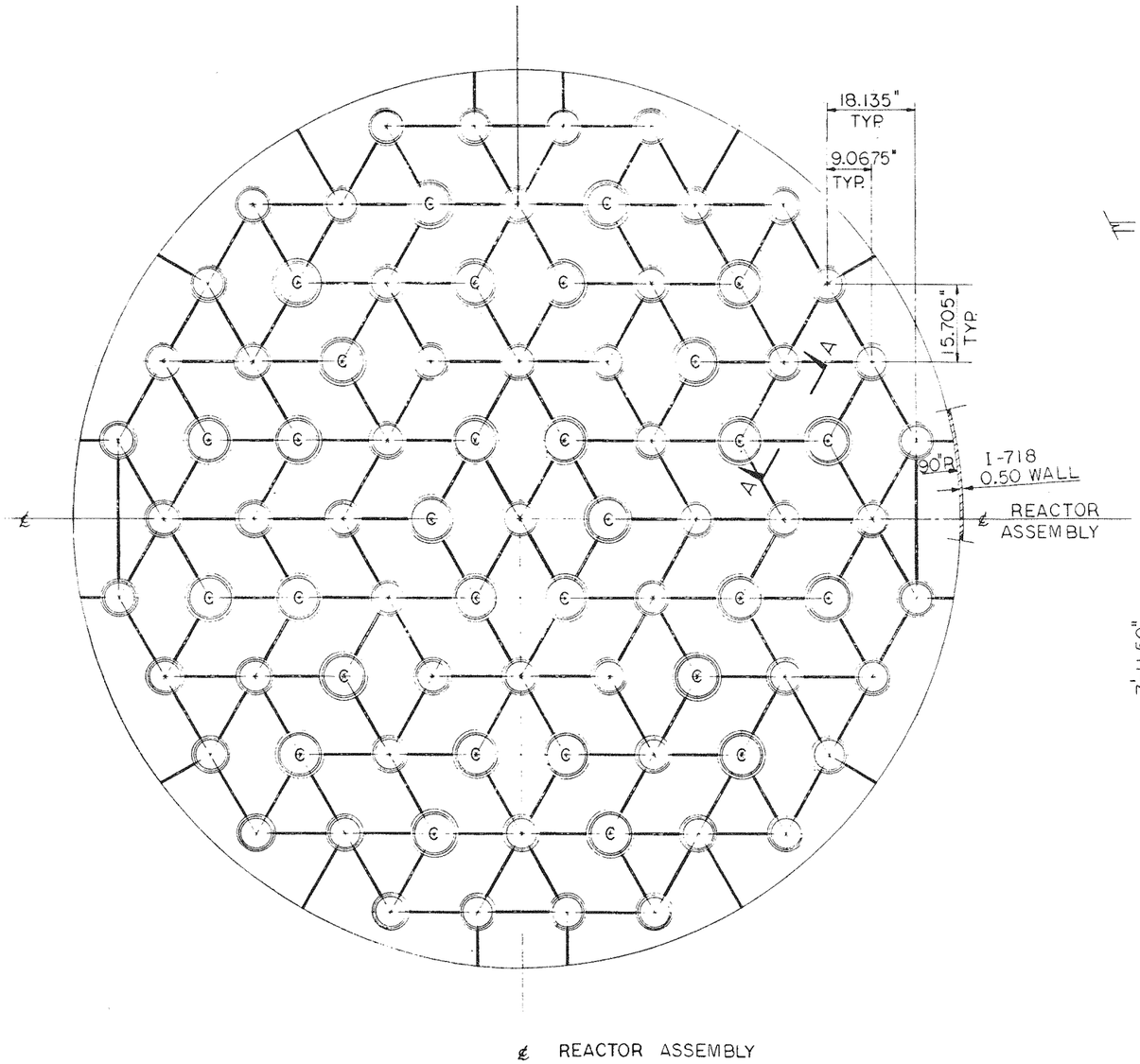

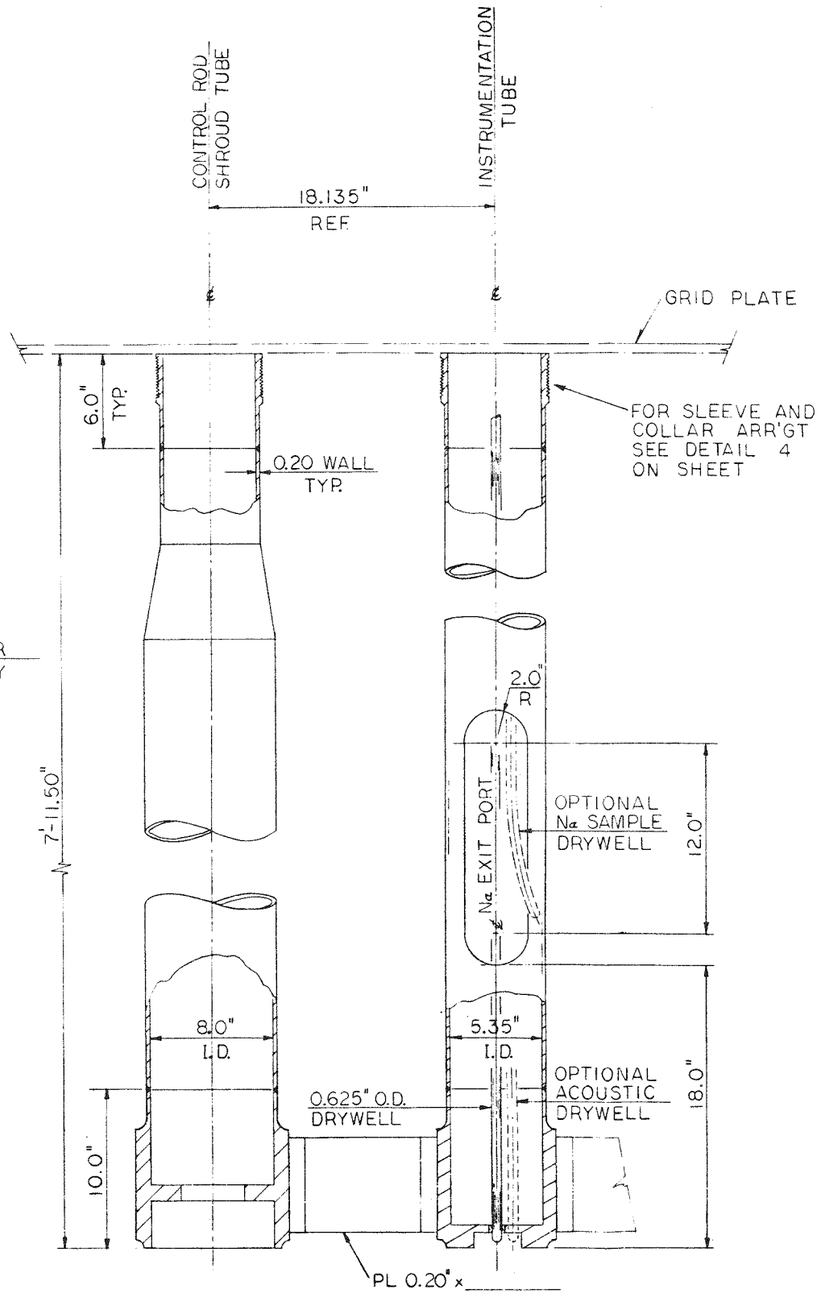

Figure 3.5.2-3 Mixing Chamber Layout, High Baffle Design

SECTION A-A
TUBE AND LIGAMENT ARR'GT
MATERIAL: INCONEL 718
SCALE: 3" = 1'-0"
NOTE: MINIMUM 1 DRYWELL REQ'D @ BOTTOM OF INSTRUMENT SHROUD TUBE. 2 REQ'D FOR ACOUSTIC MONITOR OR Na SAMPLE

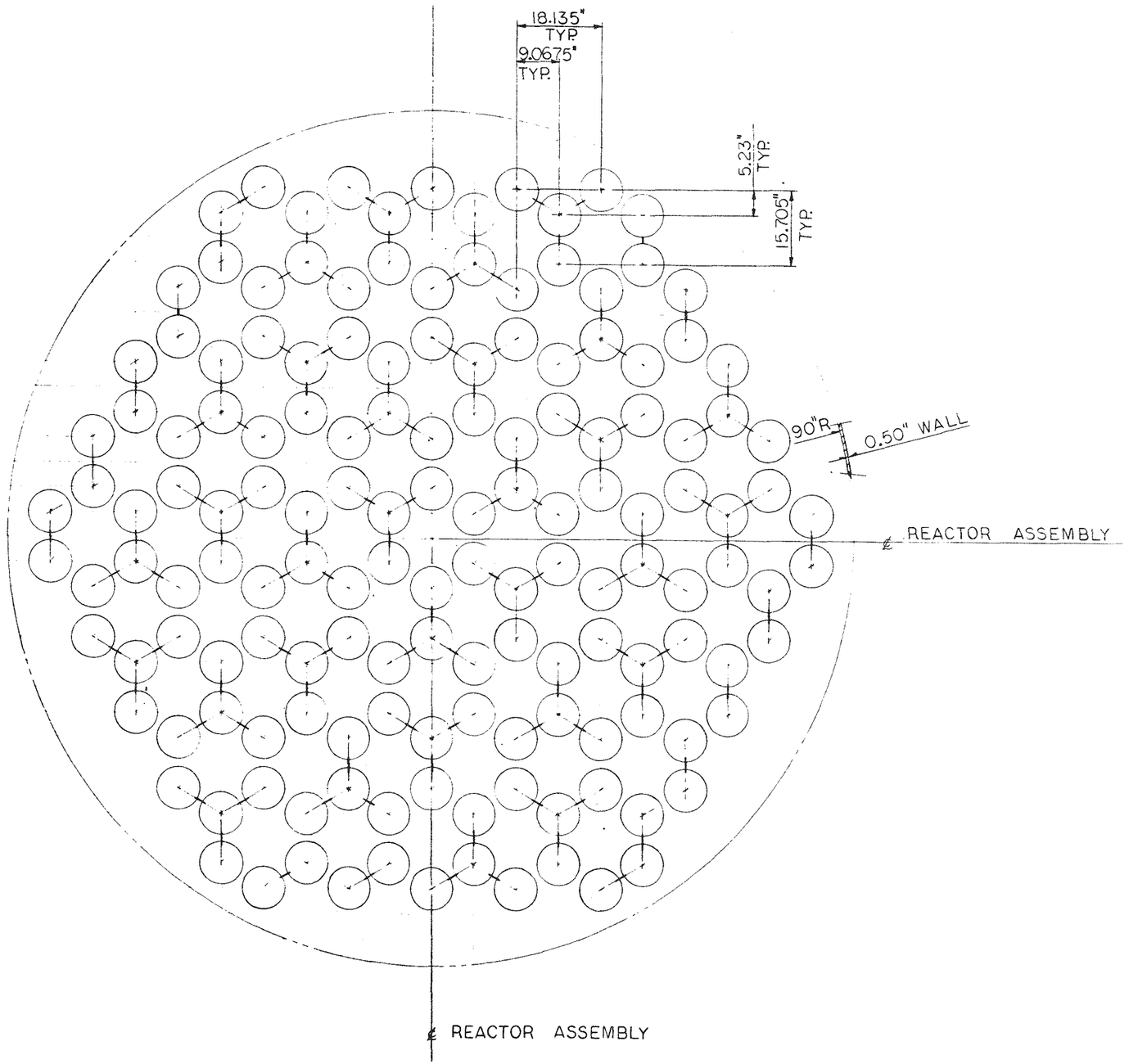

30__4-CYLINDER MODULES
2___3- " "
12___2- " "
150_CYLINDER TOTAL

Figure 3.5.2-4 Instrumentation Module Plan, High Baffle Design

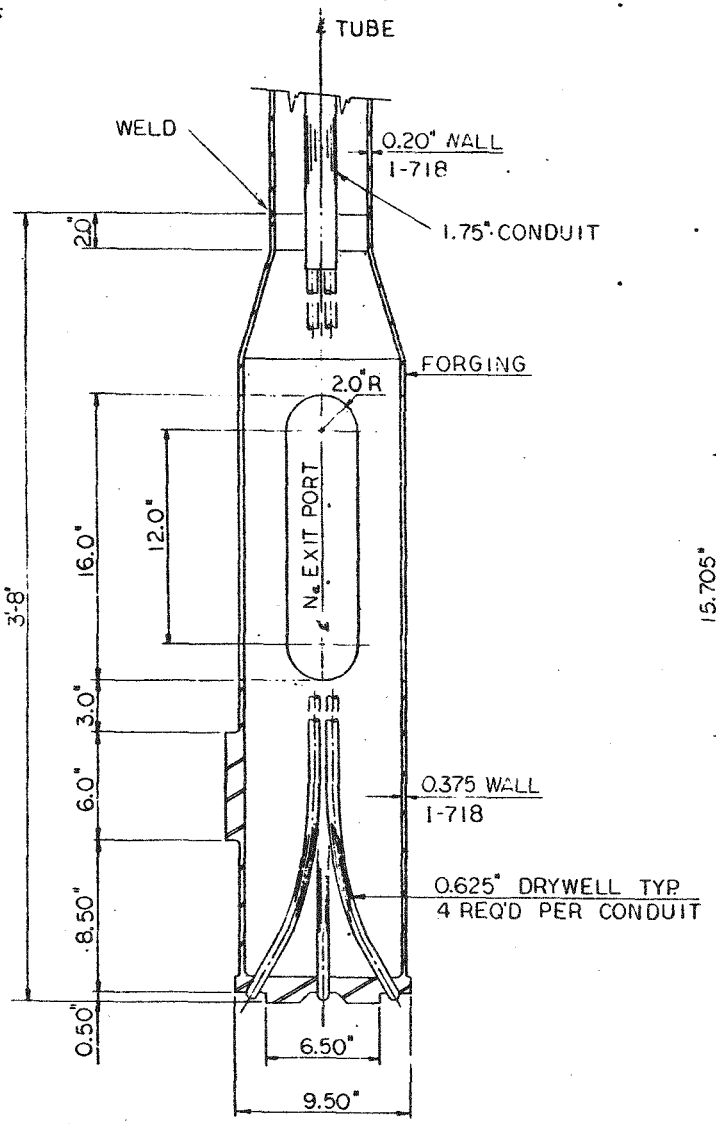

SECTION C-C
INSTRUMENTATION CYLINDER

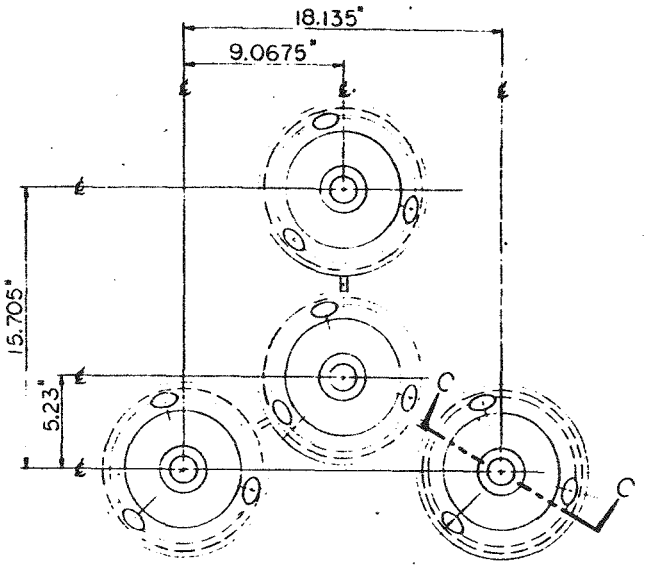

PLAN (INVERTED)
4-CYLINDER INSTRUMENT
MODULE

Figure 3.5.2-5 Instrumentation Module Detail, High Baffle Design

SECTION

GRID PLATE PENETRATION SCHEDULE

Figure 3.5.2-6 Grid Plate, High Baffle Design

REFERENCES

1. "Prototype Large Breeder Reactor, Phase II: Conceptual Design", General Electric Report GEFR-00099, June 1977.

2. Kimball, O.F., W.R. Pieren and D.I. Roberts, "Effects of Elevated Temperature Aging on the Mechanical Properties and Ductility of Ni·Cr·Mo·Cb Alloy 625, "Gulf-GA Report A12683.

3. The US estimate was based on data presented in the following reference: Jaske, C.E. and W.J. O'Donnell, "Fatigue Design Criteria for Pressure Vessel Alloys" Transactions of the ASME. Journal of the Pressure Vessel Technology, November, 1977, p. 584. These data have been used to establish the design fatigue curve for SA-637 Grade 718 Alloy, Section III, Division 1, Class 1 of the ASME B and PV Code.

PART II: REACTOR ASSEMBLY - STRUCTURES

SECTION 8: INTERNAL SHIELDING

CONTENTS

Section		Page
II-8.1	INTRODUCTION AND SUMMARY	II-8-1
II-8.2	NEUTRON SHIELD DESIGN REQUIREMENTS	II-8-3
8.2.1	Activation of IHX Steel and Secondary Sodium	II-8-3
8.2.2	Neutron Damage to Stainless Steel Structures	II-8-3
8.2.3	Helium and Tritium Gas Generation in B_4C	II-8-6
II-8.3	ANALYTICAL MODELING	II-8-7
8.3.1	Two-Dimensional R-Z Diffusion Models	II-8-7
8.3.2	One-Dimensional Radial Transport Model	II-8-12
8.3.3	Diffusion and Transport Theory Assumptions	II-8-19
II-8.4	ANALYTICAL RESULTS	II-8-21
8.4.1	Two-Dimensional Total Neutron Flux Distributions	II-8-21
8.4.2	Two-Dimensional Fast Neutron Flux Distributions ($E > 0.1$ MeV)	II-8-26
8.4.3	Two-Dimensional Neutron Flux Distributions ($0.015 < E < 0.5$ MeV)	II-8-26
8.4.4	One-Dimensional Transport Analysis	II-8-26
8.4.5	Dose Rates from Activation of IHX Steel and Secondary Sodium	II-8-38
8.4.6	Calculated Neutron Damage Response Functions for Near-Core Steel Structures	II-8-40
8.4.7	Helium and Tritium Gas Generation in B_4C Shield Assemblies	II-8-42
II-8.5	IMPACT ON REACTOR ASSEMBLY DESIGN	II-8-47
8.5.1	Fuel and Blanket Assemblies	II-8-47
8.5.2	Removable Radial Shield Assemblies	II-8-47
8.5.3	Inlet Pipe Region	II-8-48
8.5.4	Component Shielding	II-8-48
8.5.5	Shielding Design Flexibility	II-8-48
II-8.6	CONCLUSIONS AND RECOMMENDATIONS	II-8-53
	REFERENCES	II-8-59

FIGURES

		Page
3-1	GE-ARSD Pool Reactor Geometry	II-8-8
3-2	EPRI 1000 MWe Heterogeneous, "Bullseye" Core for Pool Reactor Design	II-8-9
3-3	GE-ARSD 1200 MWe Heterogeneous LMFBR Core Layout	II-8-10
3-4	Region and Material Map for Pool Reactor Design Near-Core Upper Axial R-Z Model	II-8-13
3-5	Region and Material Map for Pool Reactor Design Near-Core Lower Axial R-Z Model (Two Rows of B_4C Radial Shield Assemblies)	II-8-15
3-6	Region Geometry and Compositions for Pool Reactor Design Radial 1-D Model with 2 Rows of B_4C Shield Assemblies	II-8-18
4-1	Total Neutron Flux Distribution in Near-Core Upper Axial Region (One Row of B_4C Radial Shield Assemblies)	II-8-22
4-2	Total Neutron Flux Distribution in Near-Core Upper Axial Region (Two Rows of B_4C Radial Shield Assemblies)	II-8-23
4-3	Total Neutron Flux Distribution in Near-Core Lower Axial Region (One Row of B_4C Radial Shield Assemblies)	II-8-24
4-4	Total Neutron Flux Distribution in Near-Core Lower Axial Region (Two Rows of B_4C Radial Shield Assemblies)	II-8-25
4-5	Fast Neutron Flux Distribution ($E > 0.1$ MeV) in Near-Core Upper Axial Region (One Row of B_4C Radial Shield Assemblies)	II-8-27
4-6	Fast Neutron Flux Distribution ($E > 0.1$ MeV) in Near-Core Upper Axial Region (Two Rows of B_4C Radial Shield Assemblies)	II-8-28
4-7	Fast Neutron Flux Distribution ($E > 0.1$ MeV) in Near-Core Lower Axial Region (One Row of B_4C Radial Shield Assemblies)	II-8-29
4-8	Fast Neutron Flux Distribution ($E > 0.1$ MeV) in Near-Core Lower Axial Region (Two Rows of B_4C Radial Shield Assemblies)	II-8-30
4-9	Neutron Flux Distribution ($0.015 < E < 0.5$ MeV) in Near-Core Upper Axial Region (One Row of B_4C Radial Shield Assemblies	II-8-31
4-10	Neutron Flux Distribution ($0.015 < E < 0.5$ MeV) in Near-Core Upper Axial Region (Two Rows of B_4C Radial Shield Assemblies	II-8-32

FIGURES (Cont'd)

		Page
4-11	Neutron Flux Distribution ($0.015 < E < 0.5$ MeV) in Near-Core Lower Axial Region (One Row of B_4C Radial Shield Assemblies)	II-8-33
4-12	Neutron Flux Distribution ($0.015 < E < 0.5$ MeV) in Near-Core Lower Axial Region (Two Rows of B_4C Radial Shield Assemblies)	II-8-34
4-13	One-Dimensional Group-Dependent Neutron Fluxes for GE Pool Reactor, Core Center-to-IHX (Groups 1 to 5)	II-8-35
4-14	One-Dimensional Group-Dependent Neutron Fluxes for GE Pool Reactor, Core Center-to-IHX (Groups 6 to 9)	II-8-36
4-15	Selected Response Functions for Radial 1-D Core-to-IHX Calculation (Two Rows of B_4C Assemblies)	II-8-37
4-16	Variation of the Displacement Cross Section for Stainless Steel with Neutron Mean Energy in the FTR	II-8-44
4-17		
4-18		

TABLES

		Page
3-1	End-of-Equilibrium Cycle Regional Atom Densities for GE-ARSD 1200 MWe Heterogeneous Core	II-8-11
3-2	Region Volume Fractions for Pool Reactor Design Near-Core Upper Axial R-Z Model	II-8-14
3-3	Region Volume Fractions for Pool Reactor Design Near-Core Lower Axial R-Z Model	II-8-16
3-4	Shield Material and Sodium Atom Densities	II-8-17
3-5	Energy Group Structure for 9-Group Neutron Cross Section Library	II-8-20
4-1	Neutron Spectra and dpa Values for Selected Locations in Steel Structure of Pool R-Z Diffusion Model	II-8-43

II-8.1

INTRODUCTION AND SUMMARY

A study was performed during the Phase A Extension program to determine the amount and spatial distribution of the near-core neutron shield needed to protect the IHX's and pumps in the GE-ARSD 1000 MWe pool type reactor design. The results of the study indicate that it is possible to design an adequate shield without resorting to the introduction of massive amounts of steel radial shielding in the sodium pool region outside the working perimeter of the core assembly handling equipment. This conclusion is of primary importance since it means that adequate shielding can be provided without a major impact on the size or arrangement of the reactor assembly.

To make an adequate assessment of the shield it was necessary to evaluate 1) activation of the steel and secondary sodium in the IHX's and pumps, 2) neutron damage to stainless steel structures, and 3) helium and tritium gas generation in B_4C shield assemblies. Two-dimensional diffusion and one-dimensional transport calculations were performed and isoflux contours were plotted. The neutron shield design requirements are discussed in Section 2 and the analytical modeling and calculational results are presented respectively in Sections 3 and 4.

One of the 1000 MWe pool type LMFBR plant design criteria is to limit secondary sodium activation such that shielding of the secondary system (pipes, pumps, steam generators, etc.) is not required. Another plant design criterion places a limit on activation of the materials (steel in particular) in a primary coolant system pump or IHX. Limits of this type are needed in order to facilitate hands-on maintenance or repair to these components. The reactor core neutron shield must therefore be designed such that it provides the necessary neutron flux attenuation required to meet these limits.

However, in addition to providing protection for the IHX's and primary pumps, the reactor core neutron shield must 1) provide neutron attenuation to prevent excessive radiation damage to near-core steel structures, 2) serve

as a biological shield for regions in the vicinity of the deck, and 3) have the capability of requiring little or no maintenance for the life of the reactor. Also, it should be reasonably compact so as not to interfere with the functions of other reactor components and to offer optimum shielding capability without adding excessive weight to the system.

The GE-ARSD recommended pool reactor radial neutron shield consists of two rows of steel shield assemblies inside the core barrel and three rows of steel plus two rows of B_4C shield assemblies outside the core barrel. The B_4C assemblies are needed (instead of steel) in order to obtain the desired radial compactness for the required neutron attenuation. The diameter of the outermost ring of shield assemblies is fixed according to the outer working perimeter of the core assembly handling equipment. In addition to the radial shielding, axial shielding is provided by steel sections in both the upper and lower regions of the fuel, inner blanket, and radial blanket assemblies. Also, shielding equivalent to a two-inch thick steel or B_4C annular shell is recommended for each IHX and primary pump. This memorandum describes the results of preliminary analyses performed to evaluate the effectiveness of this neutron shielding design. Section II-8.5 describes the measures necessary to provide the shielding and assesses the impact on the reactor assembly design.

NEUTRON SHIELD DESIGN REQUIREMENTS

8.2.1 ACTIVATION OF IHX STEEL AND SECONDARY SODIUM

One of the plant design criteria is to limit secondary sodium activation to a level sufficiently low such that shielding of the secondary system (pipes, pumps, steam generators, etc.) is not required. A reasonable limit would result in a dose rate in the range 1 - 10 mR/hr, say 2 mR/hr, at a point 3 feet from the surface of a large undrained secondary sodium pipe.

Another plant design criterion places a limit on activation of the steel structure in a primary coolant system pump or IHX. Such a limit is needed in order to establish the conditions for hands-on maintenance or repair of these components. A dose rate value of 20 mR/hr at a point 3 feet from the drained component surface has been suggested as a practicable limit. Previous ARSD Phase A studies have indicated that deposit of fission products and radio-corrosion products may result in radiation levels conservatively estimated to be on the order of 1 R/hr from each of these sources (1). However, due to the approximate nature of these studies, it is possible that these sources could be overestimated by as much as a factor of 100. Furthermore, since washing or solution cleaning may remove most or all of these deposits prior to "hands-on" maintenance (2), it may be reasonable to retain the 20 mR/hr activation dose rate limit for the drained and washed primary pumps and IHX's.

8.2.2 NEUTRON DAMAGE TO STAINLESS STEEL STRUCTURES

In addition to the dose rate criteria discussed above, one must consider neutron-induced structural damage criteria for near-core steel shielding and structural components (3). The ASME Boiler and Pressure Vessel Code is generally adopted as the basis for the design criterion for permanent structures subject to potentially significant neutron exposure. However, the ASME Code acknowledges the need to account for environmental effects such as irradiation but does not give specific guidance for considering radiation damage effects

in the design. The most common approach is to restrict the neutron exposure to low enough levels such that radiation effects can be ignored. Then the design is simply based on the mechanical behavior of unirradiated material. The restriction on neutron exposure level is termed a fluence limit. A second alternative is to allow higher exposure levels which produce damage, and then modify the mechanical properties required in implementing the design criteria to assure that the radiation damage can be tolerated.

Although temporary structures within the core such as the fuel pin cladding can have a maximum temperature of 653°C (1207°F), permanent structures located at elevations below the reactor core generally operate at relatively low temperatures (∿300°C). Only those permanent structures located well above the core, where hot sodium exits from fuel assemblies, operate at substantially higher temperatures (∿500°C). The materials in these structures are primarily 304 SS and 316 SS and their welds and Alloy 718. Alloy 600 is used in non-load bearing applications as a shielding or reflector material. The low operating temperatures for many of the permanent structures reduce the tendency for significant creep effects in the materials of construction. In the region above the core where temperatures can be higher, the neutron exposure levels tend to be quite low so irradiated effects on creep are small.

The definition of a single fluence limit which restricts irradiation damage has, to date, been based on residual total elongation (RTE) as measured in a post-irradiation tension test. Both the Fast Flux Test Facility (FFTF) and the Clinch River Breeder Reactor (CRBR) projects adopted a fluence limit based on 10% RTE at end-of-life. This arbitrary fluence limit was originally proposed as a compromise between a more restrictive limit which would require large amounts of shielding and more liberal limits which might not restrict all mechanical property changes to fall within acceptable safety margins (4). The specified ductility level is generally considered to be acceptable for assuring a ductile material in the sense implied by the ASME B&PV Code, and at the same time, the limit on ductility seems to place all other deteriorations in mechanical properties within the overall safety envelope.

When service neutron exposures do not exceed the fluence limit, irradiation damage can be neglected in the design of the component or system. Hence,

the only irradiation effects information needed is the ductility data required for evaluation of fluence limits. Fluence limits for FFTF and CRBR have been evaluated based on total fluence, an exposure parameter which is independent of neutron energy spectrum. This procedure is generally considered to yield conservative fluence limits when evaluation is based on data from relatively hard spectra EBR II irradiations. Reference 4 provides an example of experimental ductility data for 304 SS and gives a minimum ductility trend curve used to define CRBR spectrum-insensitive fluence limits at 371°C. The minimum ductility trend line (which is defined to fall below essentially all the data) reaches 10% RTE at a fluence of 0.9×10^{22} n/cm^2, which becomes the fluence limit. Data of this sort were used to establish CRBR fluence limits for 304 SS and 316 SS at temperatures from 370 to 650°C (5).

Correlation of the ductility data using total displacements as a spectrum-sensitive exposure parameter leads to minimum ductility trend curves, and hence fluence limits, which depend on the neutron energy spectrum. Softer spectra have higher fluence limits. The spectrum-dependent fluence limits are 1.7×10^{22} and 2.7×10^{22} n/cm^2, respectively, for the CRBR fixed radial shield and core former support ring. These limits are a factor of 2 to 3 higher than the value obtained from the spectrum-independent total fluence model. Such increases in fluence limits can have important design implications, but more experimental data are needed to demonstrate the consistency and conservatism of spectrum-sensitive fluence limits.

Another possible approach to limiting damage is to set fluence limits at the threshold for detectable irradiation-induced change in each of the several different properties which are important in design (6). The threshold fluence limit values serve the same function as the 10% RTE fluence limit values, but should be more conservative. Design for exposures beyond the fluence limits (either threshold or 10% RTE) must account for the changes in properties which accompany irradiation damage.

The damage fluence criteria for the 1000 MWe pool type LMFBR have not yet been selected but current thinking is along the lines of maintaining the ductility of structure, such as upper internals and core barrel, above 10%.

8.2.3

HELIUM AND TRITIUM GAS GENERATION IN B_4C

An additional design criterion which must be considered concerns the problem of accommodating the helium and tritium generated in the B_4C radial shield due to the B-10 (n,α) and B-10 (n,2α) reactions:

$$_5B^{10} + {}_0n^1 \rightarrow {}_3Li^7 + {}_2He^4$$

$$_5B^{10} + {}_0n^1 \rightarrow {}_1H^3 + 2\,({}_2He^4) \quad .$$

The primary pressure buildup is due to helium since the helium production cross section is several orders of magnitude greater than that for tritium production.

The helium generation rate for a CRBR B_4C control assembly located near the center of the core has been calculated to be approximately $1.65 \times 10^{22} \frac{\text{atoms (He)}}{\text{cm}^3\ (B_4C)}$ for 328 full power days of operation. Since change-out of these assemblies does not occur until the end of such a time period, it can be postulated that this same limit could be used to determine the feasibility of using radial B_4C shield assemblies in the pool design. In the case of the shield assemblies, $1.65 \times 10^{22} \frac{\text{atoms (He)}}{\text{cm}^3\ (B_4C)}$ would be taken as the cumulative release over the 40-year life of the plant at a load factor of ≥ 0.8.

II-8.3

ANALYTICAL MODELING

8.3.1
TWO-DIMENSIONAL R-Z DIFFUSION MODELS

The primary objective of this analysis is to determine the amount and spatial distribution of the near-core neutron shielding needed to limit activation of secondary sodium and steel in the IHX's (or pumps) to acceptable levels. An accurate treatment of this shielding problem requires a full reactor geometry transport solution which is not justified at this preliminary stage of the reactor design. Rather, an approximate approach was adopted which utilizes near-core two-dimensional diffusion calculations and radial core-to-IHX one-dimensional transport calculations to gain at least some insight into potential streaming problems and to conservatively estimate the shielding needs. It should be emphasized, however, that some two-dimensional transport analysis will definitely be needed in the next work phase.

Figure 3-1 shows the entire pool reactor geometry including the location of an IHX and primary pump. The near-core upper axial and lower axial regions chosen for the two-dimensional R-Z calculations are indicated by the areas outlined by the dashed lines in the figure. The radial one-dimensional transport calculations correspond to a traverse from the center of the core outward through the center of an IHX to a point approximately 50 cm radially beyond the IHX outer wall; i.e., to R = 1038 cm.

The two-dimensional R-Z models would ideally have included the EPRI 1000 MWe heterogeneous "bullseye" core pattern shown in Figure 3-2. However, because of time constraints, it was necessary to approximate this core by using a similar core model which was already available and for which a few-group neutron cross section library had been prepared for previous ARSD studies (7,8). Therefore, an R-Z version of a GE-ARSD 1200 MWe heterogeneous core was used. The core map and compositions shown in Figure 3-3 and Table 3-1 were used and the reactor power was normalized in 2-D fixed-source calculations to the design value of 2888 MW_t. The use of this alternate core model is

FIGURE 3-1 GE-ARSD POOL TYPE REACTOR GEOMETRY*

*Dashed lines indicate regions of 2-D, R-Z diffusion calculations.

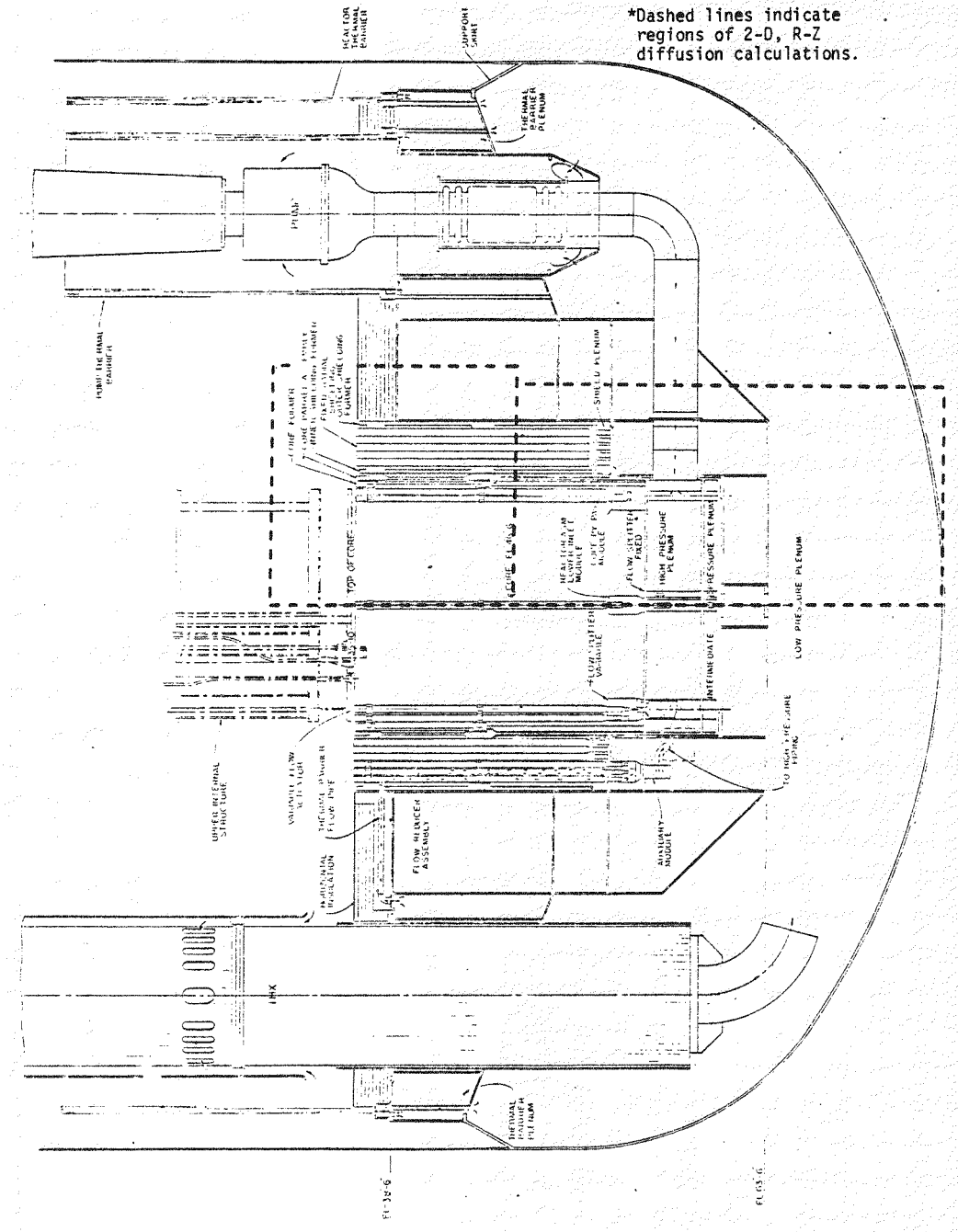

FIGURE 3-2 EPRI 1000 MWe HETEROGENEOUS, "BULLSEYE" CORE FOR POOL REACTOR DESIGN

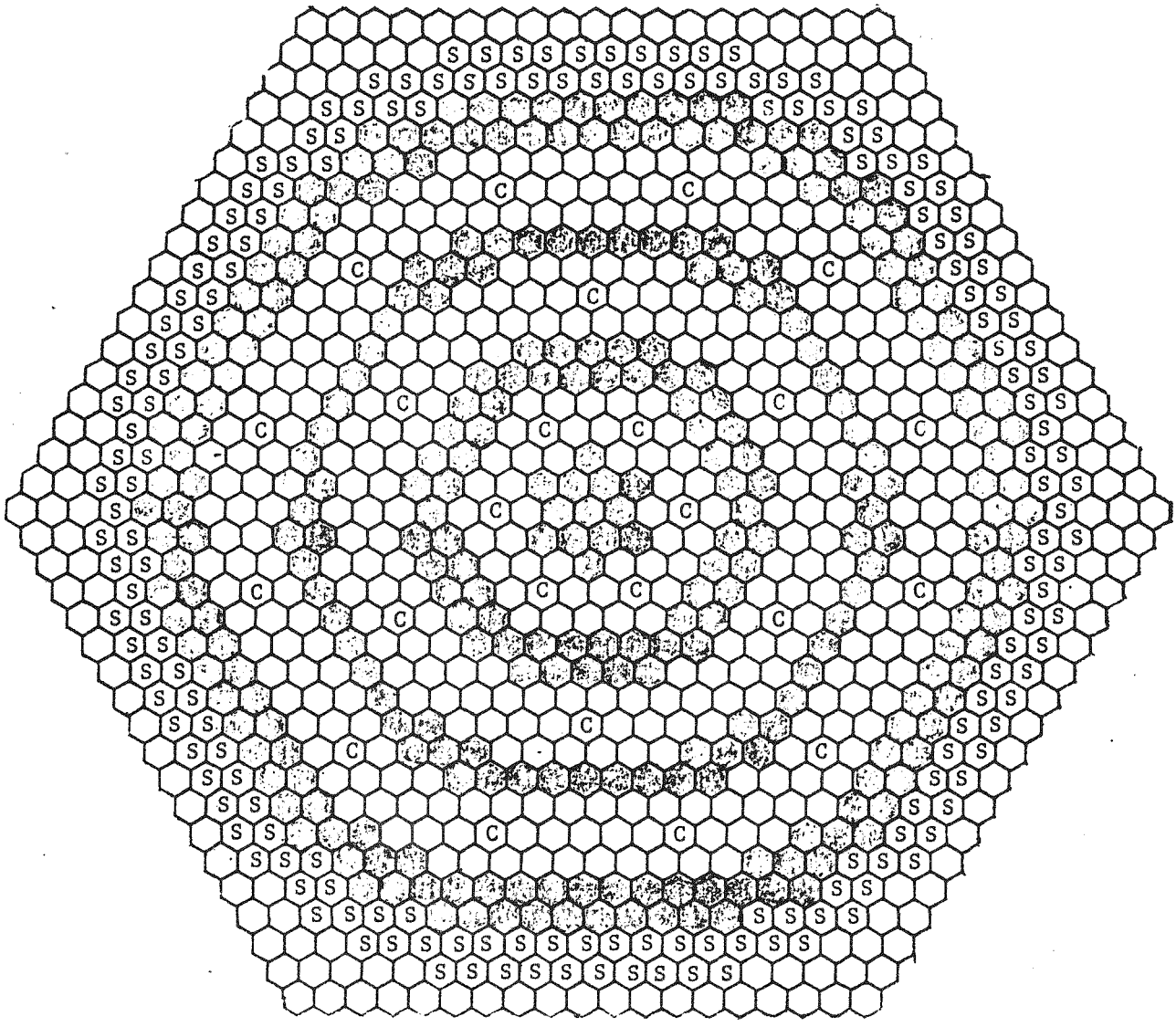

1. Blanket Assembly
   number of inner Bs = 145
   number of outer Bs = 162

   = Fuel Assembly
   number = 360

3. S = Removable Shield
   number = 180

4. C = Control Rod Assembly
   number = 24

5. Hexagonal Module
   Center-to-Center = 6.045"

6. Diameter of Circumscript Circle around Removable Shield Assemblies - 16.2'

7. Height from Seat to Top
   181"

8. Pressure Drop Pump Inlet to Pump Outlet = TBD

FIGURE 3-3 GE-ARSD 1200 MWe HETEROGENEOUS LMFBR CORE LAYOUT

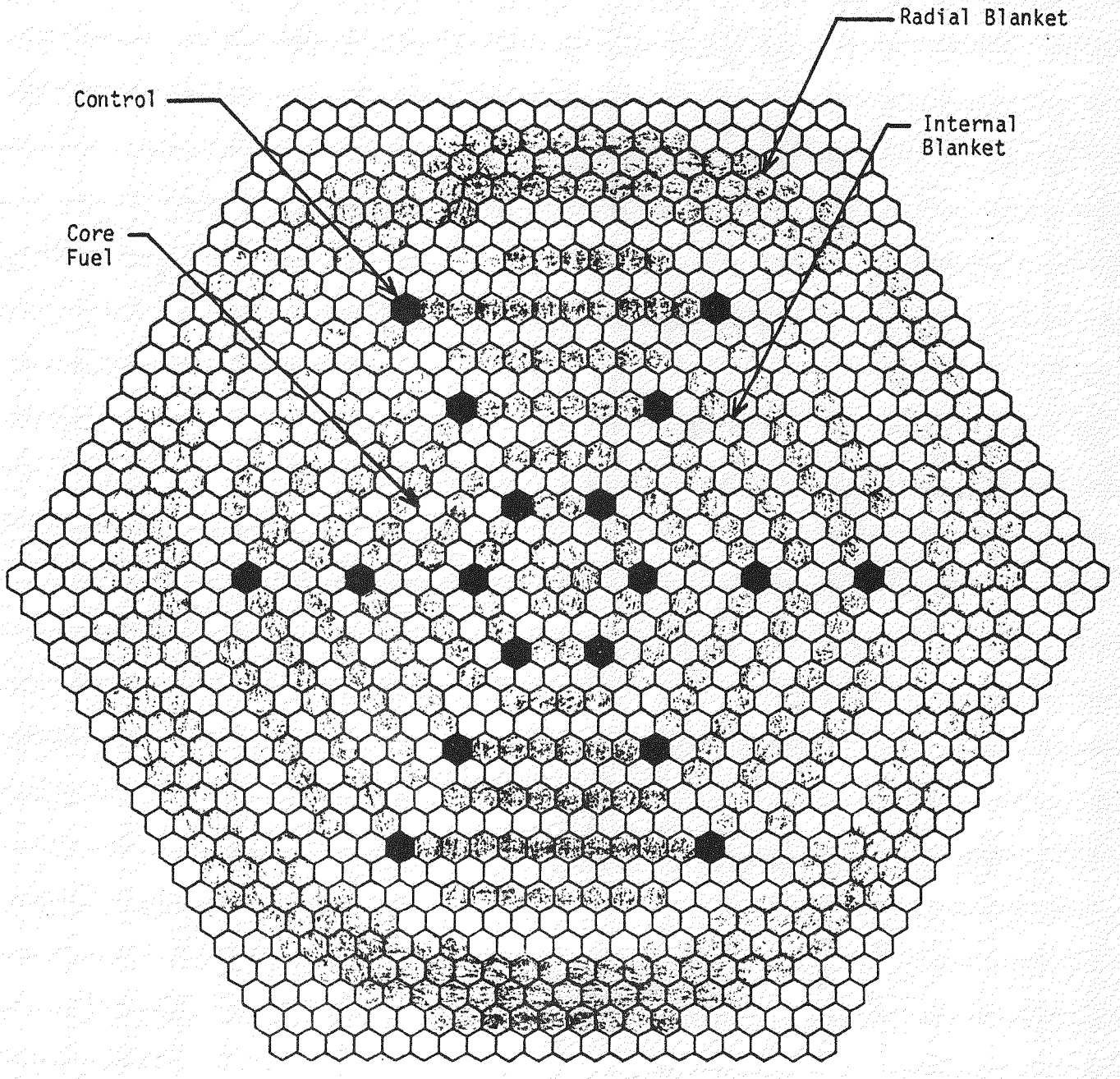

Core Assembly Totals

Core Fuel	396
Internal Blanket	235
Control	18
Subtotal	649
Radial Blanket	306
Total	955

TABLE 3-1 END-OF-EQUILIBRIUM CYCLE REGIONAL ATOM DENSITIES FOR GE-ARSD 1200 MWe HETEROGENEOUS CORE

(atoms/barn-cm)

Element	CF	IB	AB (CF)	AB (IB)	RB
Pu-239	1.308-3	2.983-4	1.045-4	1.306-4	1.542-4
Pu-240	4.991-4	1.735-5	2.258-6	2.231-6	3.823-6
Pu-241	1.659-4	5.026-7	3.464-8	2.701-8	9.688-8
Pu-242	6.395-5	1.162-8	3.379-10	2.032-10	1.137-9
U-235	6.469-6	1.594-5	1.382-5	2.059-5	1.994-5
U-238	4.499-3	1.088-2	7.697-3	1.126-2	1.123-2
FP	5.381-4	1.206-4	1.162-5	1.262-5	2.011-5
O	1.414-2	2.287-2	1.566-2	2.287-2	2.287-2
Na	9.785-3	6.970-3	9.785-3	6.970-3	6.970-3
Cr	4.015-3	3.345-3	4.015-3	3.345-3	3.345-3
Fe	1.191-2	9.921-3	1.191-2	9.921-3	9.921-3
Ni	2.371-3	1.975-3	2.371-3	1.975-3	1.975-3
Mo	2.472-4	2.059-4	2.472-4	2.059-4	2.059-4

CF : Core fuel
IB : Internal blanket
AB (CF): Axial blanket above and below core fuel
AB (IB): Axial blanket above and below internal blanket
RB : Radial blanket

considered to be a good approximation to the EPRI core for the purpose of producing neutron flux values to determine initial estimates of the necessary near-core shielding. An updated version of the core model will be used when the reactor shielding analysis is further refined.

Calculations performed with preliminary R-Z models revealed that the planned radial and axial shielding was inadequate from the standpoint of producing sufficient core midplane radial attenuation and also for preventing streaming around the radial shield. After examination of the Phase A reactor fuel assembly, internal blanket assembly, and radial blanket assembly designs, it was concluded that a total length of thirty-four inches (34") of steel shielding could be assumed for the upper axial shield. This assumption leaves an upper axial plenum length of 22.25 inches in all assemblies. One might expect that less shielding is needed in the radial blanket assemblies than in the fuel and inner blanket assemblies due to the lower neutron generation rate in the radial blanket. However, neutron streaming from the core through the regions above and below the radial blankets was evident in the preliminary R-Z calculations and indicates the desirability of this shielding. It was also found that two rows of B_4C assemblies were required at the outer periphery of the steel radial neutron shield (replacing two rows of steel shield assemblies). Figure 4.5.1 of Reference (9) shows the conceptual design of a typical B_4C shield assembly which contains B_4C pins similar to the design of a control rod assembly. Figure 3-4 and Table 3-2 show the upper axial near-core zone map and region volume fractions used for the two-dimensional R-Z diffusion calculations and correspond to the upper axial region indicated on Figure 3-1. Reflective boundary conditions were used at the left and top boundaries of this diagram and vacuum boundary conditions were used at the bottom and right boundaries. Figure 3-5 and Table 3-3 show the corresponding lower axial zone map and region volume fractions used for the lower axial diffusion calculations. Table 3-4 gives the steel, sodium, and B_4C atom densities used in all calculations.

8.3.2 ONE-DIMENSIONAL RADIAL TRANSPORT MODEL

The core center-to-IHX 1-D model region geometry and compositions are shown in Figure 3-6. This 1-D model was extended in the radial direction through the center of an IHX to R = 1038 cm. At the core midplane the distance from

FIGURE 3-4 REGION AND MATERIAL MAP FOR POOL REACTOR DESIGN
NEAR-CORE UPPER AXIAL R-Z MODEL

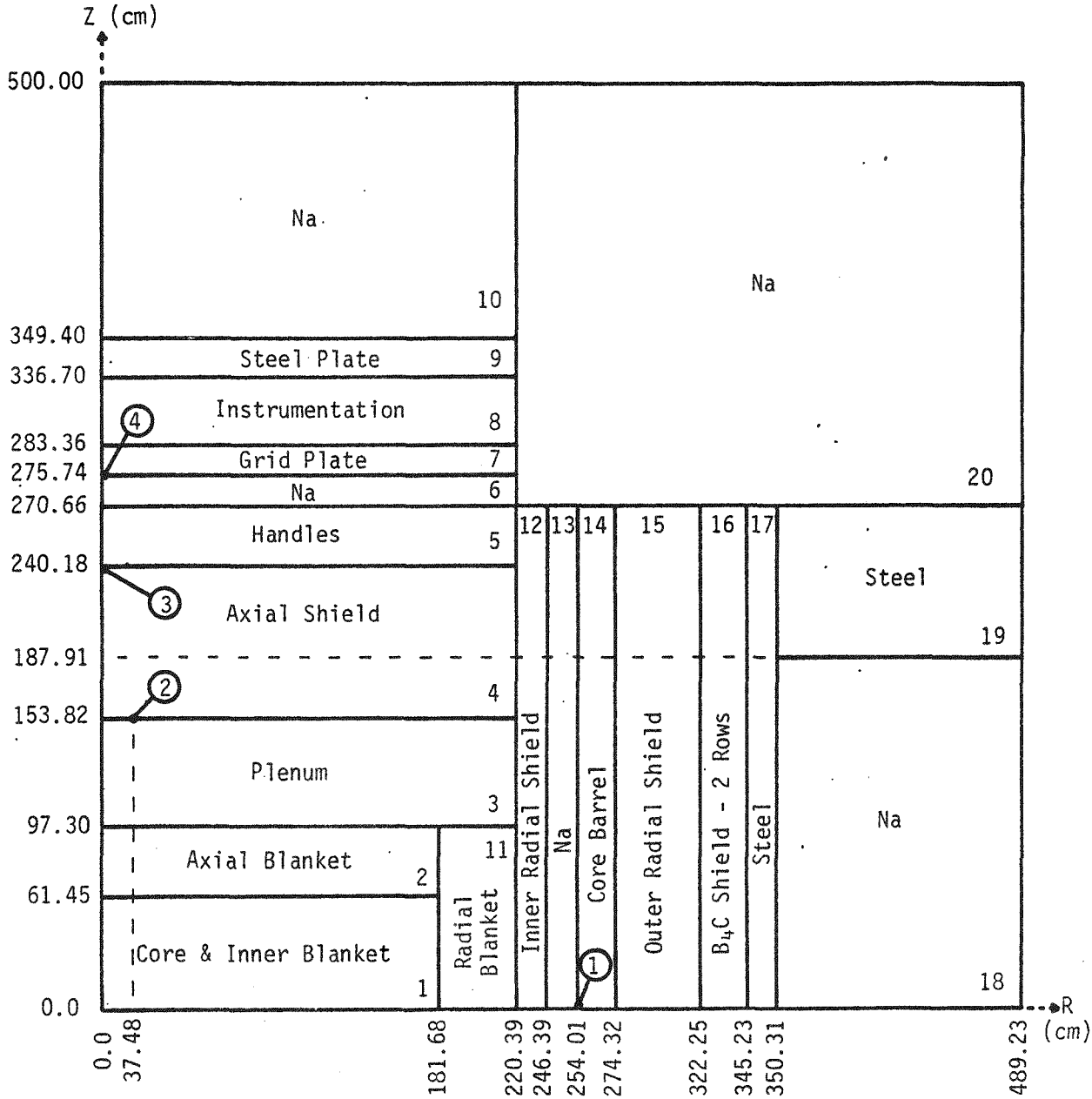

Note: Circled numbers indicate points at which the number of displacements per knock-on atom, dpa, was evaluated. See Table 4-1.

TABLE 3-2 REGION VOLUME FRACTIONS FOR POOL REACTOR DESIGN
NEAR-CORE UPPER AXIAL R-Z MODEL

Region Number	Material	Steel	Na
1	Core & Internal Blanket	*	*
2	Axial Blanket	*	*
3	Plenum	0.21	0.44
4	Axial Shield	0.56	0.44
5	Handles	0.34	0.66
6	Sodium	-	1.00
7	Grid Plate	0.92	0.08
8	Instrumentation	0.15	0.85
9	Steel Plate	0.72	0.28
10	Sodium	-	1.00
11	Radial Blanket	*	*
12	Inner Radial Shield	0.85	0.15
13	Sodium	-	1.00
14	Core Barrel	1.00	-
15	Outer Radial Shield	0.85	0.15
16	B_4C Shield (2 Rows)	0.26	0.17
17	Steel	1.00	-
18	Sodium	-	1.00
19	Steel	1.00	-
20	Sodium	-	1.00

*See Table 3-1.

FIGURE 3-5 REGION AND MATERIAL MAP FOR POOL REACTOR DESIGN

NEAR-CORE LOWER AXIAL R-Z MODEL

(Two Rows of B_4C Radial Shield Assemblies)

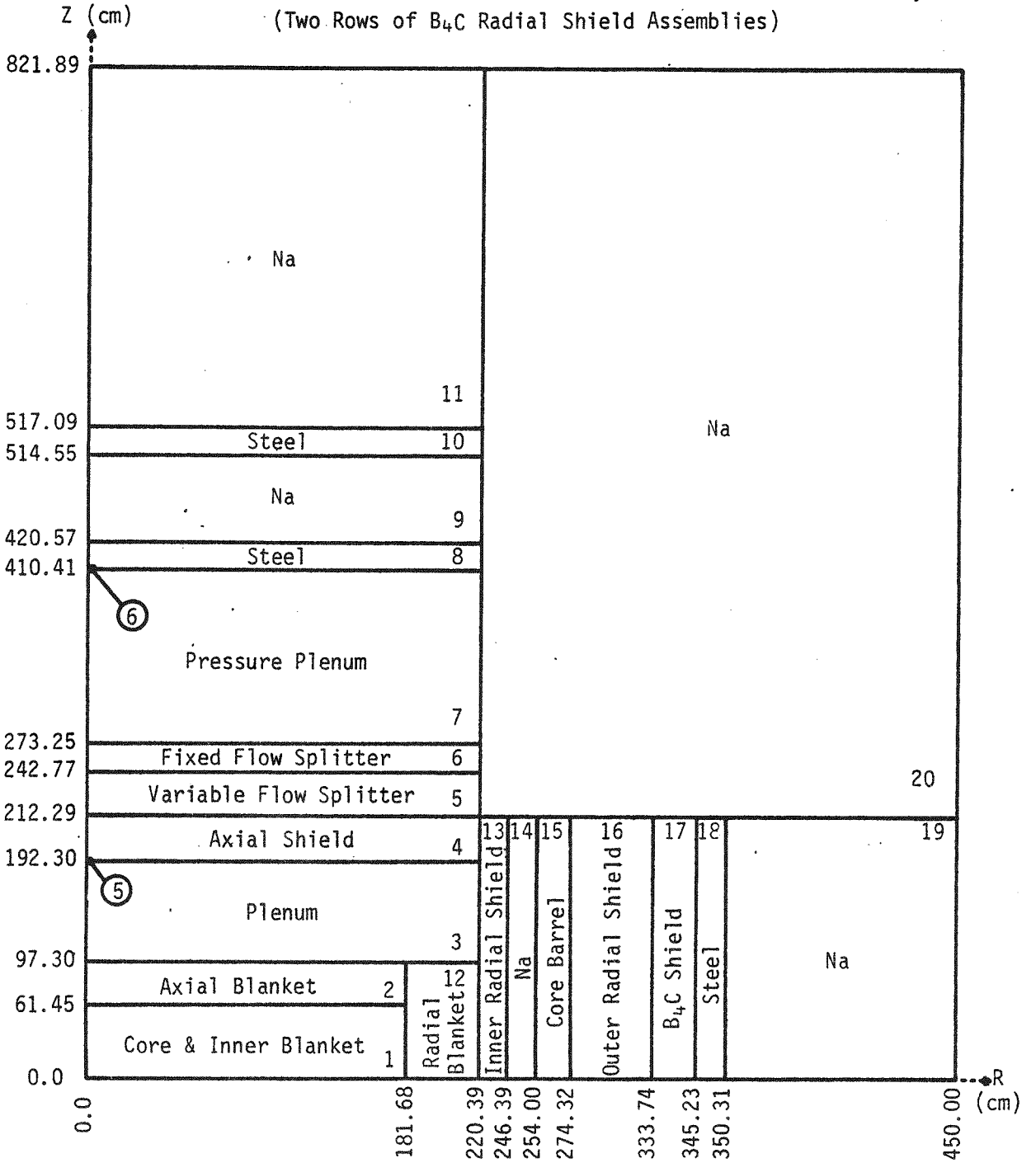

Note: Circled numbers indicate points at which the number of displacements per knock-on atom, dpa, was evaluated. See Table 4-1.

TABLE 3-3 REGION VOLUME FRACTIONS FOR POOL REACTOR DESIGN
NEAR-CORE LOWER AXIAL R-Z MODEL

Region Number	Material	Steel	Na
1	Core & Internal Blanket	*	*
2	Axial Blanket	*	*
3	Plenum	0.21	0.44
4	Axial Shield	0.56	0.44
5	Variable Flow Splitter	0.39	0.61
6	Fixed Flow Splitter	0.75	0.25
7	Pressure Plenum	0.088	0.912
8	Steel	1.00	-
9	Sodium	-	1.00
10	Steel	1.00	-
11	Sodium	-	1.00
12	Radial Blanket	*	*
13	Inner Radial Shield	0.85	0.15
14	Sodium	-	1.00
15	Core Barrel	1.00	-
16	Outer Radial Shield	0.85	0.15
17	B_4C Shield (2 Rows)	0.26	0.17
18	Steel	1.00	-
19	Sodium	-	1.00
20	Sodium	-	1.00

*See Table 3-1.

TABLE 3-4 SHIELD MATERIAL AND SODIUM ATOM DENSITIES

(atoms/barn-cm)

Element	Steel	Na	B_4C (nat.)*
C	-	-	1.959-2
B-10	-	-	1.495-2
B-11	-	-	6.354-2
Na	-	2.230-2	-
Cr	1.562-2	-	-
Fe	5.817-2	-	-
Ni	1.017-2	-	-
Mo	1.245-3	-	-
ρ (gm/cm^2)	7.93	.851	1.80*

*72% of theoretical density (2.50)

FIGURE 3-6 REGION GEOMETRY AND COMPOSITIONS FOR POOL REACTOR DESIGN
RADIAL 1-D MODEL WITH 2 ROWS OF B_4C SHIELD ASSEMBLIES

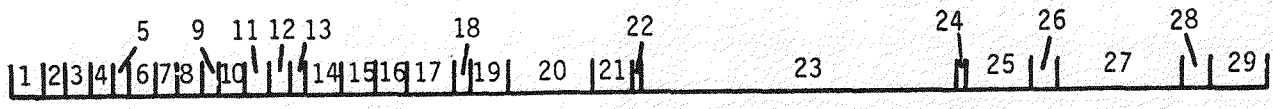

	Region	Region Thickness, cm (Distance from Core Center, cm)		Region Composition†
1	Internal Blanket 1	18.87	(18.87)	Internal Blanket*
2	Core 1	12.22	(31.09)	Core**
3	Internal Blanket 2	12.79	(43.88)	Internal Blanket*
4	Core 2	11.82	(55.70)	Core**
5	Internal Blanket 3	10.05	(65.75)	Internal Blanket*
6	Core 3	14.62	(80.37)	Core**
7	Internal Blanket 4	12.34	(92.71)	Internal Blanket*
8	Core 4	12.34	(105.05)	Core**
9	Internal Blanket 5	11.04	(116.09)	Internal Blanket*
10	Core 5	13.66	(129.75)	Core**
11	Internal Blanket 6	12.34	(142.09)	Internal Blanket*
12	Core 6	12.35	(154.44)	Core**
13	Internal Blanket 7	7.71	(162.15)	Internal Blanket*
14	Core 7	19.53	(181.68)	Core**
15	Radial Blanket 1	20.32	(202.00)	Radial Blanket*
16	Radial Blanket 2	18.39	(220.39)	Radial Blanket*
17	Inner Radial Shield	26.00	(246.39)	.15-Na, .85-Steel
18	Sodium	7.61	(254.00)	1.0-Na
19	Steel Plate	20.32	(274.32)	1.0-Steel
20	Outer Radial Shield	47.93	(322.25)	.15-Na, .85-Steel
21	B_4C Radial Shield (2 rows)	22.98	(345.23)	.17-Na, .26-Steel, .57-B_4C (72% Theor. Dens.)
22	Steel Plate	5.08	(350.31)	1.0-Steel
23	Sodium	244.61	(594.92)	1.0-Na
24	Steel Plate	5.08	(600.00)	1.0-Steel
25	Sodium	29.92	(629.92)	1.0-Na
26	IHX Vessel Wall	7.62	(637.54)	1.0-Steel
27	IHX Interior	340.36	(977.90)	.86-Na, .14-Steel
28	IHX Vessel Wall	7.62	(985.52)	1.0-Steel
29	Sodium	52.39	(1037.91)	1.0-Na

†See Table 3-1 for inner blanket and core assembly compositions.

*Internal Blanket and Radial Blanket - 0.5100 Fuel, 0.1825 Structure, 0.3075 Na.

**Core - 0.3493 Fuel, 0.2191 Structure, 0.4316 Na.

the center of the core to the nearest surface of the IHX is 630 cm. Since the outside diameter of the IHX is 11' 8" (355.60 cm), a point at R = 1038 cm represents a location 52 cm radially beyond the IHX outer wall but 90 cm inside the vessel. The cylindrical outer steel wall of the IHX was assumed to be 3" thick and the internal structure was assumed to be a homogeneous mixture consisting of approximately 14% steel and 86% sodium.

8.3.2
DIFFUSION AND TRANSPORT THEORY ASSUMPTIONS

Table 3-5 gives the energy group structure of the 9-group neutron cross section library used in both the 1-D and 2-D calculations. The R-Z diffusion calculations were performed as fixed fission source calculations with the SN2D computer code (10), and the 1-D transport calculations were performed as eigenvalue calculations with the SN1D computer code (11). Transport-corrected P_0 cross sections were used for all 2-D and 1-D cases with S_2P_0 used for diffusion calculations and $S_{16}P_0$ used for transport calculations.

It should be pointed out that shielding analyses and experiments performed by ORNL for the FFTF (12) and CRBR (13) reactors have revealed the necessity of treating fast reactor deep penetration problems with relatively high S_n quadrature and P_ℓ scattering orders in order to adequately account for associated streaming effects. It would therefore be desirable during the next phase of 1000 MWe pool type LMFBR studies to examine this problem relative to a pool reactor design and use more accurate methods. It is particularly important to perform some 2-D transport analyses to better determine the neutron streaming through the more sparsely shielded regions of the near-core shield.

TABLE 3-5 ENERGY GROUP STRUCTURE FOR 9-GROUP NEUTRON CROSS SECTION LIBRARY

Group	Energy Range	Average Energy
1	2.23 MeV - 15.0 MeV	6.680 MeV
2	821.0 keV - 2.23 MeV	1.353
3	183.0 - 821.0 keV	387.8 keV
4	40.8 - 183.0	86.53
5	9.12 - 40.8	19.31
6	2.03 - 9.12	4.308
7	454.0 eV - 2.03 keV	961.2 eV
8	0.683 - 454.0 eV	17.60
9	0.0 - 0.683	0.1847

ANALYTICAL RESULTS

8.4.1
TWO-DIMENSIONAL TOTAL NEUTRON FLUX DISTRIBUTIONS

Figures 4-1 and 4-2 are R-Z isoflux contour plots of the total neutron flux distribution in the reactor near-core upper axial region. They show conditions, respectively, for using one or two rows of B_4C radial shield assemblies. Although the absolute magnitudes of the fluxes shown in these figures are in error due to the limitations of diffusion theory, the plots are still useful because they provide insight into the degree of seriousness of neutron streaming through the near-core shield. Evidence for streaming is characterized by the "bulge" in the contours in the upper right corner of both figures. It is noted that two rows of B_4C reduces the total flux in the sodium region above the radial shield by a factor of 2 to 3. It is especially important to realize that the shape of this streaming "bulge" is a strong function of the accuracy of treatment of forward (away from the core center) scattering. Consequently, the diffusion theory calculations underestimate the neutron fluxes in this region - - probably by as much as an order of magnitude. It is suggested that the utilization of a high S_n quadrature, high P_ℓ scattering order transport model will confirm this hypothesis at a later date. The fluxes in the core midplane are not expected to be as sensitive to S_n quadrature and P_ℓ scattering assumptions because the neutron shield is essentially free of streaming "holes" in this direction. The core midplane total neutron flux at a point just outside the radial shield is approximately 2×10^9 n/cm^2-sec for the 2-D diffusion analysis and for the 1-D transport analysis (two rows of B_4C assemblies).

Figures 4-3 and 4-4 show the near-core total neutron flux distribution for the lower axial R-Z region. They are analogous to the upper axial cases and show the respective conditions for one or two rows of B_4C shield assemblies. It should be clear from the figures that the core midplane is at the bottom of the figures and the distance below the core midplane is plotted in the upward direction. Note again the evidence of streaming indicated

4-1 TOTAL NEUTRON FLUX DISTRIBUTION IN NEAR-CORE UPPER AXIAL REGION

(ONE ROW OF B_4C RADIAL SHIELD ASSEMBLIES)

Units are Neutrons · cm^{-2} · sec^{-1}

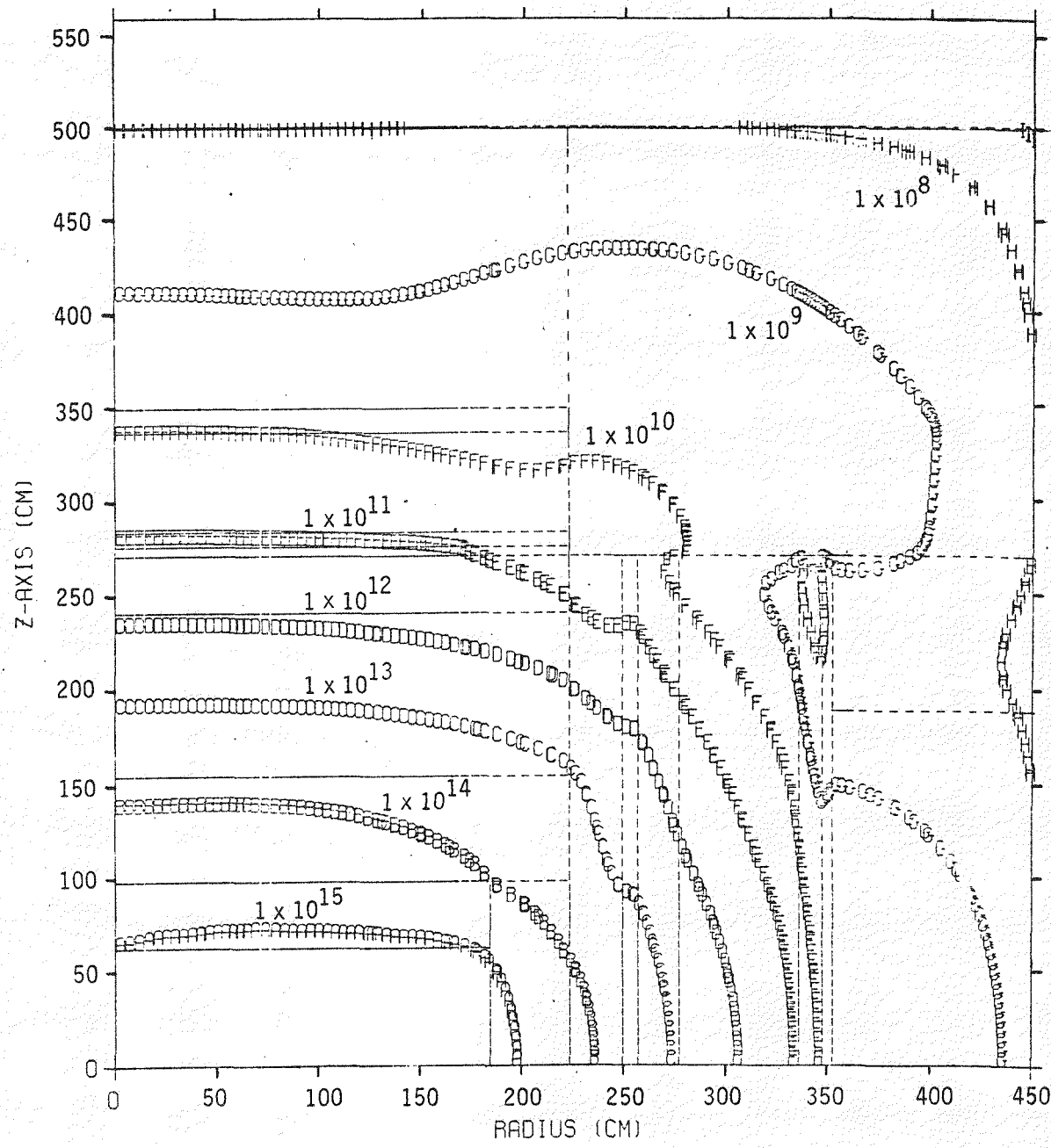

4-2 TOTAL NEUTRON FLUX DISTRIBUTION IN NEAR-CORE UPPER AXIAL REGION

(TWO ROWS OF B_4C RADIAL SHIELD ASSEMBLIES)

Units are Neutrons · cm^{-2} · sec^{-1}

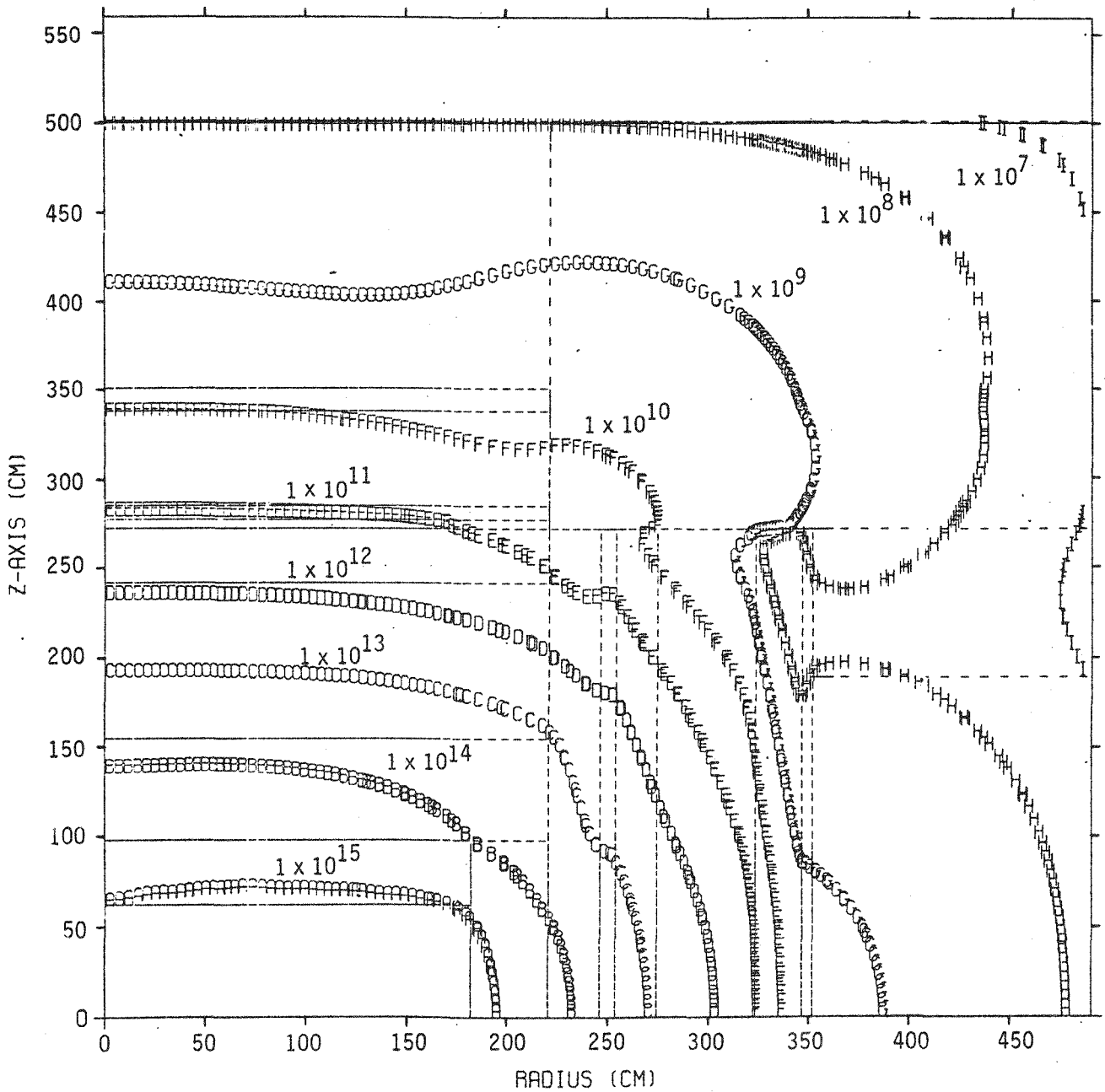

FIGURE 4-3 TOTAL NEUTRON FLUX DISTRIBUTION IN NEAR-CORE LOWER AXIAL REGION (ONE ROW OF B_4C RADIAL SHIELD ASSEMBLIES)

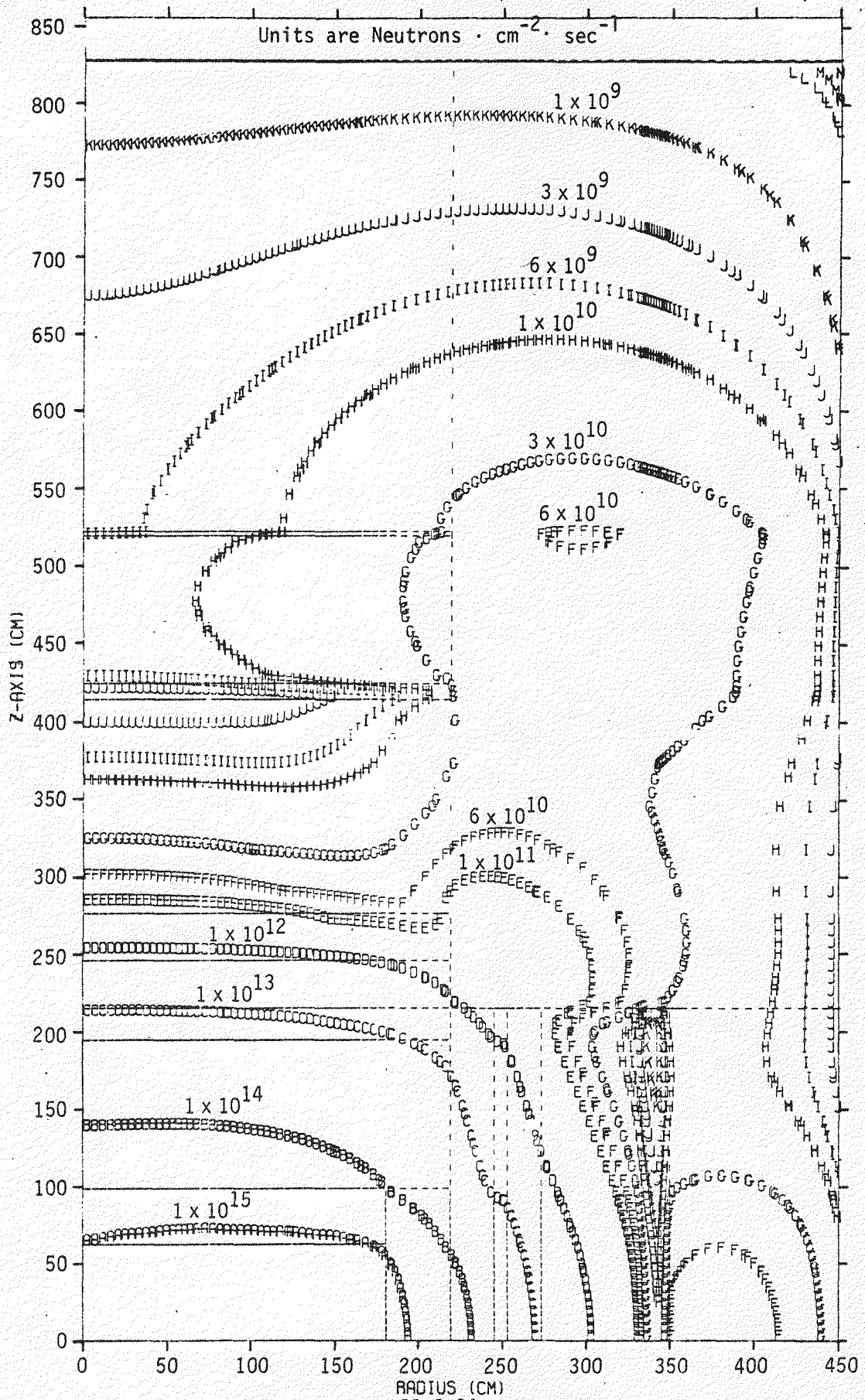

II-8-24

FIGURE 4-4 TOTAL NEUTRON FLUX DISTRIBUTION IN NEAR-CORE LOWER AXIAL REGION (TWO ROWS OF B_4C RADIAL SHIELD ASSEMBLIES)

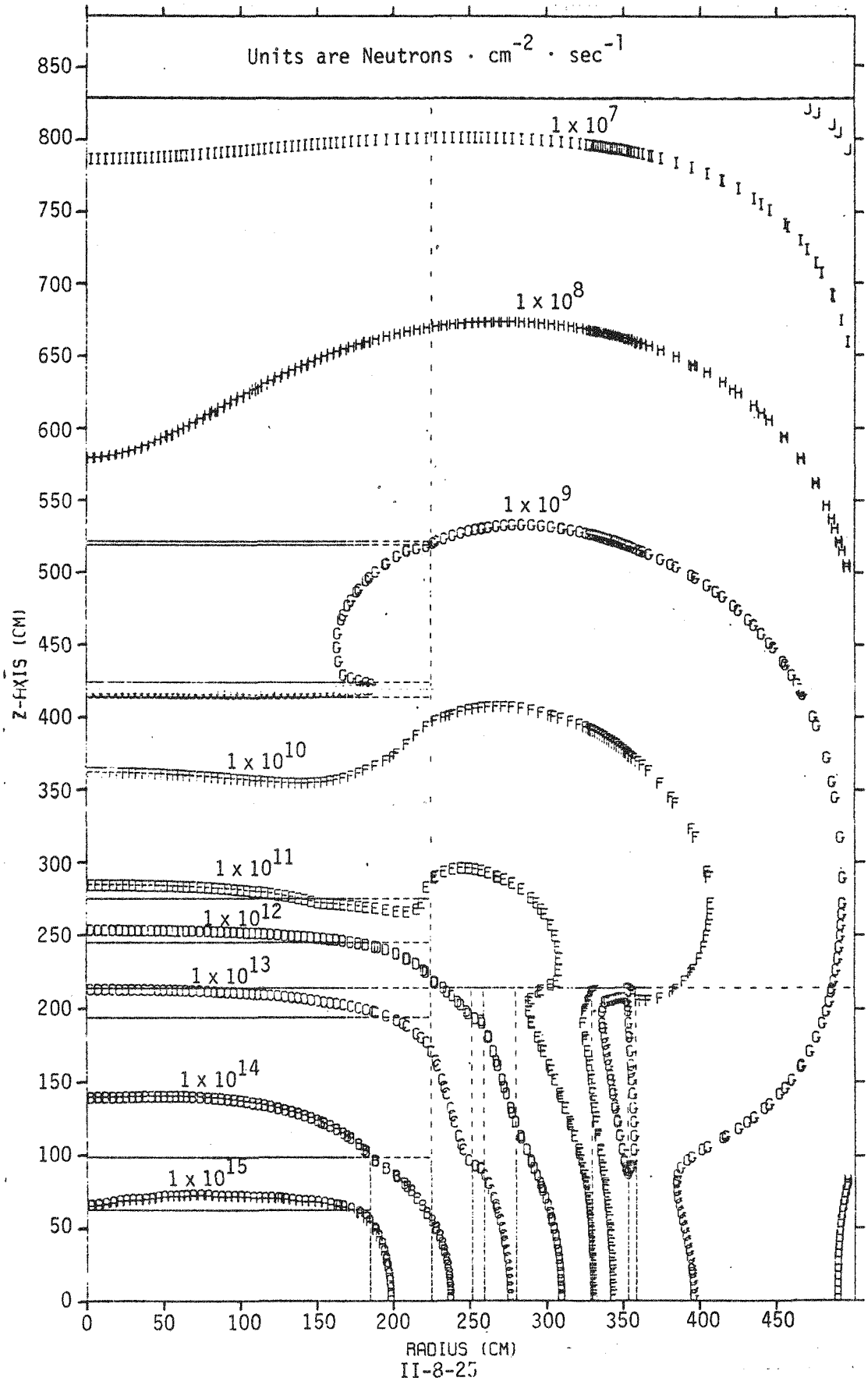

by the bulge in the contours in the upper right corner of each plot. These results suggest the need for adding additional steel shielding in the region at the bottom of the radial neutron shield. This design change is now being implemented.

As a result of preliminary 2-D diffusion calculations, the near-core neutron shielding has been increased in all directions compared to the earlier Phase A design. It is believed that the current design is adequate for the purposes of IHX and primary pump protection. However, further more accurate analysis is needed to reduce the calculational uncertainties and also to optimize the shield by considering trade-offs with other design constraints; e.g., seismic problems due to additional shield weight or primary coolant flow interference from unwarranted amounts of shielding.

8.4.2
TWO-DIMENSIONAL FAST NEUTRON FLUX DISTRIBUTIONS ($E > 0.1$ MeV)

Figures 4-5 and 4-8 are analogous to Figures 4-1 to 4-4 except that isoflux contours are given for the fast neutron flux ($E > 0.1$ MeV). This information is useful for evaluating potential neutron damage to steel and will be discussed further in a following section devoted specifically to this subject.

8.4.3
TWO-DIMENSIONAL NEUTRON FLUX DISTRIBUTIONS ($0.015 < E < 0.5$ MeV)

Figures 4-9 to 4-12 are also analogous to Figures 4-1 to 4-4 except that isoflux contours are given for the neutron flux with energies ($0.015 < E < 0.5$ MeV). This information was generated specifically at the suggesting of FRD/NPC engineering personnel in England and will be used in the near future to compare neutron damage criteria and conditions for the CFR and GE-ARSD pool reactor designs. The data is included here for the sake of completeness and for convenience in future reference. A determination of neutron damage conditions at selected locations in the GE-ARSD design has been made based on the total flux and average neutron energy at these locations. These results are discussed in the section on neutron damage.

8.4.4
ONE-DIMENSIONAL TRANSPORT ANALYSIS

The results of the 1-D, $S_{16}P_0$ transport calculations are plotted in Figures 4-13 to 4-15. Figures 4-13 and 4-14 display the group-dependent neutron

Fig. 4-5 FAST NEUTRON FLUX DISTRIBUTION (E > 0.1 MeV) IN NEAR-CORE UPPER AXIAL REGION (ONE ROW OF B_4C RADIAL SHIELD ASSEMBLIES)

Units are Neutrons · cm^{-2} · sec^{-1}

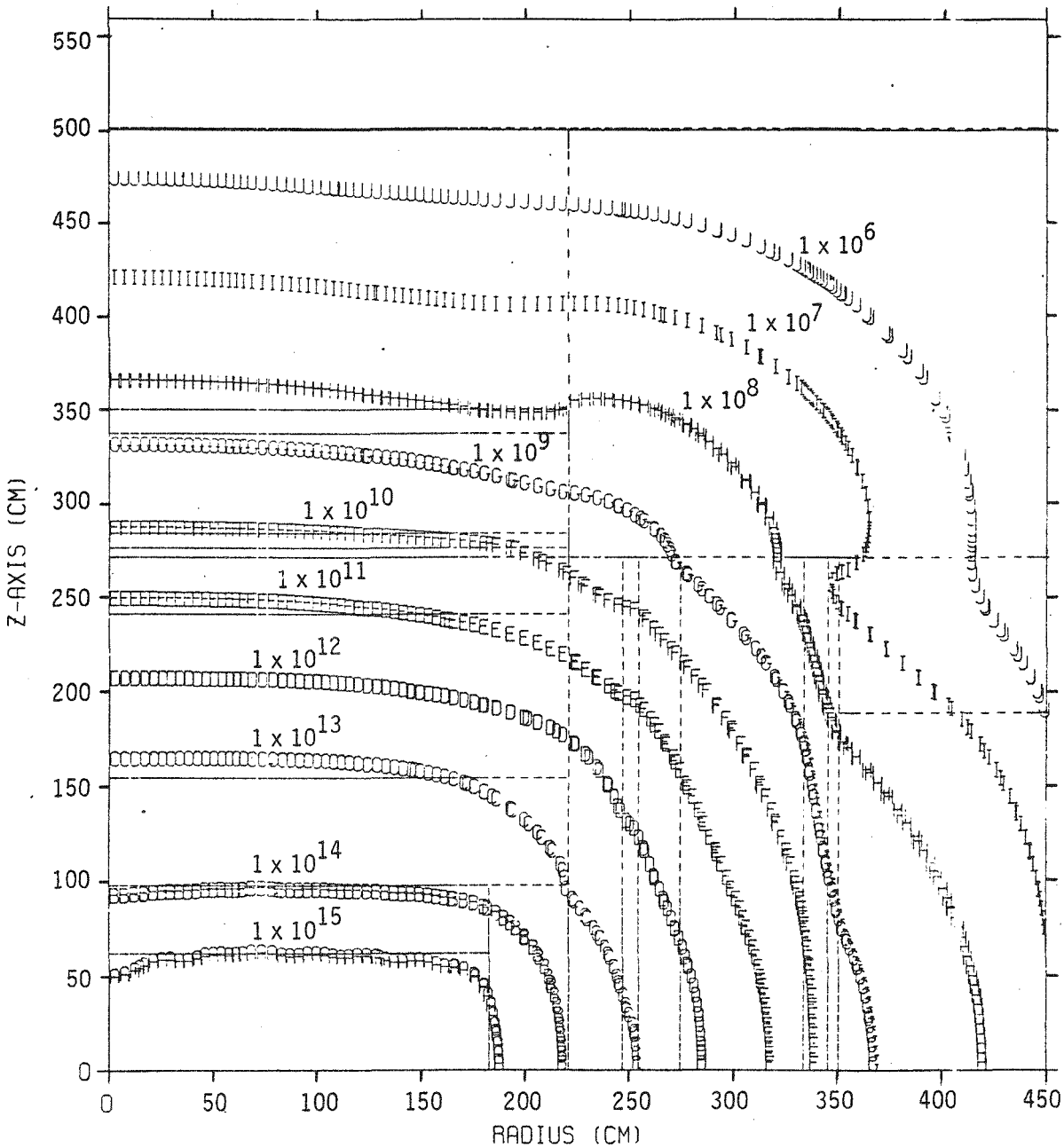

Fig. 4-6. FAST NEUTRON FLUX DISTRIBUTION (E > 0.1 MeV) IN NEAR-CORE UPPER AXIAL REGION (TWO ROWS OF B_4C RADIAL SHIELD ASSEMBLIES).
Units are Neutrons · cm^{-2} · sec^{-1}

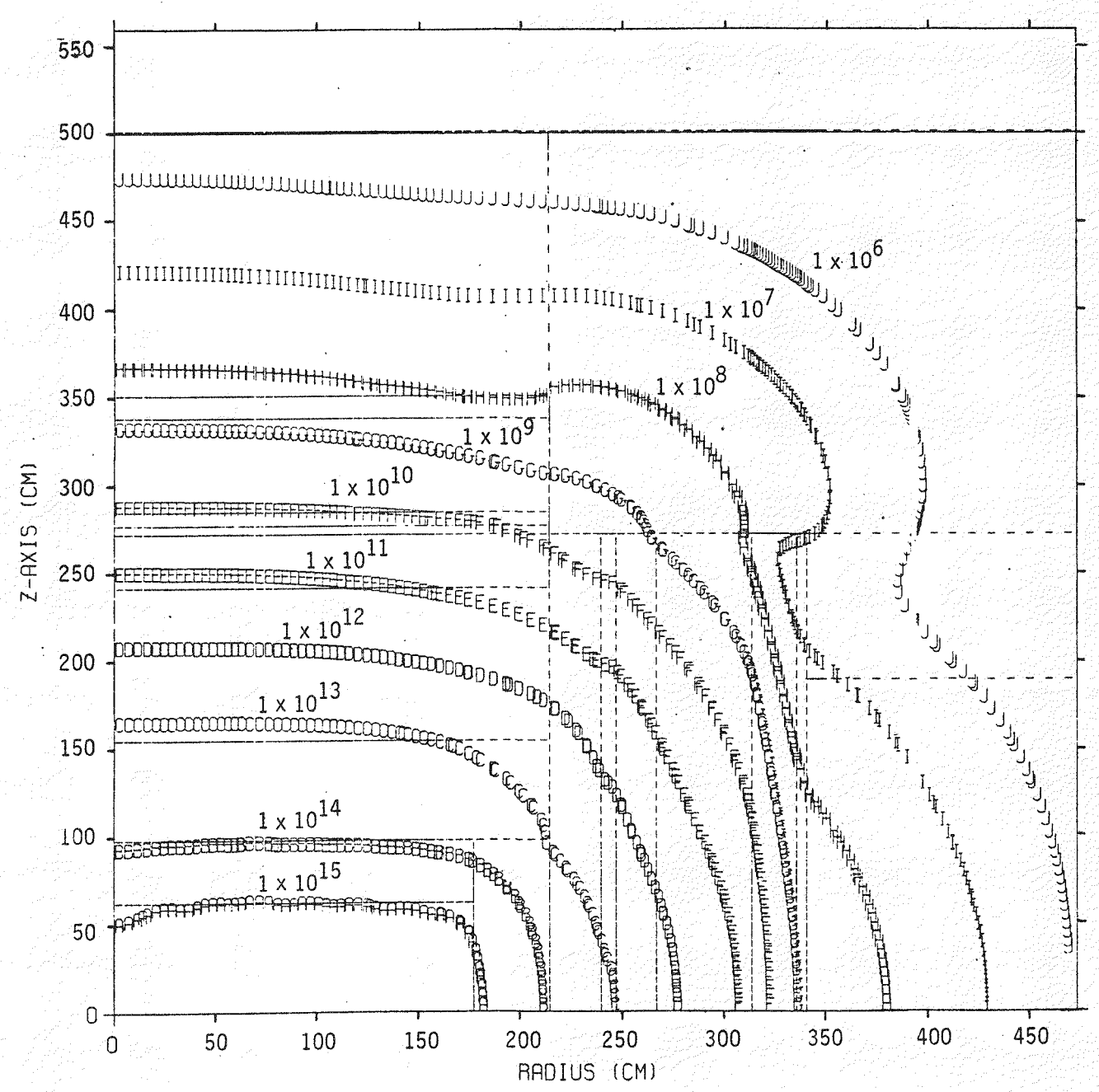

FIGURE 4-7 FAST NEUTRON FLUX DISTRIBUTION (E > 0.1 MeV) IN NEAR-CORE LOWER AXIAL REGION (ONE ROW OF B_4C RADIAL SHIELD ASSEMBLIES)

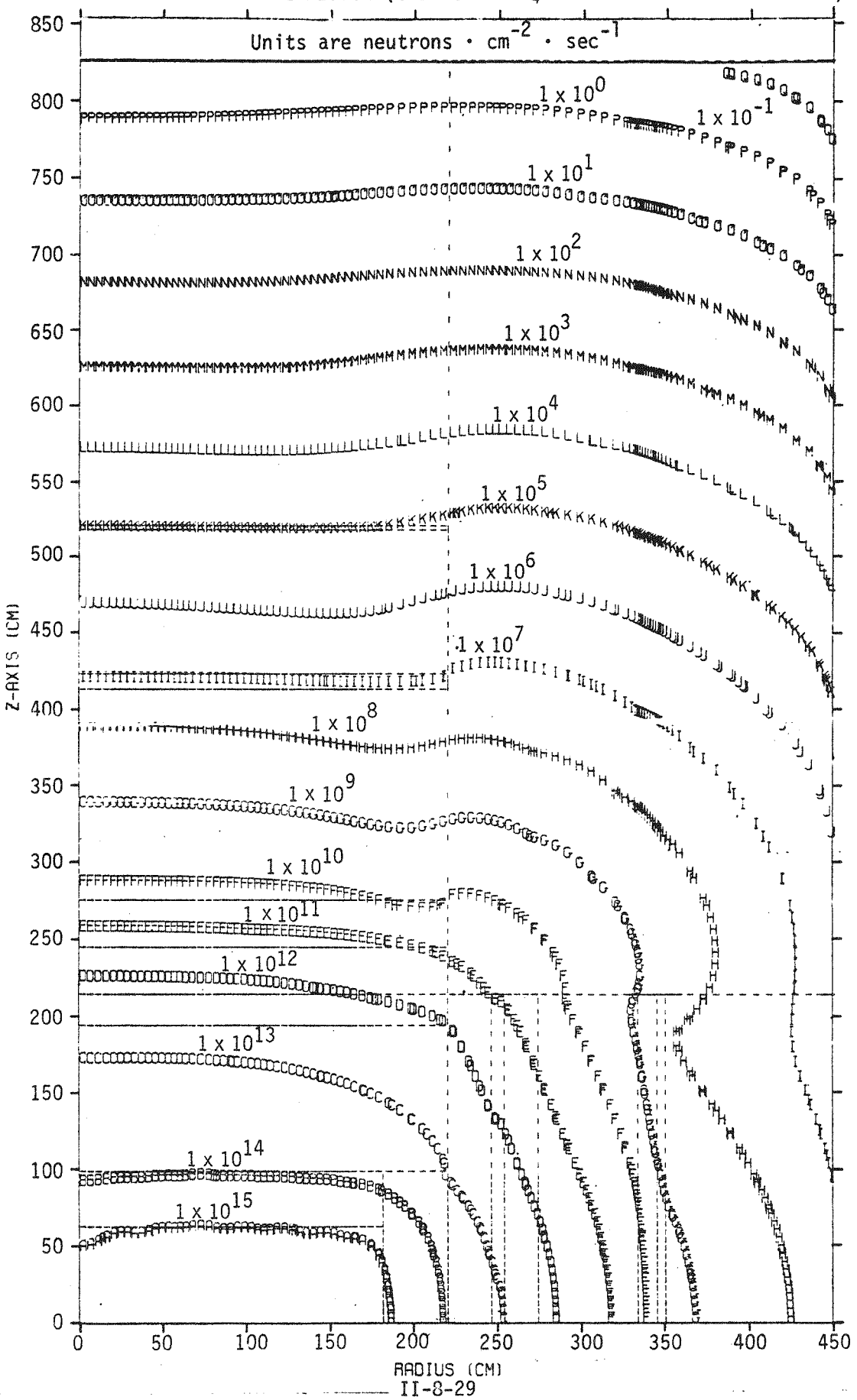

FIGURE 4-8 FAST NEUTRON FLUX DISTRIBUTION (E > 0.1 MeV IN NEAR-CORE LOWER AXIAL REGION (TWO ROWS OF B_4C RADIAL SHIELD ASSEMBLIES)

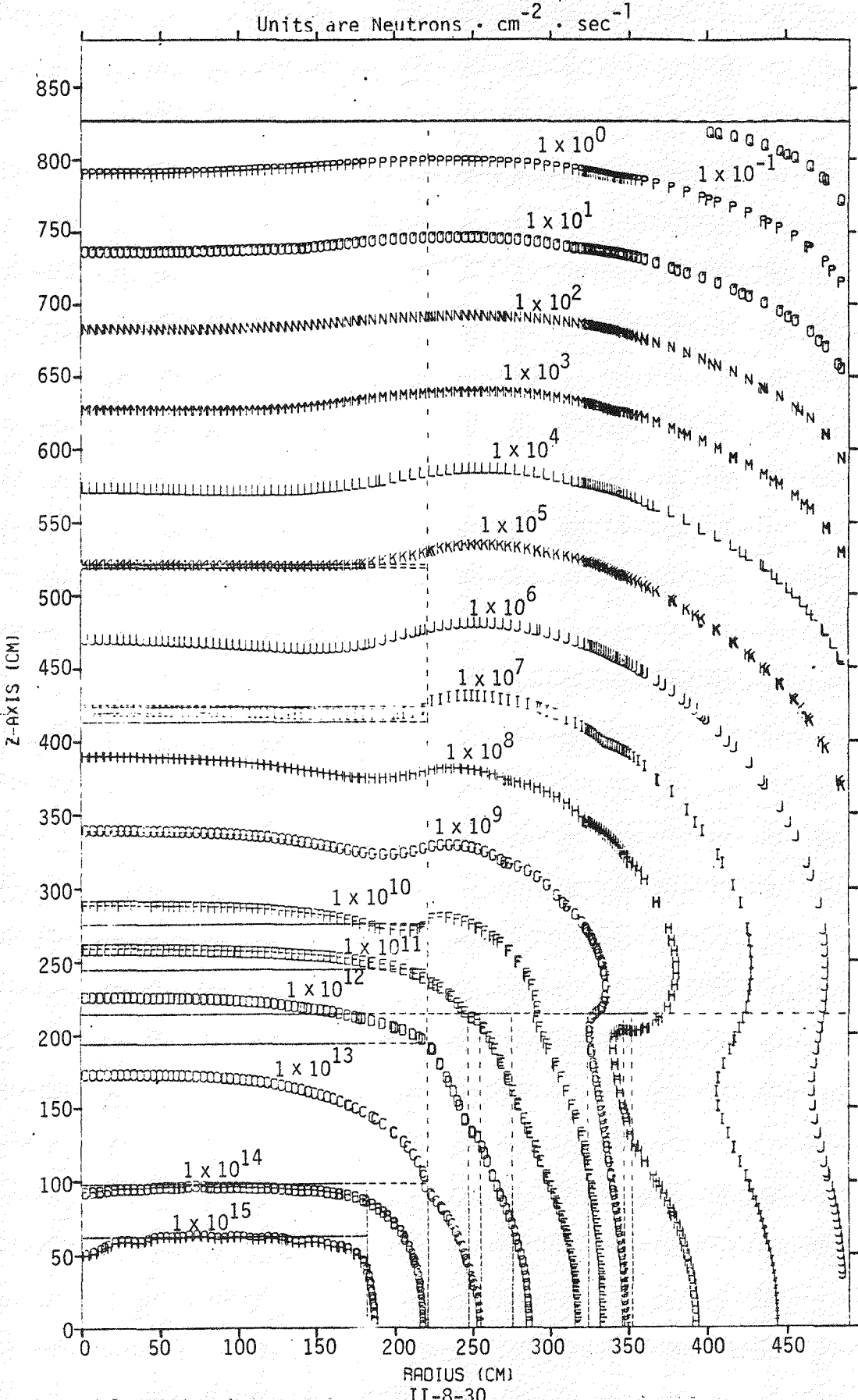

FIGURE 4-9 NEUTRON FLUX DISTRIBUTION ($0.015 < E < 0.5$ MeV) IN NEAR-CORE UPPER AXIAL REGION (ONE ROW OF B_4C RADIAL SHIELD ASSEMBLIES)

Units are Neutrons · cm^{-2} · sec^{-1}

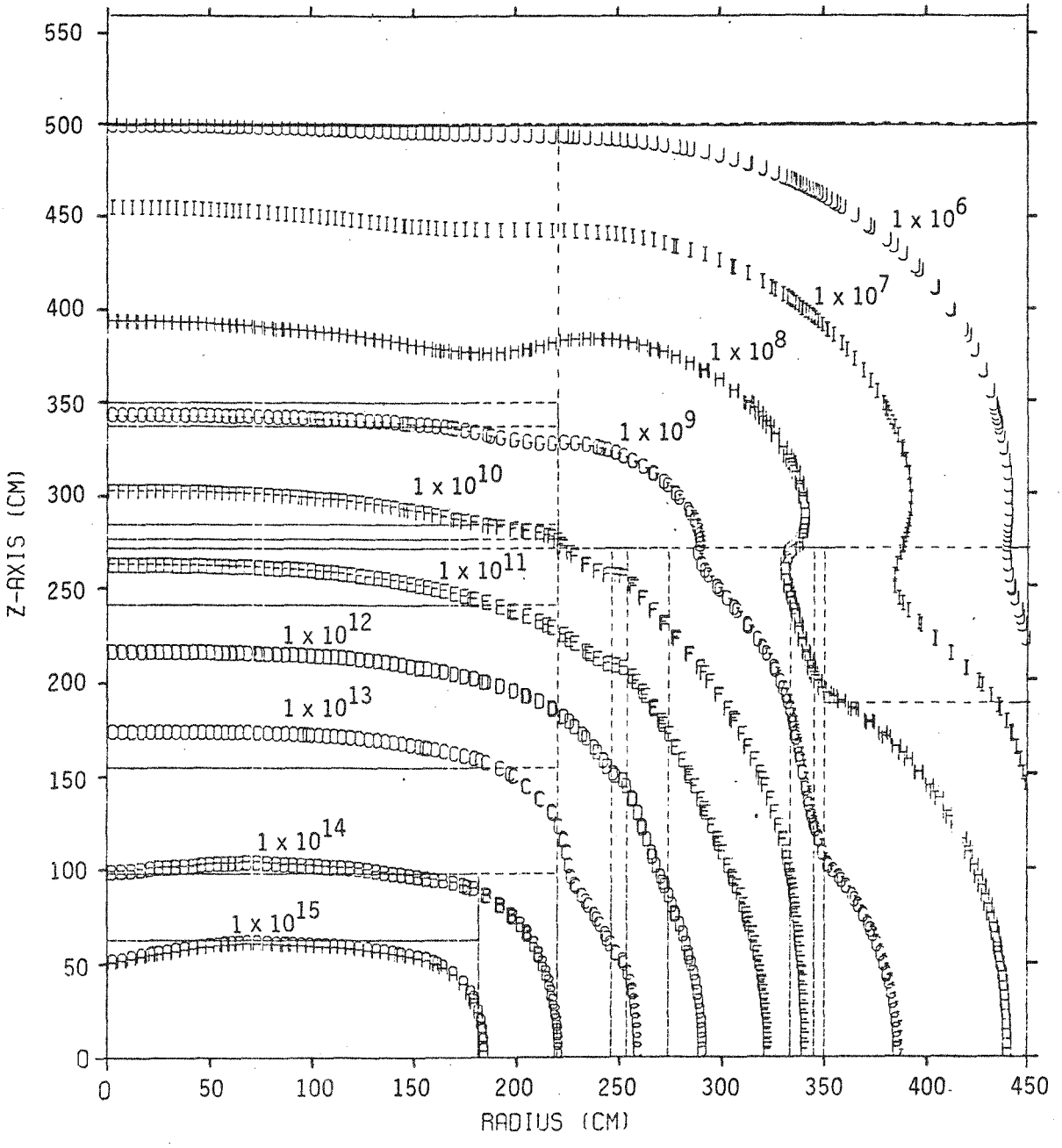

FIGURE 4-10 NEUTRON FLUX DISTRIBUTION ($0.015 < E < 0.5$ MeV IN NEAR-CORE UPPER AXIAL REGION (TWO ROWS OF B_4C RADIAL SHIELD ASSEMBLIES)

Units are Neutrons · cm^{-2} · sec^{-1}

*Displacements per primary knock-on atom

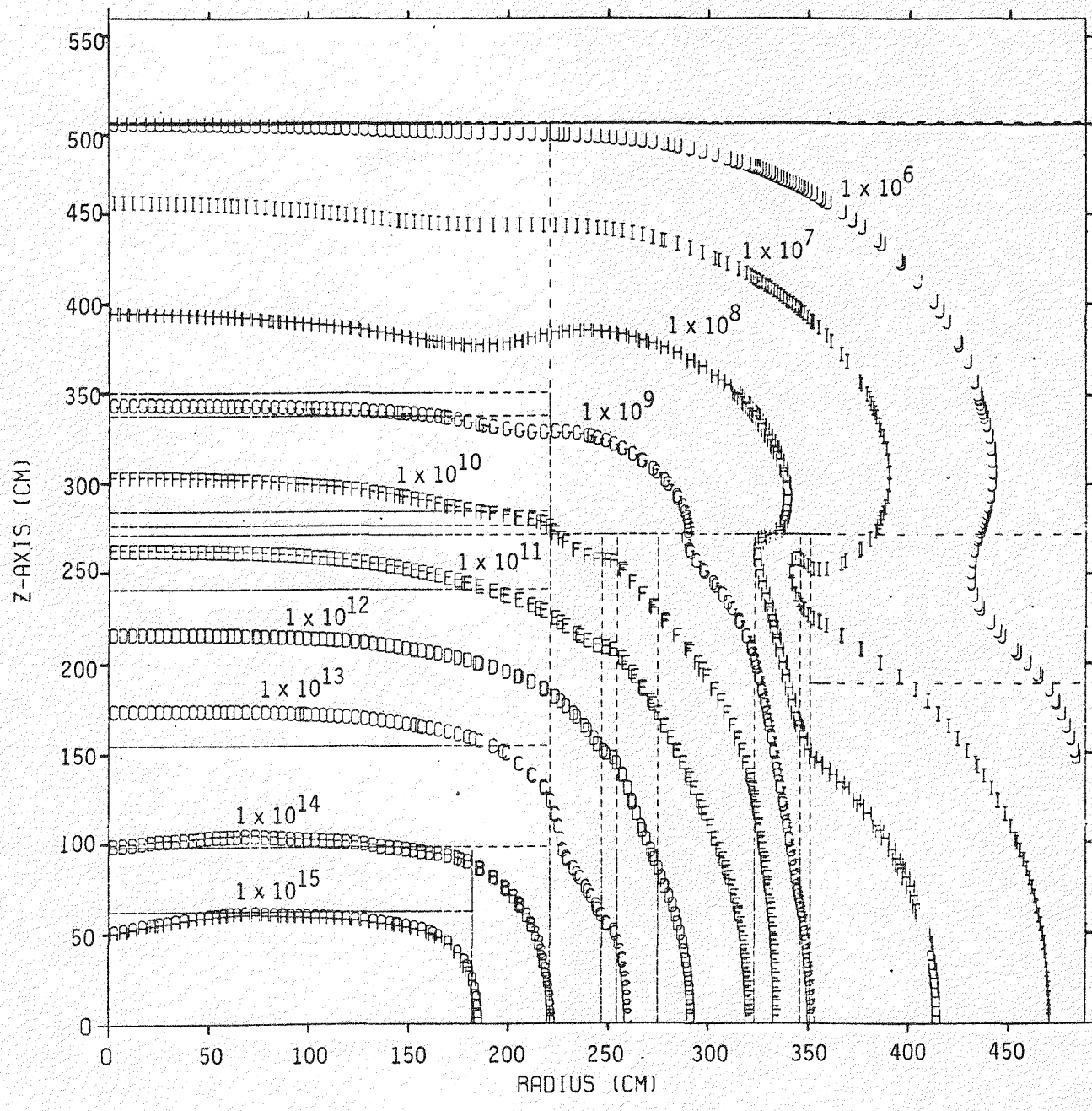

FIGURE 4-11 - NEUTRON FLUX DISTRIBUTION (0.015 < E < 0.5 MeV IN NEAR-CORE LOWER AXIAL REGION (ONE ROW OF B_4C RADIAL SHIELD ASSEMBLIES)

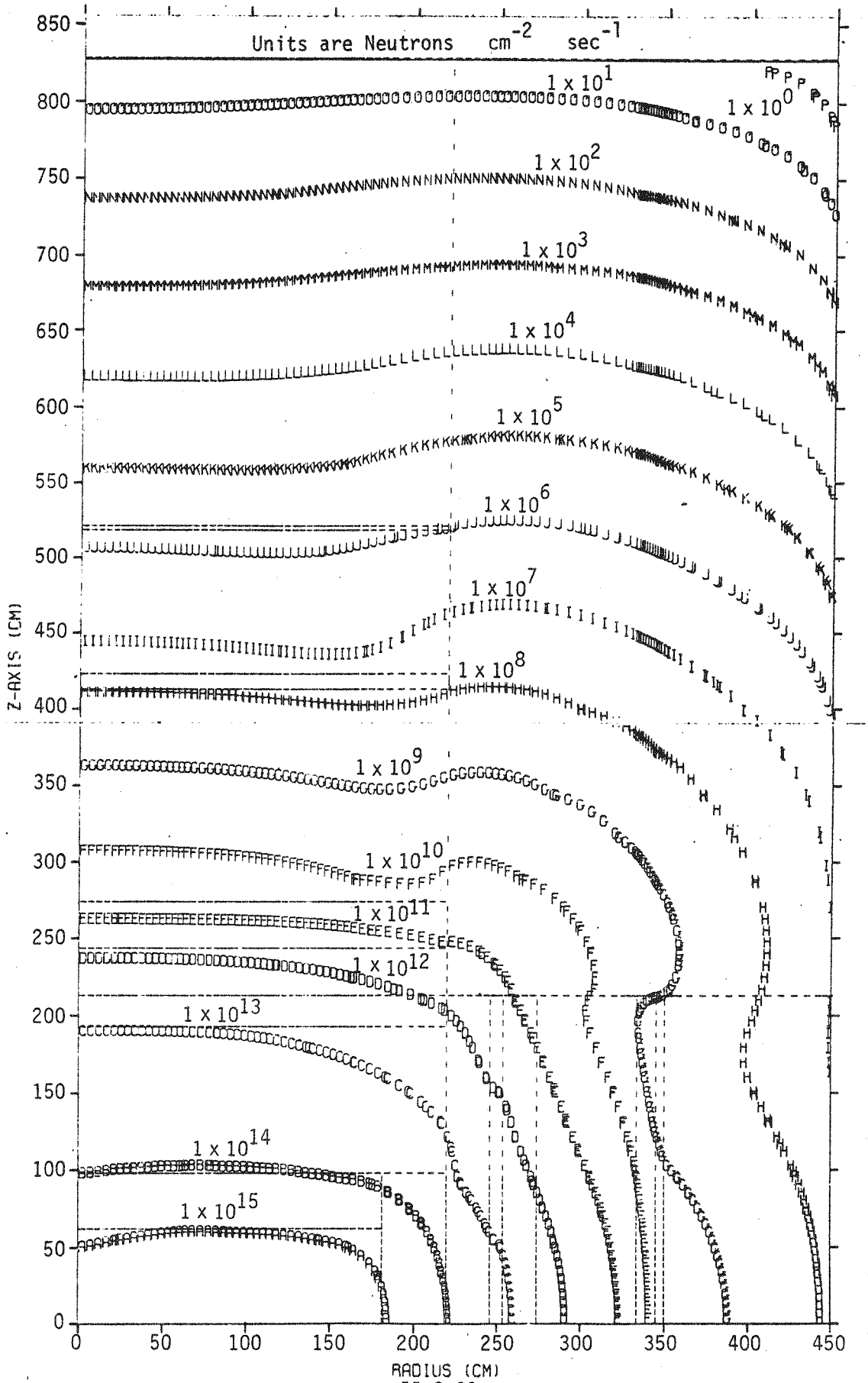

FIGURE 4-12 NEUTRON FLUX DISTRIBUTION ($0.015 < E < 0.5$ MeV IN NEAR-CORE LOWER AXIAL REGION (TWO ROWS OF B_4C RADIAL SHIELD ASSEMBLIES)

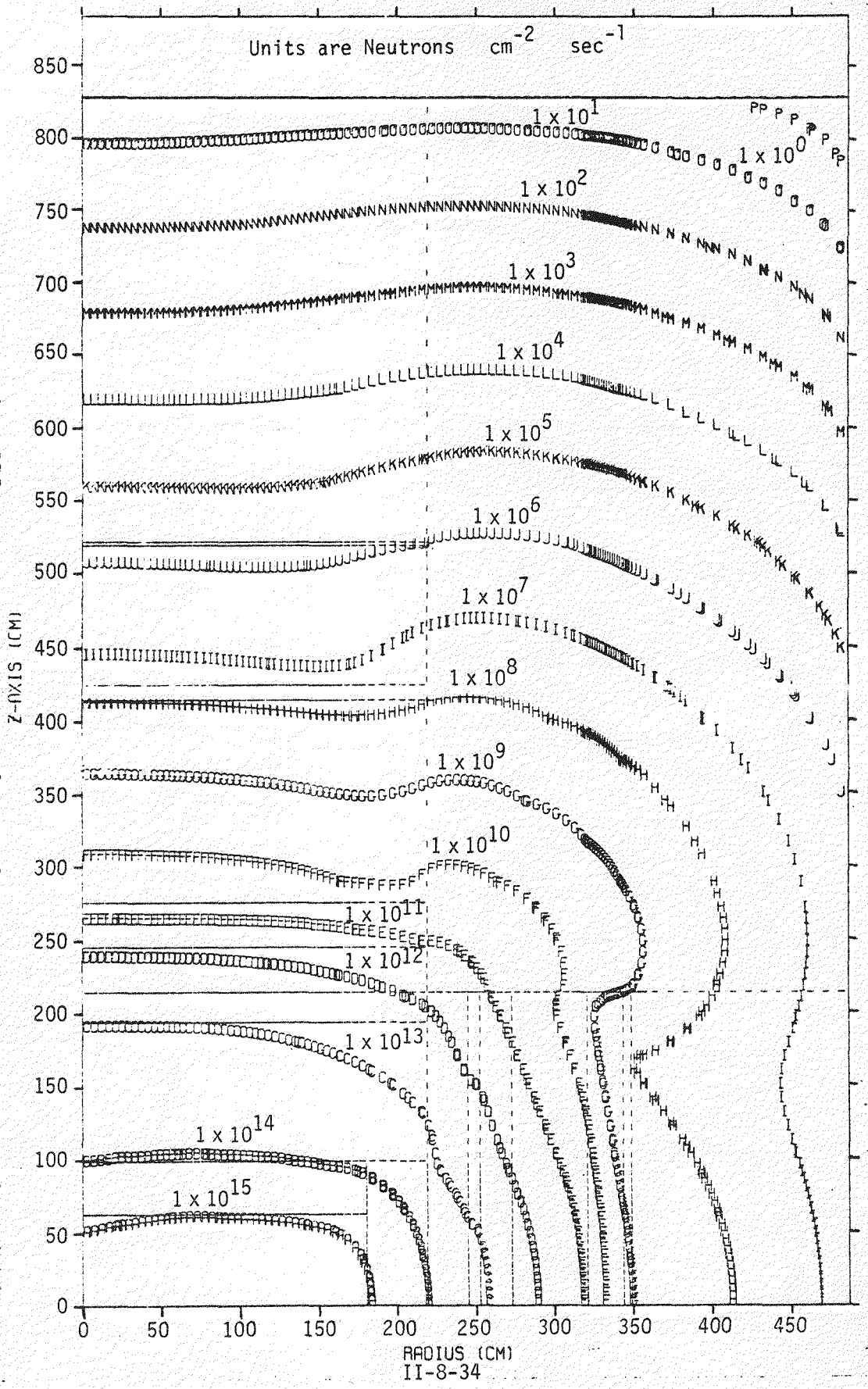

II-8-34

FIGURE 4-13 ONE-DIMENSIONAL GROUP-DEPENDENT NEUTRON FLUXES FOR GE POOL REACTOR*, CORE CENTER-TO-IHX (GROUPS 1 TO 5)

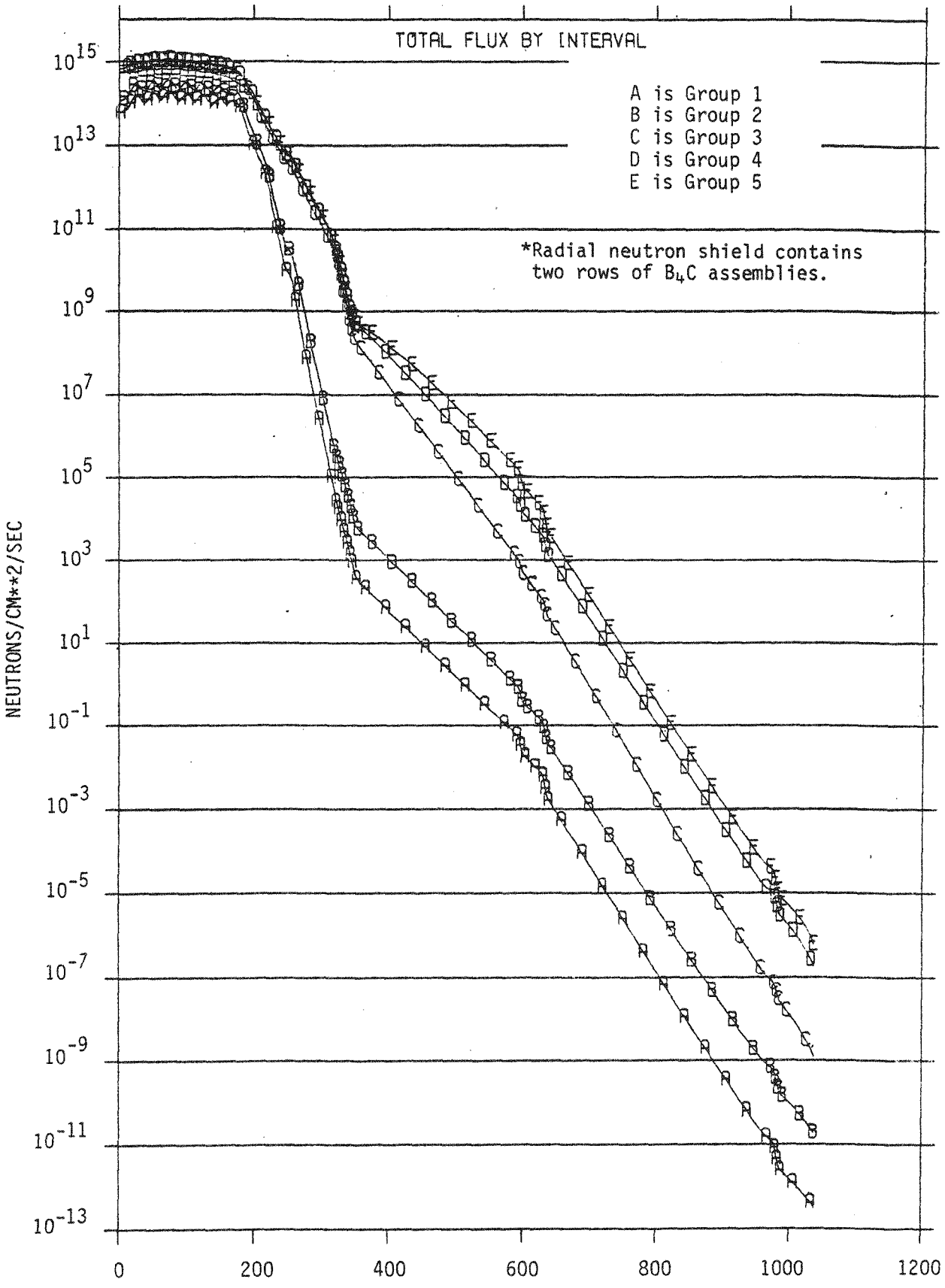

FIGURE 4-14 ONE-DIMENSIONAL GROUP-DEPENDENT NEUTRON FLUXES FOR GE POOL REACTOR*, CORE CENTER-TO-IHX (GROUPS 6 TO 9)

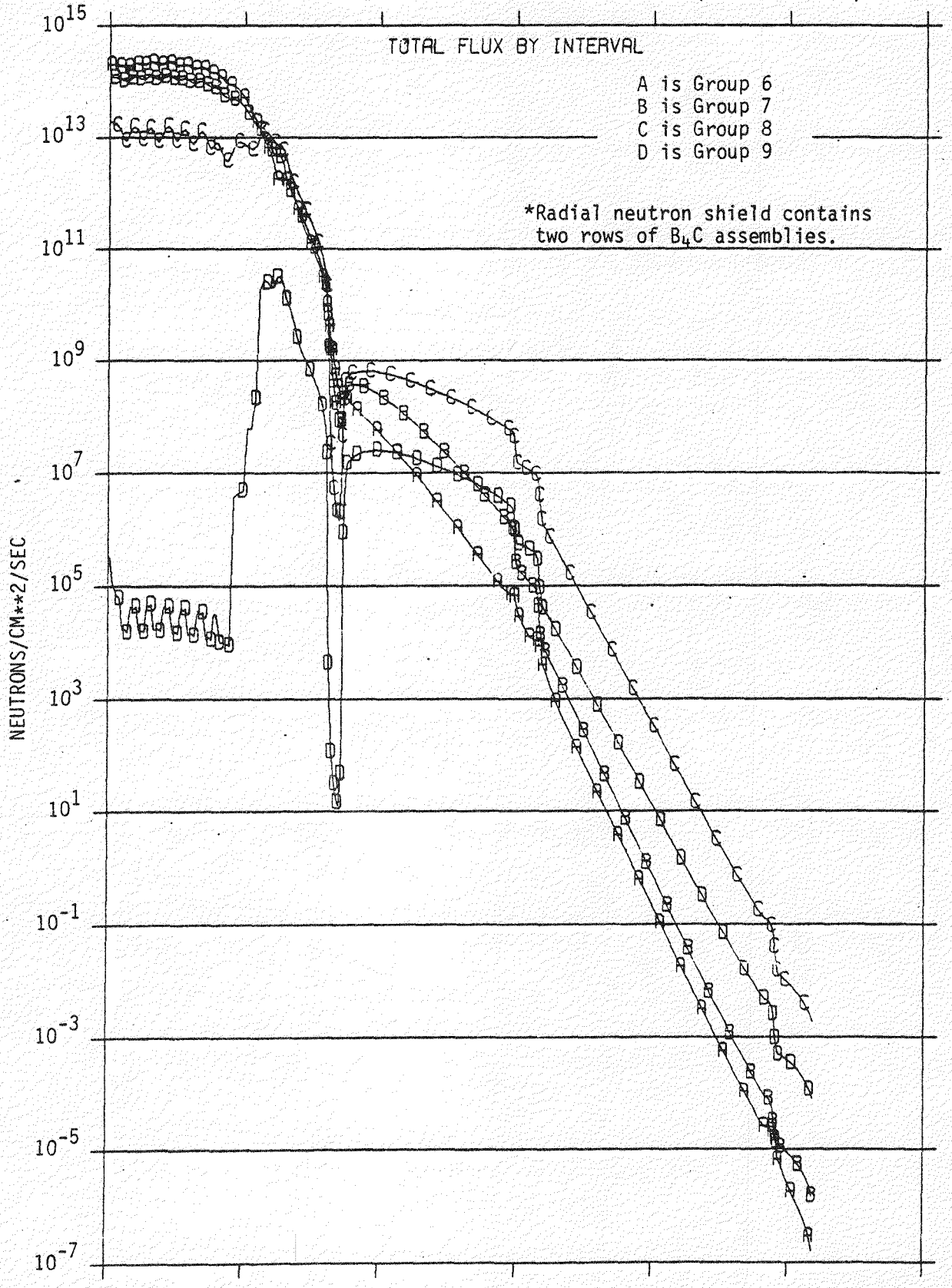

FIGURE 4-15 SELECTED RESPONSE FUNCTIONS FOR RADIAL 1-D CORE-TO-IHX CALCULATION (TWO ROWS OF B_4C ASSEMBLIES)

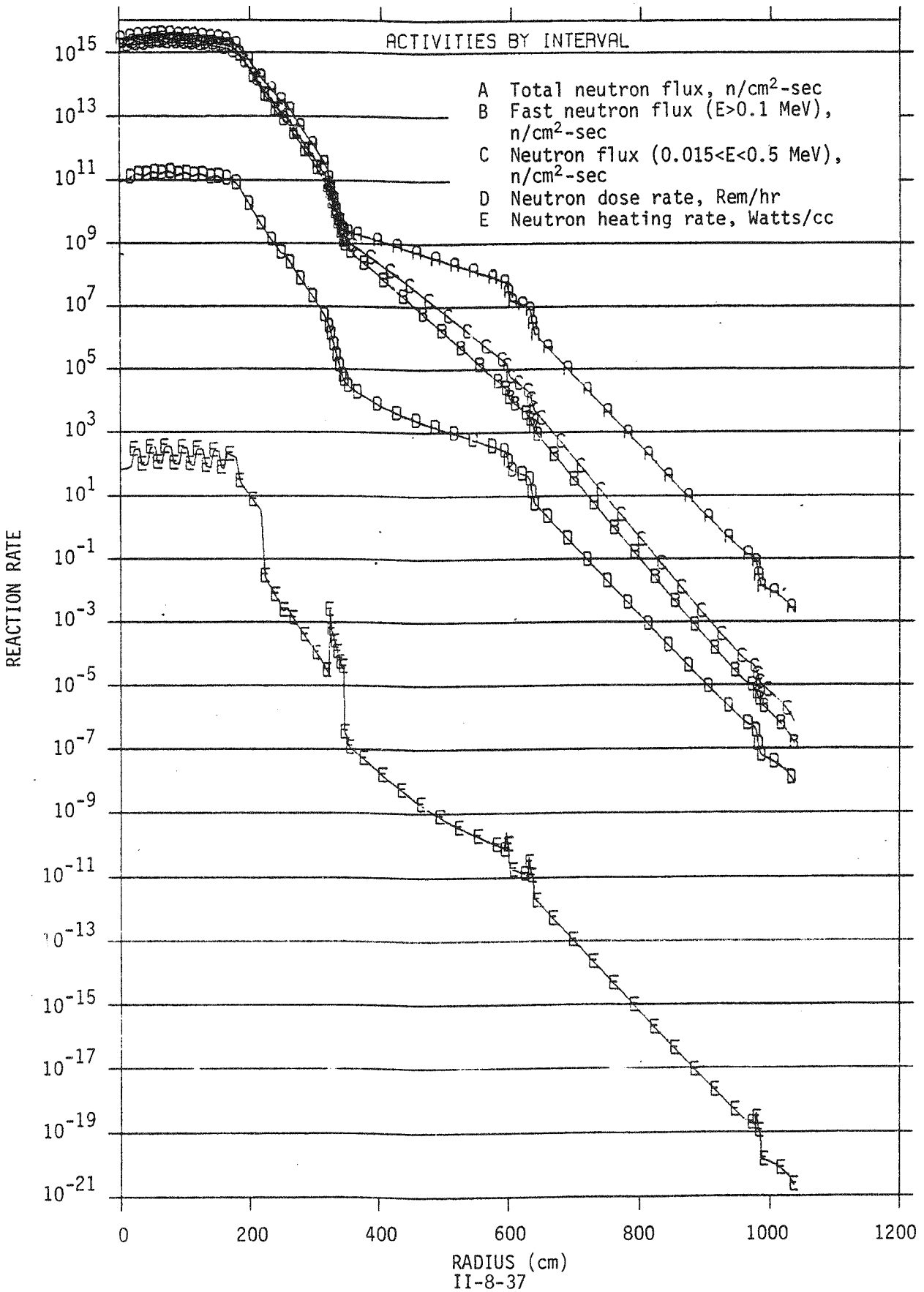

fluxes for a core midplane radial traverse from the core through the center of an IHX to a point 52 cm radially beyond the IHX (R = 1038 cm). The results shown are for a radial neutron shield containing two rows of B_4C assemblies. Figure 4-15 exhibits the radial plots for five different response functions over the same radial interval. These quantities are the 1) total neutron flux, 2) fast neutron flux ($E > 0.1$ MeV), 3) neutron flux ($0.015 < E < 0.5$ MeV), 4) neutron dose rate, and 5) neutron heating rate.

Since the radial 1-D calculations cannot accurately model the 3-D geometry in the region of an IHX, approximate methods were used to calculate the values of the response functions near or inside an IHX. For example, due to the higher transmission rate of neutrons through the sodium regions between the IHX's compared to transmission directly through an IHX, the IHX attenuation of the total neutron flux will not be as steep as is indicated by curve A in Figure 4-15. Therefore, in order to calculate the average total neutron flux inside an IHX it was assumed that 1) the flux at the rear exterior surface of the IHX (R = 986 cm) has the value that would exist at that location if the IHX were completely replaced by sodium, and 2) the flux in the interior of the IHX decreases exponentially going from any point on the IHX wall inside surface toward the IHX center. The total neutron flux shape generated from these assumptions was then used to compute a volume-weighted average for the interior of the IHX; i.e., 8.03×10^4 n/cm^2-sec. This value and the associated 9-group spectrum provide the basis for a reasonably conservative estimate of the activation of the secondary sodium in the IHX's. The value is felt to be conservative since no credit was taken for the decrease in magnitude of the neutron flux in an IHX which will probably occur both above and below the core midplane. The axial variation of the neutron flux in the IHX's should be calculated as a part of the next work phase on the pool reactor.

8.4.5 DOSE RATES FROM ACTIVATION OF IHX STEEL AND SECONDARY SODIUM

Section 2 suggests that a reasonable dose rate limit for maintenance operations is a maximum of 2 mR/hr for a detector located at a point 3 feet from the surface of a large undrained secondary sodium pipe (or 20 mR/hr for a drained IHX or pump). In order to calculate these dose rates, neutron

fluxes and spectra were taken from the radial SN1D transport calculation at a point on the surface of the IHX (R = 630 cm) and at a point corresponding to the volume averaged total flux inside the IHX as described previously. The neutron sources described above were then input to the ACT-II computer program (14) to calculate the gamma source strengths for activated IHX steel and secondary sodium under the assumption that the IHX is continuously irradiated during reactor operation at a load factor of 0.8. For the treatment of secondary sodium activation the neutron fluxes were reduced by a factor of 4.73 to account for the fact that typical volume elements of secondary sodium are irradiated only during the time they spend in the IHX during their flow around the secondary loop.

The gamma source strengths calculated with ACT-II were input to the ISOSHLD computer program (15) along with simple cylindrical models of the IHX and secondary sodium piping to calculate dose rates. The gamma dose rates due to activated steel were calculated at 0, 3, and 10 feet from the surface of the drained and washed IHX in the IHX midplane. The computed values are respectively 12.3, 8.3, and 4.0 mR/hr at reactor shutdown. It is assumed for the purposes of this discussion that, prior to any extensive maintenance, the IHX has been drained and washed so that dose rate contributions from plated-out fission products and corrosion products have been greatly reduced (by a factor 10^2 to 10^3) below their pre-washed values. Otherwise, the dose rate due to IHX steel activation would probably be dominated by these other sources by 1 to 2 orders of magnitude or more. It is encouraging to note that experience reported for Phenix plant IHX maintenance indicates that washing procedures are very effective and that dose rate reductions of up to 10^3 are achievable (16).

The gamma sources for the secondary sodium were used to calculate the dose rates at 0, 3, and 10 feet from the surface of the insulation of a 3' diameter, 100' length of secondary sodium piping. The computed values are respectively 2.4, 1.1, and 0.45 mR/hr during reactor operation and 3.4×10^{-4}, 1.5×10^{-4}, and 5.2×10^{-5} mR/hr at 10 days after shutdown. The pipe insulation was assumed to be 1 foot thick and have a density of 11 lb/ft^3.

For two rows of B_4C shield assemblies, the calculated dose rate values at 3' from the IHX or secondary sodium pipe surface are therefore seen to be

acceptable if 20 and 2 mR/hr are chosen as the respective limits. It is of interest to note that the use of only one rather than two rows of B_4C shield assemblies would result in about a factor of five increase in the quoted dose rates. It should again be emphasized, however, that there is a large uncertainty (factor of 10 to 100) in the magnitude of the neutron flux incident on the surface of the IHX. For this reason it is considered desirable to incorporate a two-inch B_4C or stainless steel shield annulus around each IHX (and possibly each pump). This design feature is suggested in order to accommodate the uncertainty in the incident neutron flux and also anticipates future identification of radial neutron streaming problems which will most likely only become fully apparent when the reactor design is more thoroughly analyzed during follow-on studies.

8.4.6
CALCULATED NEUTRON DAMAGE RESPONSE FUNCTIONS FOR NEAR-CORE STEEL STRUCTURES

Three types of damage response functions were considered in evaluating the susceptibility to neutron damage of the current pool design. First it is recalled that the discussion in Section 2 indicates that a residual total elongation (RTE) criterion of 10% was used to establish neutron fluence limits for CRBR. A value of 0.9×10^{22} n/cm^2 was quoted as a spectrum-insensitive total neutron fluence limit at 371°C (700°F). Spectrum-dependent total fluence limits of 1.7×10^{22} and 2.7×10^{22} n/cm^2 were quoted as appropriate values, respectively, for the fixed radial shield and for the core former support ring. These three fluence values translate into flux limits of 9.0×10^{12}, 1.7×10^{13}, and 2.7×10^{13} n/cm^2-sec, respectively, for a 40-year reactor life operating at a load factor of 0.8.

These limits may be used to give an approximate evaluation of the likelihood of radiation damage to near-core steel structure in the current pool design. Inspection of Figure 4-2 shows that the peak flux in the inner radial shield is about 2×10^{14} n/cm^2-sec and the peak flux in the core former is about 2×10^{13} n/cm^2-sec. It would therefore appear that consideration must be given to the possible need of periodic replacement of the inner (steel) shield assemblies and that a more refined analysis needs to be made of potential damage to the core former to assure that a reasonable design margin exists. The peak flux in the lower end of the upper axial core

shield is seen to be about 7×10^{13} n/cm^2-sec so replacement of steel shielding in the assemblies may have to be considered (e.g., due to swelling problems). Potential damage in the lower axial structure may be evaluated by inspection of Figure 4-4. It can be seen from this figure that the peak total flux in the lower axial shield is about 2×10^{13} which indicates that there will possibly be some limited damage to the steel in this region. Structures below the lower axial shield will be exposed to fluxes $\leq 1 \times 10^{13}$ n/cm^2-sec if design measures are taken to avoid the presence of significant neutron streaming paths through vertical sodium channels in this region. However, some degree of neutron streaming through lower axial sodium channels will be unavoidable and this problem should be carefully treated in future studies.

The second type of damage response function which was computed is simply the fast neutron flux (or fluence); i.e., for $E > 0.1$ MeV. A fast neutron fluence limit of 1.0×10^{22} n/cm^2 has been used frequently in the past as a design criterion. This corresponds to a fast neutron flux limit of 1.0×10^{13} n/cm^2-sec. Inspection of Figures 4-6 and 4-8 clearly shows that this criterion is not as conservative as the total fluence criteria discussed previously. The flux contours for 1×10^{13} n/cm^2-sec indicate that this limit is exceeded only in a region bounded by the core former and the upper and lower near-core axial shields. It is therefore recommended that this particular damage response function not be used as a design criterion.

The third type of damage response function which was computed is the number of metallic crystal lattice displacements per steel atom (dpa). This quantity was computed at each of the six points indicated in Figures 3-4 and 3-5. Specifically, these six locations are the:

1) Inner surface of the core former at the core midplane.
2) Bottom of the upper axial steel shield in the first ring of fuel assemblies.
3) Top of the upper axial steel shield in the first ring of fuel assemblies.
4) Bottom of the Upper Grid Plate on the core axial centerline.

5) Top of the core lower axial shield on the core axial centerline.

6) Top of the uppermost lower core support plate on the core axial centerline.

The calculations are summarized in Table 4-1. The calculational procedure used FTR 18/10 stainless steel displacement cross sections which were averaged over several neutron spectra [$\phi(E)$] of interest (16,17). These cross sections were plotted as a function of spectrum average neutron energy as shown in Figure 4-16. They provide a relative measure of the number of displacements per unit fluence in various spectral environments. The actual displacement rates (per unit time) are obtained by multiplying the cross sections by the appropriate fluxes. Thus

$$\bar{\sigma}_d = \frac{\int \phi(E)\sigma_d(E)dE}{\int \phi(E)dE} = \frac{\int \phi(E)\sigma_d(E)dE}{\phi_{TOT}}$$

and, displacements per atom per second (dpa/s) = $\bar{\sigma}_d \cdot \phi_{TOT}$

or, dpa = $\bar{\sigma}_d \cdot \phi_{TOT} \cdot t = \bar{\sigma}_d \cdot$ (fluence)

The neutron damage limit criterion currently in use for CFR is 2 dpa. Table 4-1 shows that only one of the 6 points evaluated has a dpa value that significantly exceeds this limit; i.e., the value 4.13 dpa for a point at the bottom of the upper axial steel shield.

As was mentioned in Section 2, the neutron damage fluence limits for the GE-ARSD 1000 MWe Pool-Type LMFBR have not yet been firmly established. Further analyses of the type discussed here are needed to determine these criteria.

8.4.7
HELIUM AND TRITIUM GAS GENERATION IN B_4C SHIELD ASSEMBLIES

The B-10 (n,α) reaction rate representing the helium generation can be obtained from the (n,α) power generation as given below.

The total energy release in the B-10 (n,α) reaction is 2.79 MeV as obtained from a mass balance for the reaction

$$_5B^{10} + {}_0n^1 \rightarrow {}_3Li^7 + {}_2He^4$$

TABLE 4-1 NEUTRON SPECTRA AND DPA* VALUES FOR SELECTED LOCATIONS IN STEEL STRUCTURE OF POOL R-Z DIFFUSION MODEL

9-GROUP NEUTRON FLUX AT SIX LOCATIONS
(neutrons · cm^{-2} · sec^{-1})

	$\bar{E}$ (eV)	1	2	3	4	5	6
1	6.680+6	4.39+9	5.04+10	3.14+5	4.84+3	1.90+9	1.02+1
2	1.353+6	2.26+10	6.54+10	1.95+6	6.22+4	6.09+9	6.03+2
3	3.878+5	3.58+12	6.02+12	7.19+10	7.54+9	1.87+12	2.20+6
4	8.653+4	5.80+12	9.73+12	1.32+11	2.01+10	3.28+12	2.70+7
5	1.931+4	6.26+12	1.24+13	1.74+11	2.91+10	4.55+12	6.07+7
6	4.308+3	2.55+12	3.64+12	5.44+10	1.63+10	1.34+12	5.86+7
7	9.612+2	3.68+12	8.89+12	1.22+11	2.01+10	3.42+12	8.24+7
8	1.760+1	6.73+12	1.85+13	3.06+11	6.86+10	8.92+12	8.78+8
9	1.847-1	2.53+10	4.28+10	7.42+8	1.61+9	2.08+10	2.90+7
	$\Sigma\phi$	2.86+13	5.93+13	8.61+11	1.63+11	1.89+13	1.14+9
	$\Sigma\phi\bar{E}$	2.08+18	3.86+18	4.30+16	5.32+15	1.04+18	4.71+12
	$\bar{E}$ (eV)	7.28+4	6.51+4	4.50+4	3.25+4	5.50+4	4.14+3
	$\bar{E}$ (MeV)	.073	.065	.045	.032	.055	.0041
	$\bar{\sigma}_d$ (b)	76	69	52	39	61	8.5
	dpa	2.19	4.13	.045	.0064	1.16	9.8-6

Note: See Figures 3-4 and 3-5 for location of six points.

*dpa = "Displacements per atom", i.e., no. of metallic crystal lattice atom displacements per steel atom.

$= \bar{\sigma}_d \times \phi \times t \times 10^{-24}$

where $\bar{\sigma}_d$ = displacement cross section, barns (read from Figure 4-16).

and $t = 40y @ .8 = 1.01 \times 10^9$ sec.

FIGURE 4-16 VARIATION OF THE DISPLACEMENT CROSS SECTION FOR STAINLESS STEEL WITH NEUTRON MEAN ENERGY IN THE FTR

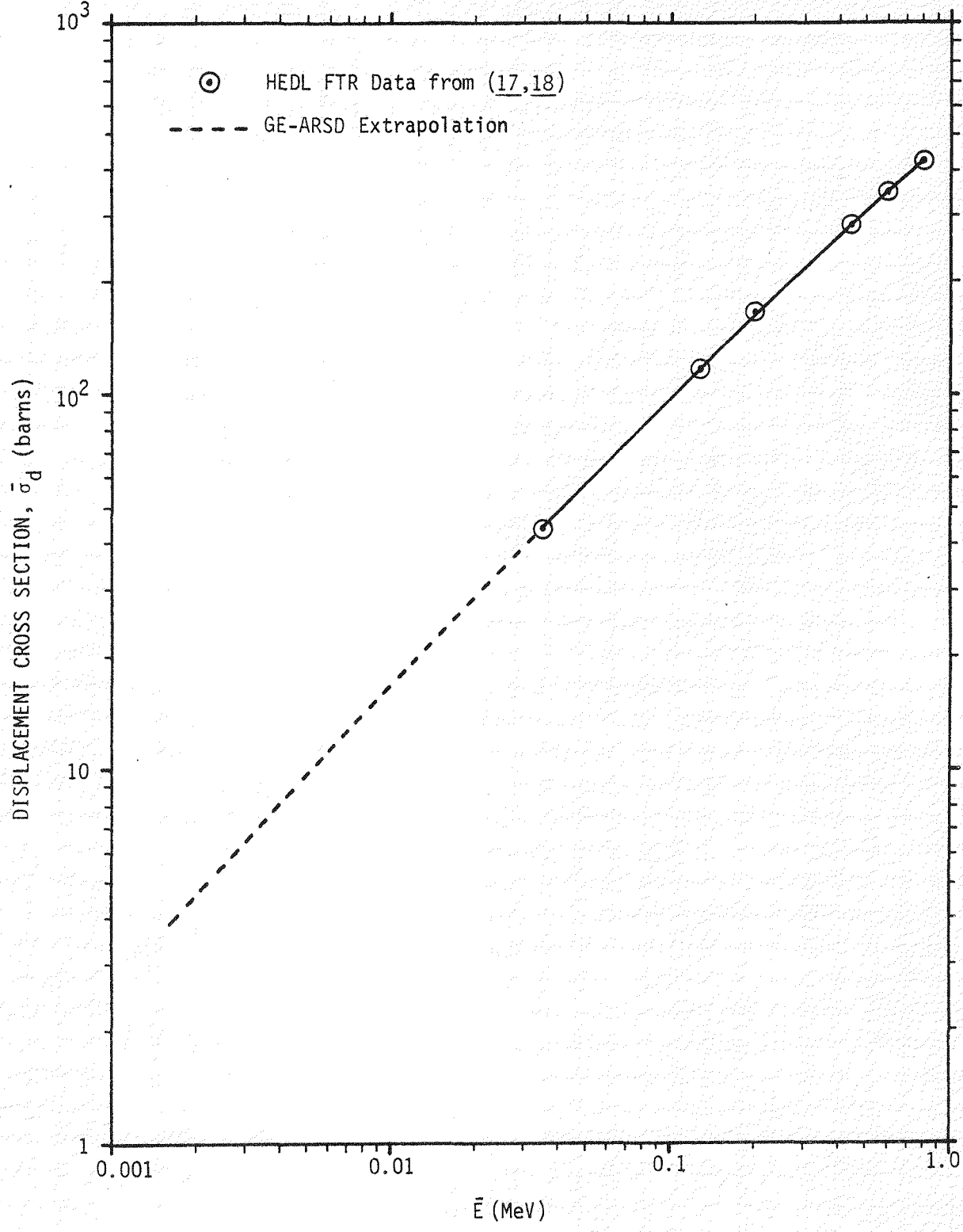

In 95% of the thermal capture events, the Li^7 nucleus is left in an excited state and a 0.478 MeV gamma is emitted. This gamma ray energy is included in the gamma ray heating rates. The net alpha energy per reaction is then:

$$2.79 \times 0.05 + (2.79 - 0.478) + 0.95 = 2.34 \text{ MeV}$$

The relation between power density and reaction rate is given by R_{He} = atom rate of helium production, PD = power density, ER = energy release per reaction):

$$R_{He} = \frac{RD}{ER} = \frac{PD \text{ Watts/cm}^3 \text{ (PN - .078)}}{2.34 \text{ MeV} \times 1.602 \times 10^{-13} \frac{\text{Joule}}{\text{MeV}}} \times \frac{1 \text{ Joule/sec}}{\text{Watt}}$$

$$R_{He} = (2.67 \times 10^{12}) \text{ (PN - .078) PD } \frac{\text{atoms}}{\text{sec-cm}^3}$$

where PD = Watts/cm^3

PN = fraction that $B_{10}(n,\alpha)$ contributes to total heating rate = 1.0.

The neutron kinetic energy deposition due to elastic scattering with Boron or Carbon is 7.8% of the (n,α) heating rates generated in the heating rates displayed in Figure 4-15. This energy is therefore included as a correction term in the above helium generation correlation.

The neutron heating rate data in Figure 4-15 was used to determine peak and average core midplane heating rates for the combined two rows of radial B_4C shield assemblies. These values were determined to be 3.85×10^{-2} and 6.62×10^{-3} watts/cm^3, respectively. A straightforward application of the above helium generation algorithm then yields 9.52×10^{19} and 1.64×10^{19} atoms/cc, respectively, for the peak and average cumulative amounts of helium generated in the B_4C assemblies for a 40 year reactor life at a load factor of 0.8.

A typical CRBR B_4C control rod design limit is approximately 1.65×10^{22} atoms/cm^3 for 328 full power days. Thus, even the peak cumulative generation of 9.52×10^{19} atoms/cc is lower than this limit by a factor of 173. The relatively low helium generation and, consequently, the lower pressure buildup

in the radial B_4C shield assemblies is primarily due to the lower neutron capture rate (lower thermal neutron flux) at this out-of-core location. In addition to the effect of the lower thermal flux, the lower temperature of the B_4C and the helium gas in the shield assemblies will lead to a further reduction in pressure relative to in-core B_4C control rod conditions. As a consequence of the above analysis, it appears that helium generation in the B_4C shield assemblies will not present a major design problem on the basis of pressure buildup considerations. However, it will probably be necessary to allow for at least a small plenum in these assemblies and this possibility should be further evaluated.

It was pointed out in Section 2 that the cross section for helium production is several orders of magnitude greater than that for tritium production. Since the cumulative helium generation in the B_4C shield assemblies is low, it was considered unnecessary to calculate the tritium production rate for the current analysis. However, this information will be generated later as the need arises for evaluation of potential biological radiation hazards.

The preceding discussion was specifically focused on the problem of helium generation in the B_4C radial shield assemblies. However, the conclusions also have implications for the feasibility of using annular B_4C shielding "blankets" around the IHX's and pumps. It can be inferred from the results for the radial shield assemblies and from the 1-D neutron heating rate curve in Figure 4-15 that the peak and average helium generation rates in such "blankets" would be about a factor of 10^6 lower than the respective values in the shield assemblies. Consequently, helium and tritium pressure build-up should not be a significant design problem for this type of shielding.

II-8.5

IMPACT ON REACTOR ASSEMBLY DESIGN

Work in Phase A did not include core design or precise shielding design. For sizing and arrangement of the reactor assembly a core envelope which included removable shield assemblies was established. From preliminary calculations and examination of other LMFBR designs additional lateral neutron shielding around the core barrel was judged necessary. That shielding is shown in Figure 3-1, and is described in Subsection 4.5 of Reference 1.

The analyses showed the Phase A shielding to be inadequate. More shielding can be installed, however, without changing the size or basic configuration of the reactor assembly, and without adding massive shielding structure.

8.5.1 FUEL AND BLANKET ASSEMBLIES

The Phase A reactor arrangement was based on fuel and blanket assemblies 225 inches long. Approximately 75 inches in the upper end of each assembly is allocated to gas plenum and shielding. For this investigation the shielding portion length has been set at 34 inches. The analyses assumed the shielding configuration to be extensions of the pins within the assemblies. When fuel assembly design proceeds, different configuration might evolve. At that time consideration can be given to optimizing cross section for flow and shielding efficiency, and to separation of the shielding from the pins to ease fabrication and reprocessing.

8.5.2 REMOVABLE RADIAL SHIELD ASSEMBLIES

To comply with the analysis results, a second row of B_4C filled shielding assemblies has been added outside of the core barrel assembly. The new B_4C row replaces a row of solid stainless steel assemblies. The new radial shielding arrangement is shown on Figure 3-1. As stated in Reference 1, if more stainless steel were used instead of B_4C, the volume and weight increases would be very large. All major

components of the reactor assembly; i.e., both vessels, the core support platform, the reactor closure, and the deck structure would need to be enlarged. Reference 1 elaborates on the B_4C /stainless steel comparison.

8.5.3
INLET PIPE REGION

Figures 4.3 and 4.4 show streaming paths in the annular structure of the core support platform through which the inlet pipes pass. Shield plates have therefore been added in this region. They are shown in Section EE-EE on Figure 4-17.

8.5.4
COMPONENT SHIELDING

To account for uncertainties the report recommends that 2 inches of steel shielding be located around the pumps and IHXs. The Phase A design is adaptable to this recommendation. Thermal barriers having a total thickness of not less than two inches now surround each pump. The thermal barriers extend two feet above the hot sodium pool surface, leaving a three foot gap to the underside of the deck insulation. The thermal barrier and the gap are shown on Figure 4-18. Should future shielding analyses show the need to close the gap, the thermal barriers can readily be extended upward.

Each heat exchanger is enveloped by an inlet shroud extending down from the underside of the deck structure to almost the top of the horizontal insulation on the core support platform. In the Phase A design the shroud needed to be only thick enough to retain its shape while serving as a flow channel. The shroud can readily be thickened to the two inches recommended for shielding purposes. The thickened shroud is shown on Figure 3-2.

8.5.5
SHIELDING DESIGN FLEXIBILITY

In each of the shielding regions discussed in previous paragraphs, good potential exists for improving the shielding more if necessary. This flexiblity is important, particularly for avoiding massive shield structures projecting above the core in the outlet flow region.

In the blanket and fuel assemblies, a few additional inches of steel seem possible. Around the core barrel another row of B_4C assemblies, or alternating rows of B_4C and stainless steel assemblies are possibilities. At the inlet pipe region,

additional steel below the pipe centerlines will further close the streaming paths. Around the IHXs, the shrouds can be thickened, and around the pumps the outer thermal barrier cylinder can be thickened. The validity of each of these measures must, of course, be confirmed by shielding and structural analyses.

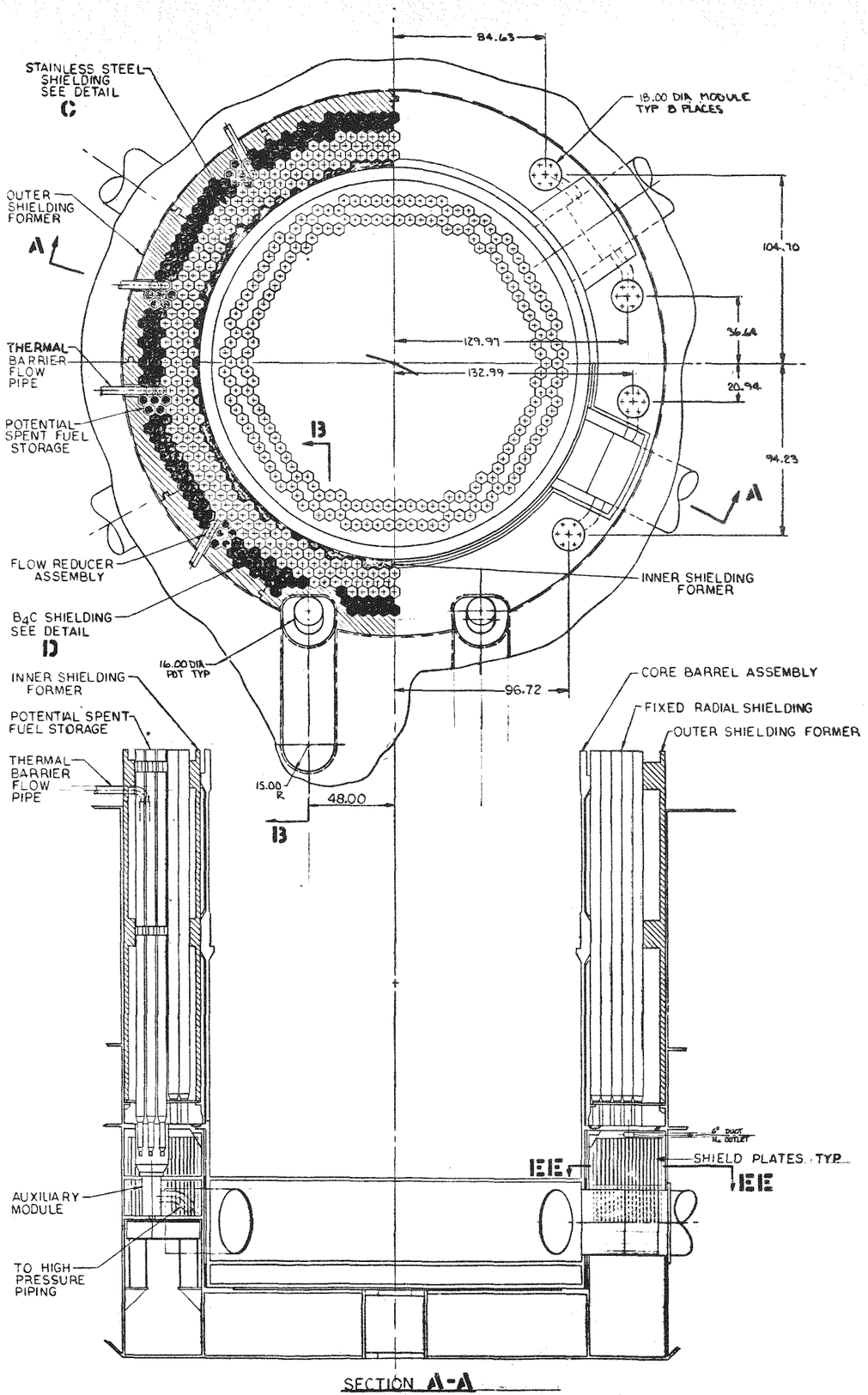

SECTION A-A

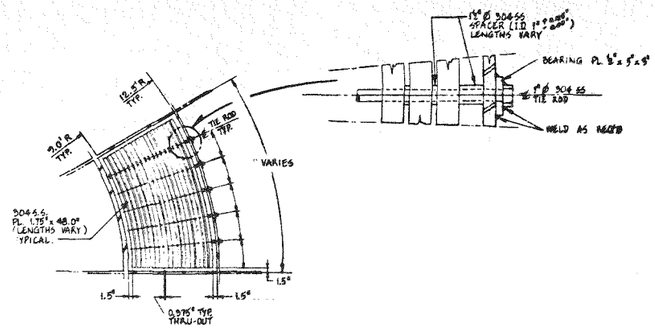

SECTION EE - EE
TYPICAL SHIELD PLATE ASSEMBLY

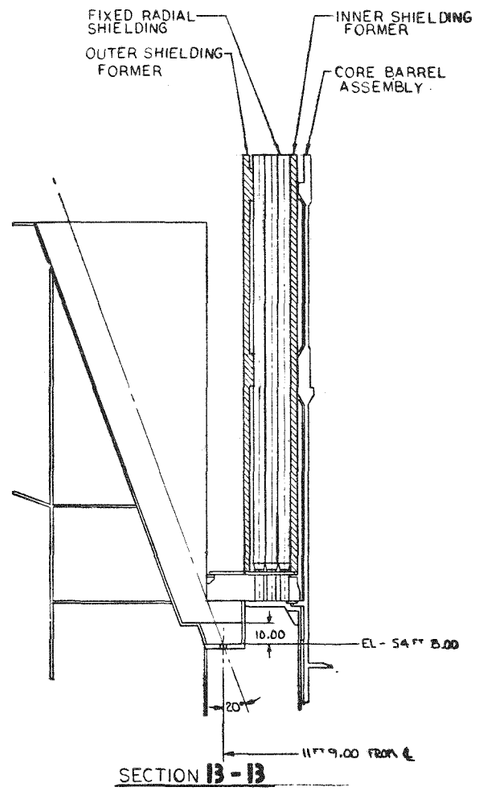

SECTION B - B

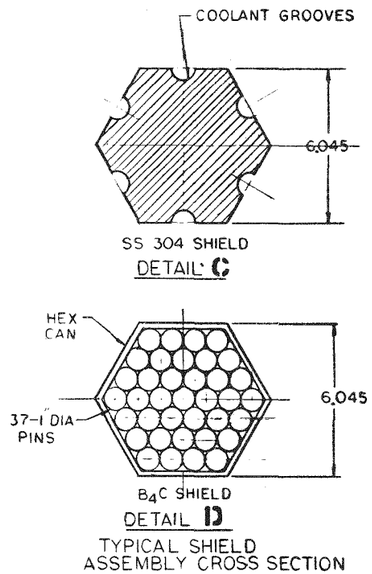

TYPICAL SHIELD ASSEMBLY CROSS SECTION

Figure 3-1 Shielding Around the Reactor

SODIUM SURFACE LEVELS - TRANSIENT AND ACCIDENT CONDITIONS

CONDITION	SODIUM SURFACE LEVEL
SHUTDOWN TO 400°F	(-) 21'-10"
SHUTDOWN TO 595°F	(-) 20'-4"
PUMPS TRIPPED & BEFORE COOLDOWN	
HOT POOL	(-) 18'-9"
COLD POOL	(-) 20'-6"
AFTER PRIMARY VESSEL	
SODIUM @ 595°F	(-) 25'-8"
SODIUM @ 550°F	(-) 25'-9"
SODIUM @ 400°F	(-) 26'-9"

* REFERENCE ELEVATION 0-0 CORRESPONDS TO BUILDING ELEVATION 60 FT 0.0

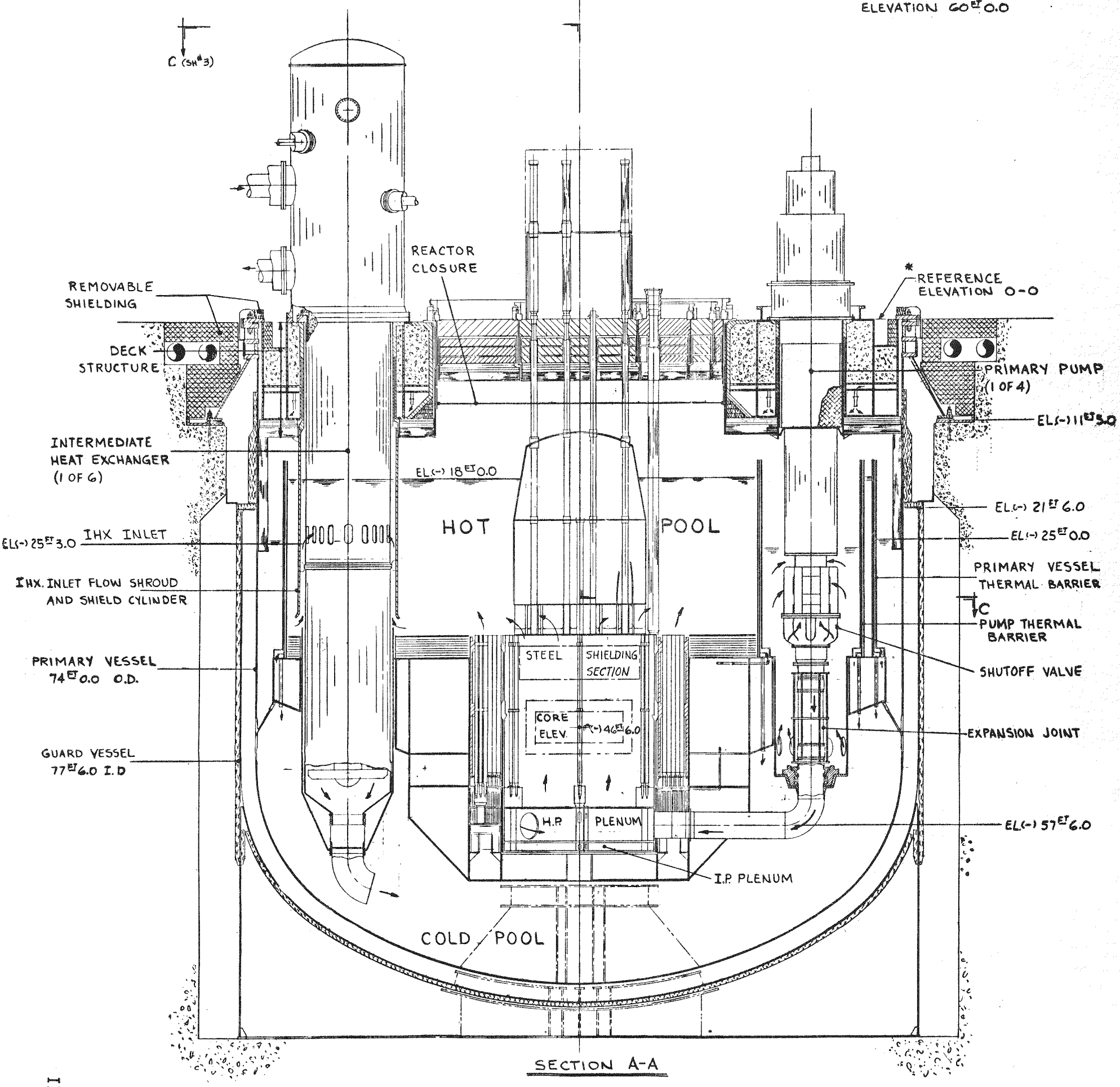

SECTION A-A

Figure 3-2 Reactor Assembly Arrangement Elevation

II-8.6

CONCLUSIONS

The work reported here has defined a near-core neutron shield for protection of IHX's and pumps in the GE-ARSD 1000 MWe Pool-Type LMFBR design. This preliminary analysis indicates that it is possible to design an adequate shield without resorting to the introduction of massive amounts of steel radial shielding in the sodium pool region outside the working perimeter of the core assembly handling equipment. This is a design decision of primary importance since the presence of massive shields in this region would introduce seismic, primary coolant circulation, and structural support problems into the design.

An examination of the core and inner blanket assembly designs has indicated that shield pin lengths of up to 34 inches of steel can be included in the upper axial regions of these assemblies. This amount of shielding was used in the present analysis and was found to be adequate within the uncertainties of the methods used. However, further analysis needs to be done using more accurate transport methods to provide some degree of optimization for the shield design. It is possible that a 34 inch upper axial assembly shield length may be found to be excessive for IHX and pump protection requirements, although it should be pointed out that the impact of this shield length on the biological shield design in the region of the deck must also be considered.

The current lower axial shield design was found to be inadequate from the standpoint of IHX and pump protection due to neutron streaming through the annular region just below the radial steel shield assemblies. A design change which adds steel shielding in this region is now being implemented.

In addition to the calculations performed to determine the attenuation provided by the reactor neutron shield, an evaluation was made of potential neutron damage to near-core steel structures. The data for three types of damage response functions were examined. It is concluded on the basis of spectrum dependent fluence limits criteria that consideration must be given

to the possible need of periodic replacement of the inner (steel) radial shield assemblies. Also, a more refined analysis needs to be performed to evaluate the potential damage to the core former and to assure that a reasonable design margin exists. In addition, there is a likelihood of some damage (e.g., swelling) in 1) the upper and lower axial shields within the fuel assemblies, and 2) the core support structure below the lower axial shield. When more refined calculations are performed, careful attention should be given to evaluating the potential for damage in these regions and the necessary accommodations in the design or design criteria should be determined.

In order to provide the required neutron attenuation in the radial neutron shield without increasing the outside diameter of the shield beyond the rather compact current design envelope it was found that two rows of B_4C shield assemblies were needed at the periphery of the radial shield. The boron in the B_4C was assumed to have the isotopic composition of natural boron. Helium and tritium gas generation rates were calculated for these assemblies and appear unlikely to present a significant design problem on the basis of a 40-year reactor life operating at a load factor of 0.8. However, it is recommended that this problem be further evaluated. If necessary these gases could be vented.

Due to the limitations of the methods which were necessary in this preliminary analysis (2-D diffusion and 1-D radial transport calculations), it is assumed that an uncertainty of at least an order of magnitude exists in the prediction of the neutron fluxes at the surface of the IHX's and pumps; i.e., the fluxes are underpredicted. It is therefore recommended that a 2 inch thick steel or B_4C "blanket" annular shield be assumed as necessary around each IHX and pump until this uncertainty can be reduced by more accurate calculations. In addition to the need for accommodating this uncertainty there is a likelihood that such annular "blanket" shields will be needed to accommodate neutron streaming through near-core shield penetrations that will only become fully apparent when the reactor design is further refined during follow-on studies.

Actually, these annular shielding "blankets" may serve other purposes besides neutron shielding. In the phase A design, each heat exchanger is enveloped

by an inlet shroud entending down from the underside of the deck structure to a plane near the top of the horizontal insulation on the core support platform. This shroud need only be thick enough to retain its shape while serving as a flow channel and can readily be thickened to the two inches recommended for shielding purposes. Also, thermal barriers having a total thickness of no less than two inches now surround each pump. The thermal barriers extend two feet above the hot sodium pool surface, leaving a three foot gap to the underside of the deck insulation. Should future shielding analyses show the need to close the gap, the thermal barriers can readily be extended upward. If necessary, the thermal barriers could also be thickened to provide more shielding.

Shielding provisions can have inordinate impact on design and cost if not given early and sufficient attention. The current analyses is necessarily based on an inexact core, assumed criteria and approximate modeling. The design has not yet examined cost effects of shielding alternatives, the loads produced by the new shielding, or the influence of the shielding on the operation of the reactor system. Also still to be considered are the shielding design requirements of auxiliary system equipment (cold traps, auxiliary cooling system heat exchangers, etc.), the reactor closure, and the deck structure.

REFERENCES

(1). Prototype Large Breeder Reactor; Phase II: Conceptual Design; Volume II: Plant Description; Part 2: Balance of Plant, Bechtel Report BTR-8, June 1977.

(2). J. Goddet, A. LaCroix, and B. Vial, "Rapsodie and Phenix Plants Intermediate Heat Exchangers Experience", Trans. Am. Nucl. Soc., 27, 221 (1977).

(3). L.D. Blackburn and R.L. Knecht, "Irradiation Effects and Design of LMFBR Permanent Reactor Structures", in Nuclear Reactor Shielding, Science Press, 1977.

(4). R.A. Moen, J.C. Tobin, and K.C. Thomas, "Neutron Fluence Limit Determinations for Some Fast Flux Test Facility Components", p. 409 in Irradiation Effects on Structural Alloys for Nuclear Reactor Applications, ASTM STP 484, American Society for Testing and Materials, Philadelphia, 1970.

(5). L.D. Blackburn, J.M. Steichen, and R.L. Knecht, "Postirradiation Tensile Properties of Annealed 304 and 316 Stainless Steels", p. 193 in Cladding and Structural Materials Semi-Annual Progress Report - January 1975 to July 1975, Report HEDL-TME 75-77 (October 1975).

(6). W.J. McAfee and T.W. Pickel, Preliminary Elevated - Temperature Core Structures Design Criteria, Report ORNL-TM-4932 (March 1976).

(7). "Nuclear Data and Methods Development and Application to LMFBR's, Fiscal Year 1977, GE-FBRD, GEFR-14073-3, November 1977.

(8). "Cooperative Nuclear Data and Methods Development - Quarterly Progress Report for Period January - March 1978", GE-FBRD, GEFR-14074-9, April 1978.

(9). "Pool-Type LMFBR Plant, 1000 MWe Phase A Design", Part IV, Sections 1-6; EPRI NP-646, April, 1978.

(10). R. Protsik, "Users Manual for SN2D, A Two-Dimensional Multigroup Discrete Ordinates Transport/Diffusion Theory Code", GE-FBRD, NEDE-13747, August 1971.

(11). R. Protsik, "SN1D - A One-Dimensional Discrete Ordinates Transport Code with General Anisotropic Scattering", GE-FBRD, FBRD-00074(IR), February 1978.

(12). L.S. Abbott and F.R. Mynatt, "Review of ORNL Radiation Shielding Analyses of the Fast Flux Test Facility Reactor", ORNL-5027, July 1975.

(13). W.W. Engle, et al., "Analyses of the Preliminary In-Vessel and Enclosure Shield System Designs for the Clinch River Breeder Reactor (July 1973 - July 1975), ORNL-TM-5338, March 1976.

(14). "ACT-II: Activation Gamma-Ray Source Strength Code - Simple Geometry, Finite Dilution", Astonuclear Laboratory, Westinghouse Electric Corporation, Pittsburgh, Pennsylvania, January 1966.

(15). R.L. Engel, J. Greenborg, and M.M. Hendrickson, "ISOSHLD - A Computer Code for General Purpose Isotope Shielding Analysis", BNWL-236, June 1966.

(16). J. Goddet, et al., "Rapsodie and Phenix Plants Intermediate Heat Exchangers Experience", ANS Transactions, Vol. 27, November 1977; also refer to full text of paper as presented at the ANS meeting.

(17). D.G. Doran, et al., "Report of the Working Group on Displacement Models and Procedures for Damage Calculations", HEDL-TME 73-76, December 1973.

(18). D.G. Doran and N.J. Graves, "Displacement Cross Sections and PKA Spectra: Tables and Applications", HEDL-TME 76-70, December 1976.

PART II: REACTOR ASSEMBLY - STRUCTURES

SECTION 9: ROTATING PLUG SIZE STUDY

CONTENTS

		Page
II-9.1	INTRODUCTION AND SUMMARY	II-9-1
	9.1.1 Introduction	II-9-1
	9.1.2 Summary	II-9-1
II-9.2	DISCUSSION	II-9-3
	9.2.1 General Requirements	II-9-3
	9.2.2 Three Rotating Plug Arrangements	II-9-4
	9.2.3 Two Rotating Plug Arrangements	II-9-4
	9.2.4 One Rotating Plug Arrangements	II-9-6
II-9.3	CONCLUSIONS	II-9-7
	REFERENCES	II-9-9

FIGURES

		Page
2-1	Arrangement Layout Requirements--Plan View	II-9-13
2-2	Arrangement Layout Requirements--Elevation View	II-9-15
2-3	Three Rotating Plugs	II-9-17
2-4	Three Rotating Plugs--Seismic Support Interference	II-9-19
2-5	Two Rotating Plugs	II-9-21
2-6	Two Rotating Plugs--with Transfer Arm	II-9-23
2-7	Two Rotating Plugs--with Transfer Arm (Relocated Support Columns)	II-9-25
2-8	Two Rotating Plugs--Eccentric	II-9-27
2-9	One Rotating Plug--Offset Handling Machine	II-9-29
2-10	One Rotating Plug--Offset Handling Machine with Removable Plug	II-9-31
2-11	Two Rotating Plugs--with Two IVTM's	II-9-33
2-12	Reactor Arrangement Comparison for Concentric and Eccentric Plugs	II-9-35

TABLES

		Page
2-1	Rotating Plug Comparison	II-9-11

II-9.1

INTRODUCTION AND SUMMARY

9.1.1 INTRODUCTION

The reactor Closure Assembly size has always been a concern for the designer during plant component design. The large size components take up valuable space as well as restrict the location of other reactor components. In addition, the larger size rotating plug components are costly and can present fabrication problems as well as limit the possible number of reliable suppliers.

The GE-ARSD recommended LMFBR refueling scheme for an Under-the-Head arrangement has been three rotating plugs. With the interest to reduce component sizes, the three rotating plug reference design was compared with other possible rotating plug schemes. This memorandum describes the results of the study and defines the relative dimensional differences between the various schemes.

9.1.2 SUMMARY

A study was performed during Phase A Extension program to make a comparison and to define the plug sizes of three, two and one rotating plug schemes. To make an adequate assessment of the plug schemes, a set of component sizes and restrictions was also established so that each arrangement layout would be based on a common set of restrictions and requirements. Each arrangement is described in Section 2.0. The three rotating plug concept is still the recommended reference design for the 1000 MWe LMFBR program.

DISCUSSION

The basic arrangement and size of components used for this study were obtained from the previous LMFBR design programs. From this information the requirements and restrictions were defined for developing various rotating plug arrangements. Each of the rotating plug arrangements is discussed in the following paragraphs with a summary of the results shown on Table 2-1.

9.2.1 GENERAL REQUIREMENTS

The interface requirements along with spacing limitation and component sizes are some of the parameters that have an impact on rotating plug sizes. For this study the restrictions were developed and defined on two layout drawings, Figures 2-1 and 2-2. Some of the specific limitations defined are as follows:

1. Core size
2. CRD arrangement in core
3. Instrumentation ports
4. Column supports for upper internals
5. Seismic support for CRD's
6. Spacing between plug flanges, between plug flanges and interfacing components

The requirements defined in the figures were used to develop the rotating plug schemes discussed in the following sections.

The obvious objective for each arrangement was to develop the smallest possible rotating plugs within the constraints shown on Figures 2-1 and 2-2. For each case the rotating plug arrangement must be capable of being positioned over every core element (including the last row of shield assemblies), and transfer each element to and from the core component pot (CCP) position. No shielding elements were considered for transfer although in several cases many of the elements could also be handled if necessary.

9.2.2
THREE ROTATING PLUG ARRANGEMENTS

The three rotating plug arrangements are shown in Figures 2-3 and 2-4. Both arrangements are the usual three rotating plug schemes; that is, the centerline of the large rotating plug is concentric to both the core centerline and reactor vessel centerline and the small rotating plug (SRP) contains the fuel handling mechanism.

Figure 2-3 is very similar to the GE reference concept reported in the PLBR Phase A Report, reference (1). The plug diameters are determined by first defining the position of each of the plug centerlines. As previously stated, the large rotating plug centerline is located on the core centerline. The intermediate rotating plug (IRP) is located midway between the core centerline and the center of the SRP that is positioned to within 1.14 inches of the CRD's seismic support. Using the SRP arrangement as shown, the In-Vessel Transfer Machine (IVTM) grapple is located on a diameter of the IRP that encircles every core element. Therefore, by rotating a combination of the LRP and IRP, each core element can be reached. Rotation of the SRP for this scheme provides the additional reach to the outer area of the core component pot (CCP) location for further ex-vessel transfers.

Figure 2-4 is very similar to the arrangement discussed above. In this case the SRP was moved inward so the IVTM is located on the diameter of the outermost core element (a shield element). All core elements and the CCP can be reached but interference is created between the CRD's seismic support and the flange of the SRP. Very little is gained in reducing the LRP diameter. Because of the interference this layout is not considered as a contender for the study.

However, from Figure 2-4 it can be concluded, to further reduce the diameters on a three rotating plug scheme, a reduction in the CRD's package must also be made.

9.2.3
TWO ROTATING PLUG ARRANGEMENTS

The two rotating plug arrangements are shown on Figures 2-5 through 2-7 and 2-11. These schemes include the usual two plug schemes and arrangements that incorporate an additional handling mechanism in place of a third rotating plug.

Figure 2-5 is the usual two rotating plug scheme where the LRP centerline is concentric with the core centerline and reactor vessel centerline. This scheme has one of the largest rotating plugs, 38'-8.33" diameter LRP. For this arrangement, the centerline of the SRP is located one-half the distance between the core centerline and the transfer path to the CCP. Having the center location for the SRP, the outer flange diameters can be located with the clearance specified around the support solumns. The LRP diameter is determined by locating the flange with the 1.50 inches clearance around the SRP.

Figure 2-6 is a two rotating plug scheme with an additional transfer arm located in the LRP and located so the transfer arm can operate between either of two CCP positions. For this scheme two locations of shield elements are utilized as the intermediate fuel transfer points.

During a refueling sequence, a fuel element is removed from the core and positioned in one of two intermediate transfer points. The transfer arm is then used to further transfer the element to the CCP position. This arrangement produces a much smaller two rotating plug scheme but requires additional steps by transferring from one machine to another along with requiring an additional mechanism. Because of this third mechanism, these types of arrangements when compared with three rotating plug schemes are very near the size of a three rotating plug arrangement.

Figure 2-7 is similar to Figure 2-6. The component restricting the reduction of size in the SRP, the support column, was repositioned. As can be seen, the diameter of the LRP is reduced very little, 7.0 inches, because the CRD envelope becomes the next obstacle.

Figure 2-8 is similar to Figure 2-5 except the centerline of the LRP was positioned 2'-0.50" eccentric to the core centerline and reactor vessel centerline. For this case the LRP is reduced by more than 6 feet and is now approximately the same size as the three rotating plug size shown in Figure 2-3. The off center location of the LRP causes an eccentric loading on the reactor internals and vessel which is undesirable.

Figure 2-11 is another two rotating plug scheme. This arrangement has two IVTM's in the SRP. For this arrangement approximately 64 of the innermost fuel elements must be handled twice. The inner IVTM must first remove an element, move to an outer position made vacant for intermediate transfer so the outer IVTM can further transfer the element to the CCP position. The outer group of fuel elements need only be handled by the outer IVTM.

This scheme produces the smallest of the LRP's but has several disadvantages that make it undesirable for consideration. The arrangement positions the core eccentric to the vessel, requires the inner group of elements to be handled by both the inner and outer IVTM's which creates a longer refueling cycle, the inner IVTM location is very sensitive to the CRD arrangement and the inner IVTM must be a very compact unit because of the space restrictions around the CRD's.

9.2.4
ONE ROTATING PLUG ARRANGEMENTS

The one rotating plug arrangements are shown on Figures 2-9 and 2-10. Both arrangements position the core eccentric to the reactor vessel. The elevation view for this is better shown in Figure 2-12. Also, both arrangements require an additional offset handling machine that is mounted to the plug and positioned on the opposite side of the CRD package. For refueling the CRD package on the rotating plug is rotated away from the core area which positions the offset handling machine above the fuel elements. The handling machine can then remove the fuel elements and by again rotating the plug the elements can be transferred to the CCP position.

Figure 2-9 is the smallest of the one rotating plug arrangements. For this arrangement the plug diameter is set by the location of the plug flange to the support columns.

Figure 2-10 is very similar to Figure 2-9. For this arrangement, provisions are made within the rotating plug for a removable plug above the core area providing access to components within the core barrel assembly diameter. Because of this the rotating plug became larger in size.

II-9.3

CONCLUSIONS

From the work performed, it is still the recommendation of GE-ARSD that the 1000 MWe pool-type LMFBR program use the three rotating plug arrangement as the reference concept. The conclusion is based on comparing the concepts that were based on the reactor assembly components as they presently exist. It should be noted that the component designs limit the flexibility of the various concepts and therefore the actual plug sizes will vary as the components change size or change location within the reactor assembly. The size difference between types of concepts should remain about the same.

A review of the Rotating Plug Comparison chart, Table 2-1, indicates that the large plug of the three rotating plug arrangement is smaller than a two rotating plug arrangement by 6 feet 1 inch, except for the versions that position the core eccentric to the large rotating plug and reactor vessel or the versions with an additional transfer arm. The eccentric loading condition is an undesirable condition. The additional transfer arm takes the place of a third rotating plug and adds complexity to the refueling operation and, therefore, is also considered undesirable.

The one rotating plug arrangements are approximately the same size as the large plug of the three rotating plug scheme. However, the one plug scheme also must utilize an additional transfer mechanism with a very large swing, 7 foot 5 inches. In addition, the arrangement has the core eccentric to the plug and vessel centerline by 7 foot 5 inches. For these reasons the one rotating plug concepts are considered undesirable.

REFERENCES

1. "Pool-Type LMFBR Plant 1000 MWe Phase A Design," EPRI NP-646, (April, 1978).

Rotating Plug Comparison

TABLE 2-1

Figure	No. Rotating Plugs	Plug Sizes (Dia.) SRP	IRP	LRP	Other Transfer Features	Plug Relation to Vessel	LRP Relation to Core	Advantages	Disadvantages	Comments
2-3	3	6'-2"	22'-0.74"	32'-7.04"	---	Concentric	Concentric	1. Larger reach to outside core area	1. 3 Plugs	
2-4	3	6'-2"	21'-9.44"	31'-11.5"	---	"	"	1. (Same as fig. 1)	1. (Same as fig. 1) 2. Interference at CRD Seismic support	
2-5	2	24'-10.02"	---	38'-8.32"	---	"	"	1. Only 2 plugs	1. Very large LRP	Impact on Vessel Size
2-6	2	22'-0"	---	32'-1.06"	Swing Arm	"	"	1. Smaller LRP 2. 3rd arm can reach outside core area	1. Has a 3rd operating mechanism	
2-7	2	21'-3"	---	31'-5.06"	Swing Arm	"	"	1. (Same as fig. 4)	1. Support Column relocated	
2-8	2	20'-2.7"	---	32'-5.96"	---	?	Eccentric	1. No 3rd arm	1. Eccentric by 2'-0.50"	Deck unsymmetrical design
2-11	2	19'-0.08"	---	28'-8.62"	---	?	Eccentric	1. Smallest LRP	1. Eccentric by 1'-11.97" 2. Inner fuel elements have double handling 3. Very sensitive to CRD arrangement 4. IVTM must be compact	Has an Inner & Outer IVTM's
2-9	1	---	---	29'-5.32"	Swing Arm	Eccentric	Eccentric	1. Only 1 plug and swing arm	1. Eccentric by 7'-4.995" 2. Large swing arm 3. Eccentric load on vessel	
2-10	1	17'-9.5"	---	33'-6.49"	Swing Arm	Eccentric	Eccentric	1. (Same as fig. 7) 2. Removable plug	1. (Same as fig. 7)	Has an Inner Non-Rotating Plug

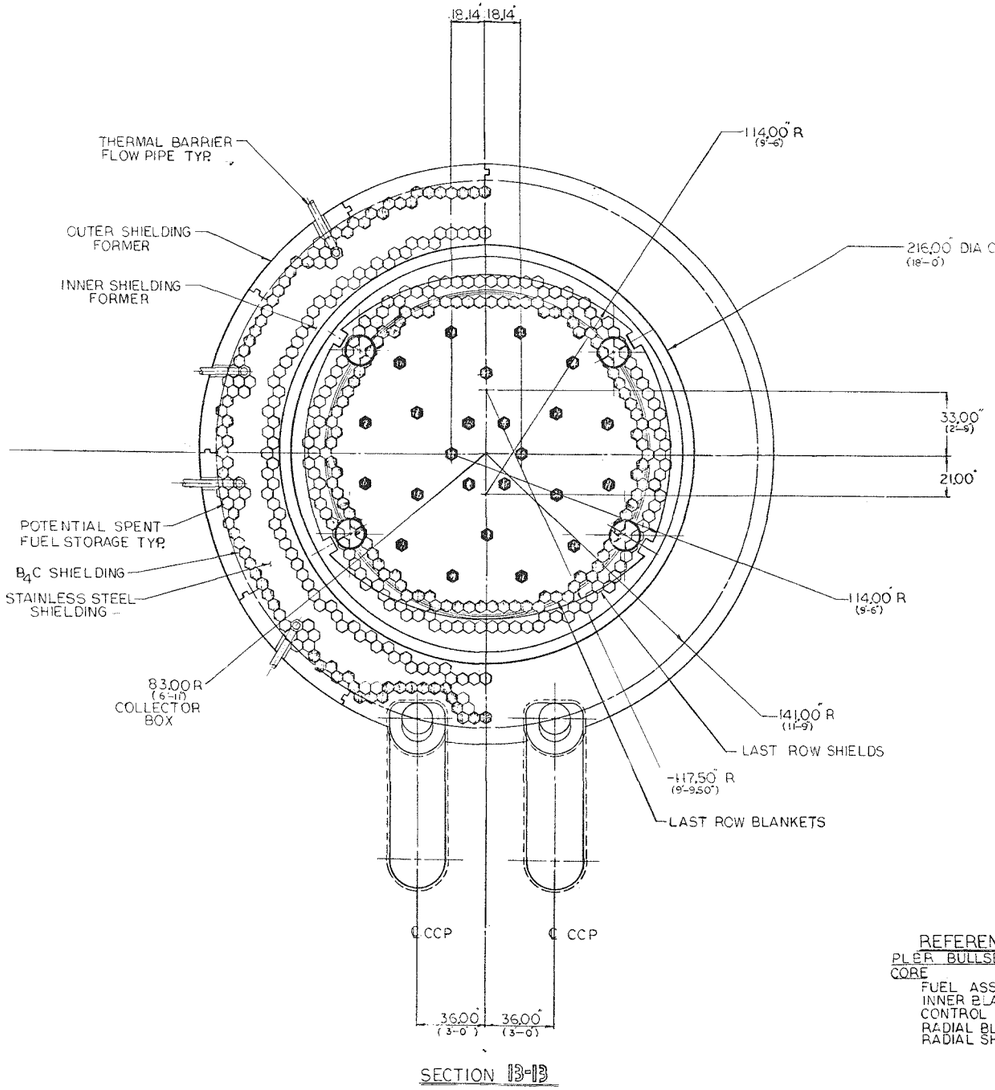

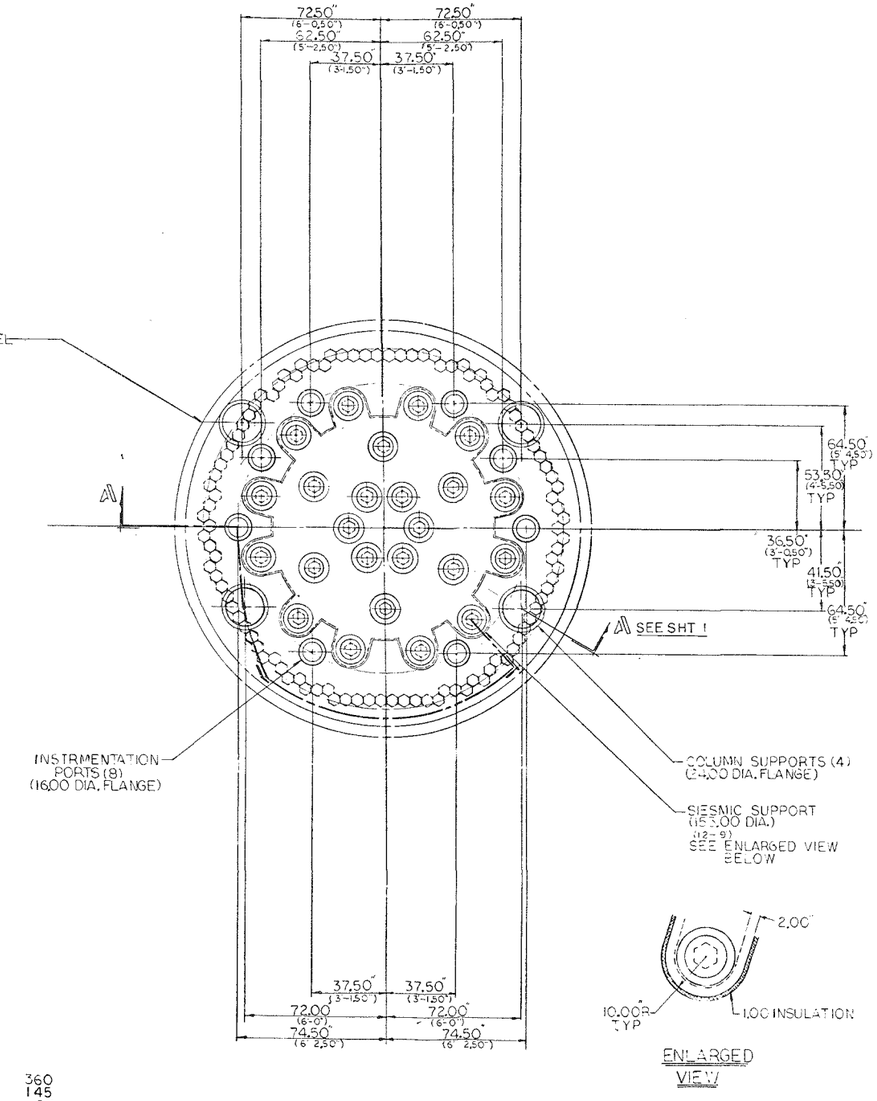

REFERENCE
PLBR BULLSEYE CORE

CORE	
FUEL ASSEMBLY	360
INNER BLANKET	145
CONTROL RODS	24
RADIAL BLANKET	162
RADIAL SHIELDING	180
TOTAL	871

PITCH — 6.045
5.235

FIGURE 2-1 ARRANGEMENT LAYOUT REQUIREMENTS--PLAN VIEW

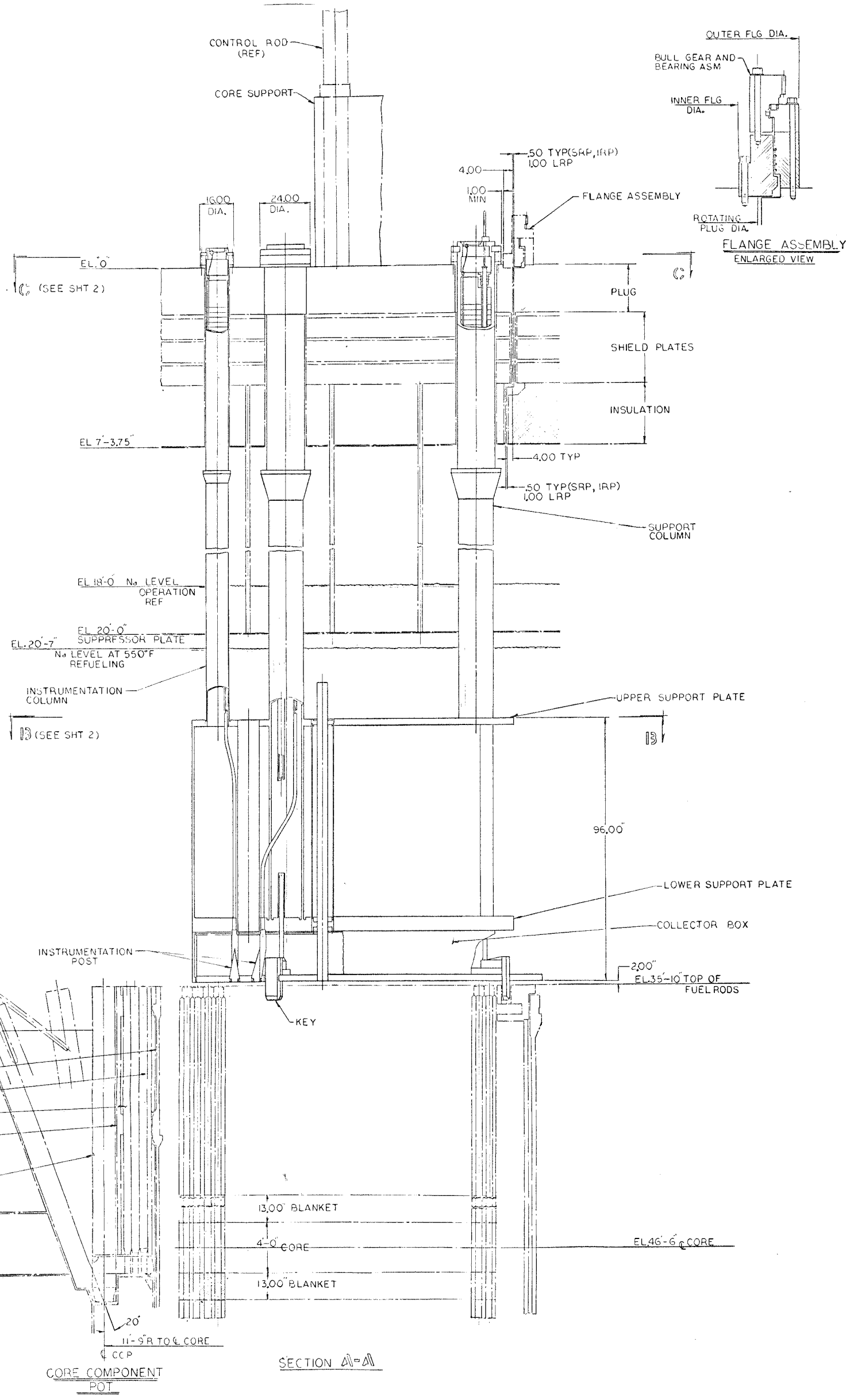

FIGURE 2-2 ARRANGEMENT LAYOUT REQUIREMENTS--ELEVATION VIEW

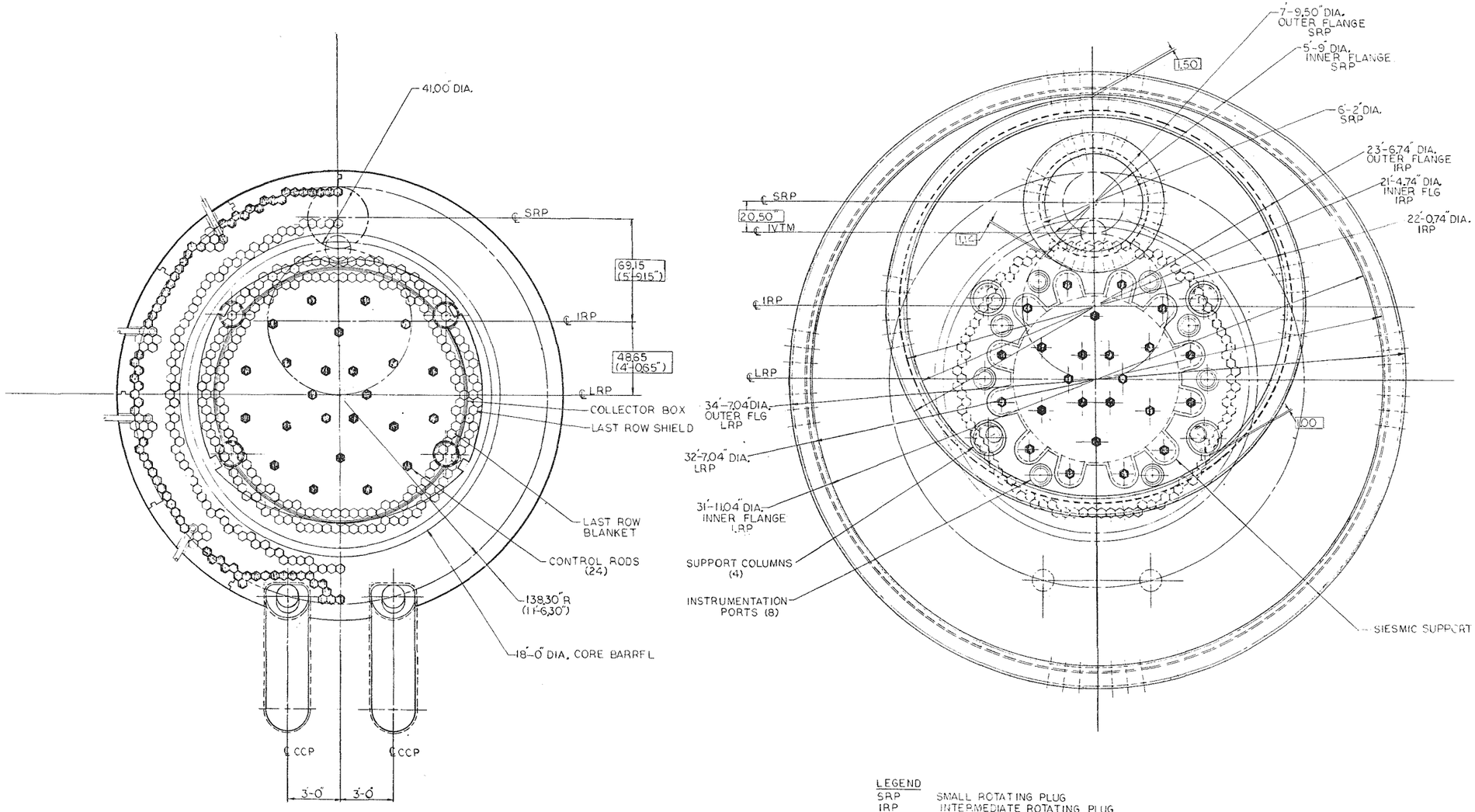

LEGEND

SRP	SMALL ROTATING PLUG
IRP	INTERMEDIATE ROTATING PLUG
LRP	LARGE ROTATING PLUG
IVTM	IN VESSEL TRANSFER MACHINE
CCP	CORE COMPONENT POT

FIGURE 2-3 THREE ROTATING PLUGS

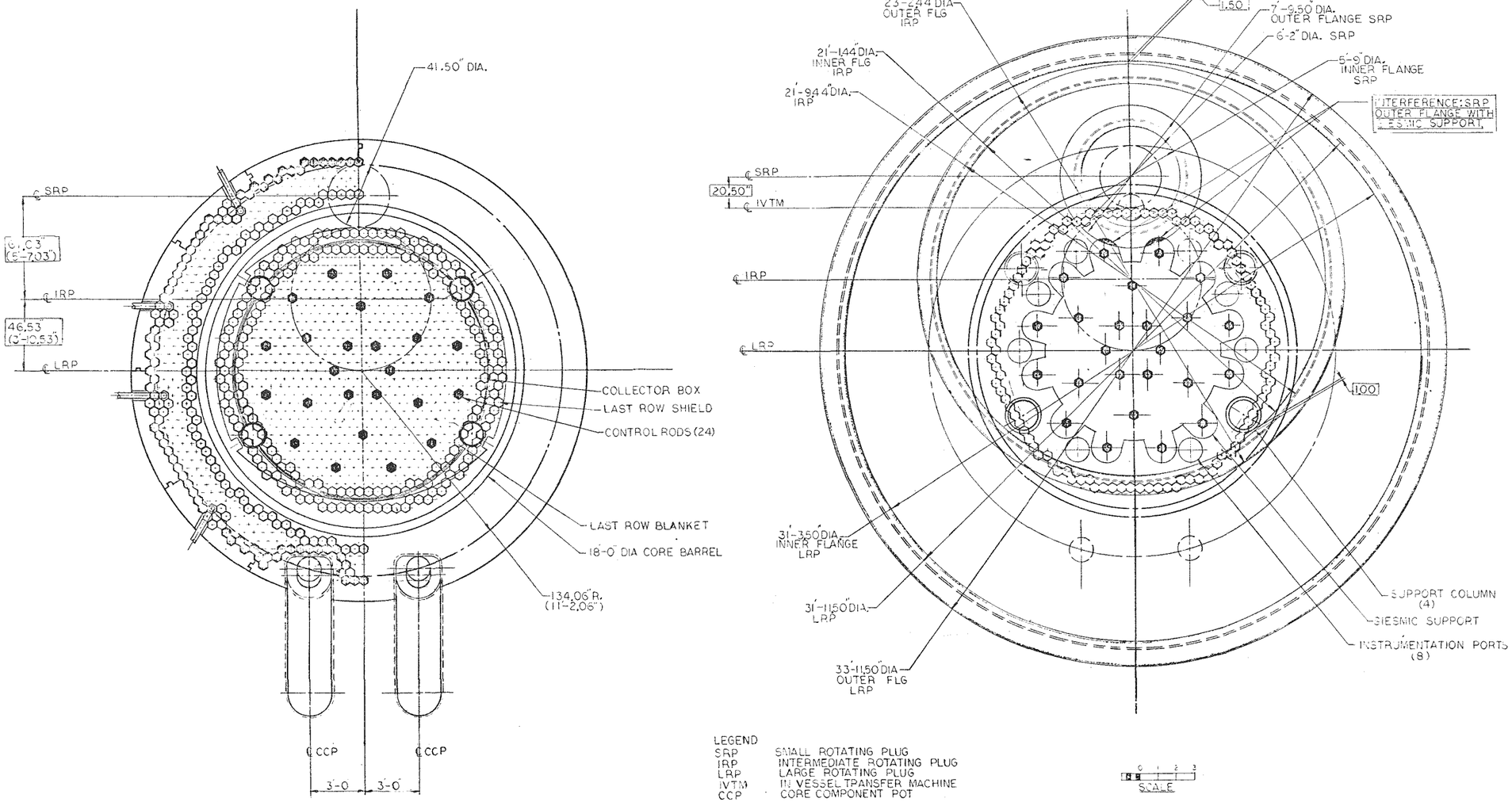

FIGURE 2-4 THREE ROTATING PLUGS--SEISMIC SUPPORT INTERFERENCE

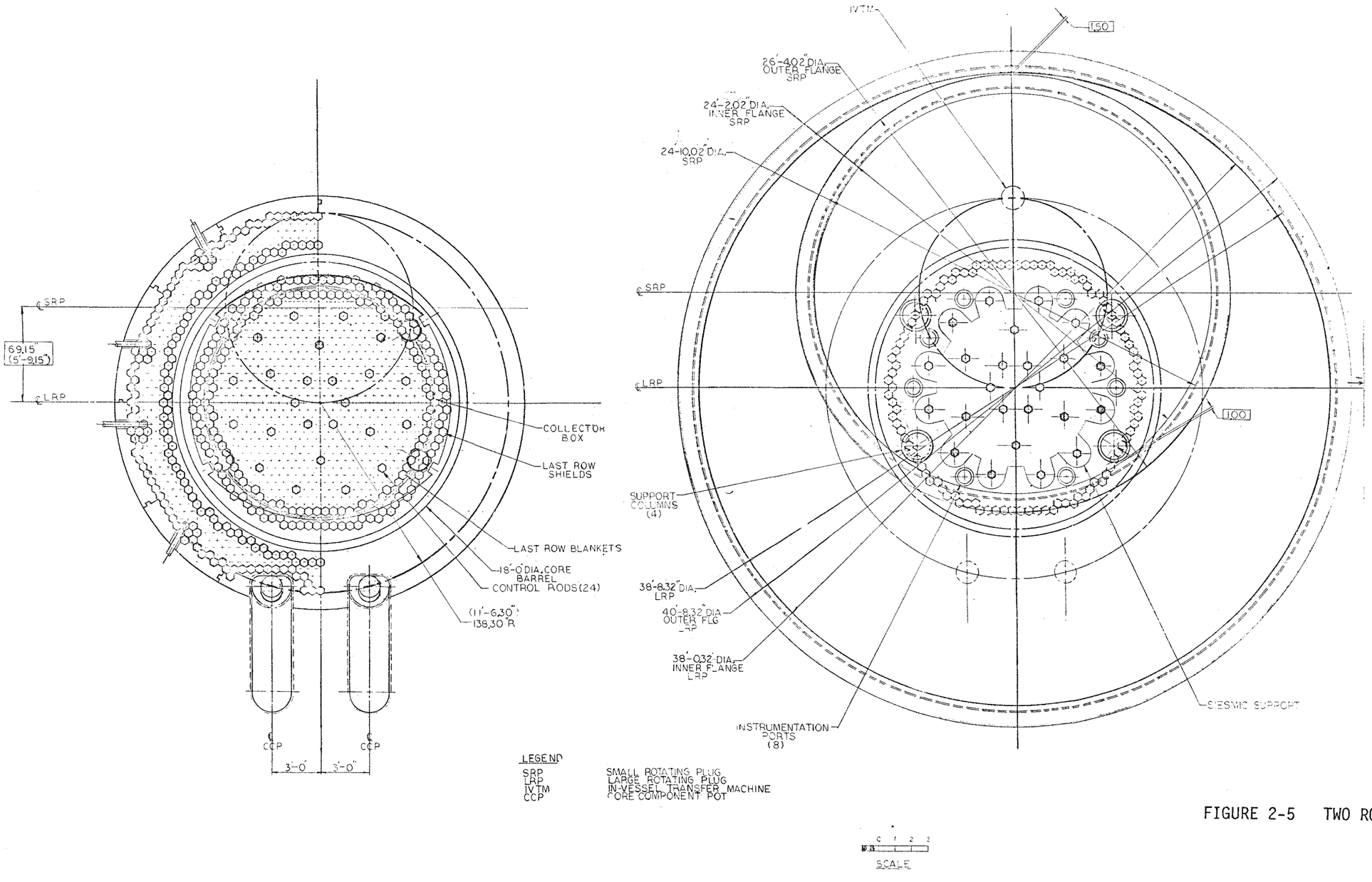

FIGURE 2-5 TWO ROTATING PLUGS

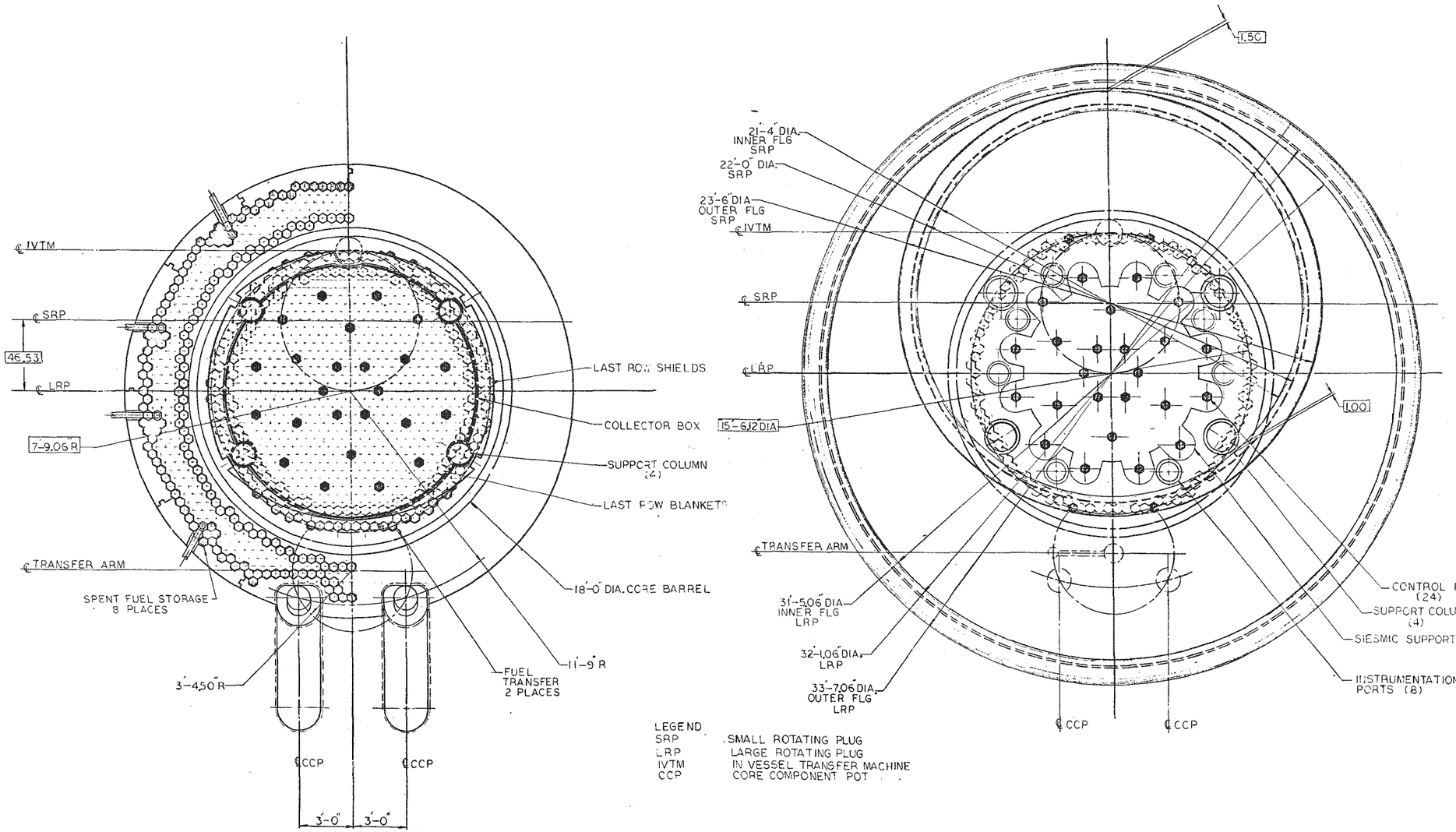

FIGURE 2-6 TWO ROTATING PLUGS--WITH TRANSFER ARM

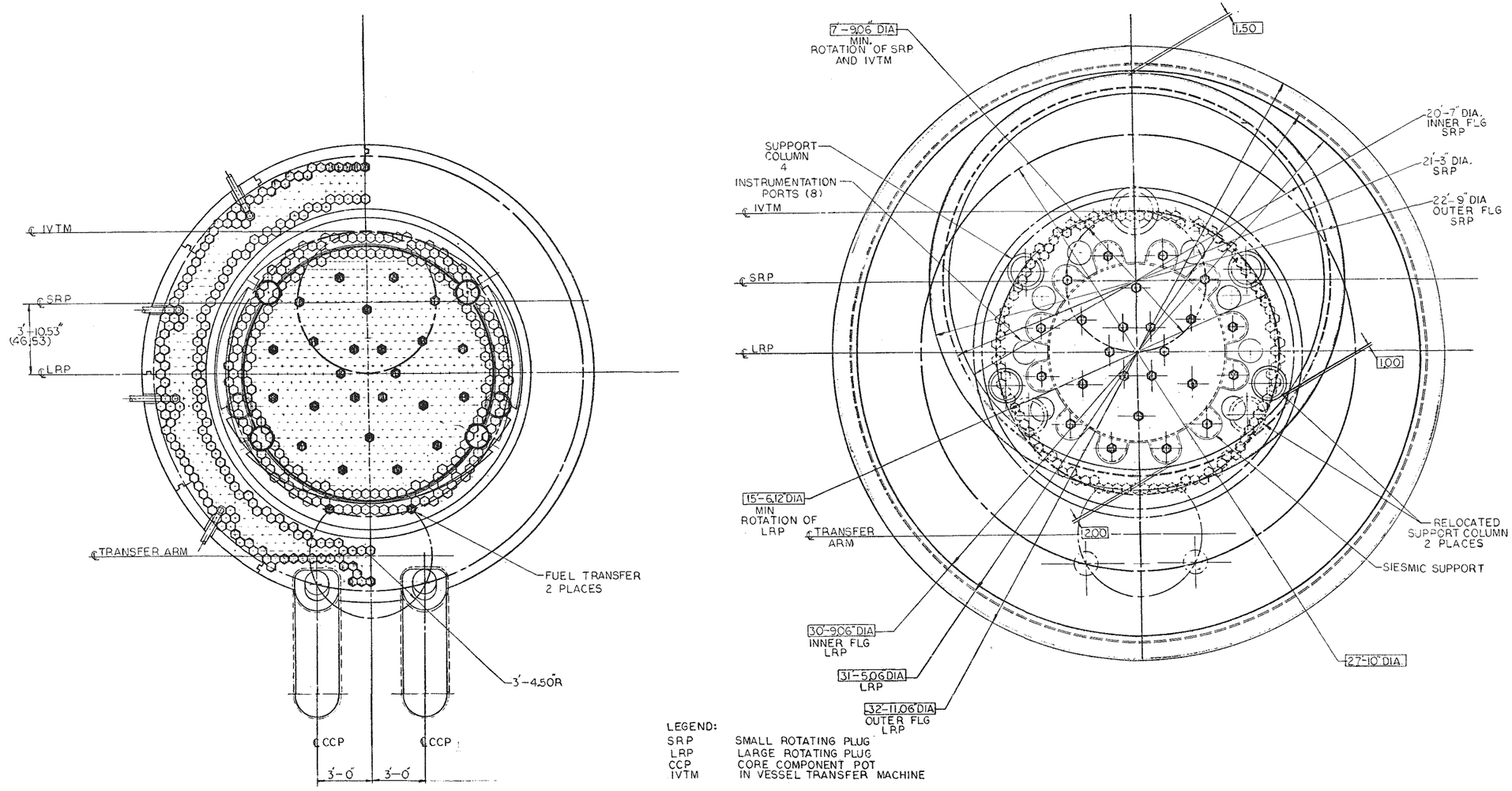

FIGURE 2-7 TWO ROTATING PLUGS--WITH TRANSFER ARM (RELOCATED SUPPORT COLUMNS)

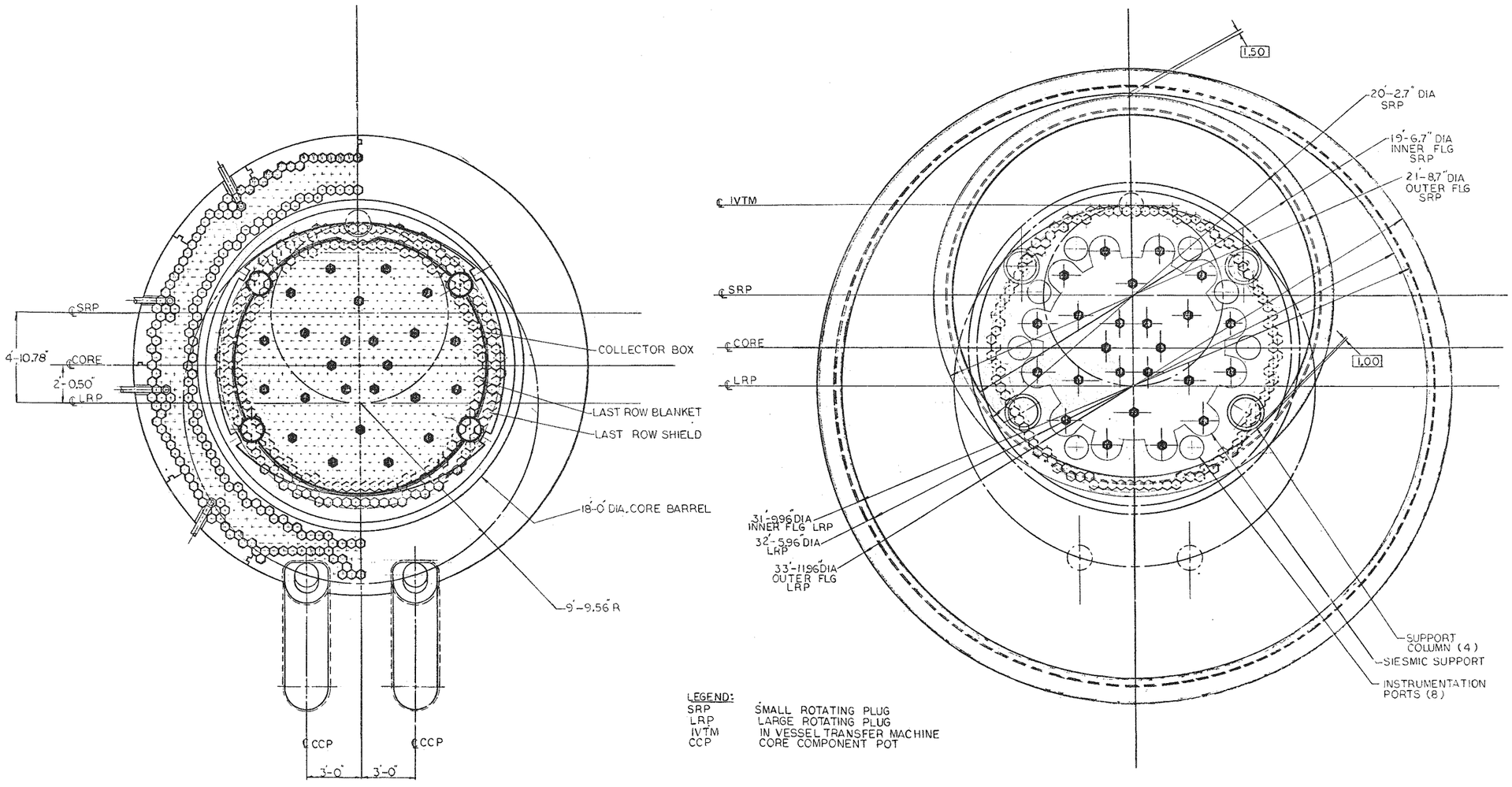

FIGURE 2-8 TWO ROTATING PLUGS--ECCENTRIC

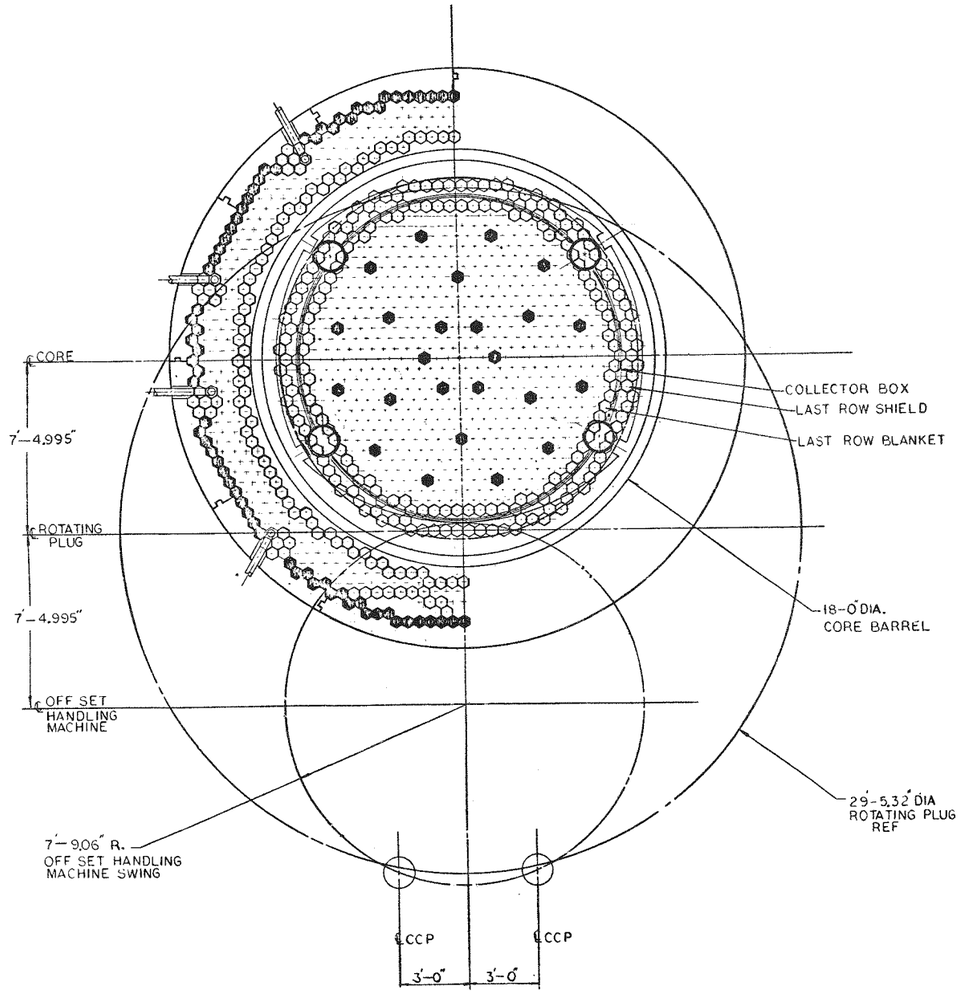

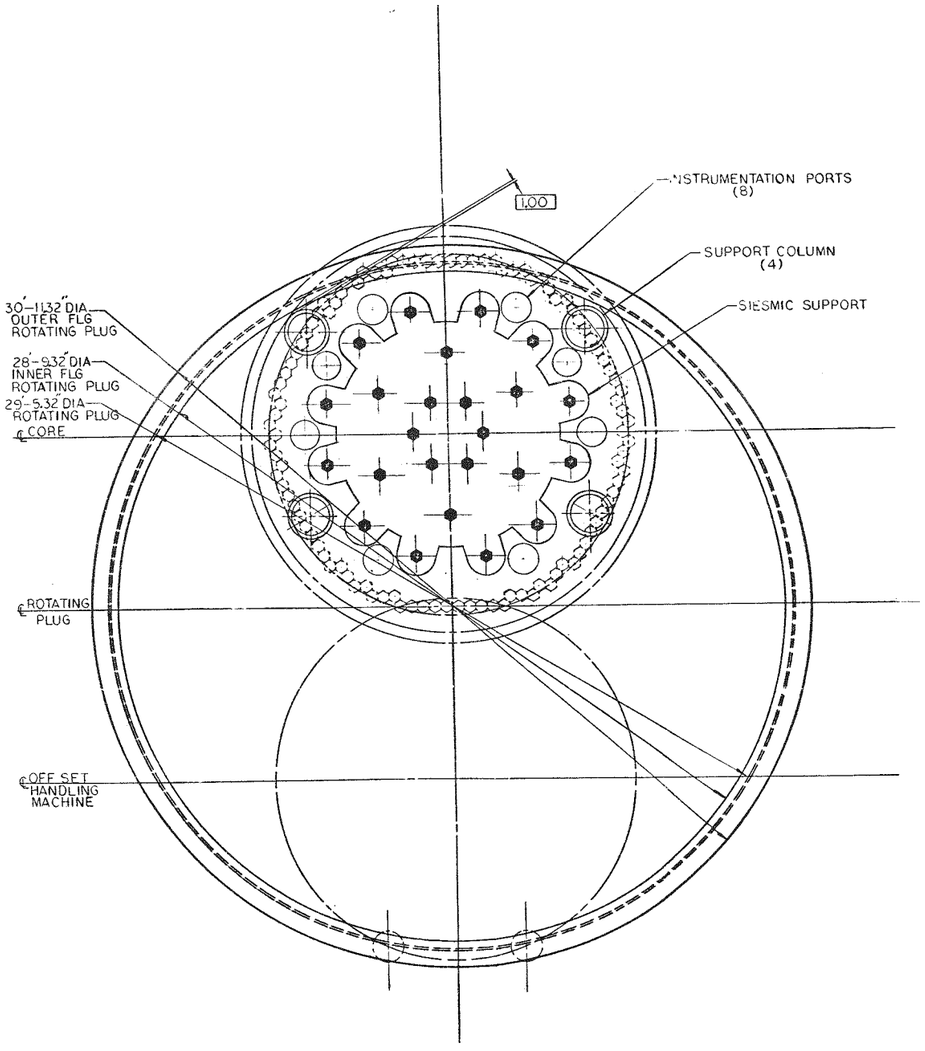

FIGURE 2-9 ONE ROTATING PLUG--OFFSET HANDLING MACHINE

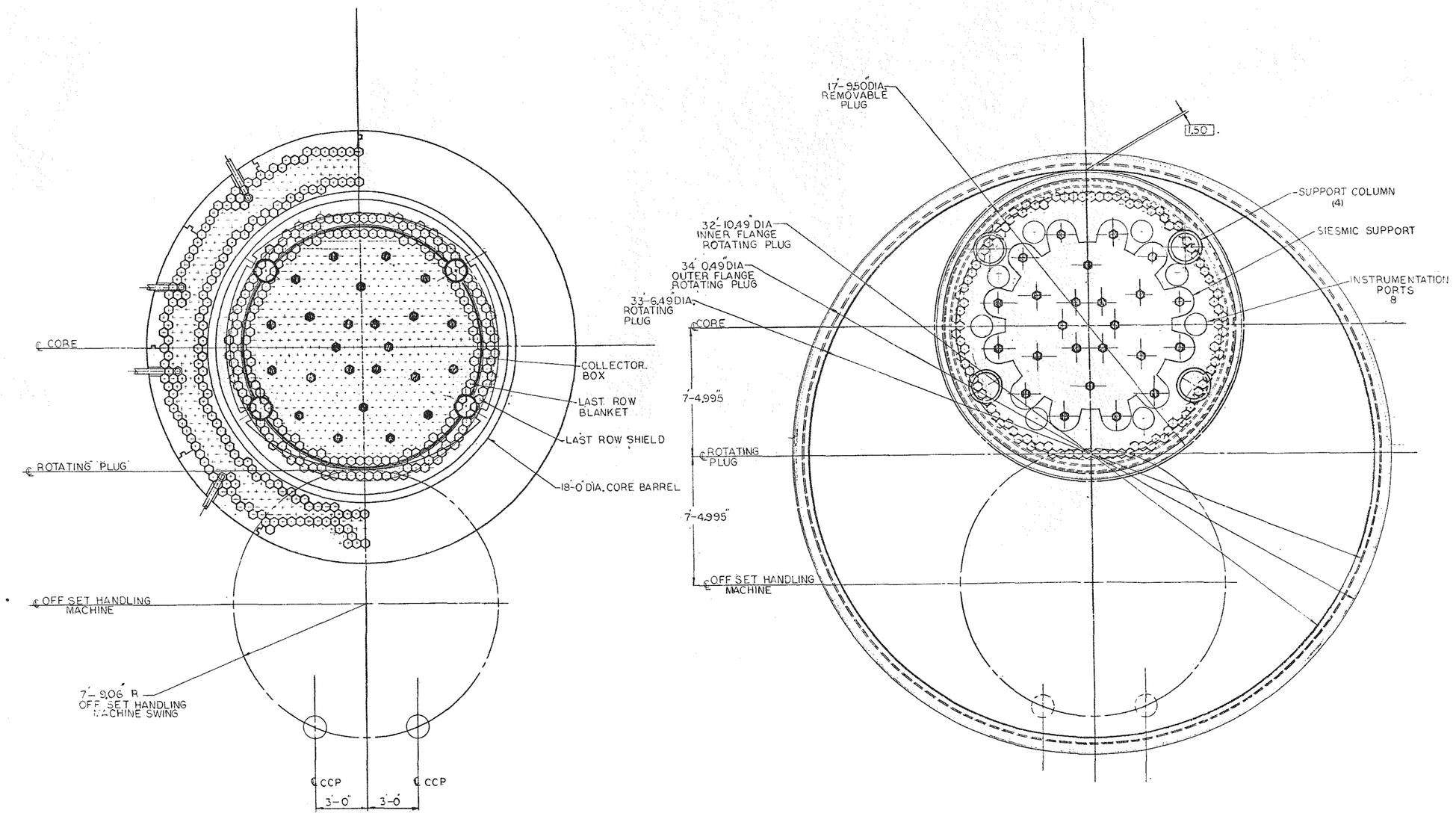

FIGURE 2-10 ONE ROTATING PLUG--OFFSET HANDLING MACHINE WITH REMOVABLE PLUG

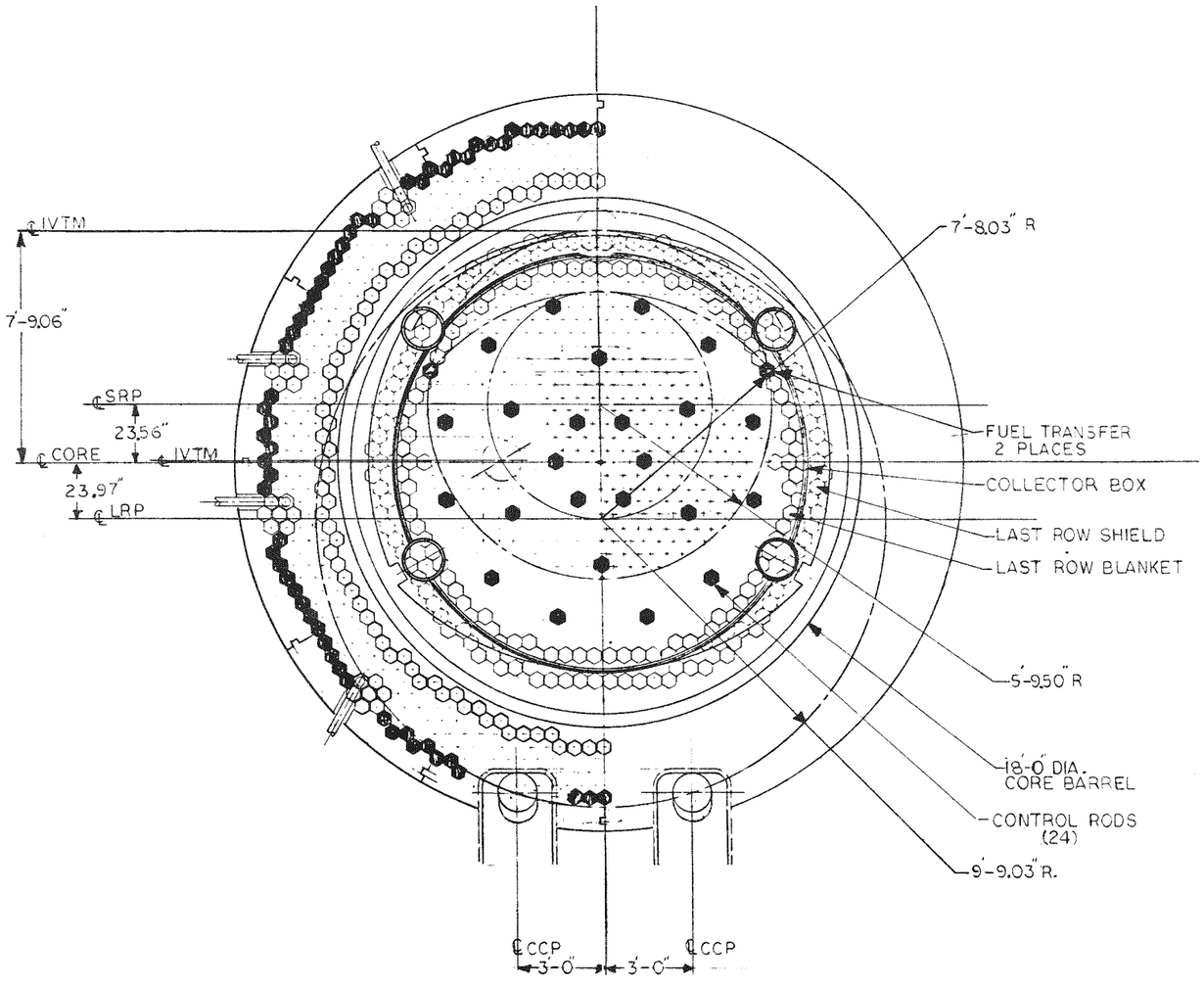

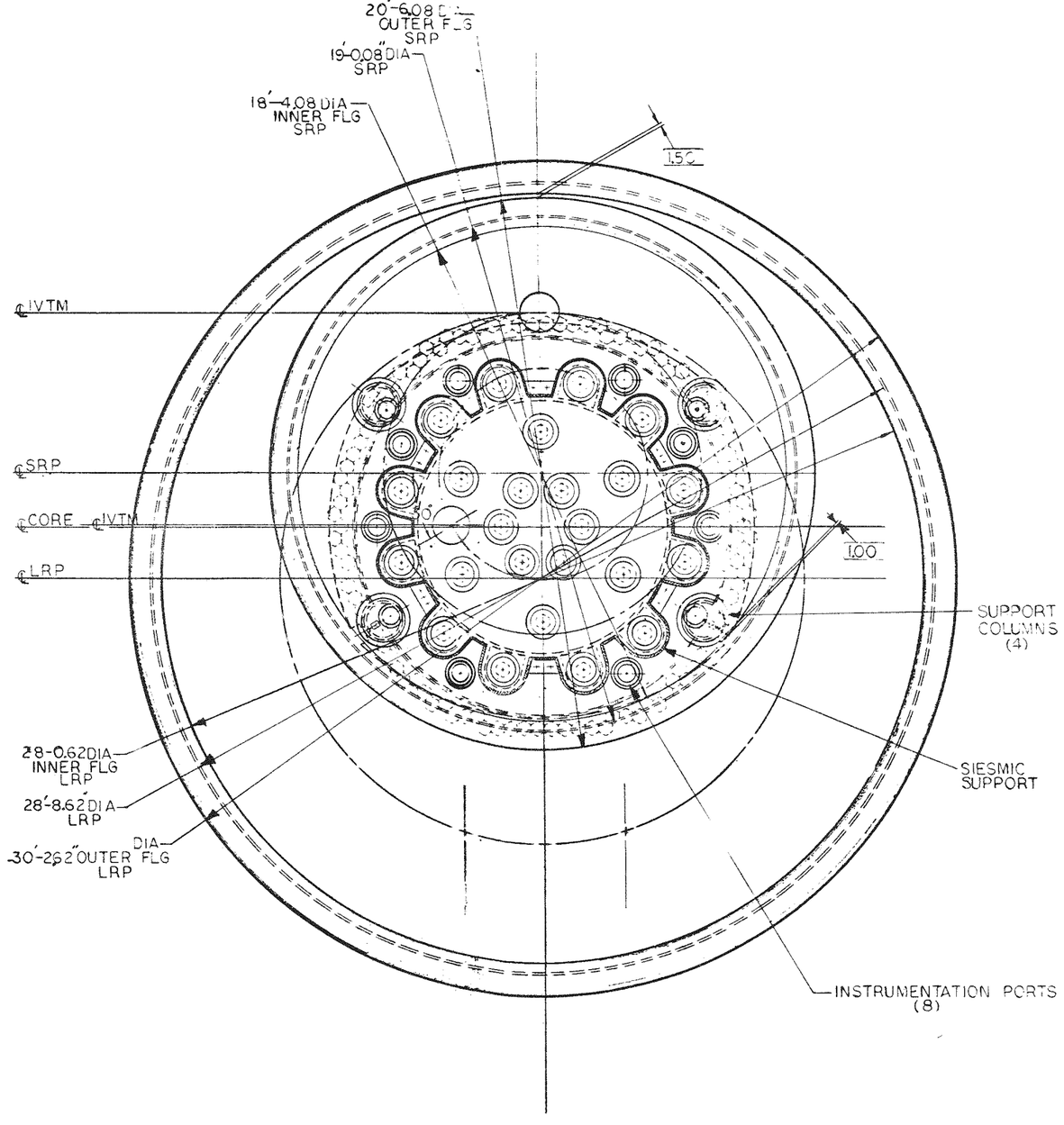

FIGURE 2-11 TWO ROTATING PLUGS -- WITH TWO IVTM'S

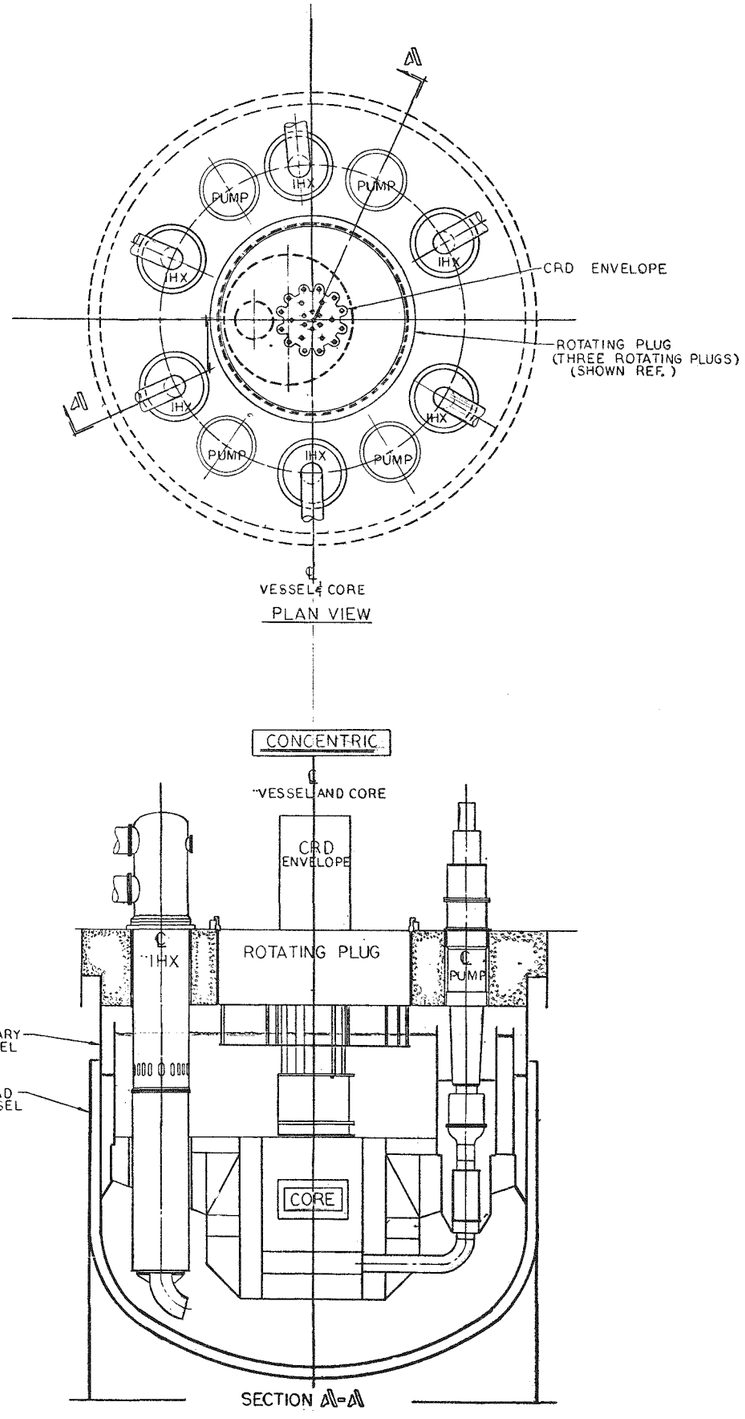

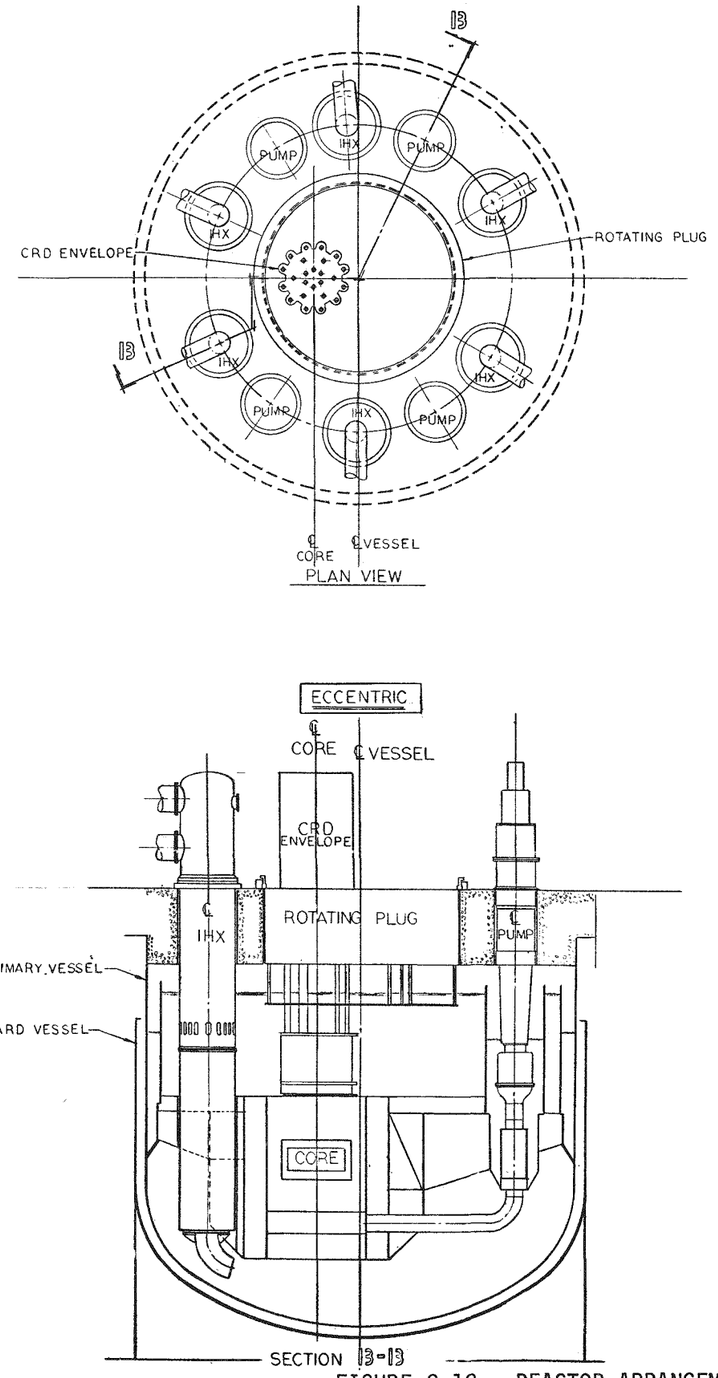

FIGURE 2-12 REACTOR ARRANGEMENT COMPARISON FOR CONCENTRIC AND ECCENTRIC PLUGS

Part II: Reactor Assembly - Structures

Section 10: Rotating Plug Thermal Analysis

CONTENTS

		Page
II-10.1	INTRODUCTION AND SUMMARY	II-10-1
	10.1.1 Introduction	II-10-1
	10.1.2 Summary	II-10-2
II-10.2	DISCUSSION	II-10-7
	10.2.1 Assumptions	II-10-7
	10.2.2 Method of Solution	II-10-8
	10.2.3 Steady State	II-10-11
	10.2.4 Transient	II-10-15
II-10.3	CONCLUSION	II-10-45
	10.3.1 Steady State	II-10-45
	10.3.2 Transient	II-10-46
	10.3.3 Recommendations	II-10-46
	REFERENCES	II-10-47
	APPENDIX II-10A	II-10A-1

FIGURES

		Page
1-1	Plan View of Reactor Closure	II-10-4
1-2	Elevation View of Reactor Closure	II-10-5
2-1	Instrument Penetrations - Steady State Results	II-10-17
2-2	Support Column Penetrations - Steady State Results	II-10-18
2-3	Deck/Large Plug - Wire Screen - Layer Plates -Steady State Results	II-10-34
2-4	Deck/Large Plug - Wire Screen - Layer Plates - Steady State Results	II-10-35
2-5	Deck/Large Plug - Kaylo - Steady State Results	II-10-36
2-6	Deck/Large Plug - Wire Screen - Layer Plate -Decay Heat Results	II-10-37
2-7	Startup Transient Condition	II-10-38
2-8	Deck/Large Plug Transient Model	II-10-39
2-9	Deck/Large Plug Startup Transient Results	II-10-40
2-10	Deck/Large Plug Startup Transient Results	II-10-41
2-11	Small Plug Transient Model	II-10-42
2-12	Small Plug Startup Transient Results	II-10-43

TABLES

		Page
2-1	Case 1 - WS & LP,* Natural Convection	II-10-19
2-2	Case 2 - WS & LP, Forced Convection	II-10-20
2-3	Case 3 - WS & LP, Natural Convection, Isolated Container	II-10-21
2-4	Case 4 - WS & LP, Forced Convection, Isolated Container	II-10-22
2-5	Case 5 - WS & LP, (24"), Natural Convection	II-10-23
2-6	Case 6 - WS & LP, (36"), Natural Convection	II-10-24
2-7	Case 7 - Kaylo, Natural Convection	II-10-25
2-8	Case 8 - Kaylo, Natural Convection, Isolated Container	II-10-26
2-9	Case 9 - Kaylo, Forced Convection, Isolated Container	II-10-27
2-10	Case 10- Kaylo & LP, Natural Convection	II-10-28
2-11	Case 11- Kaylo & LP, Forced Convection	II-10-29
2-12	Case 12- Kaylo & LP, Natural Convection, Isolated Container	II-10-30
2-13	Case 13- Kaylo & LP, Forced Convection, Isolated Container	II-10-31
2-14	Case 14- WS & LP, Natural Convection, Decay Heat Condition	II-10-32
2-15	Case 15- WS & LP, Forced Convection, Decay Heat Condition	II-10-33

* WS & LP - Wire Screen and Layered Plates

INTRODUCTION AND SUMMARY

10.1.1 INTRODUCTION

Steady state and transient temperatures were determined for the reference reactor closure and interfacing deck regions of the pool concept for several operating conditions.

The reference design shown on Figures 1-1 and 1-2 consists of a top plate, three shield plates, and a composite thermal insulation. The insulation consists of ten (10) inches of wire screen separated by thin plates (K = 9.18 BTU/hr ft °F) and twelve (12) inches of layered plate insulation (27 plates (.062m), with 3/8 inch spacing between plates). The insulation has argon gas in the spaces. The layered plates insulate by limiting gas convection and reducing the temperature difference in radiation between adjacent plates in the insulated region.

For comparison purposes, analysis was run with a solid insulation (Kaylo,* K = 0.03 BTU/hr ft °F). Forced cooling of the top of the plugs was also investigated to assess the effectiveness of a cooling system.

For further evaluation of the closure components, steady state results can be used to determine whether supplementary cooling is required for the closure region. Transient results can be used to assess the probable thermal stresses in the deck and closure region. Component temperatures will be used in the closure seal and bearing design.

The deck/large plug interface area and the small rotating plug were selected for transient thermal analysis, using the startup transient (50°F/Hr ramp). No drastic thermal gradients were uncovered. Steady state conditions had not been reached in the case of the small plug when the analysis was terminated after 10 hours of computer simulation. (Figure 2-12)

*Owens/Corning Fiberglass Corp., calcium silicate material.

The temperatures reported for the wire screen plus layered plates (Table 2-1 to 2-3) is marginal for elastomer seals operation and should be lowered. The most effective way to lower temperatures is to replace the wire screen insulation (K = .18) with Kaylo or equivalent solid insulation (K = .03). Other possible means to reduce temperatures are forced cooling of the top surface or increasing the thickness of the layered plate insulation from 12" to 36".

The wire screen insulation is not effective for a sodium environment above 608°F[1] and therefore limits the options available to reduce surface temperatures.

10.1.2
SUMMARY

Typical sections within the reactor closure and adjacent deck interface areas were analyzed for thermal effects. A typical section of the deck was analyzed for the steady state and startup transient condition. In addition, the previous analysis for the rotating plugs was reevaluated for the pool concept, using the reference design insulation and several alternates.

Local hot spots occurred at penetrations: the fuel transfer tube, the control rod drives, instrument tubes, and the plug interfaces. All temperatures were between 150°F and 200°F at the top of the plugs, in the vicinity of the penetrations, depending on the insulation material. At regions removed from the penetrations, the temperature was reduced to about 130°F in the reference design and 106°F when the plate screen insulation was replaced with Kaylo insulation. The insulation above the sodium pool is effective in isolating the plugs from the hot sodium pool. Most of the heat loss is through the penetrations and supporting structure. Forced cooling of the plugs (air velocity 16 fps) was also investigated for the reference design. The plug temperatures (away from the penetrations) were reduced from 130°F to 100°F.

The deck/large plug interface area was examined for steady state operation with various combinations of insulation and forced cooling. The reference design, consisting of wire screen and layered plate insulation with forced nitrogen cooling, gave concrete temperatures of 107°F. Another investigation using Kaylo

insulation (.03 BTU/hr ft °F) in place of the wire screen plus layered plates and no forced nitrogen cooling, gave concrete temperatures of 120°F.

The deck/large plug area was checked for a postulated decay heat removal condition (sodium temperature = 1150°F) with forced deck cooling and layered plate plus wire screen insulation. Concrete temperatures were 106° - 108°F. This was very close (>.5°) to the 875°F sodium temperature run.

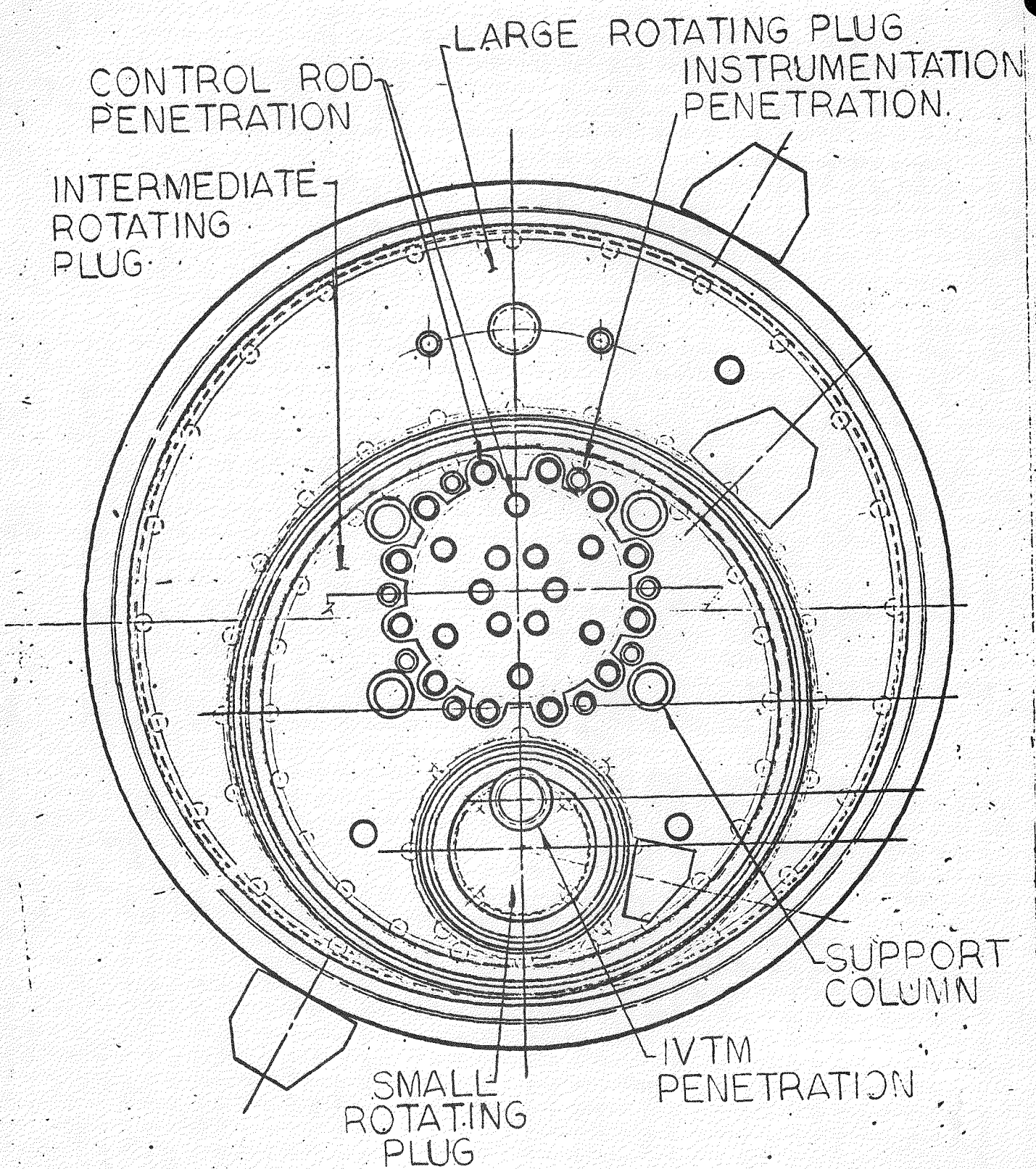

Figure 1-1 Plan View of Reactor Closure

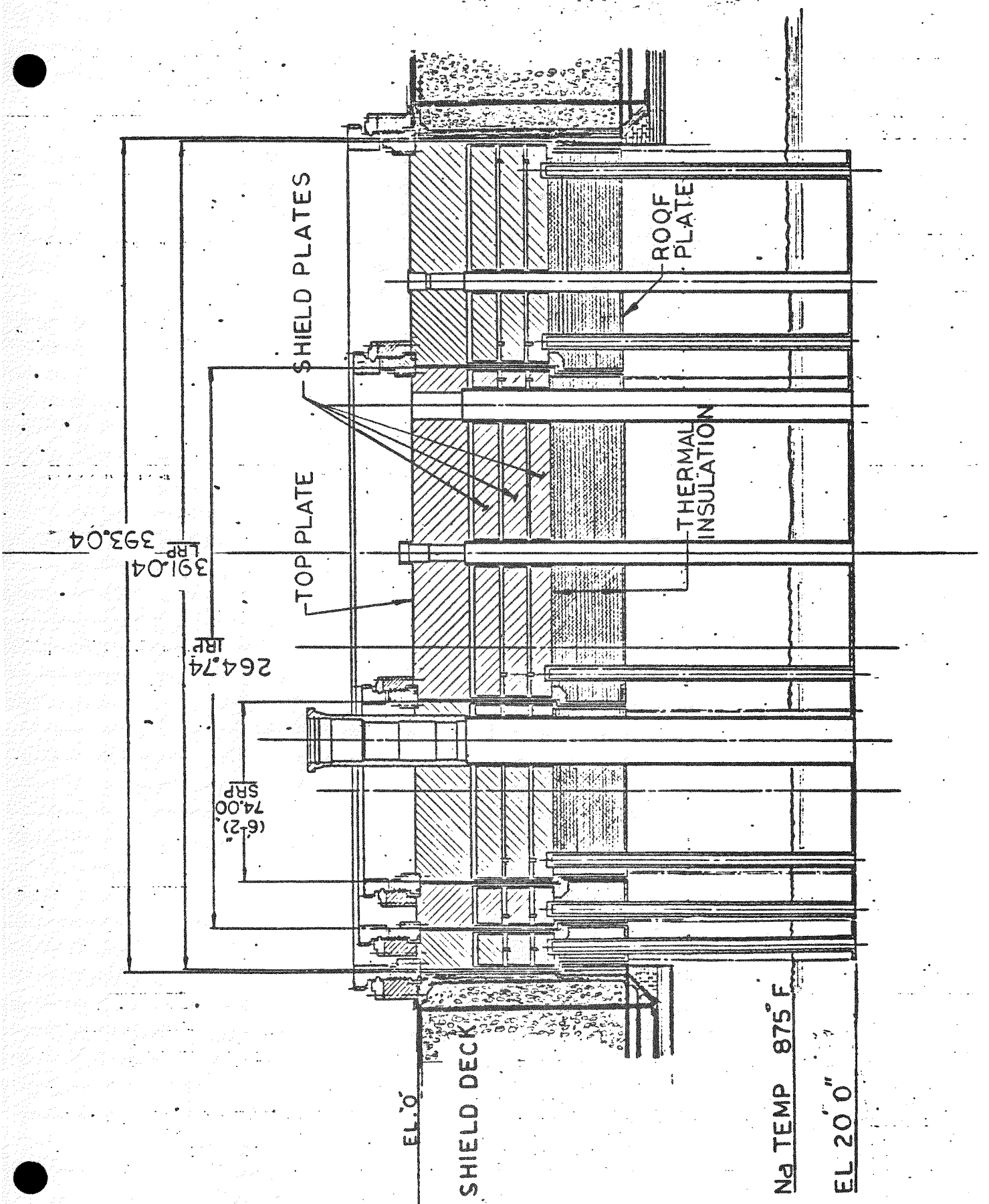

Figure 1-2 Elevation View of Reactor Closure

II-10.2

DISCUSSION

The reactor closure assembly with all the penetrations and arrangement of the components is too complex to analyze as an entire system. The strategy adopted was to separate the large system into smaller subsystems, which were chosen on the basis of their ability to influence the large system. Penetrations and interfaces meet this criterion. The sodium pool is isothermal in the radial direction to a first approximation at the free surface between the sodium and the argon cover gas. The following are the assumptions used for the analysis, the method of analysis and the summary of the results for both the steady state analysis and transient analysis.

10.2.1
ASSUMPTIONS

A. Small Rotating Plug (SRP)
   1. DT/Dr = 0 @ the outside diameter. (conservative)
   2. In each plate the vertical gradient is very small (DT/DZ $\approx$ 5°F/ft.)
   3. 10" wire screen (K = .18) and 12" layered plate (K = .35) is used as insulation.
   4. Air or nitrogen gas is in the clearance spaces above the roof.
   5. A lumped parameter model can be used to model the transient response. (This follows from A1 and A2.)
   6. A linear model is permissible. (Thermal properties are assumed to be average values independent of temperature.)

B. Deck Plug-Interface (DPI)
   1. The temperature distribution is axi-symmetric.
   2. The radial gradient at the deck plug interface equals zero (0). (conservative)
   3. The radial gradient at a radius greater than the 1.5" thick cylindrical support is zero. (conservative)
   4. 10" wire screen (K = .18) and 12" layered plate (K = .35) is used as insulation.
   5. Air or nitrogen gas is in the clearance spaces above the roof.

10.2.2
METHOD OF SOLUTION

Steady State Two Dimension Analysis

A two-dimensional axisymmetric thermal network was used to solve the steady state thermal problem.

$$\sum_{i=1}^{n} Y_{ij} \quad (T_i - T_j) = 0 \qquad j = 1, m \quad m > n$$

for the radial direction:

$$Y_{ij} = \frac{2\pi kZ(R_o - R_i)}{\ell n(R_o / R_i)}$$

for the axial direction:

$$Y_{ij} = \frac{2}{Z} r_m hk$$

r_m = mean radius

h = Thickness of cylinder

Admittances in parallel add directly. $(Y_T = Y_1 + Y_2)$

Admittances in series add as $1/Y_T = 1/Y_1 + 1/Y_2$

$$Y_T = Y_1 Y_2 / (Y_1 + Y_2)$$

Conical shapes were converted to equivalent cylinders.

The transient thermal problem was solved as follows:

$$M_j C \frac{dTj}{dt} = \sum_{i=1}^{n} Y_{ij} \quad (T_i - T_j)$$

c = specific heat (Btu/lb°F)

The only additional data needed to solve this problem is Mc matrix. The Y_{ij} matrix is the same as that used for the steady state solution.

The small rotating plug was solved using implicit methods. The dTj/dt was converted to finite differences as follows:

$$\frac{dTj}{dt} \approx \frac{T_j^{t+1} - T_j^{t}}{\Delta t} = \frac{Yij}{Mjc} (T_i - T_j)^{t+1}$$

$$\text{let } K_{ij} = \Delta t \frac{Y}{MC}$$

$$[I + K] T^{t+1} = F(t) = [I] T^{t}$$

$$\text{let } A = I + K$$

$$[A] T^{t+1} + [I] T^{t}$$

$$T^{t+1} = [A]^{-1} \{F(t) + [I] T^{t}\}$$

This solution is unconditionally stable regardless of the time increment Δt. The only limitation is the error in the solution which is a function of Δt. The smaller the Δt, the less the error.

The Deck/Large Plug Interface was solved with explicit methods because of numerical problems which developed with the implicit approach due to the large matrix to be inverted (51 x 51) and the large difference between the terms of the various rows of the matrix.

$$\frac{dTj}{dt} \approx \frac{Tj^{t+1} - Tj^{t}}{\Delta t} = \frac{Yij}{Mjc} (T_i - T_j)^{t}$$

$$T^{t+1} = [I + K] T^{t} + F(t)$$

This is only stable for $\Delta t \leq \frac{.5Mc}{Y} \left(\frac{\Delta x}{1 + H\Delta x} \right)$, k

The Δt << than that used in the implicit method. This makes this approach very expensive of computer time.

Steady State One Dimension Analysis

For a one dimension analysis, the general method can be simplified to eliminate the solution of simultaneous equations.

let $R_i = 1/Y_{ij}$

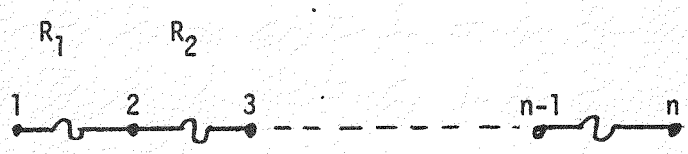

Q = Heat Flux in BTU/hr ft.^{2} T_1 & T_n are known

$$\Delta T = T_n - T_1$$

$$Q = Y \Delta T$$

$$Q = \frac{\Delta T}{\sum_{i=1}^{n} R_i}$$

ΔT is known from the boundary conditions. The R_i are temperature dependent. The Q must therefore be determined by iteration.

$$T_2 = T_1 + QR_1$$

$$T_3 = T_2 + QR_2$$

$$T_{n-1} = T_{n-2} + QR_{n-2}$$

The iterative procedure is as follows:

1. Pick a set of trial T_i
2. Determine the R_i associated with theT_i
3. Solve for Q

4. Solve for T_i using the Q from Step 3.

5. If $|T_n^{t+1} - T_n^t| < \varepsilon$: Where ε is some tolerance and t is the t^{th} iterative, the problem is solved (T_n^{t+1} are the correct temperatures). If $| T_n^{t+1} + T_n^t | > \varepsilon$ go to Step 2 and repeat the iterative process. The iterative process for the one dimensional case always converges. It usually requires less than 20 iterations for convergence to take place.

10.2.3
STEADY STATE ANALYSIS

Steady state analysis of the subsystems, using the thermal circuit analogy, identified the major heat leaks. These heat leaks cause local perturbations in the temperature fields of the rotating plugs and shield disc. The majority of the heat leaks occurs in the Intermediate Rotating Plug (IRP), where six (6) instrument probe penetrations, four (4) support columns for the upper internals and twenty-four Control Rod Drives (CRD's) are located. Results of the steady state analysis for the instrument penetrations and support column penetrations are shown on Figure 2-1 and 2-2 respectively. Details of the analysis along with the analysis for other areas of the rotating plug are included in the appendix.

Another area containing a major heat leak is the Small Rotating Plug (SRP) which includes the outer cylinder structure and the In-Vessel Transfer Machine (IVTM) penetration. This area of the reactor closure was analyzed extensively and the summary of the results for the reference design along with variations using other insulation and cooling approaches are discussed in detail below.

Another area of the reactor closure that was examined extensively is a location removed from the penetration areas, where there is a uniform field of low temperature due to the heat losses through the closure insulation. This region was examined using one dimensional heat transfer analysis. The summary of the results for the reference design and variations to reduce local hot spots are also discussed below.

For each of the cases reviewed the top steel support structure remains a constant thickness of 22.75 inches along with the three lower steel shield plates having the thickness of 10.50 inches, 10.00 inches and 9.00 inches. Below the shield plates is an area of insulation. The major variation between cases is the method of cooling and the insulation type and thickness. For the SRP, an additional variation of including or isolating the effect of the insulation container has also been included as another variation. A review of each of the cases analyzed is as follows.

Cases 1 through 6 use an insulation package of wire screen plus a series of layered plates.

Case 1 - This case uses the reference design insulation material for the area adjacent to the cover gas. The material consists of 10 inches of wire screen package plus 12 inches of a layered plate arrangement. The results of the analysis is shown on Table 2-1. The temperature at the top of the closure is 126°F for the areas where no penetrations exist. The SRP surface temperature is the highest, at 198°F. This far exceeds the limit of 150°F. The following cases show variations to reduce the surface temperature.

Case 2 - This case has the same configuration of insulation materials as analyzed for Case 1 with the addition of a forced cooling method. to the top surface only. The velocity of the air used for the forced convection is 16 fps. As shown on Table 2-2, the temperatures are reduced from 126°F to 100°F at areas without penetrations and from 198°F to 152°F at the SRP. From this analysis, it becomes apparent that the reactor closure temperature can be maintained without internal cooling complications.

Case 3 - Case 3 was devised to determine the thermal effect the penetrations and side steel container has on the top structure. For this case, only the SRP was analyzed, since the thermal leakage could be directly compared with Case 1, which utilizes free convection cooling at the top surface. The results are shown on Table 2-3. The top surface temperature is reduced from 198°F to 163°F and utilizes natural convection cooling at the top surface. The 35°F reduction in temperature shows that isolating the thermal leakage through the insulation container walls can significantly reduce the temperature on the top structure. Design methods should be investigated to insulate this leakage path. Additional benefit could also be gained by isolating the IVTM penetration.

Case 4 - This case also analyzes the SRP with the insulation side container thermal leakage isolated from the remaining top structure. For this case, forced convection cooling was included and the results are shown on Table 2-4. As shown, the top surface temperature is further reduced to 126°F, well below the limit of 150°F. The result further indicate that by isolating thermal leaks along with simple top surface forced cooling, the reactor closure can be maintained at temperature well below the 150°F limit.

Case 5 - The thickness of insulation was also investigated because the under surface of the reactor closure has room for increase thickness. For this case, the 12 inch layered plates shown for Case 1 were increased to 24 inches. To determine the average heat leakage through the plugs, the analysis was only performed where no penetrations exist. The results for this case are shown on Table 2-5. Compared with Case 1 the top surface is reduced from 126°F to 115°F.

Case 6 - This case further increased the layered plates to a thickness of 36 inches. The results are shown on Table 2-6. As shown, the temperature is further reduced to 108°F, an additional 7°F.

Cases 7 through 9 use an insulation package of Kaylo (K = 0.03 BTU/hr Ft °F).

Case 7 - This case analyzes the closure with the entire insulation package replaced with Kaylo. This case uses natural convection cooling on the top surface. The results are shown on Table 2-7. For this case, the top surface temperature at areas where no penetrations exist is approximately the same as the Case 1 reference design, 129°F. However, on the SRP, the top surface temperature decreases from 198°F to 177°F, a considerable decrease in temperature. For this arrangement, it is estimated that the seals in the flange may be near the design temperature limit, but this would only exist at localized spots.

Case 8 - This case also used the Kaylo insulation material, but considers that the thermal leakage through the insulation container is isolated from the top surface. Because of this, the top surface temperatures of the SRP is reduced to 144°F as shown on Table 2-8, considerably less that what is required.

Case 9 - This case evaluates the Kaylo insulation material arrangement further by including forced convection cooling on the top surface. As shown on Table 2-9, the SRP top surface is further reduced to only 113°F . The forced cooling is again considered only at local spots where penetrations exist.

Case 10 through 13 consider the use of Kaylo in place of the screen package of Case 1 reference design.

Case 10 - The thermal results of using Kaylo for the screen package with natural convection cooling are shown on Table 2-11. Only the SRP was analyzed and only an 8°F benefit was gained. The top surface of 191°F is considered high.

Case 11 - This case is the same as Case 10 with the addition of forced convection cooling. As shown on Table 2-11, the top surface on the SRP is reduced to 145°F, which is below the 150°F design limit.

Case 12 - This case is also similar to Case 10, but considers the thermal penetration leaks isolated. As shown on Table 2-12, the SRP temperature is reduced to 152°F, very close to Case 11 using forced convection and near the 150°F design limit temperature.

Case 13 - This case uses the combination of forced convection cooling of the top surface of the SRP and isolating the thermal leak paths. The results for this case are shown on Table 2-13. The top surface temperature is reduced to 118°F.

Case 14 and 15 are two additional cases that consider the temperature effect on the closure when the condition occurs that the decay heat drives the sodium pool temperature from 875°F to 1150°F, For both these cases, only the areas where no penetrations exist were analyzed.

Case 14 - This case is the same arrangements as Case 1. From Table 2-14 the surface temperatures go from 126°F to 149°F, an increase of 23°F.

Case 15 - This case considers the effect of forced convection cooling. As shown on Table 2-15, the temperature is reduced to 113°F, 13°F less than the surface temperature in Case 1.

Another area where steady state analysis was performed was at the interface of the support deck and large rotating plug. In each case, the material arrangement of the LRP was as stated for Case 1, Table 2-1. For the deck the following cases were evaluated.

1. Insulation - Wire screen plus layered plates
   Cooling - N_2 cooling of bottom of concrete
   Results - Figure 2-3
2. Insulation - Wire screen plus layered plates
   Cooling - N_2 cooling of bottom of concrete
   Radial heat flow from rotating plugs included
   Results - Figure 2-4
3. Insulation - Kaylo
   Cooling - None
   Results - Figure 2-5
4. Insulation - Wire screen plus layered plates
   Cooling - N_2 cooling of bottom of concrete
   Decay Heat Sodium Pool temperature
   Results - Figure 2-6

For each of the above four cases, there is very little difference in the top deck temperature. The range is 81°F to 88°F.

The use of Kaylo insulation with no nitrogen cooling of the lower area near the concrete has a steel structure temperature of approximately 125°F at areas away from the large penetrations. The design limit for the concrete has been set at 125°F. Once again, the Kaylo type insulation shows great promise for reducing the forced cooling requirements in the deck area where the large heat source from the large (IHX) penetrations does not exist.

10.2.4
TRANSIENT ANALYSIS

Two startup transient conditions were considered for the analysis. As shown on Figure 2-7, one transient condition had a 50°F/Hr ramp. while the other transient condition had a 67.5°F/Hr ramp. Also, for this analysis, two regions

of the closure area were considered as being representative of the system for the transient analysis at this point in the design. The two regions considered were the deck-plug interface area and the small rotating plug. From the results of the analysis, either the reference insulation, previously discussed or Kaylo AF insulations could be considered.

The deck-plug interface area utilized the comprehensive steady state analysis previously run. Conversion to the transient analysis was accomplished by the addition of a Mass X specific heat matrix. The results for this analysis are based on the 50°F/Hr ramp condition, with a maximum temperature of 900°F for this case. The model for the analysis is shown on Figure 2-8 with the results shown on Figure 2-9 and 2-10. From the results, the only member with any significant thermal response is the supporting containers for the thermal insulation. This member sees the full effect of the startup transient condition. The main structural members of the deck have only a very gradual thermal response. As shown on Figure 2-10, the thermal response logs the excitation in time.

The small rotating plug was analyzed by a one-dimensional lumped mass model (7 nodes). This method was selected instead of the more complex 3D model due to the complex geometry of the SRP (assymetric due to the offset fuel transfer tube). This method of analysis will show the transient response at the selected points with a loss of detail, due to the integrated effect of the surrounding areas. The model for this analysis is shown on Figure 2-11. As shown, on Figure 2-12, there is very little temperature effect on the structure.

CODE: STAP3 DATA: TARS13

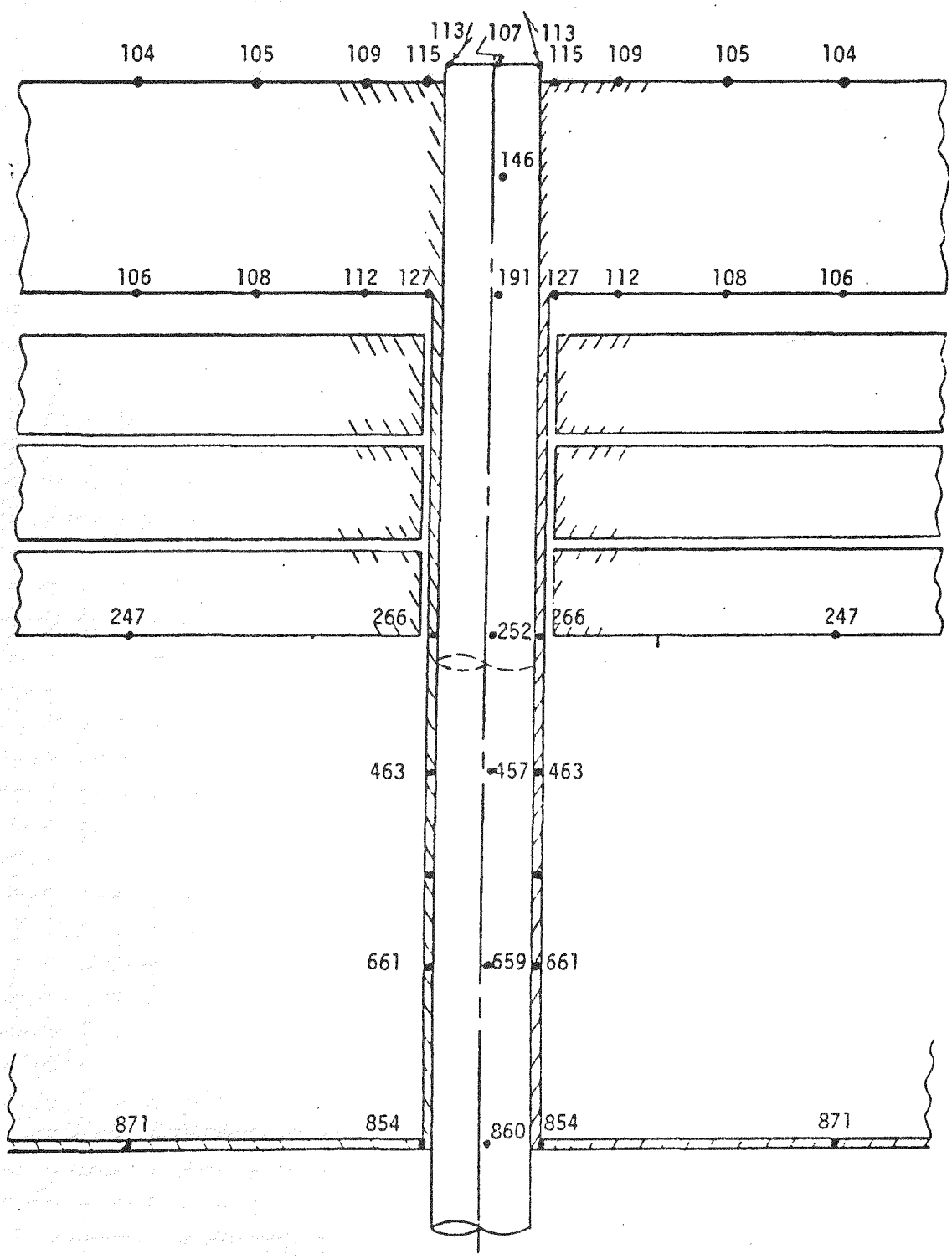

Figure 2-1 Instrument Penetrations - Steady State Results

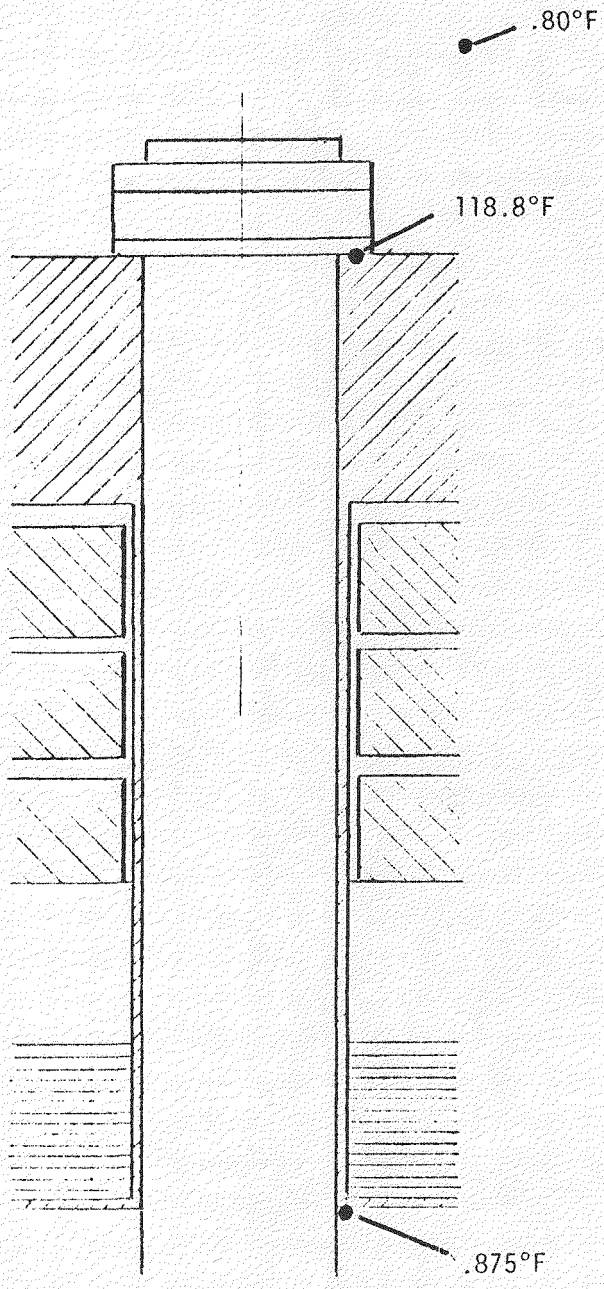

Figure 2-2 Support Column Penetrations - Steady State Results

Table 2-1

I. Condition - Case 1

1.	Temperature in Head Access Area	- 80°F
2.	Temperature of Sodium Pool	- 875°F
3.	Insulation material	- 10" Wire Screen+12" Layered Plates
4.	Insulation can	- Considered Attached
5.	Cooling	- Natural Convection

II. Location

at SRP with IVTM Penetration

Configuration Temperature °F

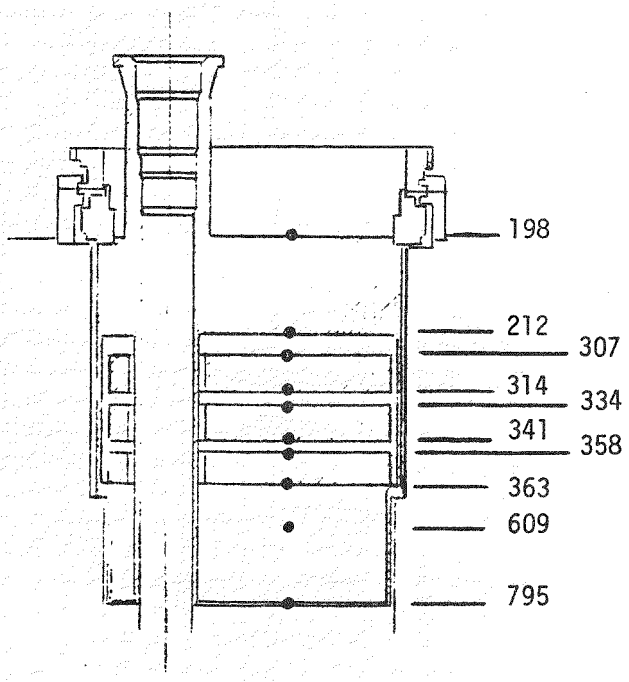

at a no Penetration Area

Temperature °F Configuration

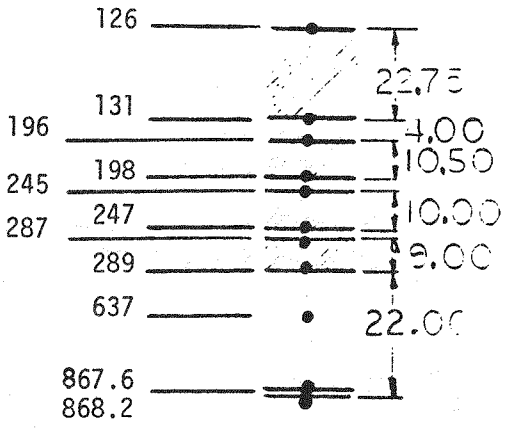

Table 2-2

I. Condition - Case 2

1.	Temperature in Head Access Area	- 80°F
2.	Temperature of Sodium Pool	- 875°F
3.	Insulation material	- 10" Wire Screen+12" Layered Plates
4.	Insulation can	- Considered Attached
5.	Cooling	- Forced Convection

II. Location

at SRP with IVTM Penetration

Configuration Temperature °F

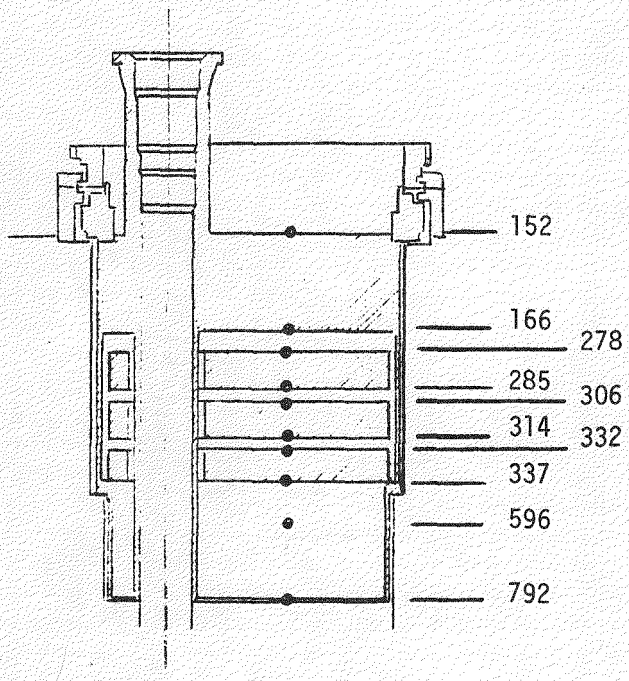

at a no Penetration Area

Temperature °F Configuration

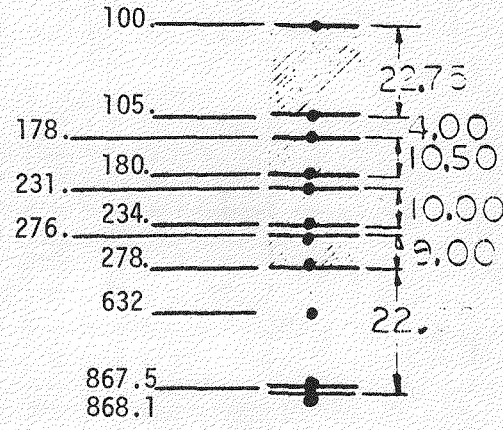

Table 2-3

I. Condition - Case 3

1.	Temperature in Head Access Area	-80°F
2.	Temperature of Sodium Pool	-875°F
3.	Insulation material	-10" Wire Sreen+12" Layered Plates
4.	Insulation can	-Assumed Isolated for Thermal Analysis
5.	Cooling	-Natural Convection

II. Location

at SRP with IVTM Penetration

Configuration Temperature °F

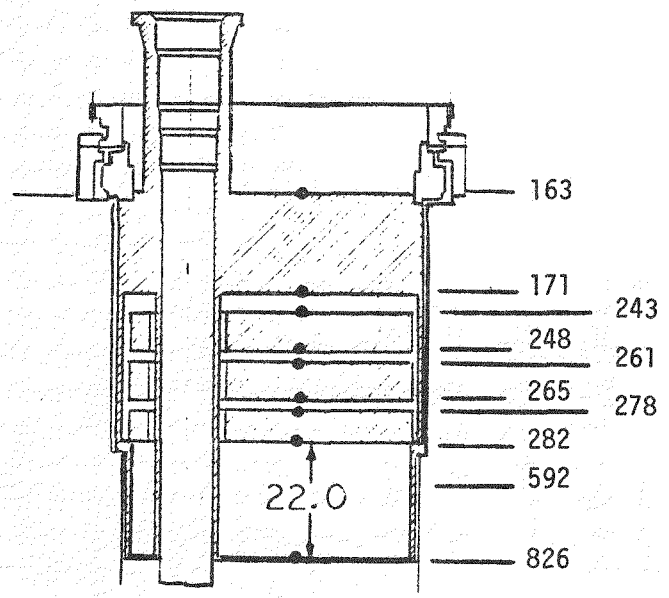

Table 2-4

I. Condition - Case 4

1.	Temperature in Head Access Area	-80°F
2.	Temperature of Sodium Pool	-875°F
3.	Insulation material	-10" Wire Screen+12" Layered Plates
4.	Insulation can	-Assumed Isolated for Thermal Analysis
5.	Cooling	-Forced Convection

II. Location

at SRP with IVTM Penetration

Configuration Temperature °F

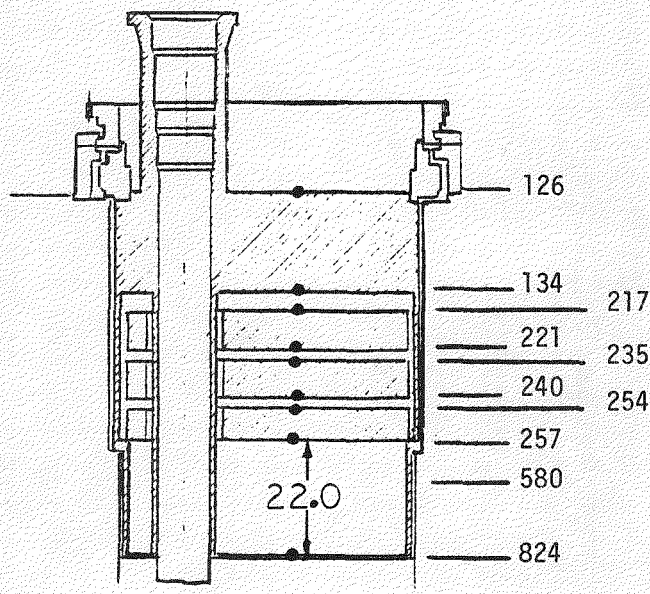

Table 2-5

I. Condition - Case 5

1.	Temperature in Head Access Area	- 80°F
2.	Temperature of Sodium Pool	- 875°F
3.	Insulation material	- 10" Wire Screen + 24" Layered Plates
4.	Insulation can	- N/A
5.	Cooling	- Natural Convection

II. Location

at a no Penetration Area

Temperature °F | Configuration

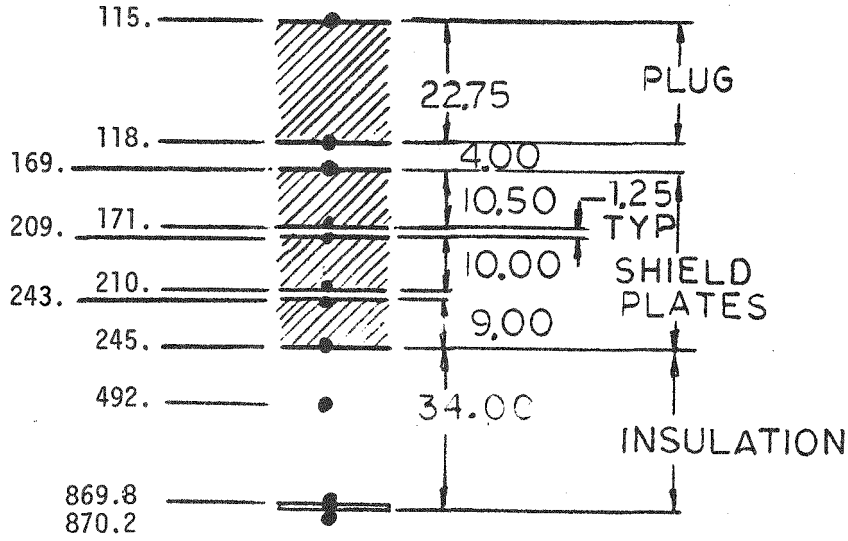

Table 2-6

I. Condition - Case 6

1.	Temperature in Head Access Area	- 80°F
2.	Temperature of Sodium Pool	- 875°F
3.	Insulation material	- 10° Wire Screen + 36" Layered Plate
4.	Insulation can	- N/A
5.	Cooling	- Natural Convection

II. Location

at a no Penetration Area

Temperature °F — Configuration

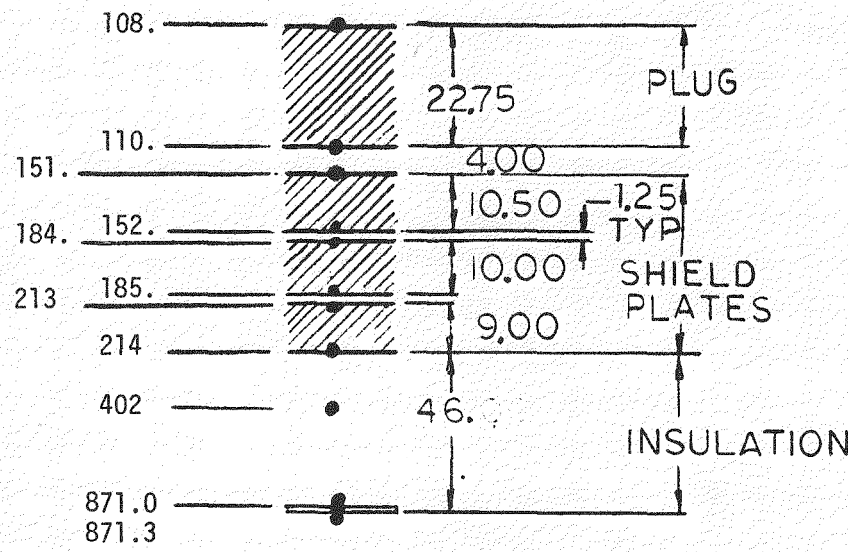

Table 2-7

I. Condition

1.	Temperature in Head Access Area	-	80°F
2.	Temperature of Sodium Pool	-	875°F
3.	Insulation material	-	Kaylo
4.	Insulation can	-	Considered Attached
5.	Cooling	-	Natural Convection

II. Location

at SRP with IVTM Penetration

Configuration Temperature °F

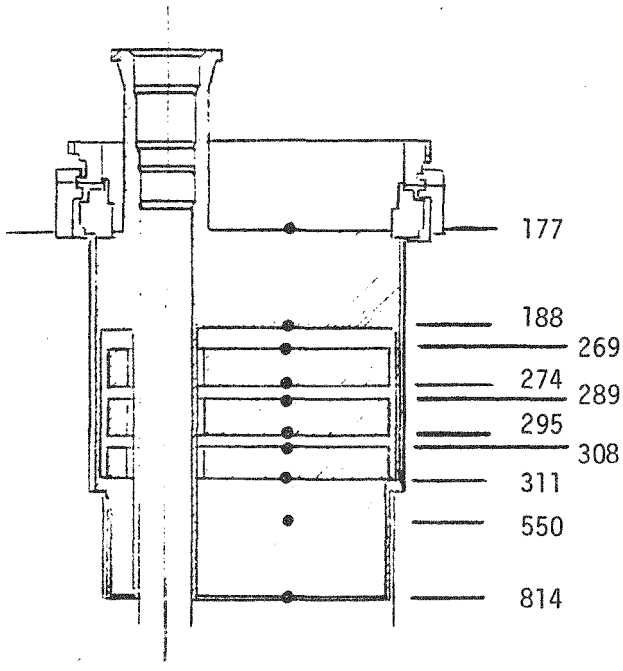

at a no Penetration Area

Temperature °F Configuration

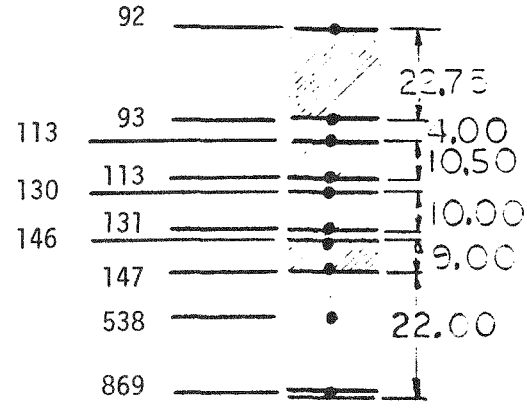

Table 2-8

I. Condition - Case 8

1. Temperature in Head Access Area - 80°F
2. Temperature of Sodium Pool - 875°F
3. Insulation material - Kaylo
4. Insulation can - Assumed Isolated for Thermal Analysis
5. Cooling - Natural Convection

II. Location

at SRP with IVTM Penetration

Configuration Temperature °F

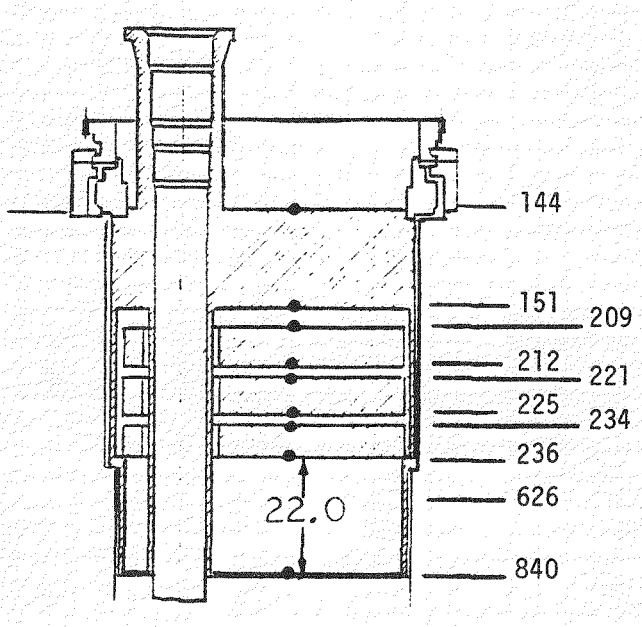

Table 2-9

I. Condition - Case 9

1. Temperature in Head Access Area - 80°F
2. Temperature of Sodium Pool - 875°F
3. Insulation material - Kaylo
4. Insulation can - Assumed Isolated for Thermal Analysis
5. Cooling - Forced Convection

II. Location

at SRP with IVTM Penetration

Configuration Temperature °F

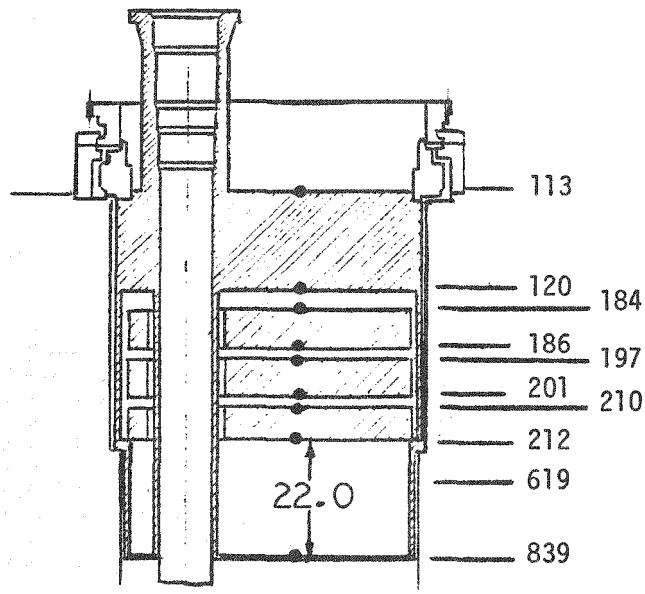

Table 2-10

I. Condition - Case 10

1.	Temperature in Head Access Area	- 80°F
2.	Temperature of Sodium Pool	- 875°F
3.	Insulation material	- 10" Kaylo + 12" Layered Plates
4.	Insulation can	- Considered Attached
5.	Cooling	- Natural Convection

II. Location

at SRP with IVTM Penetration

Configuration Temperature °F

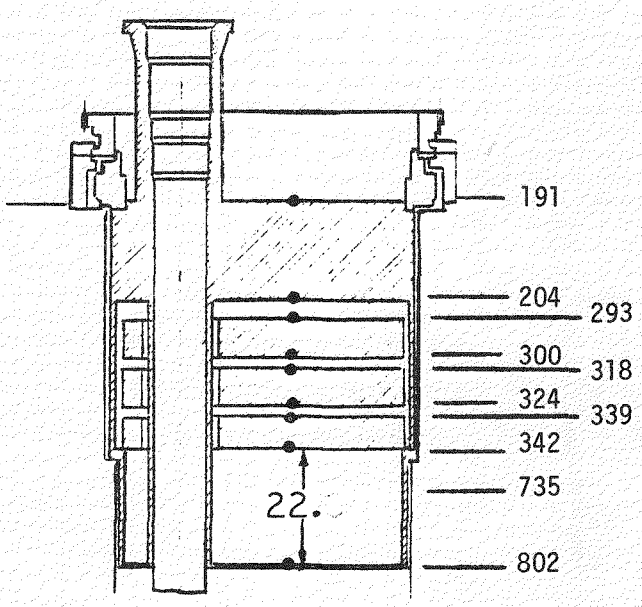

Table 2-11

I. Condition - Case 11

1.	Temperature in Head Access Area	- 80°F
2.	Temperature of Sodium Pool	- 875°F
3.	Insulation material	- 10" Kaylo + 12" Layered Plates
4.	Insulation can	- Considered Attached
5.	Cooling	- Forced Convection

II. Location

at SRP with IVTM Penetration

Configuration Temperature °F

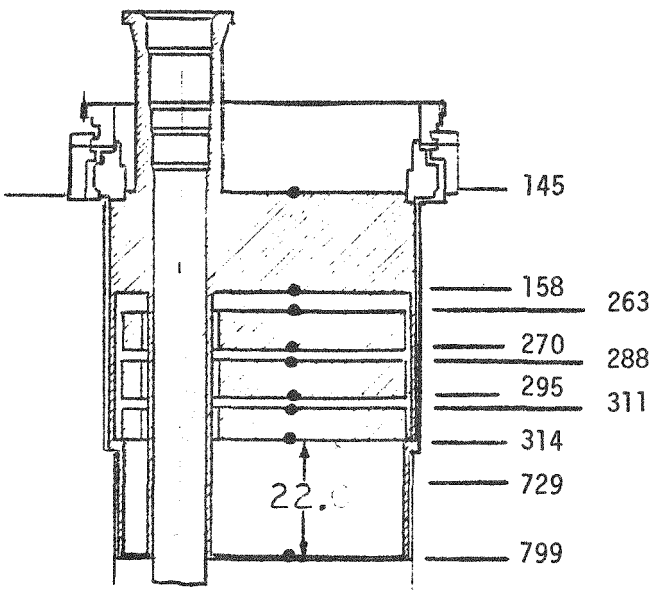

Table 2-12

I. Condition - Case 12

1. Temperature in Head Access Area - 80°F
2. Temperature of Sodium Pool - 875°F
3. Insulation material - 10" Kaylo + 12" Layered Plates
4. Insulation can - Assumed Isolated for Thermal Analysis
5. Cooling - Natural Convection

II. Location

at SRP with IVTM Penetration

Configuration Temperature °F

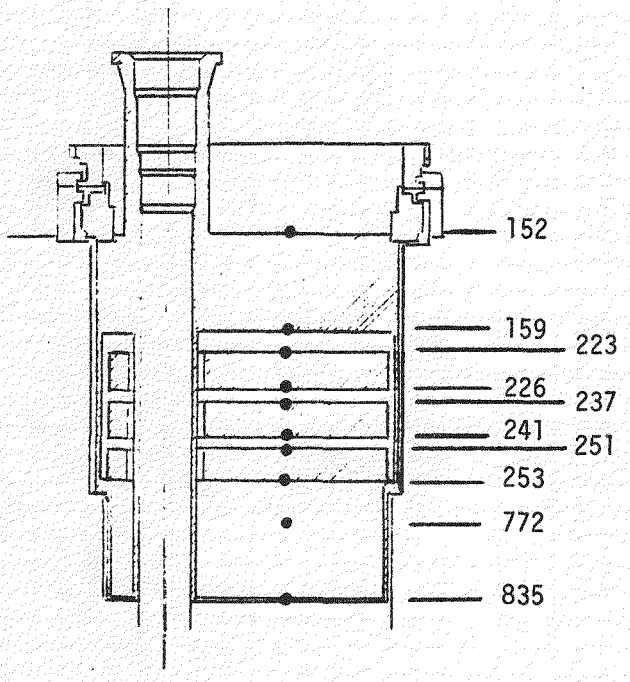

at a no Penetration Area

Temperature °F Configuration

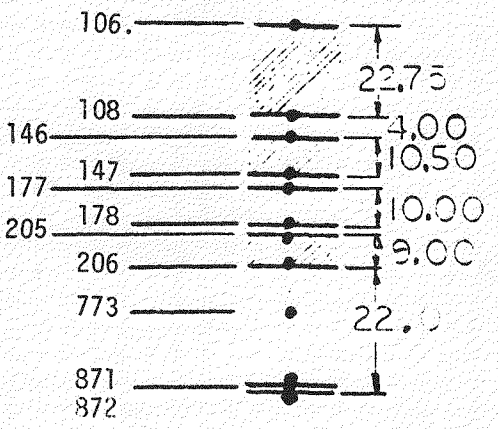

Table 2-13

I. Condition - Case 13

1.	Temperature in Head Access Area	- 80°F
2.	Temperature of Sodium Pool	- 875°F
3.	Insulation material	- 10" Kaylo + 12" Layered Plates
4.	Insulation can	- Assumed Isolated for Thermal Analysis
5.	Cooling	- Forced Convection

II. Location

at SRP with IVTM Penetration

Configuration Temperature °F

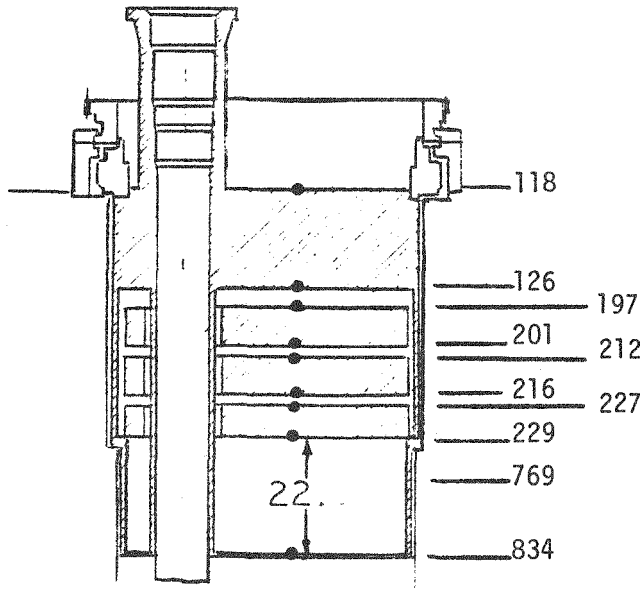

Table 2-14

I. Condition - Case 14

1. Temperature in Head Access Area - 80°F
2. Temperature of Sodium Pool - 1150°F (Decay Heat)
3. Insulation material - 10° Wire Screen + 12" Layered Plate
4. Insulation can - N/A
5. Cooling - Natural Convection

II. Location

at a no Penetration Area

Temperature °F | Configuration

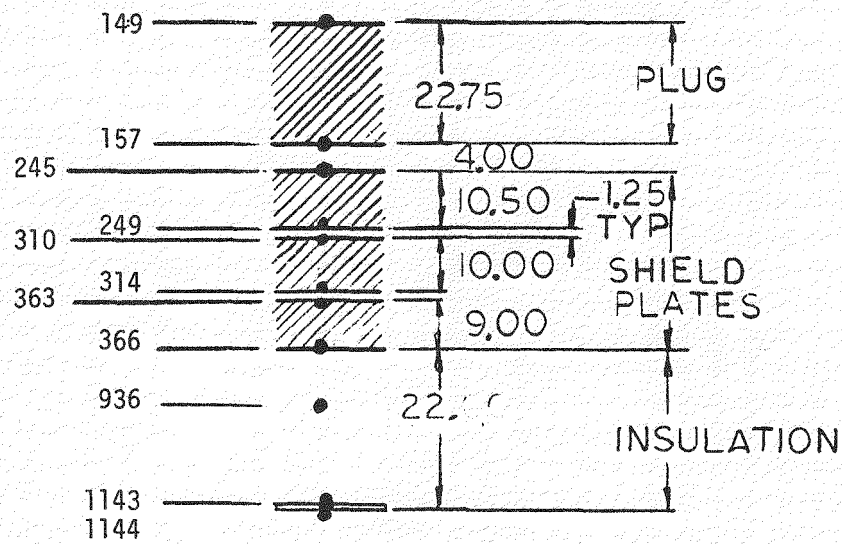

Table 2-15

I. Condition - Case 15

1.	Temperature in Head Access Area	- 80°F
2.	Temperature of Sodium Pool	- 1150°F (Decay Heat)
3.	Insulation material	- 10" Wire Screen + 12" Layered Plate
4.	Insulation can	- N/A
5.	Cooling	- Forced Convection

II. Location

at a no Penetration Area

Temperature °F — Configuration

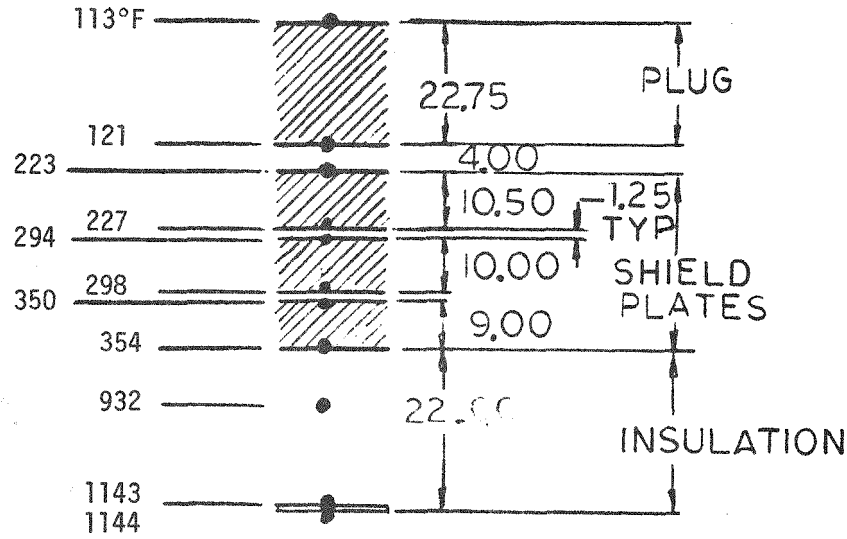

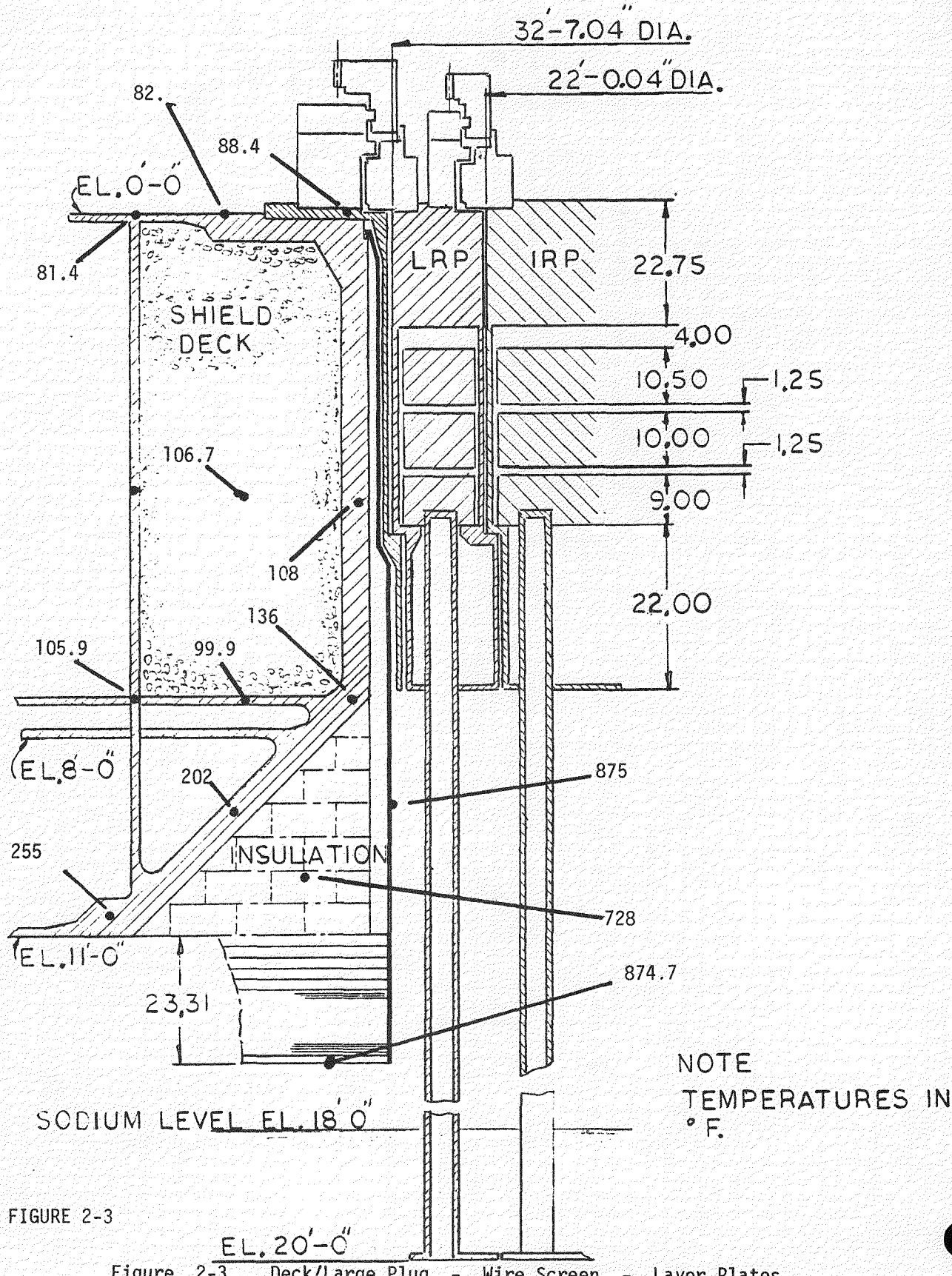

FIGURE 2-3

Figure 2-3 Deck/Large Plug - Wire Screen - Layer Plates -Steady State Results

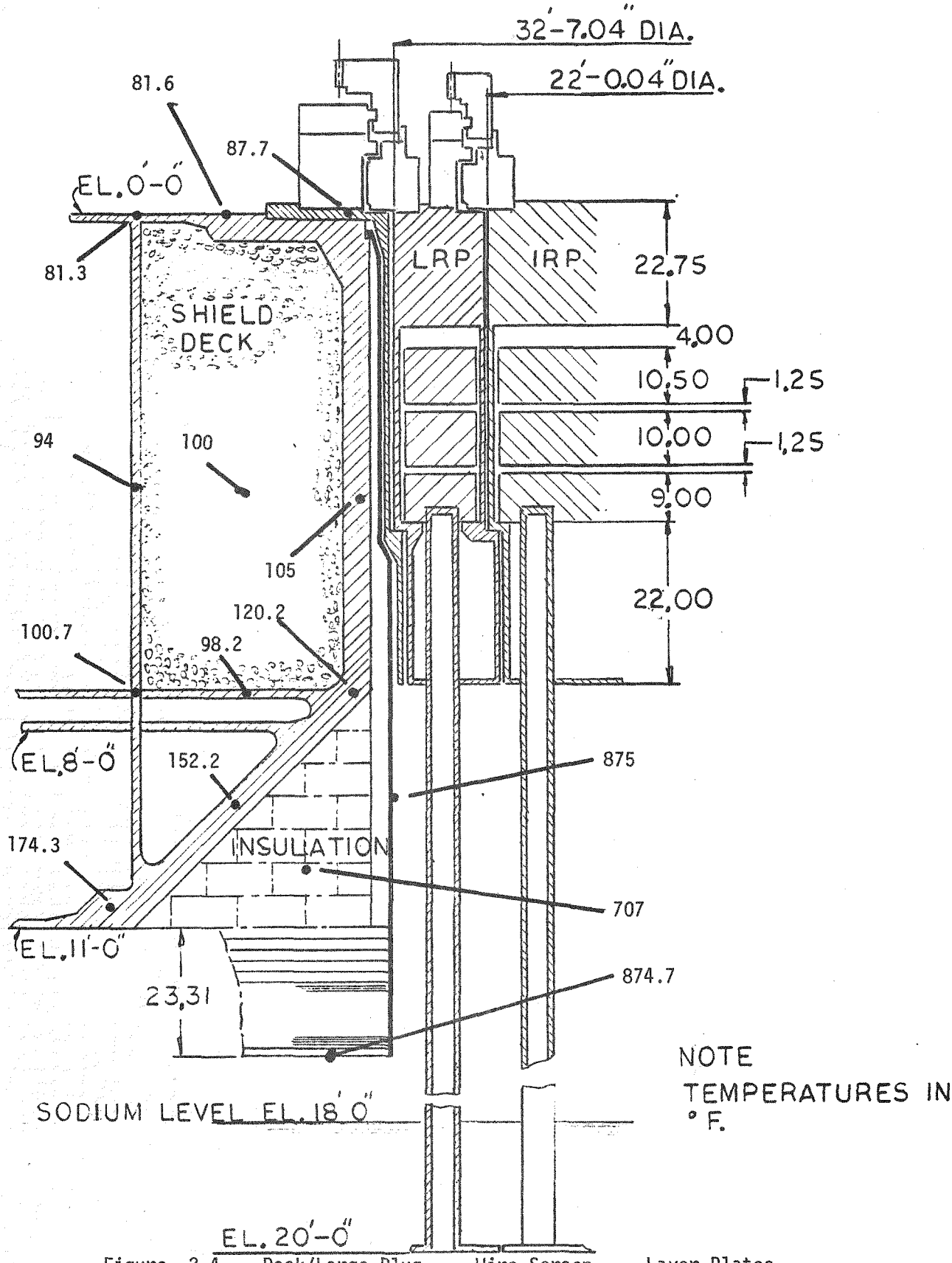

Figure 2-4 Deck/Large Plug - Wire Screen - Layer Plates -Steady State Results

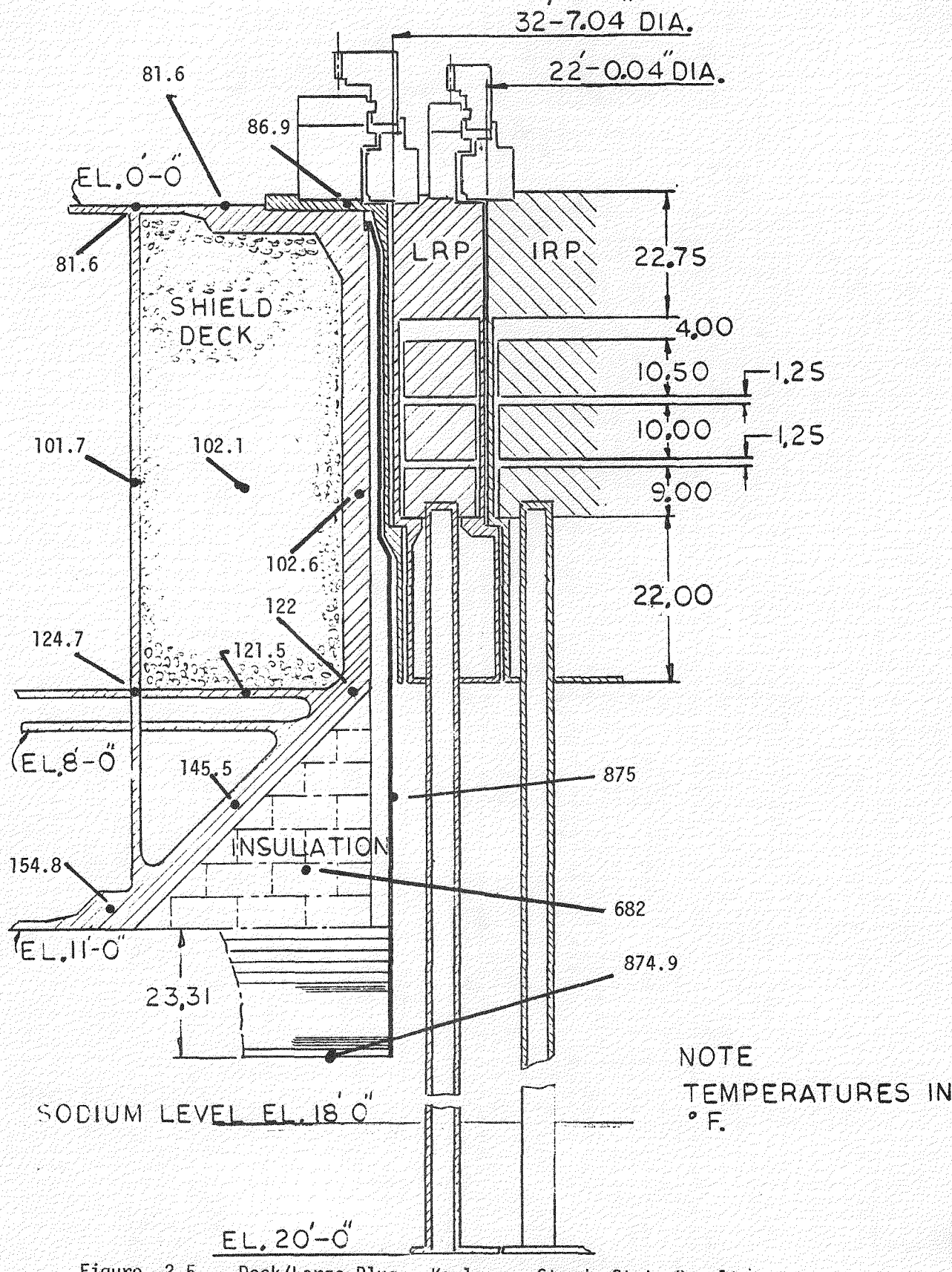

Figure 2-5 Deck/Large Plug - Kaylo - Steady State Results

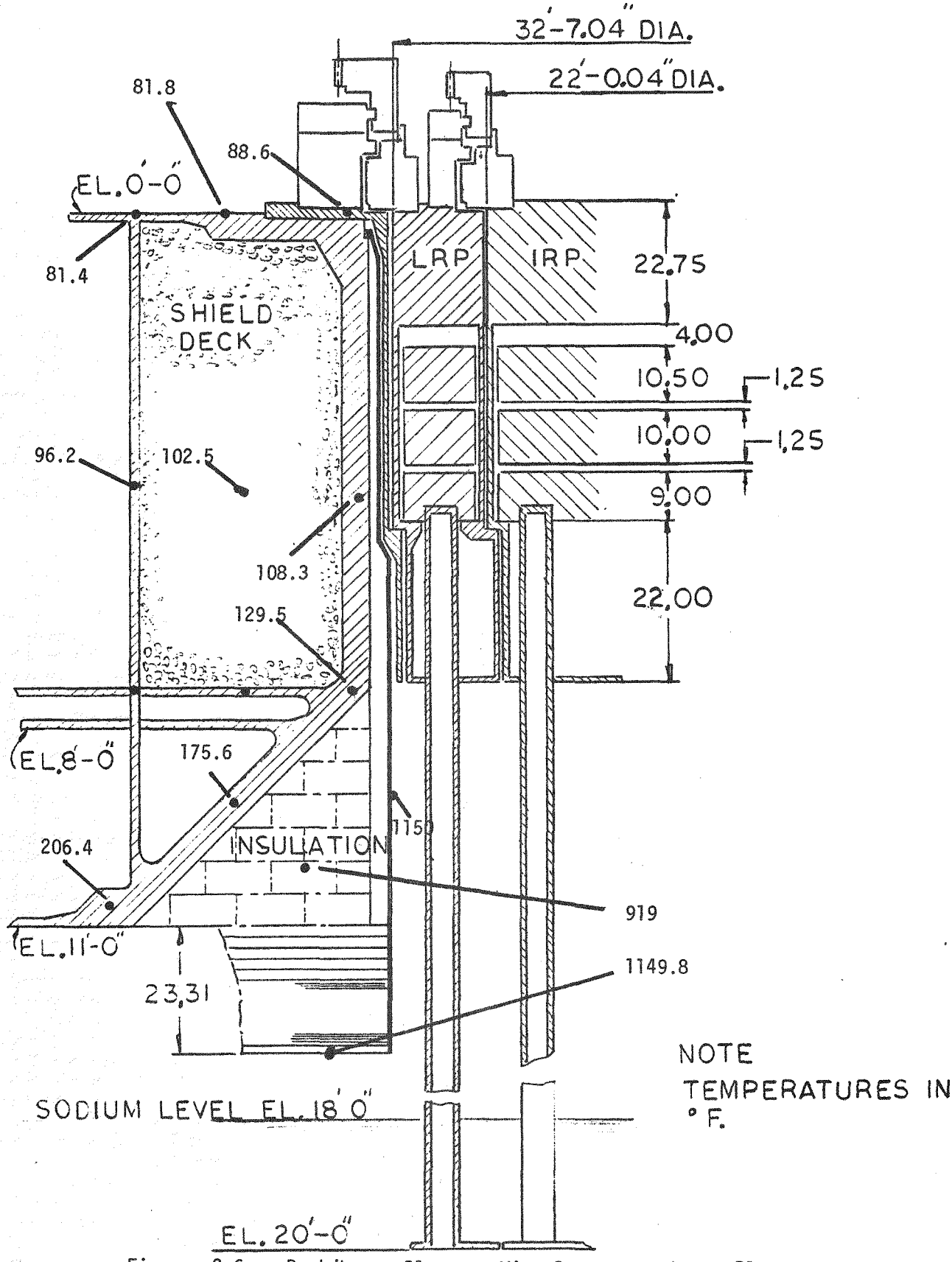

Figure 2-6 Deck/Large Plug - Wire Screen - Layer Plate -Decay Heat Results

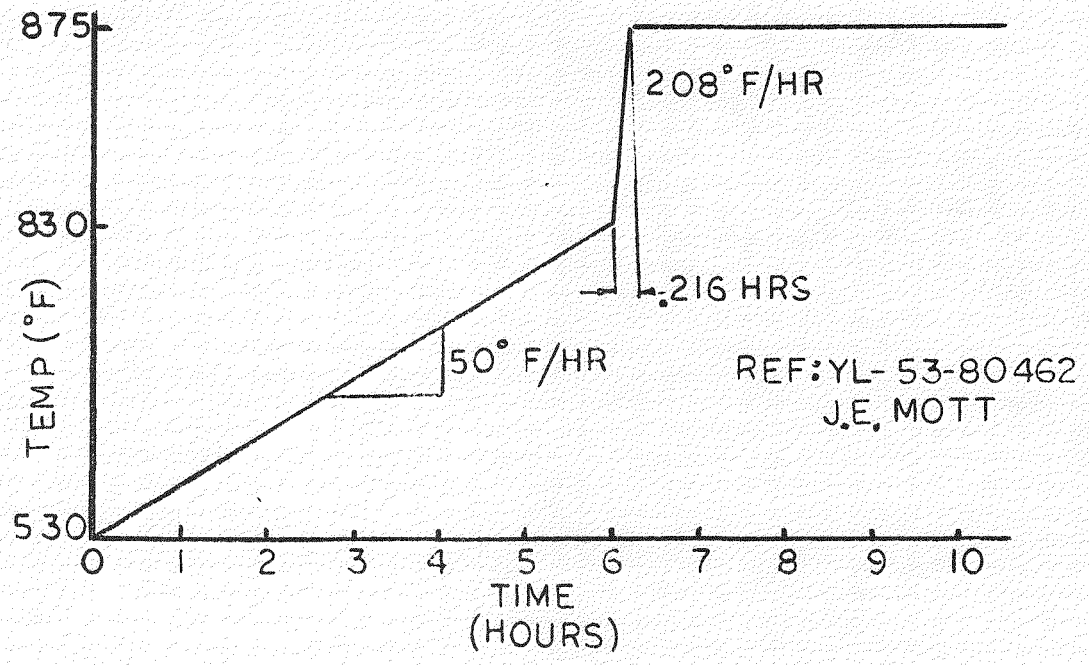

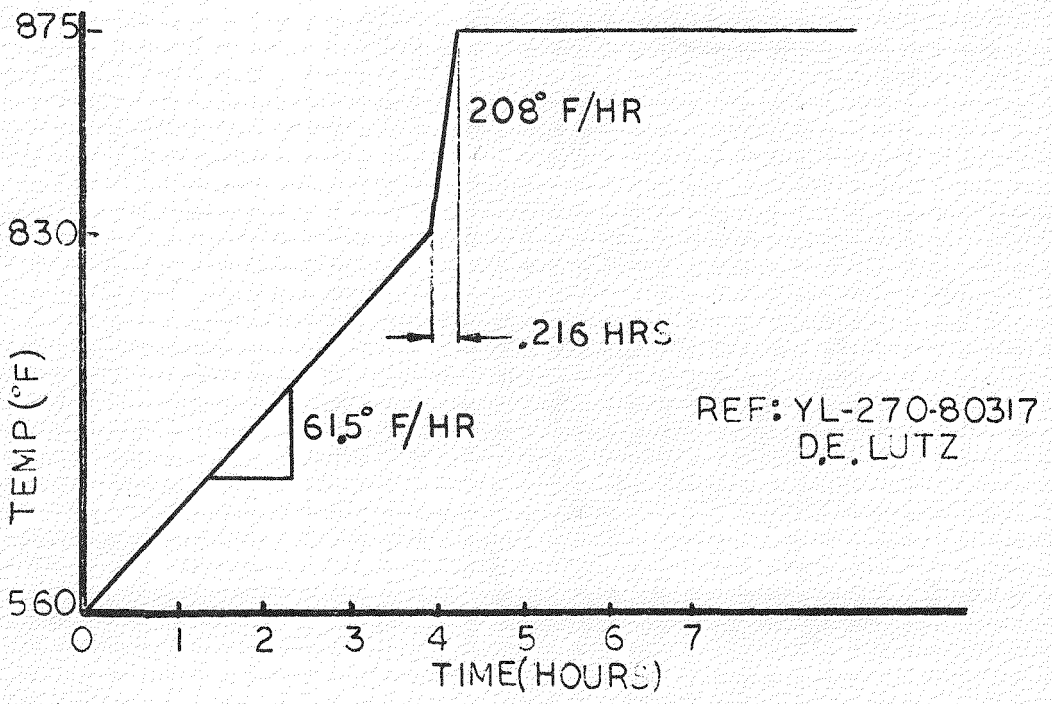

Figure 2-7 Startup Transient Condition

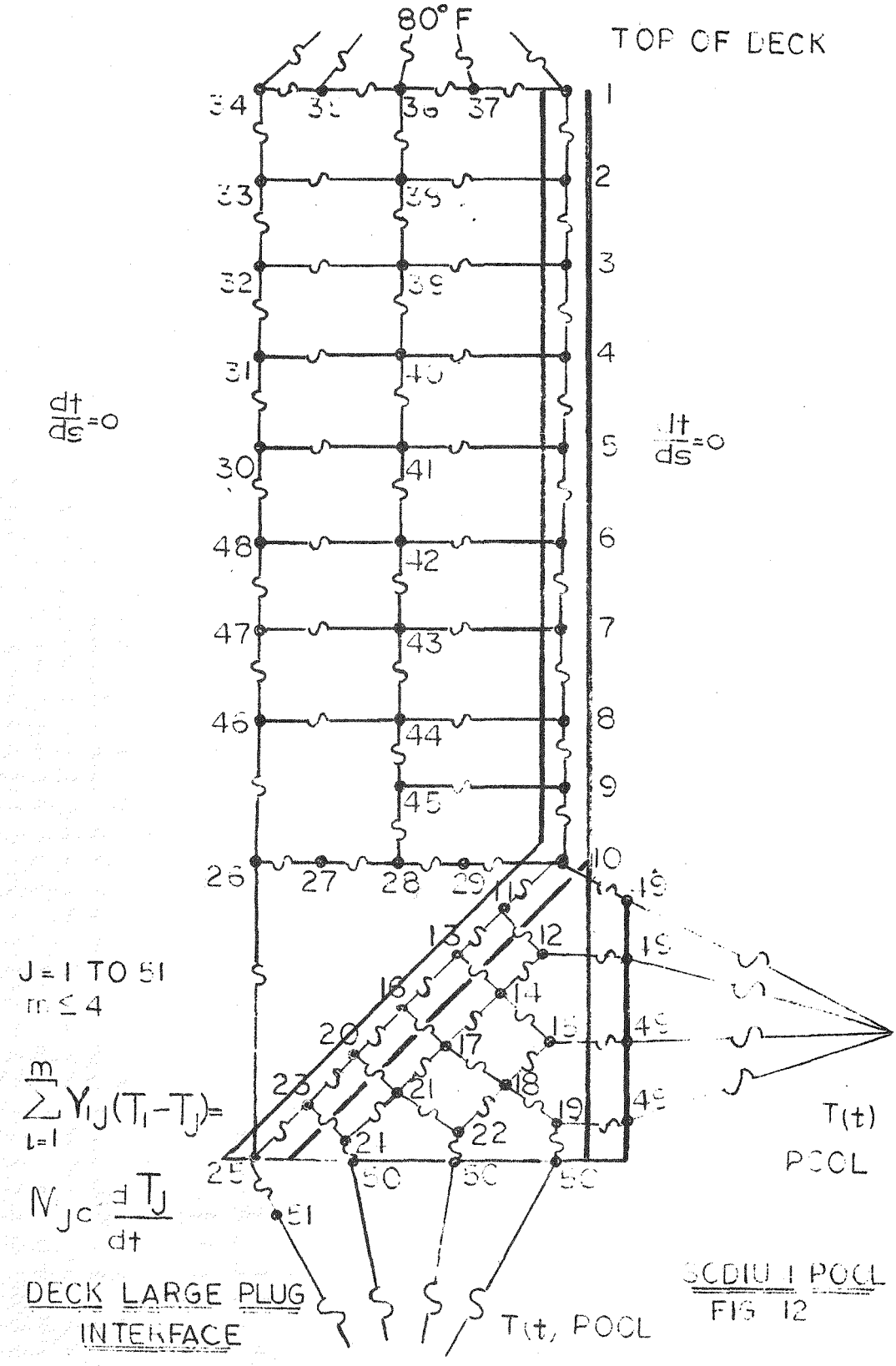

Figure 2-8 Deck/Large Plug Transient Model

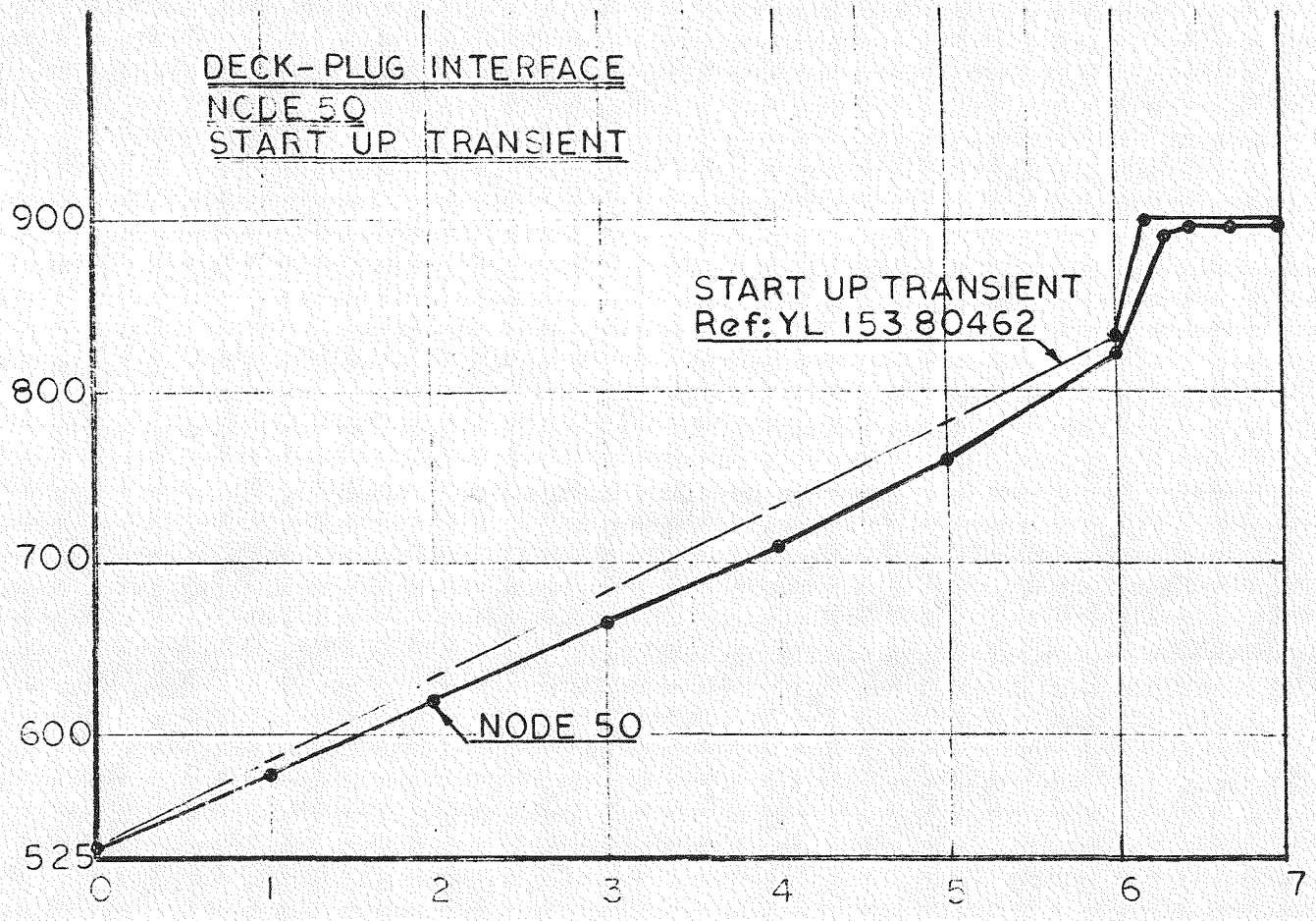

Figure 2-9 Deck/Large Plug Startup Transient Results

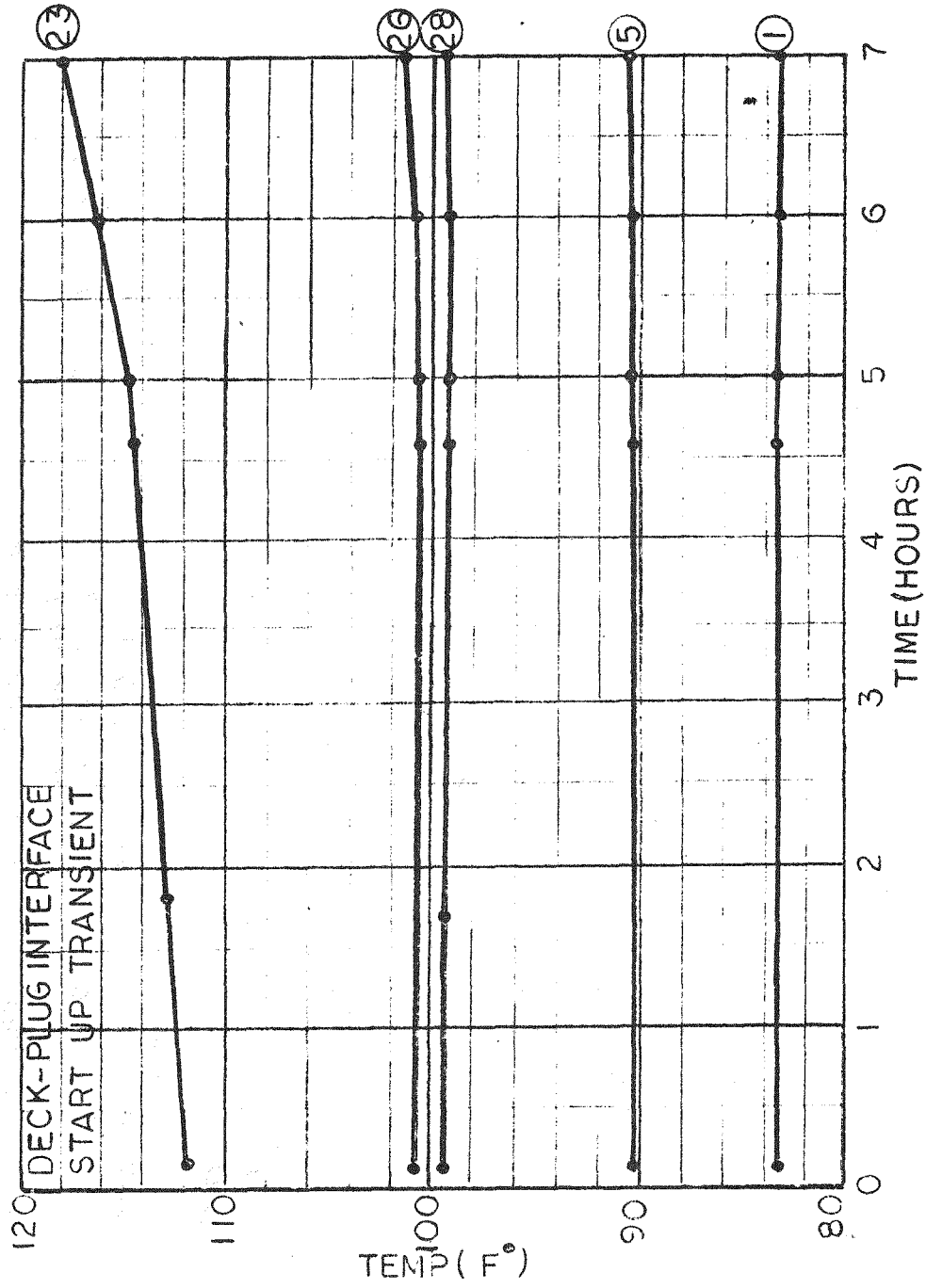

Figure 2-10 Deck/Large Plug Startup Transient Results

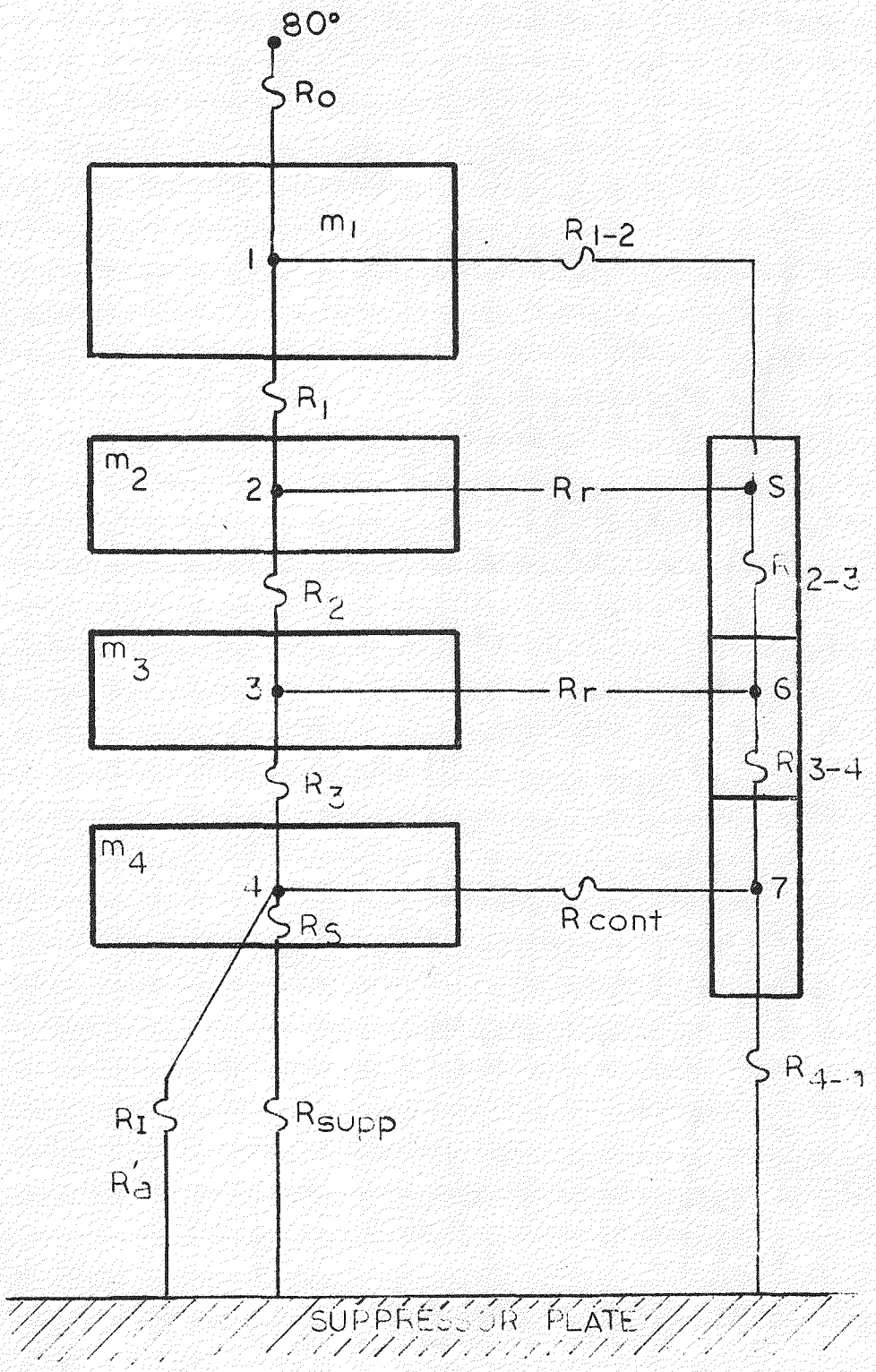

Figure 2-11 Small Plug Transient Model

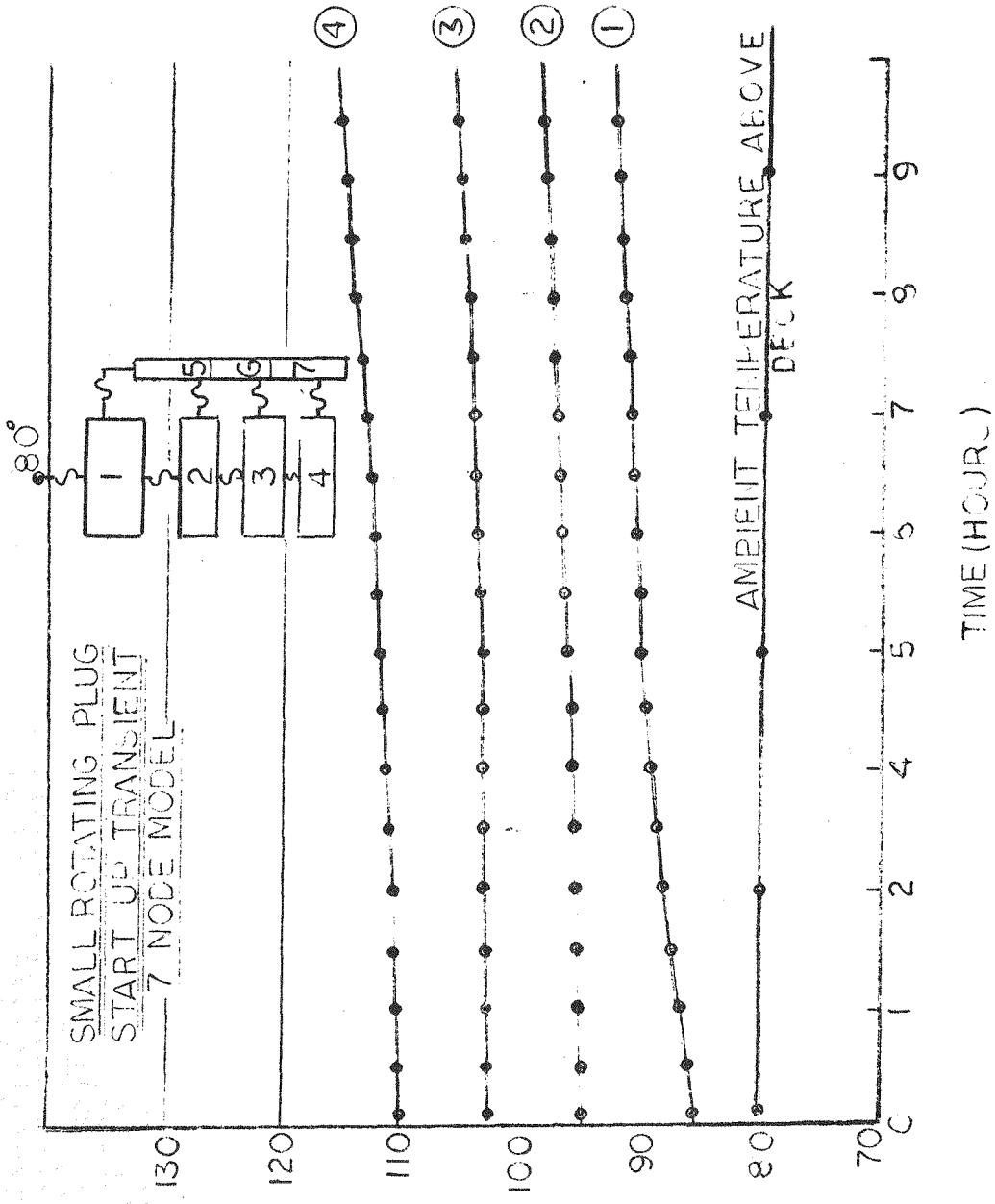

Figure 2-12 Small Plug Startup Transient Results

II-10.3

CONCLUSIONS

10.3.1 STEADY STATE

The reactor closure reference design, wire screen plus layered plates of insulation, can be made to work, but local forced cooling near penetrations would be required to maintain a limit of 150°F. To reduce the surface temperature further, a method must be devised to reduce the thermal leakage through the penetrations. Increasing the layered plate thickness by an additional 12 inches is a help, but only reduces temperatures by approximately 10°F per 12 inches of insulation.

The substitution of Kaylo insulation for the screen and layered plate package has shown excellent results in reducing the temperature on the top surface of the reactor closure. If localized hot spots exists around penetrations, forced cooling can be added. Insulating materials like Kaylo should be investigated to a greater degree along with isolating the thermal leakage through penetrations. (See Tables 2-7, 2-8, 2-9)

The use of Kaylo insulation in place of the screen package of the reference design has also shown good results, but not quite as good as the entire insulation package being Kaylo. This method should be considered if lower layered plates are found necessary for other reasons. (See Tables 2-10, 2-11, 2-12, 2-13)

The deck/rotating plug area was also evaluated for the steady state condition. Again the reference design of screen plus layered plates with the addition of nitrogen cooling can be made to work. The analysis shows that a Kaylo type

insulation has great promise and can possibly greatly reduce internal cooling requirements. For the deck. (See Figure 2-5)

10.3.2
TRANSIENT

The shape of the reactor startup curve has very little effect on the thermal response because of the large time constant of the structures. The large mass of the deck and plugs smoothes out the transient thermal response.

10.3.3
RECOMMENDATIONS

It is recommended that Kaylo or equivalent be evaluated as an alternative to the reference design of screen plus layered plate insulation. The long term effects of sodium vapor on the insulation should be investigated.

Also further design effort is required to devise a method to reduce the thermal effect of the penetrations on the top structure.

Additional thermal analysis is required on the rotating plugs as a complete system, to better define the temperature fields and heat losses. The analysis should include a three dimensional analysis with an extensive model.

For the reference design insulation, wire screen and layered plates, further thermal analysis is required to define the temperature field at penetrations.

REFERENCES

1. "Pool-type LMFBR Plant, 1000 MWe Phase A Design," EPRI NP-646, (April 1978).

APPENDIX II-10A

The following thermal analysis calculations, heat transfer programs and computer print outs are included in this appendix:

1. Radiation and Convection Calculations
2. Support Column for Upper Internals, Steady State Calculations
3. Computer listing of one dimensional heat transfer program and some print out.
4. Computer listing of two dimensional steady state axisymmetric heat transfer program and some print out.
5. Computer listing of two dimensional transient axisymmetric heat transfer program and some print out.
6. Seven Node Model of the Small Rotating Plug
   a. Steady state analysis
   b. Transient analysis

RADIATION BETWEEN PARALLEL SURFACES

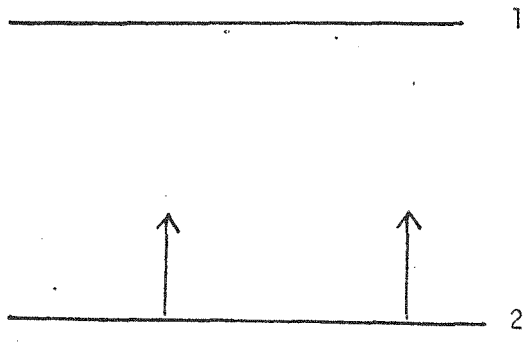

$$h_r = \frac{\sigma}{\frac{1}{\varepsilon_1} + \frac{1}{\varepsilon_2} - 1} (T_1^3 + T_1^2 T_2 + T_1 T_2^2 + T_2^3)$$

$$Q = h_r A (T_2 - T_1)$$

ε = Emissivity

σ = Stefan-Boltzmann Constant = 1.671219×10^{-10}

A = area in inches^2

$\varepsilon_{ss} \approx .26$

Reference: McAdams, Heat Transmission 3rd Edition McGraw-Hill Book Company

FREE CONVECTION IN THE ARGON FILLED INTERFACE BETWEEN THE PLUGS

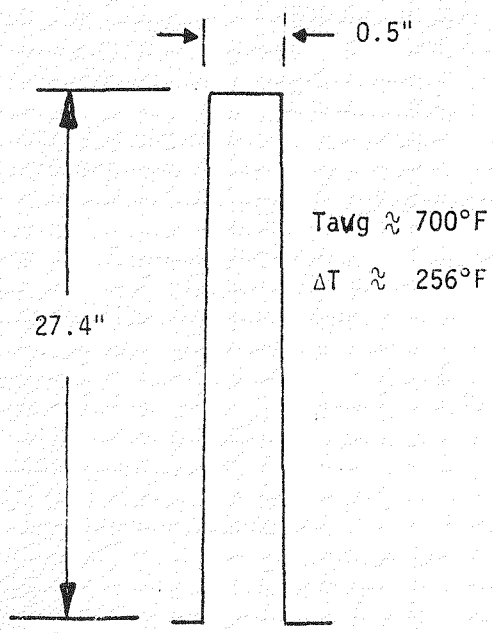

$$N_{Gr} = \frac{X^3 \rho^2 g \beta \Delta t}{u^2}$$

$$N_{pr} = Cp\,{}^{u}/_{k}$$

$$\frac{hX}{k} = \frac{C}{(L/X)}\ 1/9\ [N_{Gr} \cdot N_{pr}]^n$$

for Argon @ 700°F

Cp = 0.124

k = .018

u = .096 lb/hr ft.

ρ = .0453 lb/ft^3

$N_{pr} = 0.652$

$\frac{N_{Gr}}{X^3 \Delta T} = 330506$

$L = {}^{2714}/_{12} = 2.283$ ft.

$X = {}^{.5}/_{12} = 0.0416$ ft.

from McAdams

$C = 0.071$

$n = 1/3$

$N_{Gr} \approx 330506(.0416)^3(256) = 6091.$

$N_{pr} \times N_{Gr} = 6091 \times .652 = 3971.$

$$\frac{.0416h}{.018} = \frac{.071}{(54.8)^{.11111}\ (3971)^{.3333}}$$

$2.3111\ h = 4.5505 \times 10^{-2} \times 15.8355548$

$h_{argon} = 0.31179$ BTU/hr ft^2

$k_{ss} = 8.4696$ BTU/hr ft^2°F/ft.

$R_{cond} = \frac{L}{K}$

$R_{conv} = {}^{1}/_{h}$

$R_{cond} = \frac{.0416}{.0133} = 3.1278$

$R_{conv} = {}^{1}/_{.31179} = 3.207$

$R_{conv} \approx R_{cond}$

Most of the heat will be passed by conduction. Convection can be ignored in the gap region.

ARGON CONVECTION ABOVE SODIUM SURFACE

Ref: McAdams, Heat Transfer

Temperature $\approx$ 875°F

$$\frac{hL}{k_f} = 0.14 [N_{Gr} * N_{pr}]^{1/3}$$

L = 5 ft.

$k_f \approx 0.0194$

$$\frac{N_{Gr}}{L\Delta T} = 54771.$$

$N_{pr} = 0.6519$

$\therefore h = 0.03058\Delta T^{1/3}$

AIR CONVECTION ABOVE DECK

Ref: McAdams p. 180

$h = 0.22\Delta T^{1/3}$

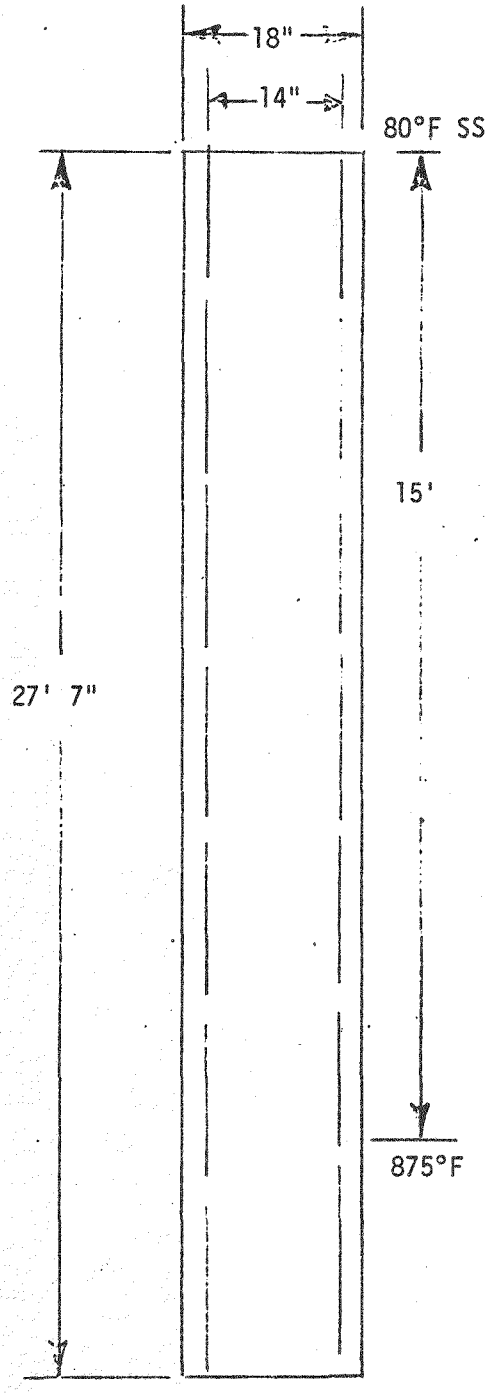

SUPPORT COLUMNS FOR UPPER INTERNALS

$$A = \frac{\pi}{4}(18^2 - 14^2) = .698 \text{ ft}^2$$

$$Q = \frac{AK}{L}\Delta T = \frac{.698 \times 8.4}{15}\Delta T$$

$$Q = 0.3908\Delta T$$

$$R = \frac{L}{Ak} = 2.5588$$

Support Column - Top of Plate
Iterative Solution

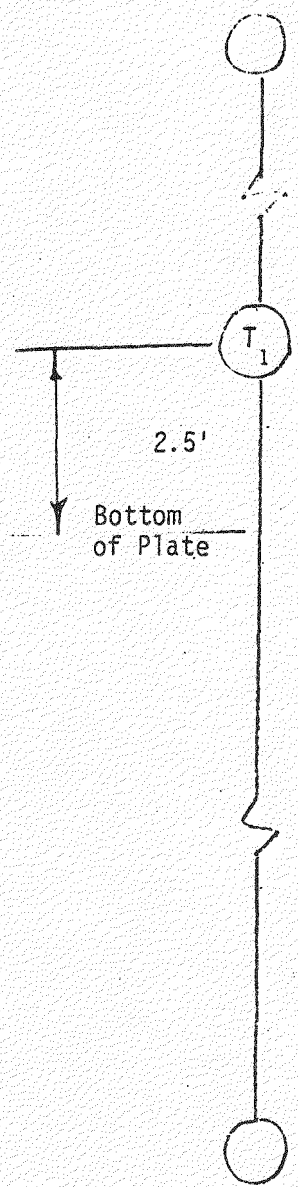

$h = .22\Delta T^{1/3}$

$\Sigma R = 5.8888$

$Q = \frac{\Delta T}{R} = \frac{795}{5.8888}$

$Q = 135.00 \frac{BTU}{hr}$

$T_1 = 529.5°F$

$A_1 \quad \frac{\pi}{4} 3^2 = 7.0686 \text{ ft}^2$

$h_c = 1.694$

$R_1 = \frac{1}{hA} = \frac{1}{1.699x7} = .08433$

$\dot{\Sigma} R = 2.64313$

$Q = \frac{795}{2.64313} = 300.779 \text{ BTU/hr}$

$T_1 = 80 + .08433 \times 300.779 = 105.3°F$ (1ST ITERATION)

ITERATIVE SOLUTION CONTINUED

$h_c = .22\ (25.364)^{1/3} = .6424$

$R_1 = \frac{1}{hA} = \frac{1}{.6424 \times 7.0686} = 0.2202$

$\Sigma R = .2202 + 2.5588 = 2.77902$

$Q = \frac{795}{2.77902} = 286.071$ BTU/hr

$T_1 = 80 + .2202 \times 286.071 = 62.99 + 80 = 143.°F$ (2ND ITERATION)

$h_c = .8646$

$R_1 = \frac{1}{hA} = 0.163$

$Q = \frac{795}{2.72242} = 292.02$ BTU/hr

$T_1 = 80 + .163 \times 292.02 = 80 + 47.6 = 127.6°F$ (3RD ITERATION)

$h_c = 1.1176$

$R_1 = 0.1265$

$Q = \frac{795}{2.68578} = 296.05$

$T_1 = 80 + 296.05 \times .265 = 80 + 37.45 = 117.4°F$ (4TH ITERATION)

$h_c = 1.078$

$R = 0.1312$

$\Sigma R = 2.69$

$Q = \frac{795}{2.69} = 295.5$

$T_1 = 80 + 295.5 \times .1312 = 80 + 38.8 = 118.8°F$ (5TH ITERATION)

1 DIMENSIONAL HEAT TRANSFER PROGRAM

```
      DIMENSION T(99),T1(99),R(99)
      READ(5,899)JJR
      DO 200 JRUN=1,JJR
      READ(5,900)NUM,NODE,TA,TF
      READ(5,950) BL,BKIWS
      NODE1=NODE+1
      T(1)=TA
      DO 12 I=2,NODE
   12 T(I)=T(I-1)+5.
      T(NODE1)=TF
      WRITE(6,2500)JJR,NUM,NODE,NODE1,TA,TF
      WRITE(6,2510)(T(I),I=1,NODE1)
      II=0
      DO 20 I=1,NODE1
   20 T1(I)=T(I)
   25 II=II+1
      CALL ATP(T,YO,99,1)
      R(1)=1.0/YO
      R(2)=1.91E/BKCS(T,2)
      R(3)=.33333/BKARG(T,3)*1.0/HRAD(T,2,3)/(.33333/BKARG(T,3)+
     1 1.0/HRAD(T,2,3))
      R(4)=.875/BKCS(T,4)
      R(5)=.10416/BKARG(T,5)*1.0/HRAD(T,4,5)/(.10416/BKARG(T,5)+
     1 1.0/HRAD(T,4,5))
      R(6)=.8333333/BKCS(T,6)
      R(7)=.10416/BKARG(T,7)*1.0/HRAD(T,6,7)/(.10416/BKARG(T,7)+
     1 1.0/HRAD(T,6,7))
      R(8)=.75/BKCS(T,8)
      R(9)= BL/BKIWS
      IF(JRUN.GE.4)R(9)=BL/BKI(T,9)
      NNN=NODE-1
      DO 93 I=10,NNN
      JJ=I+1
   93 R(I)=.03125/BKARG(T,I)*1.0/HRAD(T,I,JJ)                    /(
     1 .031250/BKARG(T,I)+1.0/HRAD(T,I,JJ))
      R(NODE)=.083333333/BKSS(T,NODE)
      CON=.03058*(TF-T(NODE))**.333333
      CON=1.0/CON
      CON1=1.0/HRAD(T,NODE,NODE1)
      R(NODE1)=CON*CON1/(CON+CON1)
      RT=0.0
      DO 50 I=1,NODE1
   50 RT=RT+R(I)
      Q=(TF-TA)/RT
      T(1)=TA+Q*R(1)
      DO 60 I=2,NODE
   60 T(I)=T(I-1)+Q*R(I)
      DO 65 I=1,NODE
```

```
      TG=.5*(T(I)+T1(I))
      T1(I)=T(I)
   65 T(I)=TG
      IF(II.LT.NUM)GO TO 25
      WRITE(6,2020)
      DO 75 I=1,NODE
   75 WRITE(6,2000) I,T(I),R(I)
      WRITE(6,2030)
      WRITE(6,2010)Q,RT,R(NODE1)
  899 FORMAT(I5)
  900 FORMAT(2I5,2F10.0)
  950 FORMAT(2F10.0)
 1000 FORMAT(7F10.0)
 2000 FORMAT(1H ,5X,I5,2(5X,F10.3))
 2010 FORMAT(1H ,3(5X,F10.3))
 2020 FORMAT(1H1,5X,'ONE DIMENSIONAL HEAT TRANSFER ANALYSIS'//5X,
     1'NODE',6X,'TEMPERATURE',4X,'RESISTANCE')
 2030 FORMAT(1H ,5X,'FLUX(BTU/HR)',3X,'TOTAL RESIST',3X,'R(11)')
 2500 FORMAT(1H ,'JJR=',  ,I3,5X,'NUM=',I3,5X,'NODE=',I3,5X,'NODE1=',I3/
     1 'AIR TEMP=',F8.2,5X,'SODIUM TEMP=',F8.2)
 2510 FORMAT(1H ,5(5X,F8.2))
  200 CONTINUE
      STOP
      END
```

```
      SUBROUTINE AIR(T,YO,III,N)
      DIMENSION T(III)
      TEMP=T(N)    +459.
      Z=0.11659E-08*( 1.565908E+08+290521.*TEMP+539.*TEMP*TEMP+
     1TEMP**3)
      S=ABS(TEMP-539.)
      HO=.22*S**.3333333333
      YO=ABS(Z)+ABS(HO)
      RETURN
      END
```

```
      FUNCTION HRAD(T,N1,N2)
      DIMENSION T(99)
      T1=T(N1)     +459.
      T2=T(N2)    +459.
      HRAD =0.11659E-08 *(T1*T1*T1+T1*T1*T2+T1*T2*T2+T2*T2*T2)
      RETURN
      END
```

```
      FUNCTION BKCS(T,N)
      DIMENSION T(99)
      S=T(N)
      S=ABS(S)
      BKCS=32.-.01111*S
      RETURN
      END
```

```
      FUNCTION BKSS(T,N)
      DIMENSION T(99)
      S=T(N)
      BKSS=7.21+.0042*S
      RETURN
      END
```

```
      FUNCTION BKARG(T,N)
      DIMENSION T(99)
       S=T(N)
      S=ABS(S)
      BKARG=.0100333+1.15E-05*S
      RETURN
       END
```

```
      FUNCTION BKI(T,N)
      DIMENSION T(99)
       S=T(N)
      BKI=0.08333*(0.369+7.316E-05*S+5.654E-07*S*S-2.339E-10*S*S*S)
      RETURN
      END
```

ONE DIMENSIONAL HEAT TRANSFER ANALYSIS

NODE	TEMPERATURE	RESISTANCE
1	126.420	0.617
2	131.140	0.063
3	195.707	0.859
4	197.956	0.029
5	245.126	0.627
6	247.269	0.028
7	286.592	0.523
8	288.552	0.026
9	636.876	8.630
10	647.669	0.143
11	658.183	0.140
12	668.433	0.136
13	678.435	0.133
14	688.201	0.130
15	697.745	0.127
16	707.076	0.124
17	716.206	0.121
18	725.144	0.119
19	733.899	0.116
20	742.480	0.114
21	750.894	0.112
22	759.148	0.110
23	767.250	0.108
24	775.205	0.106
25	783.020	0.104
26	790.700	0.102
27	798.250	0.100
28	805.675	0.099
29	812.980	0.097
30	820.169	0.096
31	827.247	0.094
32	834.216	0.093
33	841.082	0.091
34	847.847	0.090
35	854.515	0.089
36	861.088	0.087
37	867.610	0.087
38	868.188	0.008

FLUX(BTU/HR)	TOTAL RESIST	P(11)
75.238	10.564	0.091

JJR= 5 NUM= 20 NODE= 38 NODE1= 39

AIR TEMP= 80.00 SODIUM TEMP= 875.00

initial guess

80.00	100.00	120.00	140.00	160.00
180.00	200.00	220.00	240.00	260.00
280.00	300.00	320.00	340.00	360.00
380.00	400.00	420.00	440.00	460.00
480.00	500.00	520.00	540.00	560.00
580.00	600.00	620.00	640.00	660.00
680.00	700.00	720.00	740.00	760.00
780.00	800.00	820.00	875.00	

ONE DIMENSIONAL HEAT TRANSFER ANALYSIS

NODE	TEMPERATURE	RESISTANCE
1	100.276	0.265
2	105.030	0.062
3	177.905	0.953
4	180.136	0.029
5	231.345	0.669
6	233.513	0.028
7	275.492	0.549
8	277.476	0.026
9	631.613	4.630
10	642.721	0.145
11	653.532	0.141
12	664.065	0.138
13	674.334	0.134
14	684.355	0.131
15	694.141	0.128
16	703.703	0.125
17	713.054	0.122
18	722.203	0.120
19	731.161	0.117
20	739.936	0.115
21	748.536	0.112
22	756.969	0.110
23	765.243	0.108
24	773.364	0.106
25	781.338	0.104
26	789.172	0.102
27	796.871	0.101
28	804.440	0.099
29	811.884	0.097
30	819.208	0.096
31	826.416	0.094
32	833.512	0.093
33	840.500	0.091
34	847.384	0.090
35	854.168	0.089
36	860.853	0.087
37	867.446	0.087
38	868.073	0.008

FLUX(BTU/HR)	TOTAL RESTST	R(11)
76.494	10.397	0.091

$h = 3.$ BTU/Hr FT^2 °F

```
I=  1      NUM= 20      NODF= 3A      NODE1= 39
TEMP=   80.00      SODIUM TEMP=  875.00
     80.00          85.00          90.00          95.00         100.00
    105.00         110.00         115.00         120.00         125.00
    130.00         135.00         140.00         145.00         150.00
    155.00         160.00         165.00         170.00         175.00
    180.00         185.00         190.00         195.00         200.00
    205.00         210.00         215.00         220.00         225.00
    230.00         235.00         240.00         245.00         250.00
    255.00         260.00         265.00         875.00
```

```
      SUBROUTINE AIR(T,YO,III,N)
      DIMENSION T(III)
      TEMP=T(N)   +459.
     Z=0.11659E-08*( 1.565908E+08+290521.*TEMP+539.*TEMP*TEMP+
     1TEMP**3)
      S=ABS(TEMP-539.)
      HO=.22*S**.3333333333
C
C     FORCED CONVECTION COEFFICIENT FOR TOP OF PLUG.
C
      HO=3.0
      YO=ABS(Z)+ABS(HO)
      RETURN
      END
```

```
26-78   08.472   NTERFACE BETWEEN THE DECK AND THE LARGE PLUG.

      1        C       TNTERFACE BETWEEN THE DECK AND THE LARGE PLUG.
      2        C
      3        C       STEADY STATE TEMPERATURES AT SELECTED LOCATIONS.
      4        C
      5              INTEGER HELP
      6              DIMENSION HELP(3)    ,YOT(5)
      7              DIMENSION TF(51),CHECK(51),NODE(51,4),Y(51,52),C(51),T(51),
      8             1 ADM(51,51),HR(12),AREA(12)
      9              DATA HELP/ 49,50,51/
     10        C
     11        C       INPUT NUMBER OF AREAS,ROW INDEX, COLUMN INDEX
     12        C
     13              READ(5,1150)NAN,III,JJJ
     14         1150 FORMAT(3I5)
     15        C
     16        C        INPUT AREA, NODAL ASSOCIATION AND ERROR DATA
     17        C
     18              READ(5,900)(AREA(I),I=1,NAN)
     19              WRITE(6,2550)(AREA(I),I=1,NAN)
     20         2550 FORMAT(1H ,'AREA',4(5X,F12.6))
     21              DO 20 I=1,III
     22           20 READ(5,1000)(NODE(I,J),J=1,4)
     23              DO 23 I=1,III
     24           23 WRITE(6,2300)I,(NODE(I,J),J=1,4)
     25         2300 FORMAT(1H ,I3,4(5X,I3))
     26              DO 21 I=1,III
     27              TF(I)=800.
     28           21 T(I)=800.
     29              ICON=0
     30        C
     31        C        CALCULATE INDIVIDUAL ADMITTANCES
     32        C
     33           25 CALL ADMIT(T,ADM,III)
     34              ICON=ICON+1
     35              IF(ICON.     LT.2)GO TO 49
     36              CALL AIR(T,YO,III,1)
     37              YOT(1)=YO *9104.
     38              CALL AIR(T,YO,III,37)
     39              YOT(2)=YO *13634.
     40              CALL AIR(T,YO,III,36)
     41              YOT(3)=YO *14263.
     42              CALL AIR(T,YO,III,35)
     43              YOT(4)=YO *14891.
     44              CALL AIR(T,YO,III,34)
     45              YOT(5)=YO*15519.
     46           49 CONTINUE
     47        C
     48              DO 50 I=1,III
     49              DO 50 J=1,III
     50           50 Y(I,J)=0.0
     51        C        SET UP ADMITTANCE MATRIX
     52        C
```

```
06.472    NTERFACE BETWEEN THE DECK AND THE LARGE PLUG.                    L
          DO 55 I=1,III
          DO 55 J=1,4
          NUM=NODE(I,J)
          IF(NUM.EQ.0)GO TO 55
          ADM(I,NUM)=ABS(ADM(I,NUM))
          Y(I,I)=Y(I,I)+ADM(I,NUM)
          Y(I,NUM)=-ADM(I,NUM)
       55 CONTINUE
C
C         CALCULATE RADIATION ADMITTANCES
C
          CALL RADH(T,HR,AREA,HELP,III,7.0)
C
C         ADD RADIATION TERMS TO Y(I,J)
C         SET UP BOUNDARY TERMS
C
C
          DO 70 I=1,NAN
          J=HELP(I)
          Y(J,J)=Y(J,J)+HR(I)
       70 C(J)=HR(I)*1334.
          C(1)=539.*YOT(1)
          C(37)=539.*YOT(2)
          C(36)=539.*YOT(3)
          C(35)=539.*YOT(4)
          C(34)=539.*YOT(5)
C         NITROGEN GAS COOLING TERMS
          C(26)=8.1918E+05
          C(27)=7.8588E+05
          C(28)=7.5313E+05
          C(29)=7.1983E+05
          DO 77 I=1,III
       77 Y(I,JJJ)=-C(I)
          Y(1,1)=Y(1,1)+YOT(1)
          Y(37,37)=Y(37,37)+YOT(2)
          Y(36,36)=Y(36,36)+YOT(3)
          Y(35,35)=Y(35,35)+YOT(4)
          Y(34,34)=Y(34,34)+YOT(5)
C         NITROGEN GAS COOLING TERMS
          Y(29,29)=Y(29,29)+1297.
          Y(26,26)=Y(26,26)+1476.
          Y(27,27)=Y(27,27)+1416.
          Y(28,28)=Y(28,28)+1357.
          CALL GAUS(Y,III,JJJ,T,DET)
          DO 190 I=1,III
          TG=0.5*(TF(I)+T(I))
          TF(I)=T(I)
      190 T(I)=TG
          DO 787 I=1,III
      787 T(I)=T(I)-459.
          WRITE(6,2900)
     2900 FORMAT(1H1,5X,'S.STATE  HEAT TRANSFER FOR THE INTERFACE BETWEEN-
```

```
-78    08.472   NTERFACE BETWEEN THE DECK AND THE LARGE PLUG.

105             1 THE DECK AND THE LARGE PLUG.'///)
106             DO 90 I=1,III,5
107             WRITE(6,2800)I,(I+1),(I+2),(I+3),(I+4)
108          2800 FORMAT(1H ,5(10X,I5))
109            90 WRITE(6,2200)T(I),T(I+1),T(I+2),T(I+3),T(I+4)
110           900 FORMAT(4F10.0)
111          1000 FORMAT(4I5)
112          1010 FORMAT(7F10.0)
113          2200 FORMAT(1H ,5(5X,F10.2))
114             DO 776 I=1,III
115           776 T(I)=T(I)+459.
116             IF(ICON.LT.8)GO TO 25
117             STOP
118             END
```

```
:-78   09.661

      1            FUNCTION BKARG(T,N)
      2            DIMENSION T(51)
      3            S=T(N)    -459.
      4            S=ABS(S)
      5            BKARG=.0100333+1.15E-05*S
      6            RETURN
      7             END
```

```
31-78   09.662

      1            FUNCTION BKN(T,N)
      2            DIMENSION T(51)
      3            S=T(N)     -459.
      4            S=ABS(S)
      5            BKN=.01328429+2.4107801E-05*S-4.576793E-09*S*S
      6            RETURN
      7            END
```

```
31-78   09.661

      1            FUNCTION BKCS(T,N)
      2            DIMENSION T(51)
      3            S=T(N)    -459.
      4            S=ABS(S)
      5            BKCS=32.-.01111*S
      6            RETURN
      7            END
```

```
-78   09.660

      1           FUNCTION BKSS(T,N)
      2           DIMENSION T(51)
      3           S=T(N)   -459.
      4           BKSS=7.21+.0042*S
      5           RETURN
      6           END
```

```
-78   09.660

      1           FUNCTION BKI(T,N)
      2           DIMENSION T(51)
      3           S=T(N)   -459.
      4            S=ABS(S)
      5           BKI=0.08333*(0.369+7.316E-05*S+5.654E-07*S*S-2.339E-10*S*S*S)
      6           RETURN
      7           END
```

```
-78   09.660

  1              SUBROUTINE AIR(T,YO,III,N)
  2             DIMENSION T(III)
  3             TEMP=T(N)
  4             Z=1.671219E-10*(1.565908E+08*290521.*TEMP+539.*TEMP*TEMP+
  5            1TEMP**3)
  6             S=ABS(TEMP-539.)
  7             HO=0.22*0.006944*S**0.3333
  8             YO=ABS(Z)+ABS(HO)
  9             RETURN
 10             END
```

```
1-78   09.659

  1              SUBROUTINE RADH(T,HR,A,NHELP,NN,TIME)
  2              DIMENSION T(NN),HR(12),A(12),NHELP(3)
  3              IF(TIME.GT.6.0)GO TO 12
  4              TEMP=1359.*(1.-50.*TIME)
  5              GO TO 14
  6           12 TEMP=1059.
  7           14 CONTINUE
  8              DO 50 I=1,3
  9              N=NHELP(I)
 10           20 Z=1.671219E-10*A(I)*(TEMP**3+TEMP*TEMP*T(N)+TEMP*T(N)*T(N)+
 11             1T(N)*T(N)*T(N))
 12              SEE=ABS(T(N)-TEMP)
 13              Y=2.123E-04*SEE**.33333333*A(I)
 14           50 HR(I)=ABS(Y)+ABS(Z)
 15              RETURN
 16              END
```

```
      SUBROUTINE ADMIT(T,ADM,III)
      DIMENSION T(III),ADM(III,III)
      DO 50 I=1,III
      DO 50 J=1,III
   50 ADM(I,J)=0.0
      ADM(28,45)=316.952090*1.05
      ADM(36,38)=237.714080*1.05
      ADM(38,39)=237.714080*1.05
      ADM(39,40)=237.714080*1.05
      ADM(40,41)=237.714080*1.05
      ADM(41,42)=237.714080*1.05
      ADM(42,43)=237.714080*1.05
      ADM(43,44)=237.714080*1.05
      ADM(44,45)=237.714080*1.05
      ADM(30,41)=58.667
      ADM(31,40)=58.667
      ADM(32,39)=58.667
      ADM(33,38)=58.667
      ADM(42,48)=58.667
      ADM(43,47)=58.667
      ADM(44,46)=58.667
      ADM(36,37)= 48.424792*BKCS(T,36)
      ADM(35,36)= 50.606884*BKCS(T,35)
      ADM(34,35)= 15.836660*BKCS(T,34)
      ADM(33,34)= 19.320793*BKCS(T,33)
      ADM(32,33)= 19.320793*BKCS(T,32)
      ADM(31,32)= 19.320793*BKCS(T,31)
      ADM(30,31)= 19.320793*BKCS(T,30)
      ADM(47,48)= 19.320793*BKCS(T,47)
      ADM(46,47)= 19.320793*BKCS(T,46)
      ADM(26,46)= 11.709571*BKCS(T,26)
      ADM(25,26)=  4.110806*BKCS(T,25)
      ADM(28,29)=  15.83666 *BKCS(T,29)
      ADM(27,28)=  15.83666 *BKCS(T,28)
      ADM(26,27)=  15.83666 *BKCS(T,27)
      ADM(45,46)=0.0
      ADM( 1, 2)=108.38507*BKCS(T, 1)
      ADM( 2, 3)=108.38507*BKCS(T, 2)
      ADM( 3, 4)=108.38507*BKCS(T, 3)
      ADM( 4, 5)=108.38507*BKCS(T, 4)
      ADM( 5, 6)=108.38507*BKCS(T, 5)
      ADM( 6, 7)=108.38507*BKCS(T, 6)
      ADM( 7, 8)=108.38507*BKCS(T, 7)
      ADM( 8, 9)=108.38507*BKCS(T, 8)
      ADM( 9,10)=135.48133*BKCS(T, 9)
      ADM( 2,38)= 1.05*BKCS(T,38)/(.0116958 +.0105452*BKCS(T,38))
      ADM( 3,39)= 1.05*BKCS(T,39)/(.0116958 +.0105452*BKCS(T,39))
      ADM( 4,40)= 1.05*BKCS(T,40)/(.0116958 +.0105452*BKCS(T,40))
      ADM( 5,41)= 1.05*BKCS(T,41)/(.0116958 +.0105452*BKCS(T,41))
      ADM( 6,42)= 1.05*BKCS(T,42)/(.0116958 +.0105452*BKCS(T,42))
      ADM( 7,43)= 1.05*BKCS(T,43)/(.0116958 +.0105452*BKCS(T,43))
      ADM( 8,44)= 1.05*BKCS(T,44)/(.0116958 +.0105452*BKCS(T,44))
```

```
78    09.662                                                                    L
53              ADM( 9,45)= 1.05*BKCS(T,45)/(.0116958 +.0105452*BKCS(T,45))
54              ADM( 1,37)= 46.242831*BKCS(T,37)
55              ADM(30,48)= 19.320793*BKCS(T,48)
56              ADM(10,29)=  15.83666 *BKCS(T,10)
57              ADM(10,11)= 50.762343*BKCS(T,11)
58              ADM(11,13)=  52.61347*BKCS(T,13)
59              ADM(13,16)= 54.464308*BKCS(T,16)
60              ADM(16,20)= 56.315325*BKCS(T,20)
61              ADM(20,23)= 58.166232*BKCS(T,23)
62              ADM(23,25)= 60.017159*BKCS(T,25)
63              ADM(12,14)=50.762343*BKI(T,14)
64              ADM(14,17)=52.613471*BKI(T,17)
65              ADM(17,21)=54.464308*BKI(T,21)
66              ADM(21,24)=56.315325*BKI(T,24)
67              ADM(15,18)=50.762343*BKI(T,18)
68              ADM(18,22)=52.613471*BKI(T,22)
69              ADM(11,12)=BKCS(T,11)*BKI(T,12)/(.01367*BKI(T,12)+.014*BKCS(T,12))
70              ADM(13,14)=BKCS(T,13)*BKI(T,14)/(.01367*BKI(T,13)+.014*BKCS(T,14))
71              ADM(16,17)=BKCS(T,16)*BKI(T,17)/(.01367*BKI(T,16)+.014*BKCS(T,17))
72              ADM(20,21)=BKCS(T,20)*BKI(T,21)/(.01367*BKI(T,20)+.014*BKCS(T,21))
73              ADM(23,24)=BKCS(T,23)*BKI(T,24)/(.01367*BKI(T,23)+.014*BKCS(T,24))
74              ADM(14,15)=72.082374*BKI(T,15)
75              ADM(17,18)=74.757534*BKI(T,18)
76                ADM(21,22)=77.425592*BKI(T,22)
77              ADM(18,19)=72.082374*BKI(T,19)
78              ADM(10,49)=69.549102*BKI(T,10)
79              ADM(12,49)=69.549102*BKI(T,12)
80              ADM(15,49)=69.549102*BKI(T,15)
81              ADM(19,49)=69.549102*BKI(T,19)
82              ADM(25,51)=415.39*BKI(T,51)*BKCS(T,25)/(2.*BKCS(T,25)+.083333*
83             1BKI(T,51))
84              ADM(50,51)=10.5267*BKCS(T,51)
85              ADM(19,50)=260.11*BKI(T,19)
86              ADM(22,50)=278.96*BKI(T,22)
87              ADM(24,50)=297.81*BKI(T,24)
88              DO 20 I=1,III
89              DO 20 J=I,III
90              IF(ADM(I,J))21,20,21
91           21 ADM(J,I)=ADM(I,J)
92           20 CONTINUE
93              RETURN
94              END
```

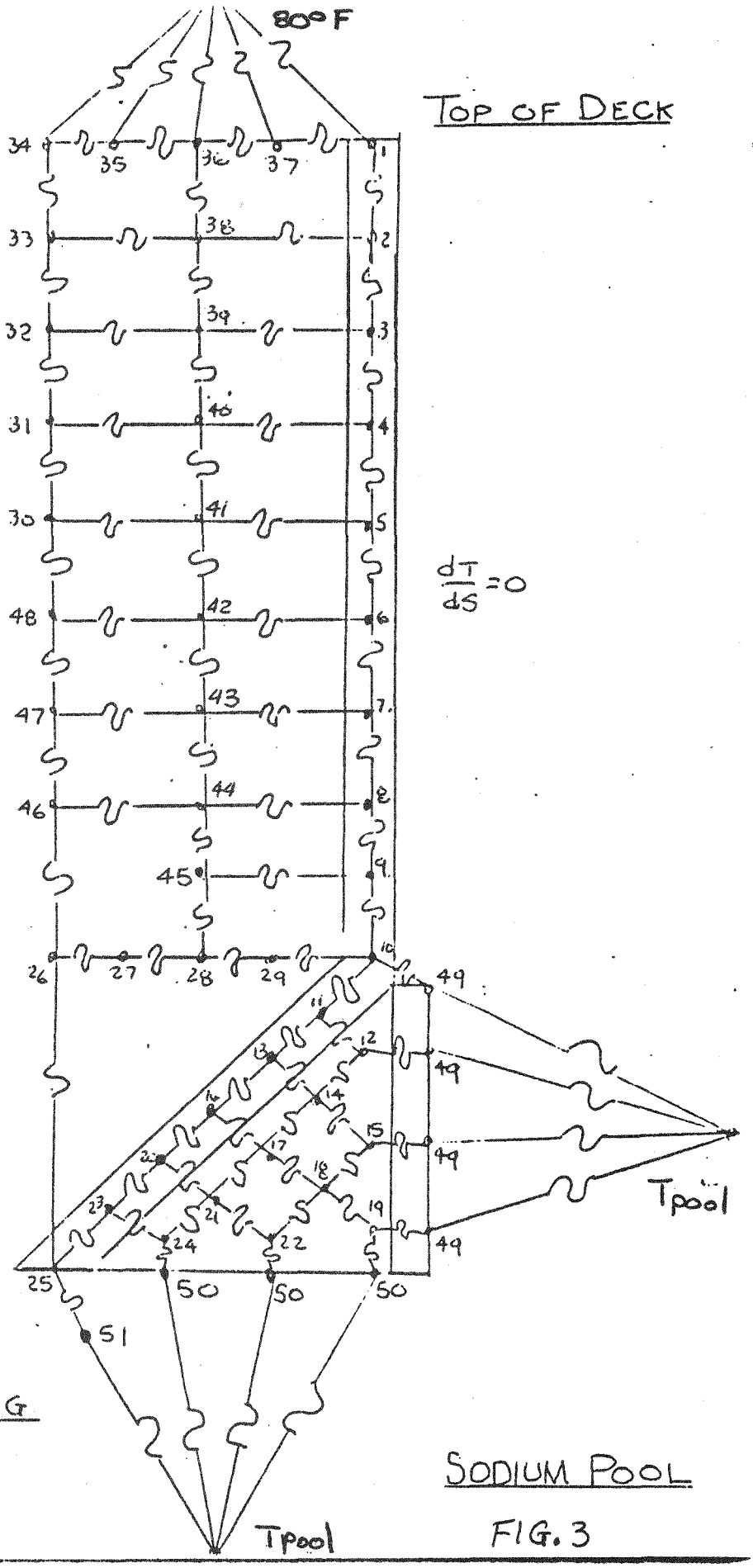
800° F
TOP OF DECK
$\frac{dT}{ds}=0$
$\frac{dT}{ds}=0$
J= 1 To 51
m ≤ 4
$\sum_{i=1}^{m} Y_{ij}(T_i - T_j) = 0.0$
Tpool
Tpool
DECK-LARGE PLUG INTERFACE
SODIUM POOL
FIG. 3

S.STATE HEAT TRANSFER FOR THE INTERFACE BETWEEN THE DECK AND THE LARGE PLUG. (530° Sodium Pool)

Kaylo Insulation

1	2	3	4	5
85.41	88.39	91.46	94.60	97.80
6	7	8	9	10
101.08	104.46	107.96	111.66	114.87
11	12	13	14	15
127.41	313.48	139.24	297.07	420.64
16	17	18	19	20
150.45	319.95	445.74	527.13	161.05
21	22	23	24	25
382.95	523.23	170.97	515.20	179.94
26	27	28	29	30
100.81	97.33	97.68	100.40	92.41
31	32	33	34	35
89.87	87.10	84.13	81.02	80.64
36	37	38	39	40
81.16	82.16	85.54	89.15	92.36
41	42	43	44	45
95.29	97.92	100.11	101.45	101.04
46	47	48	49	50
98.19	96.60	94.66	529.99	529.83
51	52	53	54	55
529.33	534615.23	0.	0.	0.

Table 53

S.S. HEAT TRANSFER ALONG THE INTERFACE BETWEEN THE DECK AND THE LARGE PLUG.

1	2	3	4	5
86.93	90.75	94.67	98.64	102.65
6	7	8	9	10
106.68	110.72	114.77	118.82	122.07
11	12	13	14	15
129.78	462.33	136.54	427.38	656.66
16	17	18	19	20
142.51	449.46	682.53	640.36	147.70
21	22	23	24	25
525.33	783.96	151.96	685.64	154.76
26	27	28	29	30
124.71	123.09	121.47	121.77	101.72
31	32	33	34	35
96.82	91.84	86.78	81.64	80.89
36	37	38	39	40
81.55	82.78	87.69	92.87	97.59
41	42	43	44	45
102.10	106.48	110.76	114.88	118.67
46	47	48	49	50
116.48	111.50	106.60	874.99	874.87
51	52	53	54	55
874.91	537938.27	0.	0.	0.

LOCATION
TEMPERATURE(°F)

Pool Temperature 875°F
Kaylo Insulation

TABLE 9

S.STATE HEAT TRANSFER FOR THE INTERFACE BETWEEN THE DECK AND THE LARGE PLUG. (Plate Insulation N_2 Cooling of Concrete area)

1	2	3	4	5
88.44	93.14	97.98	102.94	108.03
6	7	8	9	10
113.28	118.73	124.46	130.59	136.04
11	12	13	14	15
159.30	483.40	181.21	463.43	682.55
16	17	18	19	20
201.97	505.63	728.26	868.60	221.56
21	22	23	24	25
613.16	859.49	239.73	838.06	255.64
26	27	28	29	30
105.43	98.68	99.71	105.32	97.12
31	32	33	34	35
93.81	90.02	85.86	81.45	80.97
36	37	38	39	40
81.79	83.36	88.44	93.90	98.69
41	42	43	44	45
102.99	106.72	109.54	110.62	108.09
46	47	48	49	50
103.25	101.93	99.86	874.99	874.73
51	52	53	54	55
874.19	541126.59	0.	0.	0.

TABLE 10

S.STATE HEAT TRANSFER FOR THE INTERFACE BETWEEN THE DECK AND THE LARGE PLUG. (Radial Heat Flow From The Plugs Included)

N_2 Cooling of Concrete Area

1	2	3	4	5
87.71	91.99	96.40	100.94	105.15
6	7	8	9	10
108.93	112.21	114.77	117.60	120.20
11	12	13	14	15
131.89	465.51	142.50	437.26	667.02
16	17	18	19	20
152.21	471.11	706.95	858.31	160.99
21	22	23	24	25
569.52	833.06	168.62	780.27	174.31
26	27	28	29	30
100.70	97.42	98.24	101.65	94.47
31	32	33	34	35
91.75	88.58	85.04	81.26	80.87
36	37	38	39	40
81.62	83.06	87.54	92.35	96.47
41	42	43	44	45
99.98	102.80	104.71	105.25	103.56
46	47	48	49	50
99.15	98.22	96.64	874.99	874.74
51	52	53	54	55
874.66	539602.38	2606.00	2606.00	4195.00

1.0" of Wire screen insulation

12" of plate insulation (27 plates - 1/16" thick, 3/8" spacing

TABLE II

S.STATE HEAT TRANSFER FOR THE INTERFACE BETWEEN THE DECK AND THE LARGE PLUG.

1	2	3	4	5
88.57	93.34	98.26	103.34	108.27
6	7	8	9	10
113.01	117.54	121.41	125.64	129.48
11	12	13	14	15
146.38	587.94	161.68	556.72	867.29
16	17	18	19	20
175.62	600.63	919.00	1123.89	188.15
21	22	23	24	25
724.52	1083.32	198.89	994.51	206.42
26	27	28	29	30
102.67	98.00	99.10	103.81	96.17
31	32	33	34	35
93.14	89.59	85.63	81.40	80.97
36	37	38	39	40
81.80	83.40	88.43	93.82	98.49
41	42	43	44	45
102.54	105.90	108.23	108.85	106.45
46	47	48	49	50
101.17	100.27	98.58	1150.00	1149.86
51	52	53	54	55
1149.84	541385.75	2578.00	2578.00	3620.00

Decay Heat Sodium Pool 1150°F
plate & screen Insulation
N_2 forced cooling of Concrete

Table 12

```
10,089    FAT TRANSFER NETWORK ANALYZER PROGRAM.

C       HEAT TPANSFER NETWORK ANALYZER PROGRAM.
C
C       TRANSIENT ANALYSIS DECK(MAIN CONTROL DECK)
C
        DIMENSION TOT(51),YOT(5),B(51,51),TF(51),TTT(51),NODE(51,4),
       SY(51,51),C(51),T(51),ADM(51,51),HR(12),AREA(12),CONE(51),NHELP(3
        DATA NHELP/49,50,51/
        READ(5,1150)NAN,III,JJJ,TIME
 1150 FORMAT(3I5,F10.0)
        READ(5,901)ICT,DT
  901 FORMAT(I2,F10.0)
        READ(5,900)(AREA(I),I=1,NAN)
        WRITE(6,2550)(AREA(I),I=1,NAN)
 2550 FORMAT(1H ,'AREA',4(5X,F12.6))
        DO 20 I=1,III
        TOT(I)=0.0
        C(I)=0.0
   20 READ(5,1000)(NODE(I,J),J=1,4)
        DO 23 I=1,III
   23 WRITE(6,2300)I,(NODE(I,J),J=1,4)
 2300 FORMAT(1H ,I3,4(5X,I3))
        READ(5,1010)(TF(I),I=1,III)
        READ(5,1010)(T (I),I=1,III)
         WRITE(6,2742)
 2742 FORMAT(1H1,'MASS X SPECIFIC HEAT FOR TRANSIENT ANALYSIS')
        WRITE(6,3098)(TF(I),I=1,III)
        WRITE(6,2743)
 2743 FORMAT(1H1,'INITIAL TEMPERATURES IN DEGREES FAH.')
        WRITE(6,3098)(T(I),I=1,III)
 3098 FORMAT(1H ,5(5X,F12.4))
        ICON=0
        TPRNT=0
        DO 50 I=1,III
        T(I)=T(I)+459.
        TOT(I)=T(I)
        CONE(I)=DT/TF(I)
        DO 50 J=1,III
        B(I,J)=0.0
   50 Y(I,J)=0.0
   24 TIME=TIME+DT
   25 CALL ADMIT(T,ADM,III)
        ICON=ICON+1
        CALL AIR(T,YO,III,1)
        YOT(1)=YO *9104.
        CALL AIR(T,YO,III,37)
        YOT(2)=YO *13634.
        CALL AIR(T,YO,III,36)
        YOT(3)=YO *14263.
        CALL AIR(T,YO,III,35)
        YOT(4)=YO *14891.
        CALL AIR(T,YO,III,34)
        YOT(5)=YO*15519.
```

```
      49 CONTINUE
         DO 55 I=1,III
          Y(I,I)=0.0
         DO 55 J=1,4
         NUM=NODE(I,J)
         IF(NUM.EQ.0)GO TO 55
         ADM(I,NUM)=ABS(ADM(I,NUM))
         Y(I,I)=Y(I,I)+ADM(I,NUM)
         Y(I,NUM)=-ADM(I,NUM)
      55 CONTINUE
         CALL RADH(T,HR,AREA,NHELP,III,TIME)
         DO 70 I=1,NAN
         J=NHELP(I)
         HR(I)=ABS(HR(I))
         Y(J,J)=Y(J,J)+HR(I)
      70 CONTINUE
         C(1)=539.*YOT(1)
         C(37)=539.*YOT(2)
         C(36)=539.*YOT(3)
         C(35)=539.*YOT(4)
         C(34)=539.*YOT(5)
          Y(1,1)=Y(1,1)*YOT(1)
         Y(37,37)=Y(37,37)+YOT(2)
         Y(36,36)=Y(36,36)+YOT(3)
         Y(35,35)=Y(35,35)+YOT(4)
         Y(34,34)=Y(34,34)+YOT(5)
         DO 150 I=1,III
         DO 150 J=1,III
         Y(I,J)=Y(I,J)*CONE(I)
     150 CONTINUE
         DO 400 I=1,III
         B(I,I)=-Y(I,I)+1.0
         DO 400 J=1,III
         IF(J.EQ.I)GO TO 400
         B(I,J)=-Y(I,J)
     400 CONTINUE
      74 ICONT=0
      73 DO 71 I=1,NAN
         J=NHELP(I)
         IF(TIME.GT.6.0)GO TO 72
         C(J)=989.*HR(I)*(1.+.0465116279*TIME)
         GO TO 71
      72 IF(TIME.GT.6.221A6)GO TO 75
         C(J)=1289.*HR(I)*(1. +.1613653*(TIME-6.))
          GO TO 71
      75 C(J)=1359.*HR(I)
      71 CONTINUE
C        EXPLICIT SCHEME FOR SOLUTION OF PDE.
C
         DO 600 I=1,III
         TTT(I)=B(I,I)*T(I)
         DO 601 J=1,4
```

```
78   10.089   HEAT TRANSFER NETWORK ANALYZER PROGRAM.

105              NUM=NODE(I,J)
106              IF(NUM.EQ.0)GO TO 601
107              TTT(I)=TTT(I)+B(I,NUM)*T(NUM)
108           601 CONTINUE
109           600 TTT(I)=TTT(I)+CONE(I)*C(I)
110              DO 190 I=1,III
111              TG=.5*(TTT(I)+TOT(I))
112              TOT(I)=TTT(I)
113           190 T(I)=TG
114              DO 936 I=1,III
115           934 IF(T(I).GT.2000.)GO TO 6000
116              IF(ICON.LT.6)GO TO 25
117              ICON=0
118              IPRNT=IPRNT+1
119              IF(IPRNT.LT.JJJ)GO TO 779
120              DO 787 I=1,III
121           787 T(I)=T(I)-459.
122              WRITE(6,2900)
123           2900 FORMAT(1H1,5X,'TRANSIENT HEAT TRANSFER FOR THE INTERFACE BETWEEN
124                 1 THE DECK AND THE LARGE PLUG.'///)
125              WRITE(6,3000)TIME
126           3000 FORMAT(1H ,10X,'TIME=',F10.4,'HOURS')
127              IPRNT=0
128              DO 90 I=1,III,5
129              WRITE(6,2800)I,(I+1),(I+2),(I+3),(I+4)
130           2800 FORMAT(1H ,5(10X,I5))
131             90 WRITE(6,2200)T(I),T(I+1),T(I+2),T(I+3),T(I+4)
132           900 FORMAT(4F10.0)
133          1000 FORMAT(4I5)
134          1010 FORMAT(7F10.0)
135          2200 FORMAT(1H ,5(5X,F10.2))
136              DO 776 I=1,III
137           77A T(I)=T(I)+459.
138           779 CONTINUE
139               IF(TIME.LT.7.0)GO TO 24
140          6000 STOP
141              END
```

SNUMB = 6827A, ACTIVITY # = 02. , REPORT CODE = 06, RECORD COUNT = 000268

AREA	50295.199219		23437.134033	59816.298805
1	2	37	0	0
2	1	38	3	0
3	2	39	4	0
4	3	40	5	0
5	4	41	6	0
6	5	42	7	0
7	6	43	8	0
8	7	44	9	0
9	8	45	10	0
10	9	29	11	48
11	10	12	13	0
12	11	14	49	0
13	11	14	16	0
14	12	13	17	15
15	14	18	49	0
16	13	17	20	0
17	14	16	21	18
18	15	17	22	19
19	18	49	50	0
20	16	23	21	0
21	17	20	24	22
22	18	21	50	0
23	20	25	24	0
24	21	23	50	0
25	23	26	51	0
26	25	27	46	0
27	26	28	0	0
28	27	29	45	0
29	28	10	0	0
30	48	41	31	0
31	30	40	32	0
32	31	39	33	0
33	32	38	34	0
34	33	35	0	0
35	34	36	0	0
36	35	38	37	0
37	36	1	0	0
38	33	39	2	36
39	38	32	40	3
40	39	31	41	4
41	40	30	42	5
42	41	48	43	6
43	42	47	44	7
44	43	46	45	8
45	44	46	28	9
46	26	45	47	0
47	46	43	48	0
48	47	42	30	0
49	10	12	15	19
50	19	22	24	51
51	25	50	0	0

MASS X SPECIFIC HEAT FOR TRANSIENT ANALYSIS

1288.0000	2576.0000	2576.0000	2576.0000	2576.0000
2576.0000	2576.0000	2576.0000	2576.0000	2576.0000
2670.0000	248.0000	2767.0000	258.0000	248.0000
2864.0000	267.0000	258.0000	248.0000	2962.0000
276.0000	267.0000	3059.0000	286.0000	1579.0000
3668.0000	884.0000	850.0000	805.0000	917.0000
917.0000	917.0000	917.0000	1376.0000	884.0000
850.0000	805.0000	8954.0000	8954.0000	8954.0000
8954.0000	8954.0000	8954.0000	8954.0000	8954.0000
917.0000	917.0000	917.0000	1711.0000	2750.0000
1384.0000				

TRANSIENT HEAT TRANSFER FOR THE INTERFACE BETWEEN THE DECK AND THE LARGE PLUG.

TIME= 0.1400HOURS

1	2	3	4	5
83.17	84.90	86.68	88.48	90.29
6	7	8	9	10
92.11	93.94	95.77	97.61	99.07
11	12	13	14	15
102.45	296.87	105.37	270.66	402.80
16	17	18	19	20
107.94	281.67	415.94	509.52	110.15
21	22	23	24	25
327.13	476.88	111.94	426.24	113.13
26	27	28	29	30
100.06	99.40	98.78	98.91	99.80
31	32	33	34	35
87.60	85.36	83.07	80.75	80.41
36	37	38	39	40
80.71	81.28	83.50	85.84	87.98
41	42	43	44	45
90.01	91.99	93.92	95.78	97.83
46	47	48	49	50
96.39	94.18	91.99	536.42	534.43
51	52	53	54	55
536.00		0.	0.	0.

TRANSIENT HEAT TRANSFER FOR THE INTERFACE BETWEEN THE DECK AND THE LARGE PLUG.

TIME= 0.2800HOURS

1	2	3	4	5
83.17	84.90	86.68	88.48	90.29
6	7	8	9	10
92.11	93.94	95.77	97.61	99.08
11	12	13	14	15
102.45	296.92	105.37	270.66	402.86
16	17	18	19	20
107.94	281.67	415.94	509.77	110.15
21	22	23	24	25
327.13	477.06	111.95	426.42	113.16
26	27	28	29	30
100.06	99.41	98.80	98.92	89.80
31	32	33	34	35
87.60	85.36	83.07	80.75	80.41
36	37	38	39	40
80.71	81.28	83.50	85.84	87.98
41	42	43	44	45
90.01	91.99	93.92	95.79	97.81
46	47	48	49	50
96.40	94.18	91.99	542.86	540.83
51	52	53	54	55
542.45		0.	0.	0.

TRANSIENT HEAT TRANSFER FOR THE INTERFACE BETWEEN THE DECK AND THE LARGE PLUG.

TIME= 0.4200HOURS

1	2	3	4	5
83.17	84.90	86.68	88.48	90.29
6	7	8	9	10
92.11	93.94	95.78	97.61	99.09
11	12	13	14	15
102.45	297.01	105.37	270.67	402.96
16	17	18	19	20
107.94	281.67	415.95	510.23	110.15
21	22	23	24	25
327.14	477.40	111.96	426.74	113.20
26	27	28	29	30
100.06	99.42	98.82	98.93	89.80
31	32	33	34	35
87.60	85.36	83.07	80.75	80.41
36	37	38	39	40
80.71	81.28	83.50	85.84	87.98
41	42	43	44	45
90.01	91.99	93.92	95.79	97.80
46	47	48	49	50
96.40	94.18	91.99	549.30	547.29
51	52	53	54	55
548.89	--	0.	0.	0.

TRANSIENT HEAT TRANSFER FOR THE INTERFACE BETWEEN THE DECK AND THE LARGE PLUG.

TIME= 0.5600HOURS

1	2	3	4	5
83.17	84.90	86.68	88.48	90.29
6	7	8	9	10
92.11	93.94	95.78	97.62	99.09
11	12	13	14	15
102.46	297.14	105.38	270.67	403.09
16	17	18	19	20
107.94	281.67	415.96	510.87	110.16
21	22	23	24	25
327.15	477.88	111.98	427.20	113.25
26	27	28	29	30
100.07	99.43	98.83	98.94	89.80
31	32	33	34	35
87.60	85.36	83.07	80.75	80.41
36	37	38	39	40
80.71	81.28	83.50	85.84	87.98
41	42	43	44	45
90.01	91.99	93.92	95.80	97.79
46	47	48	49	50
96.40	94.18	91.99	555.74	553.76
51	52	53	54	55
555.34		0.	0.	0.

TRANSIENT HEAT TRANSFER FOR THE INTERFACE BETWEEN THE DECK AND THE LARGE PLUG.

TIME= 0.7000HOURS

1	2	3	4	5
83.17	84.90	86.68	88.48	90.29
6	7	8	9	10
92.12	93.95	95.78	97.62	99.10
11	12	13	14	15
102.46	297.30	105.38	270.67	403.27
16	17	18	19	20
107.94	281.67	415.98	511.69	110.17
21	22	23	24	25
327.16	478.50	112.00	427.80	113.31
26	27	28	29	30
100.07	99.44	98.83	98.95	89.80
31	32	33	34	35
87.60	85.36	83.07	80.75	80.41
36	37	38	39	40
80.71	81.28	83.49	85.84	87.98
41	42	43	44	45
90.01	91.99	93.92	95.80	97.78
46	47	48	49	50
96.40	94.18	91.99	562.18	560.22
51	52	53	54	55
561.79		0.	0.	0.

TRANSIENT HEAT TRANSFER FOR THE INTERFACE BETWEEN THE DECK AND THE LARGE PLUG.

TIME= 0.8400HOURS

1	2	3	4	5
83.17	84.90	86.66	88.48	90.29
6	7	8	9	10
92.12	93.95	95.79	97.63	99.11
11	12	13	14	15
102.46	297.49	105.36	270.68	403.48
16	17	18	19	20
107.95	281.67	416.01	512.68	110.18
21	22	23	24	25
327.19	479.26	112.04	428.52	113.37
26	27	28	29	30
100.08	99.45	98.84	98.96	89.80
31	32	33	34	35
87.60	85.36	83.07	80.75	80.41
36	37	38	39	40
80.71	81.28	83.49	85.84	87.98
41	42	43	44	45
90.01	91.99	93.92	95.81	97.78
46	47	48	49	50
96.40	94.18	91.99	568.62	566.69
51	52	53	54	55
568.24		0.	0.	0.

TRANSIENT HEAT TRANSFER FOR THE IN[illegible]

TIME= 0.9800HOURS

1	2	3	4	5
83.17	84.00	86.68	88.48	90.29
6	7	8	9	10
92.12	93.95	95.79	97.64	99.12
11	12	13	14	15
102.47	297.72	105.39	270.69	403.72
16	17	18	19	20
107.96	281.68	416.06	513.85	110.20
21	22	23	24	25
327.22	480.15	112.07	429.37	113.44
26	27	28	29	30
100.09	99.45	98.84	98.97	89.80
31	32	33	34	35
87.60	85.36	83.07	80.75	80.41
36	37	38	39	40
80.71	81.28	83.49	85.84	87.98
41	42	43	44	45
90.01	91.00	93.92	95.61	97.77
46	47	48	49	50
96.40	94.18	91.99	575.07	573.16
51	52	53	54	55
574.68	[illegible]	0.	0.	0.

TRANSIENT HEAT TRANSFER FOR THE INTERFACE BETWEEN THE DECK AND THE LARGE PLUG.

TIME= 1.1200HOURS

1	2	3	4	5
83.17	84.90	86.66	88.48	90.29
6	7	8	9	10
92.12	93.96	95.80	97.64	99.12
11	12	13	14	15
102.47	297.98	105.39	270.70	404.01
16	17	18	19	20
107.97	281.68	416.12	515.17	110.22
21	22	23	24	25
327.27	481.17	112.11	430.35	113.52
26	27	28	29	30
100.09	99.46	98.84	98.98	89.80
31	32	33	34	35
87.60	85.36	83.07	80.75	80.41
36	37	38	39	40
80.71	81.98	83.49	85.84	87.98
41	42	43	44	45
90.01	91.99	93.92	95.81	97.76
46	47	48	49	50
96.41	94.18	91.99	581.51	579.62
51	52	53	54	55
581.13		0.	0.	0.

SEVEN NODE TRANSIENT MODEL

OF THE SMALL ROTATING PLUG

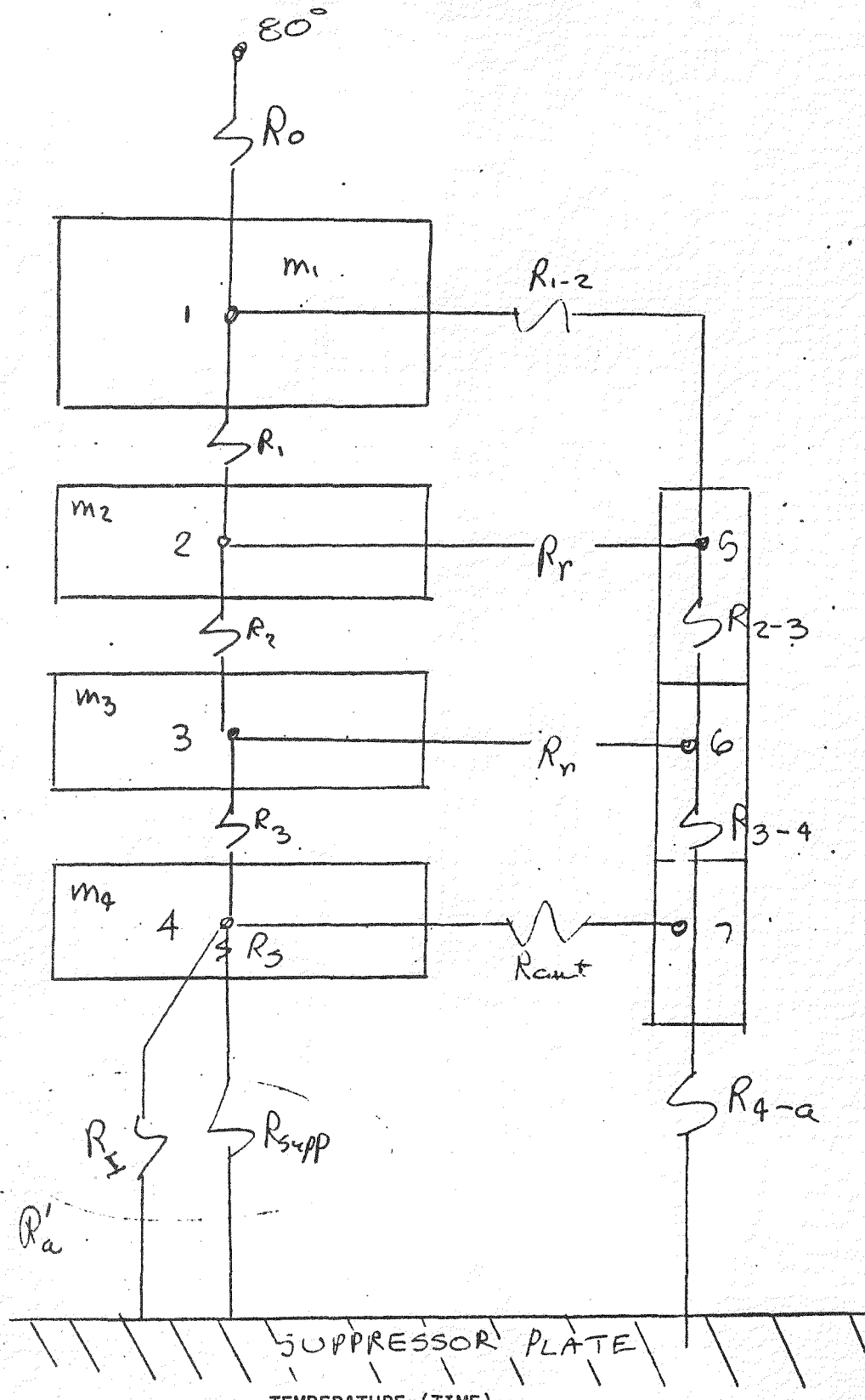

TEMPERATURE (TIME)

STEADY STATE THERMAL CIRCUIT

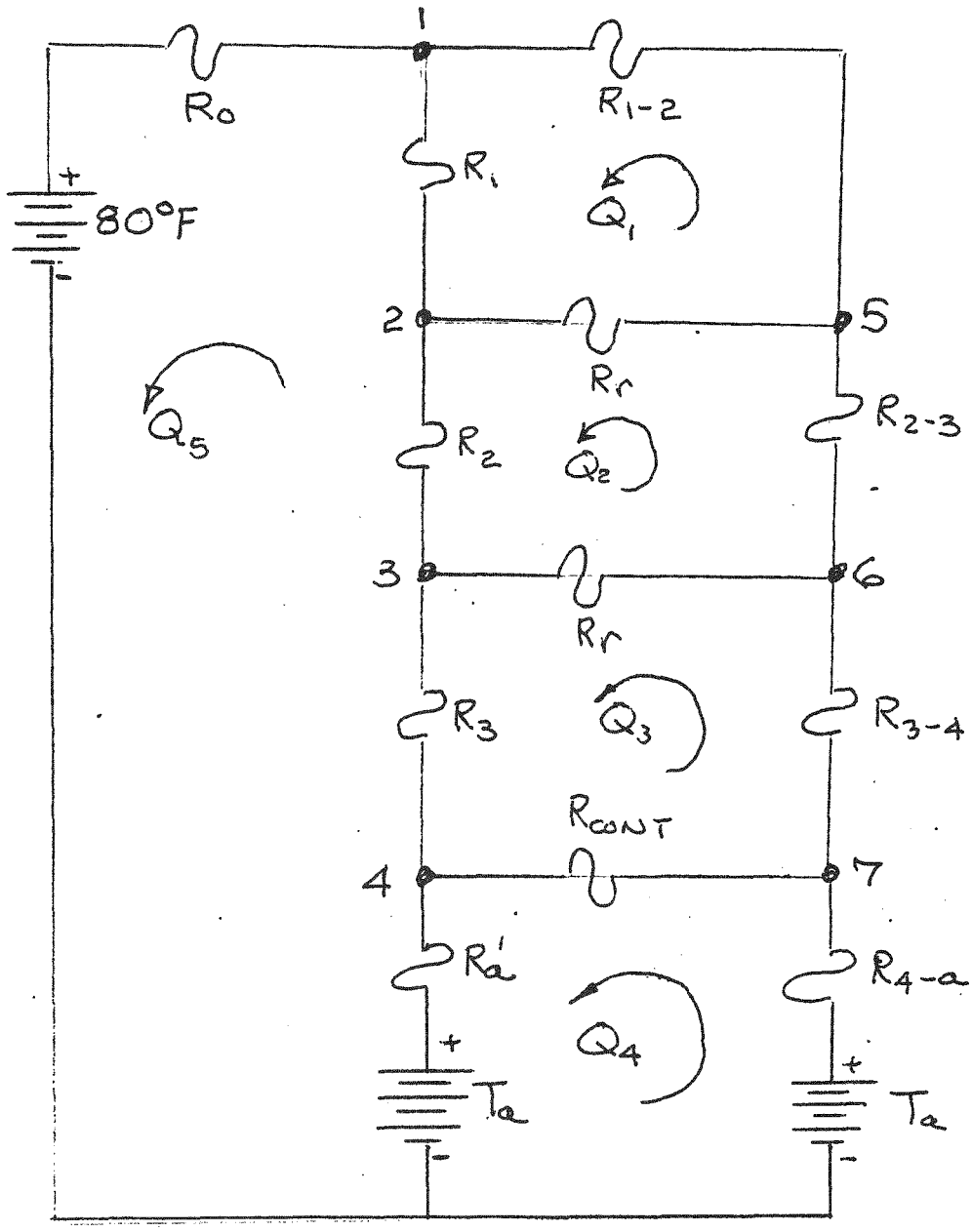

$QR - T = 0$

$\Sigma Q = 0$ @ any node

$Ta = \begin{matrix} 545°F \text{ @ start} \\ 875°F \text{ @ finish} \end{matrix}$ of startup transient

STEADY STATE NETWORK PROGRAM

```
LIST PLUGL

     DIM A(6,6),C(6),B(6)
     MAT READ A
     MAT A=INV(A)
     INPUT C(5)
     IF C(5)=0.0 THEN 100
     MAT B=A*C
     PRINT "C(5)=";C(5)
     MAT PRINT B
     PRINT\PRINT
     GO TO 22
     DATA .0814,-.5466E-03,0,0,-.0413
     DATA -.5466E-03,.08747,-.5466E-03,0,-.03411
     DATA 0,-.5466E-03,.0935536,-.4129E-03,-.03033
     DATA 0,0,-.4129E-3,.7263534,-.5489984
     DATA -.3413,-.03411,-.03033,-.54899,.6982
     END
```

STEADY STATE TEMPERATURES

T_a = 545°F

Q_1 = 999.0

Q_2 = 774.6

Q_3 = 723.3

Q_4 = 1480.9

Q_5 = 1958.8

$Q_5 R_o$ = 85.15°F

T_1 = 80 + $Q_5 R_o$ = 165.15°F.

T_2 = 165.15 + .04138 x (1958.8 - 999) = 204.86°

T_3 = 204.86 + .03411 (1958.8 - 774.6) = 245.26°

T_4 = 245.26 + .03033 (1958.8 - 723.3) = 282.73°

T_5 = 165.15 + .03955 (999) = 204.66°

T_6 = 204.66 + .052269 (774.6) = 245.15°F

T_7 = 245.15 + .052269 (723.3) = 282.96°F

STEADY STATE TEMPERATURES

T_A = 875°F

Q_1 = 1708.

Q_2 = 1324.36

Q_3 = 1236.65

Q_4 = 2531.92

Q_5 = 3348.92

$Q_5 R_o$ = 145.58°F

T_1 = 80 + $Q_5 R_o$ = 225.57°F

T_2 = 225.57 + .04138 (3398.92 - 1708) = 293.48

T_3 = 293.48 + .03411 (3348.92 - 1324.4) = 362.54

T_4 = 362.54 + .03033 (3348.9 - 1236.65) = 426.6

T_5 = 225.57 + .03955 (1708) = 293.12

T_6 = 293.12 + .052269 (1324.) = 362.32

T_7 = 362.32 + .052269 (1236) = 426.93

TRANSIENT DIFFERENCE EQUATIONS

7 NODE MODEL OF SMALL ROTATING PLUG

$$CM_1 \frac{\partial T_1}{\partial t} = \frac{1}{R_o}(80 - T_1) + \frac{1}{R_1}(T_2 - T_1) + \frac{1}{R_{1-2}}(T_5 - T_1)$$

$$CM_2 \frac{\partial T_2}{\partial t} = \frac{1}{R_1}(T_1 - T_2) + \frac{1}{R_2}(T_3 - T_2) + \frac{1}{R_r}(T_5 - T_2)$$

$$CM_3 \frac{\partial T_3}{\partial t} = \frac{1}{R_2}(T_2 - T_3) + \frac{1}{R_3}(T_4 - T_3) + \frac{1}{R_r}(T_6 - T_3)$$

$$CM_4 \frac{\partial T_4}{\partial t} = \frac{1}{R_3}(T_3 - T_4) + \frac{1}{R_c}(T_7 - T_4) + \frac{1}{R_a}(T_a - T_4)$$

$$CM_5 \frac{\partial T_5}{\partial t} = \frac{1}{R_{1-2}}(T_1 - T_5) + \frac{1}{R_r}(T_2 - T_5) + \frac{1}{R_{2-3}}(T_6 - T_5)$$

$$CM_6 \frac{\partial T_6}{\partial t} = \frac{1}{R_{2-3}}(T_5 - T_6) + \frac{1}{R_{3-4}}(T_7 - T_6) + \frac{1}{R_r}(T_3 - T_6)$$

$$CM_7 \frac{\partial T_7}{\partial t} = \frac{1}{R_{3-4}}(T_6 - T_7) + \frac{1}{R_c}(T_4 - T_7) + \frac{1}{R_{4-a}}(T_a - T_7)$$

$$\frac{\partial T}{\partial t} = \frac{T^{t+1} - T^t}{\Delta t}$$

$CM_5 = CM_6 = CM_7 = 255.88$

$CM_1 = 3880.$

$CM_2 = 1792.$

$CM_3 = 1706.$

$CM_4 = 1536.$

$R_1 = 0.0413$

$R_2 = 0.03411$

$R_3 = 0.03033$

$R_a = 0.54899$

$R_{1-2} = 0.03955$

$R_{4-a} = 0.17694$

$R_{2-3} = 0.05226$

$R_c = 0.0004129$

$R_r = 5.466 \times 10^{-4}$

$R_o = 0.04347$

$R_{3-4} = 0.052269$

$\Delta t = 0.05$ hours

TRANSIENT TEMPERATURE PROGRAM STARTUP
TRANSIENT, SMALL ROTATING PLUG

*LIST PLUGT

```
100DIM A(7,7),D(7),T(7),T1(7),Z(7),Z1(7),B(7,7)
200INPUT D1,E1,T2,N1
300MAT READ A
50 MAT A=(D1)*A
60FOR I=1 TO 7
64 A(I,I)=A(I,I)+1
67 NEXT I
70PRINT "A           MATRIX"
90PRINT
100 MAT A=INV(A)
110 MAT READ T1
120PRINT"   A   INVERSE  MATRIX"
140PRINT
150PRINT\PRINT
160 T2=T2-Z1
165 I=N+1
170 IF N<>0 GOTO 190
180 D(1)=.4742
190 D(4)=.3211853E-4
200 D(7)=.3222867E-4
210 FOR I=1 TO 7
211 Z(I)=D(I)-T1(I)
212 NEXT I
213 MAT T=A+Z
140 MAT T1=(1)*T
245 IF N<>N1 THEN 160
250PRINT"TIME=";T2;"AMBIENT TEMP=";F/81
255FOR I=1 TO 7
260PRINT I,T1(I)
265 NEXT I
270PRINT
275 N=0
280 IF T2<> E1 THEN 160
285 GO TO 470
290DATA .31868,-.8952,0,0,-.3365,0,0
300DATA -.0195,1.8079,-.8136,0,-1.3289215,0,0
310DATA 0,-.01710,1.1.08695,-.81982,0,-1.870866,0
320DATA 0,0,-.0214,1.599462,0,0,-1.57575
330DATA -.8988862,-7.1498022,0,0,7.3233718,-.874688,0
340DATA 0,0,-7.1497978,0,-.87476885,7.29998895,-.8747688E
350DATA 0,0,0,-9.4649598,0,-.87476885,9.5618496
360DATA 91.25,96.95,104.39,113.16
370DATA 76.88,104.06,114.63
380GO TO 470
390IF T2>6 THEN 420
400F=D1*(545+46.6*T2)
410 GO TO 460
420 IF T2>1.12166 THEN 450
430 F=D1*(520+209*(T2-6))
440GO TO 460
450 F=D1*675
460RETURN
470 END
```

PART II: REACTOR ASSEMBLY - STRUCTURES

SECTION 11: ROTATING PLUG SEALS

CONTENTS

		Page
II-11.1	INTRODUCTION	II-11-i
II-11.2	SUMMARY	II-11-3
II-11.3	CONCLUSIONS AND RECOMMENDATIONS	II-11-5
II-11.4	DISCUSSION	II-11-7
	11.4.1 General Arrangement and Requirements	II-11-7
	11.4.2 Elastomer Seals	II-11-7
	11.4.3 Freeze Seals	II-11-10
	11.4.4 Sodium Dip Seals	II-11-13
	REFERENCES	II-11-19

FIGURES

		Page
4-1	Reactor Closure – Plan View	II-11-21
4-2	Reactor Closure – Elevation View	II-11-23
4-3	Three-Flange Assembly – Elastomer Seals	II-11-25
4-4	Details of Three-Flange Assembly – Elastomer Seals	II-11-27
4-5	Operating Modes	II-11-29
4-6	Three-Flange Assembly – Freeze Seals	II-11-31
4-7	Detail of Three-Flange Assembly – Freeze Seals	II-11-33
4-8	Typical Freeze Seal/Flange Arrangement	II-11-35
4-9	Three-Flange Assembly -Small Sodium Seals	II-11-37
4-10	Sodium Dip Seal - Small	II-11-39
4-11	Typical Small Sodium Seal/Flange Arrangement	II-11-41
4-12	Sodium Dip Seal – Large	II-11-43
4-13	Three-Flange Assembly – Large Sodium Seals	II-11-45
4-14	Typical Large Sodium Seal/Flange Arrangement	II-11-47
4-15	Typical Large Sodium Seal – Pressure Fluctuations	II-11-49
4-16	Seal Inspection Method	II-11-51

TABLES

		Page
4-1	Environment and Requirements for Seals for Rotating Plugs	II-11-8
4-2	60% Bi - 35% Sn - 5% In Fundamental Characteristics	II-11-12

II-11.1

INTRODUCTION

The reactor closure assembly is a continuation of the reactor vessel roof structure that forms the coolant and pressure boundary around the reactor assembly. The reactor closure has three rotating plugs to perform refueling operations. Each plug includes seal arrangements to confine the radioactive gas and prevent air from entering and contacting the sodium coolant.

All components of the seal systems must have an adequate usable life and be reliable. Elastomer seals, both static and dynamic arrangements, have been the recommended choice for 1000 MWe Pool-Type LMFBR in previous studies. For this study alternate seals have been developed along with various combinations. This memorandum describes the alternate seal designs and compares the results of each design with the reference elastomer seals. The memorandum also discusses the advantages and disadvantages of each type of seal design.

II-11.2

SUMMARY

Alternate seal designs have been developed for the rotating plugs of the reactor assembly. These seals are the freeze type dip seal and the sodium dip seal. During the study the requirements and limitations for the closure seals were defined. Each type of seal was evaluated and a list of advantages and disadvantages was developed and compared with the reference inflatable elastomer seal. The inflatable elastomer design is still recommended as the reference design with the freeze seals as an acceptable but more complex alternate.

II-11.3

CONCLUSIONS AND RECOMMENDATIONS

Two types of alternate seals were designed for the use on the rotating plugs during this study. These are the freeze seals and the sodium dip seals. Each of the seal designs can be implemented into the reactor closure reference design and can be used successfully within the limitations stated. However, when compared with the reference elastomer seals, the alternate seal designs add complication to the closure design.

The freeze seal system complicates the reactor closure design by requiring a liquid-metal supply along with a temperature control system. In addition, the closure design must incorporate a method to maintain the blade and trough should oxides or foreign matter become part of the liquid metal seal. This seal system is considered the backup alternate.

Neither the large nor small type sodium dip seal arrangement is recommended for the closure design. Since the reactor closure is considered a cool plug design, the optimum position of the sodium seals is at the lower level of the closure. However, at this position the seals are inaccessible for maintenance and add considerable complication to the closure design by requiring a sodium supply system with temperature control. In addition the sodium seals are very sensitive to pressure changes and require a high column of sodium to resist the pressure or allow gas bypass should pressures be higher than the sodium seal permits.

The inflatable elastomer seals are still considered the recommended reference design for the reactor closure. The elastomer seals are currently being limited to an operating temperature of 150°F. The seal area temperature in the flange of the small rotating plug is near this limit temperature. Thermal studies conducted on the reactor closure define ways of reducing this temperature to well below the limit. In addition, elastomer materials having higher limits are currently being investigated at LMEC. As better materials become evident, they will be incorporated in the design. Very successful testing results have been obtained on the CRBRP elastomer seals which are similar to the design being recommended for this program.

It is recommended elastomer seals continue to be tested, as presently being conducted at ETEC, to obtain additional useful design data and develop higher temperature elastomer materials. A higher temperature elastomer material will permit a higher temperature of the top surface of the reactor closure as discussed in the report "Part II-10, Rotating Plug Thermal Analysis". It is also suggested that shielding calculations be performed to define the radiation levels at the seal locations and the radiation streaming effects on the seals. Further studies should be made of the reactor closure flange area to increase the dynamic seal width and thus allow larger tolerance for plug rotation.

DISCUSSION

11.4.1 GENERAL ARRANGEMENT AND REQUIREMENTS

The reactor closure assembly is shown on Figures 4-1 and 4-2. Figure 4-1 is a plan view showing the arrangement of the three rotating plugs. Figure 4-2 is an elevation view showing a cross-section of the closure. As can be seen in Figure 4-2, a flange area is located at the top of the annulus between adjacent plugs. For the design shown, the flange of each of the plugs contains the bull gear, the bearing and two sets of elastomer seals. It is these seals that isolate the head access area from the reactor cover gas and for which alternate seals were developed.

General requirements and general environments of the rotating plug seals are tabulated in Table 4-1.

11.4.2 ELASTOMER SEALS

For review purposes, the following is a summary of the inflatable type elastomer seals.

Two types of elastomer seals are used in the reactor closure to prevent reactor cover gas with fission products from entering the head access area. They are the static (stationary) elastomer seals and the dynamic (moving) elastomer seals and are shown with the three plug arrangement on Figure 4-3. Both types of seals are the inflatable type using argon and are arranged in sets with a buffer gas pressure between each seal and its neighbor. The material for the elastomer seals is EPDM (Ethylene propylene di-monomer).

The static set of seals is attached to the vertical surface of the inner flange ring and shown in more detail on Figure 4-4. During the refueling mode of operation, the static inflatable seals are deflated and permit easier rotation of the plugs.

TABLE 4-1

Environment and Requirements for Seals for Rotating Plugs

Items \ Conditions	Normal Operating Condition (NOC)	Refueling Maintenance Condition
1) Environment		
Reactor Cover Gas	Argon Gas + Sodium Vapor	Same As NOC
Head Access Areas	Air	Same As NOC
2) Pressure		
Reactor Cover Gas	-6" ± 3" W.G.* (-0.22 psi ± 0.11 psi) (Normal Operating Condition)	-6" W.G. (-0.22 psi) ± 0.11 psi (Normal Condition)
	-6" W.G.* (-0.22 psi) ± 0.5 psi (Design Condition)	
	-0.22 ± 2.5 psi (± 2.5 psi/10^3 sec) (Rapid Pressure Change)**	
3) Temperature		
Sodium Surface	875°F	595°F
Rotating Plug Flange Seal Surface	<150°F	<150°F
4) Rotating Plug Peripheral Speed	Stationary	15 fpm
5) Allowable Leak Rate	To Be Determined	To Be Determined

*Water-Gage

**Assumption

For power operation of the reactor, the rotating plugs are placed in the stationary or locked position, and the static seals are inflated to create a buffered seal arrangement between the gas in the annulus between the plugs and the head access area. Also shown in Figure 4-3 is a ledge type seal that is located at the lower end of each plug. The ledge seal is used only during power operation of the plant, when the sodium pool temperature is approximately 875°F and the sodium aerosol is at maximum density in the reactor cover gas. Prior to power operation, each plug is lowered onto a ledge that creates a restriction to impede entry of the cover gas sodium aerosol into the annulus between the plugs. Restricting the sodium-laden gas from entering the annulus eliminates the possible deposition of sodium frost on the cooler wall areas. Should sodium accumulate near or on the ledge surface, the irregularities will be filled or coated and the ledge will become a better seal. Sodium deposited on the wall surface below the ledge seal will be in contact with surfaces at temperatures above the sodium melting point and therefore the deposited sodium can run freely downward into the sodium pool.

The dynamic elastomer seals are attached to a horizontal surface between the inner and outer rings of the flange. These seals are used primarily during the refueling outage period, when the plugs are rotated to perform the transfer of fuel elements. As shown on Figure 4-4, the upper surface of the flange has a set of striker plates that maintains a surface in contact with the inflatable seals. The concave shape of the contact surface forms a good seal along with providing a well area for holding the Dow 55M lubricant. Tests on this type of seal have been conducted at ETEC with excellent results(2). Like the static seals discussed above, the dynamic seals are also buffered between the sets to insure the integrity of the seal arrangement. In addition, the dynamic seals can also be used during power operation along with the static seals as an additional barrier against cover gas entry to the head access area.

Maintenance considerations have also been reviewed for the elastomer seals. Figure 4-5 shows the arrangement for the maintenance mode along with arrangement for the power and refueling modes. To replace the elastomer seals, the outer ring area of the flange is removed to give clear access to all four elastomer seals. Following removal of the outer ring, an inflatable maintenance seal is placed in the cavity to restrict leakage of gas from the annulus area to the head access area. This maintenance seal permits seal replacement and maintenance without necessity for speedy accomplishment.

Advantages and disadvantages of the (2) elastomer seals are:

Advantages:

1. Established design, and technology.
2. Located in the cool flange area of the reactor closure.
3. Materials and configuration used by industry.
4. Excellent test results (CRBRP, FFTF, and Rapsodie).
5. Feasible to fabricate large sizes.
6. Feasible to replace seals and maintain seal area.
7. Minimum number of seal surfaces requiring close tolerance.
8. Shipping, storage and handling is simple.
9. Accessible for surveillance.
10. Not sensitive to pressure changes in reactor cover gas.

Disadvantages:

1. Requires a lubricant.
2. Requires tight control of material and fabrication to obtain a quality product.
3. May require replacement during plant life.
4. Methods to prevent sticking should be considered.
5. Temperature limit at present is 150°F.
6. Requires a lower ledge seal to reduce sodium deposition on annular walls.

11.4.3
FREEZE SEALS

Freeze seals for the three rotating plugs are shown in Figures 4-6 and 4-7. The freeze seal has the function of providing a gas-tight, pressure-proof seal between the reactor cover gas and the head access area. The freeze seal consists of a vertical steel blade and an annular double-wall trough filled with Bi-Sn-In alloy. Nitrogen is blown into the space adjacent to the trough wall for cooling the seal alloy. Several heaters and thermocouples are put in the blade for heating the metal and controlling the metal temperature. During power operation, this metal is solidified to form the pressure barrier between the cover gas and the head access area. During refueling, this metal is melted, and the rotating plug can be rotated without any leakage of reactor cover gas.

The blade of the large plug is 7.5 inches high and 1.18 inches thick. The annular trough of the large plug shown on Figure 4-8 has a 0.39 inch thick wall, is 7.87 inches deep and 2.76 inches wide, and the width between the double wall is 0.78 inches. The blade of the intermediate plug and small plug has the same dimensions as the blade of large plug. The annular trough has the same dimensions as the large plug trough. Each plug trough is filled to a depth of 4.25 inches with about 4250 lbs, 2890 lbs, 860 lbs of the bismuth-tin-indium alloy in the LRP, IRP and SRP, respectively.

The alloy consists of 60% bismuth, 35% tin and 5% indium, and has a melting point of 261°F. The fundamental characteristics are shown in Table 4-2(3). During plug rotation, the alloy is maintained completely molten by a series of electrical heaters.

The bismuth-tin-indium alloy of these proportions was chosen for the freeze seals for the following reasons:

1. The alloy has a low melting point of 261°F.
2. The alloy resists cracking on solidifying.
3. The alloy is reasonably stable chemically and resists oxidation.
4. The seal using this alloy has a negligible leak rate.
5. Thermal expansion coefficient of this alloy is very close to that of stainless steel.
6. The alloy has relatively high thermal conductivity.
7. The alloy has good compatibility with sodium vapor.
8. The alloy is not toxic and is definitely not hazardous to personnel.
9. The alloy has minimal induced radioactivity.
10. The alloy has a low viscosity.
11. Because of the alloys high density it has low surface elevation change (0.32 inch per 0.1 psi).
12. This type of alloy has been used on other reactors for years.

In the freeze seal design, the outer side of the seal blade is constantly pressurized with fresh argon gas 0.1 psi higher than the reactor cover gas pressure (-0.22 psi). This is maintained by having a set of inflatable elastomer seals located in the flange area. Should a small leak develop in the freeze seal, the clean argon will always leak into the reactor cover gas space. The argon buffer gas also further limits oxidation of the alloy.

Table 4-2 60%Bi-35%Sn-5%In
Fundamental Characteristics

Item	Content	
	Metric unit	British unit
Melting Point	77.8°C ∿ 127.4°C	172 261°F
Thermal expansion rate	8.0×10^{-6}/°C at 25°C ∿ 75°C	4.4×10^{-6}/°F at 77°F ∿ 167°F
Specific heat	0.1000 cal/g°C at 125°C	0.1 Btu/lb°F at 257°F
Thermal conductivity	0.0794 cal/cm.s.°C at 125°C	1.6 Btu/in h °F at 257°F
Density	8.63 g/cc	0.31 lb/in^3
Tensile strength	6.06 kg/mm^2	8.62×10^3 lb/in^2
Latent heat	8.29 cal/g	14.92 Btu/lb
Viscosity	≦ 20 C.P.	≦ 20 C.P.
Anti-oxidation	good	good
Sodium compatibility	good	good

Advantages and disadvantages of the freeze seal are as follows:

Advantages:

1. Good sealing quality.
2. Accessible for maintenance and surveillance.
3. Experience of similar type seals (EBR II, Raposdie, Phenix, Joyo).
4. Not sensitive to pressure changes during power operation.
5. Located in cool part of reactor closure.
6. Simple geometry.

Disadvantages:

1. Requires temperature control system.
2. Requires metal supply system.
3. Requires a backup boundary seal to atmospheric air.
4. Difficult to provide maintenance of trough and blade.
5. Requires a backup ledge seal to reduce sodium deposition on annulus walls.
6. Shrinkage by solidification might cause cracking and leakage paths.
7. Alloy oxidation might present maintenance problems.
8. Larger sizes difficult to fabricate and maintain design configuration.

11.4.4
SODIUM DIP SEALS

The sodium dip seal fulfills the primary function of preventing the reactor cover gas including fission products from entering the Head Access Area. In addition, it prevents the deposition of sodium in the annular gap between the rotating plugs.

Two types of sodium dip seals were studied. One type (Sodium Dip Seal--Small), has the capability of sealing in the normal plant operating condition. The other type has the capability of sealing both under normal conditions and possibly during rapid scram shutdown (Sodium Dip Seal--Large).

Sodium Dip Seal--Small

A small sodium dip seal design for the three rotating plugs that would meet the noted General Requirements previously stated is shown in Figure 4-9. For the

pressure fluctuation of ± 0.5 psi the equivalent sodium height is 15.7 inches. As shown on Figure 4-10 the trough must be 17.4 inches high to assure sealing capability. Because of this very large seal size, the design is not considered reasonable for the Reactor Closure Assembly.

To consider a sodium dip seal for a rotating plug design the pressure conditions must be modified. The suggested modified pressure conditions are similar to CRBRP and are as follows:

Condition / Pressure	Normal Operating Condition	Refueling Maintenance Condition
Reactor Cover Gas	-0.22 psi ± 0.1* psi (Normal Pressure Fluctuation) -0.22 ± 2.5 psi (Rapid Pressure Change) 2.5 psi/1000 sec.	-0.22 psi ± 0.1* psi (Normal Pressure Fluctuation)

*This pressure does not fluctuate sharply.

Other requirements are the same as the General Requirements.

The small sodium dip seals for each of the three plugs are shown in Figure 4-11. The dip seals are located on the ledge at the lower elevation of the rotating plugs.

The small sodium dip seals consist of a vertical steel blade and an annular trough which is filled with sodium at about 570°F. The blade of the large plug is 5.09 inches high and 0.75 inches thick. The annular trough of the large plug is 2.25 inches wide and 5.64 inches deep. The blade of the intermediate plug and the small plug is the same as the large plug. The annular trough of the intermediate plug and the small plug is also the same as the large plug.

Each plug trough is filled to a depth of 2.7 inches with 180 pounds, 120 pounds, and 30 pounds of sodium in the LRP, IRP and SRP, respectively. In this design, the outer side of this seal blade is always constantly pressurized with fresh argon gas which is the same pressure as the reactor cover gas. Figure 4-11 shows the sodium dip seal at the normal and maximum permitted pressure conditions.

In the case of the reactor cover gas pressure fluctuating + 0.1 psi (-0.12 psi),

the sodium surface goes up to 3.54 inches from the bottom of the blade. The inner sodium surface elevation drops down to an elevation of 0.39 inches from the bottom of the blade, and still prevents cover gas leakage. In the case of the reactor cover gas pressure fluctuating -0.1 psi (0.32 psi), the outer sodium surface elevation drops to 0.39 inches and the inner sodium surface elevation rises to 3.54 inches from the bottom of the blade. Leakage through the seal is still prevented. In the case of rapid pressure change, the reactor cover gas pressure (-0.22 psi) fluctuates $\pm$ 2.5 psi. One side of the sodium surface drops down to the bottom of the blade, and the reactor cover gas or fresh backup argon can leak by the blade and through the sodium seal. Therefore the small sodium dip seal can not withstand a $\pm$ 2.5 psi pressure fluctuation but with the high ledge there can be no sodium overflow.

Advantages and disadvantages of the small sodium seal are as follows:

Advantages:

1. Effective seal at low pressures.
2. Efficient sodium deposition barrier.
3. Excellent fission product barrier.

Disadvantages:

1. Poor, limited, accessibility for surveillance, maintenance and handling.
2. Requires sodium supply system.
3. Very sensitive to pressure changes.
4. Temperature of components of the plug limits location of seal.
5. Sodium oxides present maintenance problems.
6. Requires heaters and controls of supply lines.
7. Difficult to know sodium level.
8. Larger sizes difficult to fabricate and maintain configuration.
9. Difficult to assure configuration after years of operation.
10. Large volume of sodium required for three rotating plugs.
11. Wetting of blade after maintenance can be difficult.

Sodium Dip Seal--Large

The large sodium dip seal was also examined for the general requirement pressure fluctuation of ± 0.5 psi. The column of sodium to resist this fluctuation is 15.73 inches high. For a large type (reservoir) sodium dip seal it is not realistic to have a large area of sodium at a height of around 15.73 inches. For the large type dip seal, only a + 0.5 psi pressure fluctuation was considered on the cover gas side. The sodium dip seal design for this condition is shown on Figure 4-12. The dip seal arrangement appears to be a reasonable size except that when the cover gas pressure fluctuates + 0.5 psi (+ .28 psi) the sodium will rise up the annulus between the rotating plugs to a height of 16.89 inches from the bottom of the trough. This condition can cause sodium and sodium oxide buildup on the walls and eventually restrict rotation of the plugs. For this reason the pressure conditions were also revised to the same values as indicated for the small sodium dip seal (± 0.1 psi). This arrangement is shown in Figure 4-11.

The large sodium dip seal arrangement for the three plugs is shown in Figure 4-13. These sodium dip seals are located at the same elevation as the small sodium dip seal.

Figure 4-14 shows the typical mode of the sodium dip seal. In the case of rapid pressure change, the reactor cover gas pressure changes ± 2.5 psi. So for the change of + 2.5 psi (+ 2.28 psi), the outer side of the sodium surface goes up to 79.02 inches and the inner side drops down to 0.39 inches from the bottom of the blade as shown in Figure 4-15. Leakage of the reactor cover gas is still prevented. For the change of - 2.5 psi (-2.72 psi), the outer side of the sodium surface comes down to the bottom of the blade, the inner sodium surface goes up to 6.73 inches. In this case, the fresh argon gas leaks into the reactor cover gas space. Because of the large vertical height (79.02 inches) needed for the sodium column with a ± 2.5 psi reactor cover gas pressure change, this sodium seal, if considered, would have to be relocated to a much lower elevation. No attempt was made to relocate the seals in the assembly drawings to meet this requirement. This part of the study was limited to defining the size and space required for the seal.

Advantages of the large sodium seal are identical to those of the small sodium seal described earlier.

Disadvantages of the large sodium seal are also the same as those of the small sodium seal, with the addition that the large seal requires a large reservoir area in the reactor closure structure.

Inspection Mode

Inspection method for the sodium dip seals is shown in Figure 4-16. The bore scope is used for the surveillance of the sodium surface. This scope is installed in the annular gap near the top of the flange.

All of the sodium surface can be viewed with this bore scope by rotating the plug.

REFERENCES

1. "Pool-Type LMFBR Plant 1000 MWe Phase A Design", EPRI NP-646, (April, 1978).

2. "Quarterly Technical Progress Report Sodium Technology and Cover Gas Seal Development Programs, January - March 1977", AI-ERDA-13195.

3. "Shield Plug for Monju", ERDA/PNC Joint Seminar of Plant Components held at LMEC, October 1977. Power Reactor and Nuclear Fuel Development Corp. Report SA-013 KWG77-13(16).

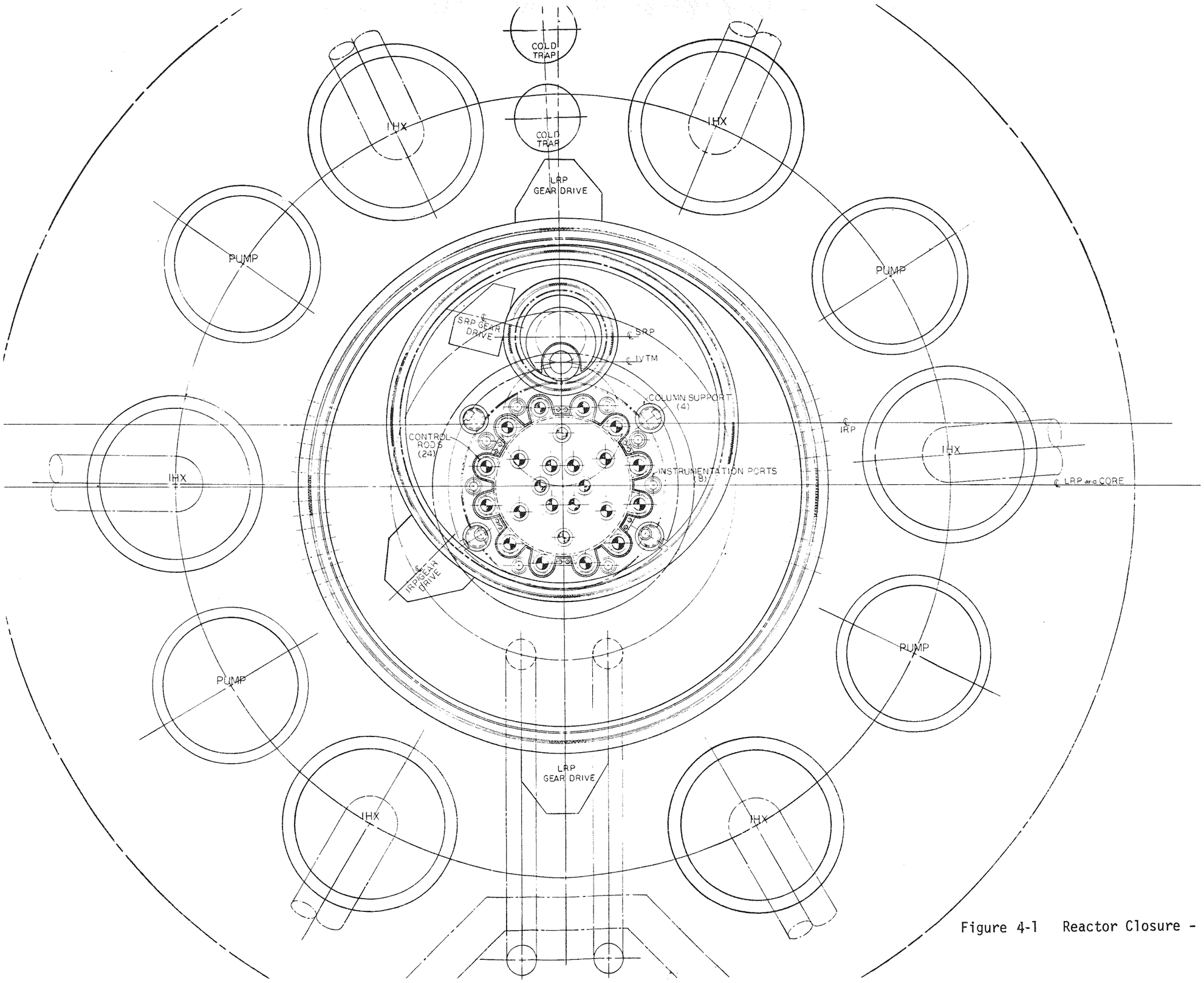

Figure 4-1 Reactor Closure - Plan View

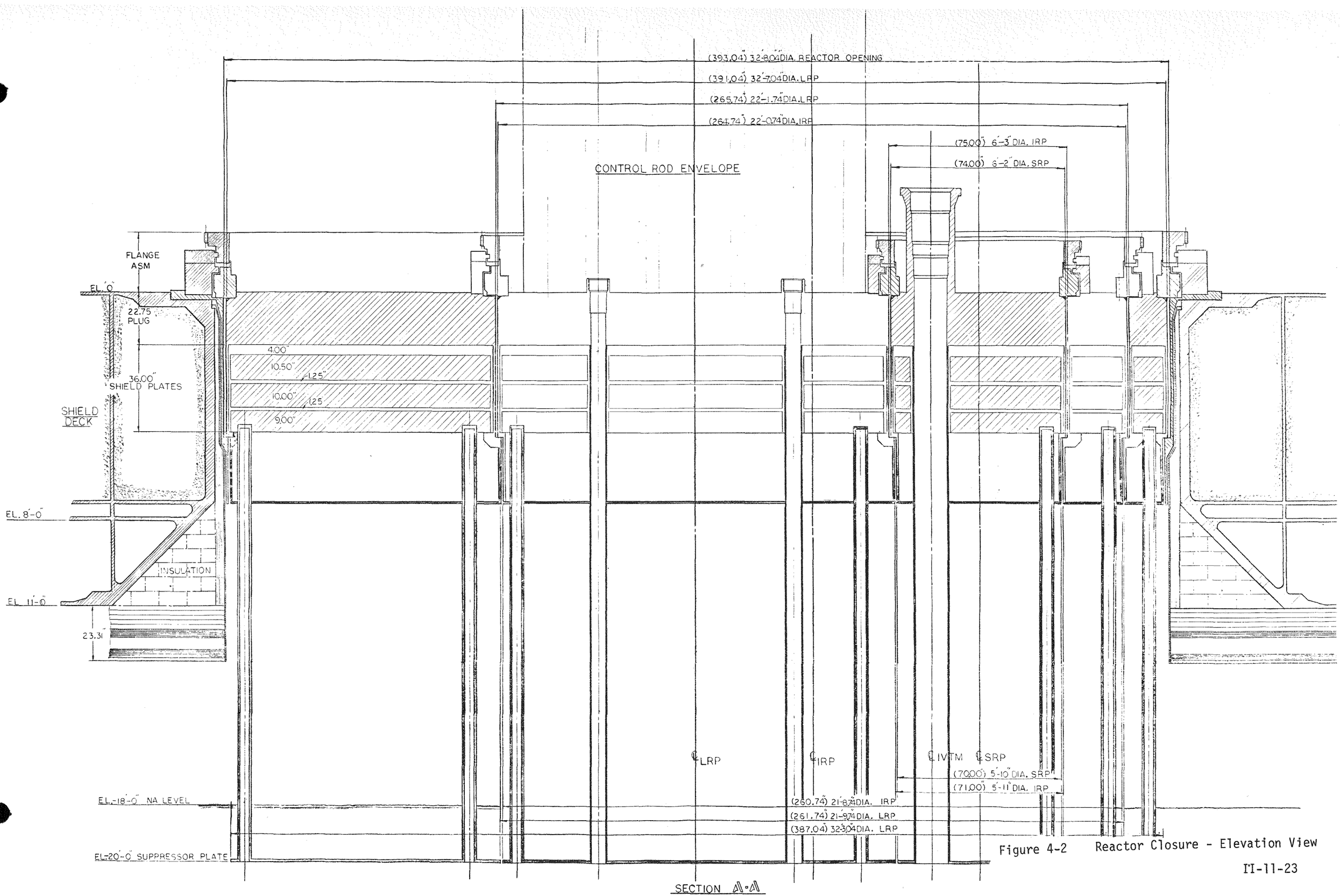

SECTION A-A

Figure 4-2 Reactor Closure - Elevation View

II-11-23

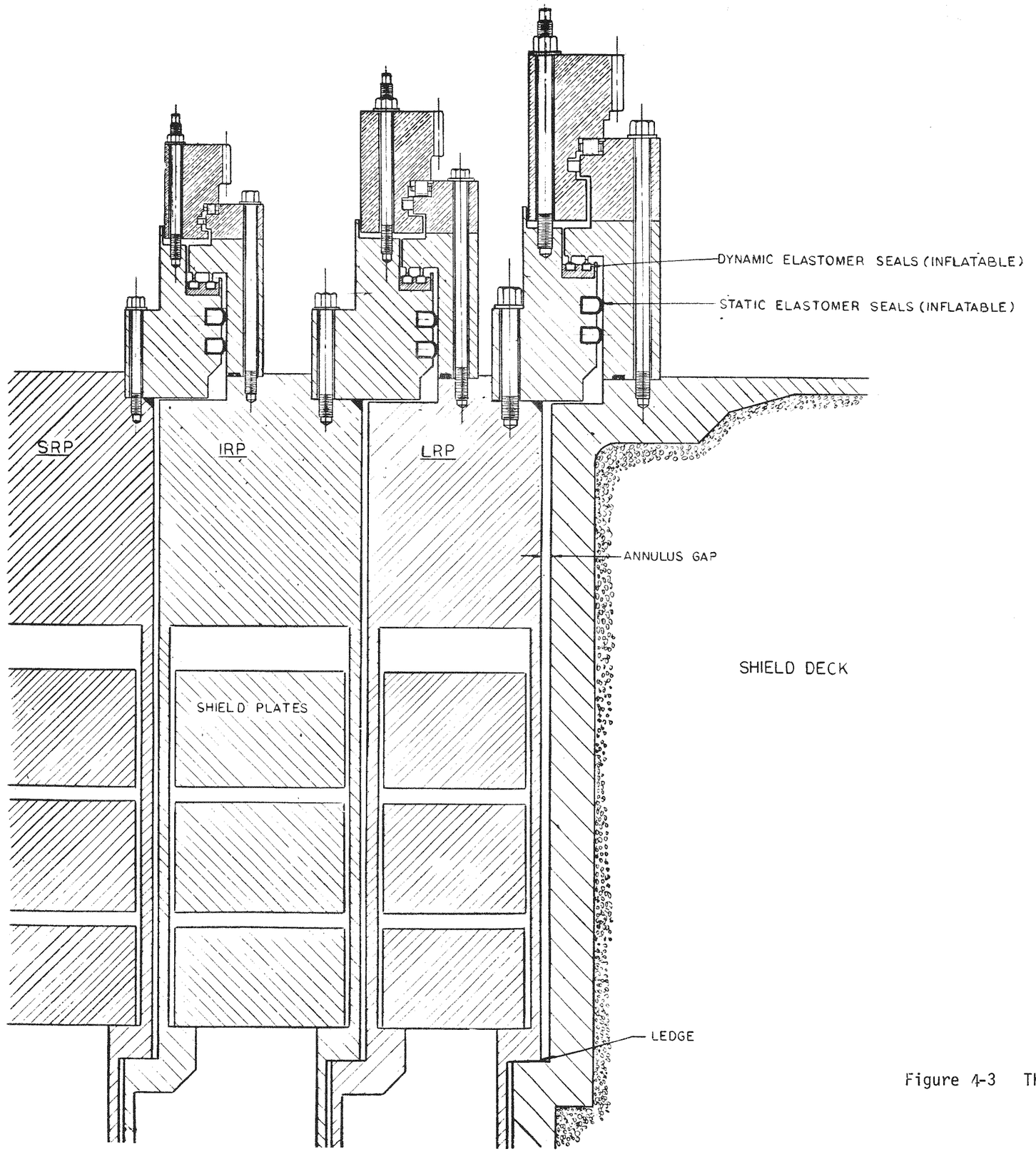

Figure 4-3 Three-Flange Assembly - Elastomer Seals

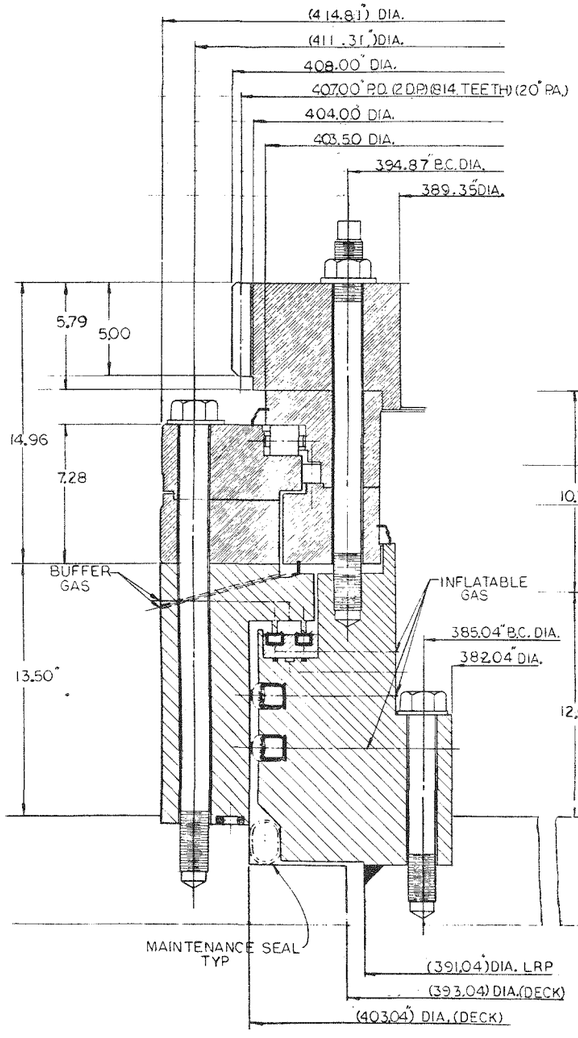

LRP FLANGE ASSEMBLY
1.65"DIA-120 HOLES EQ SPACED FOR 1.50"-6UNC BOLT
3 PLACES

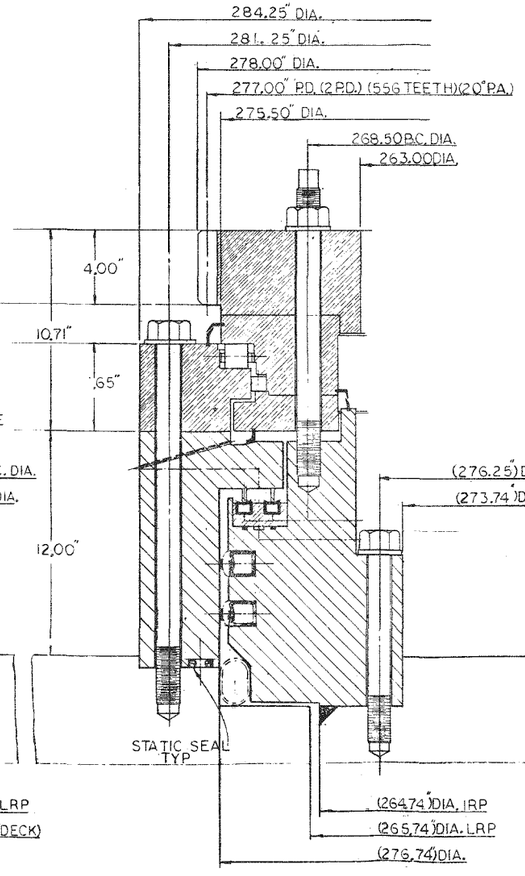

IRP FLANGE ASSEMBLY
1.378 DIA.-90 HOLES EQ SPACED FOR 1.25"-7UNC BOLT
3 PLACES

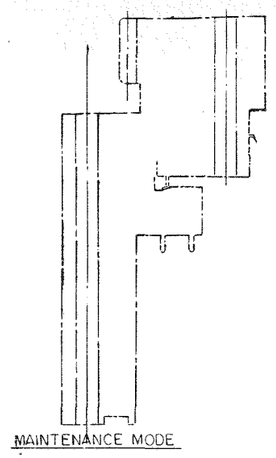

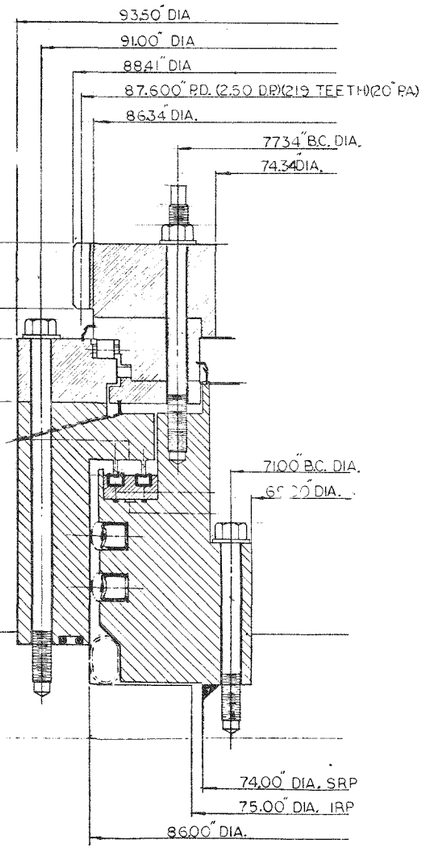

SRP FLANGE ASSEMBLY
1.12 DIA.-40 HOLES EQ SPACED FOR 1.00"-8UNC BOLT
3 PLACES

Figure 4-4 Details of Three-Flange Assembly - Elastomer Seals

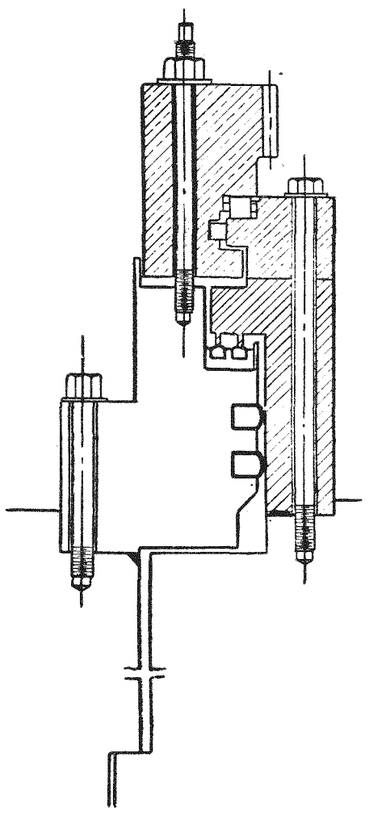

POWER MODE

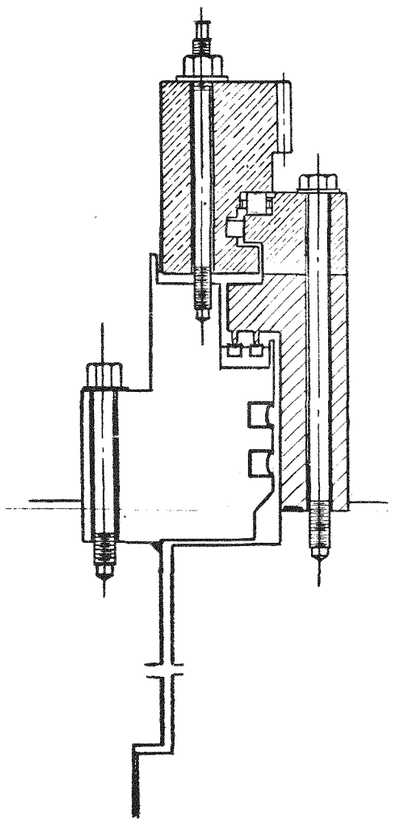

REFUELING MODE

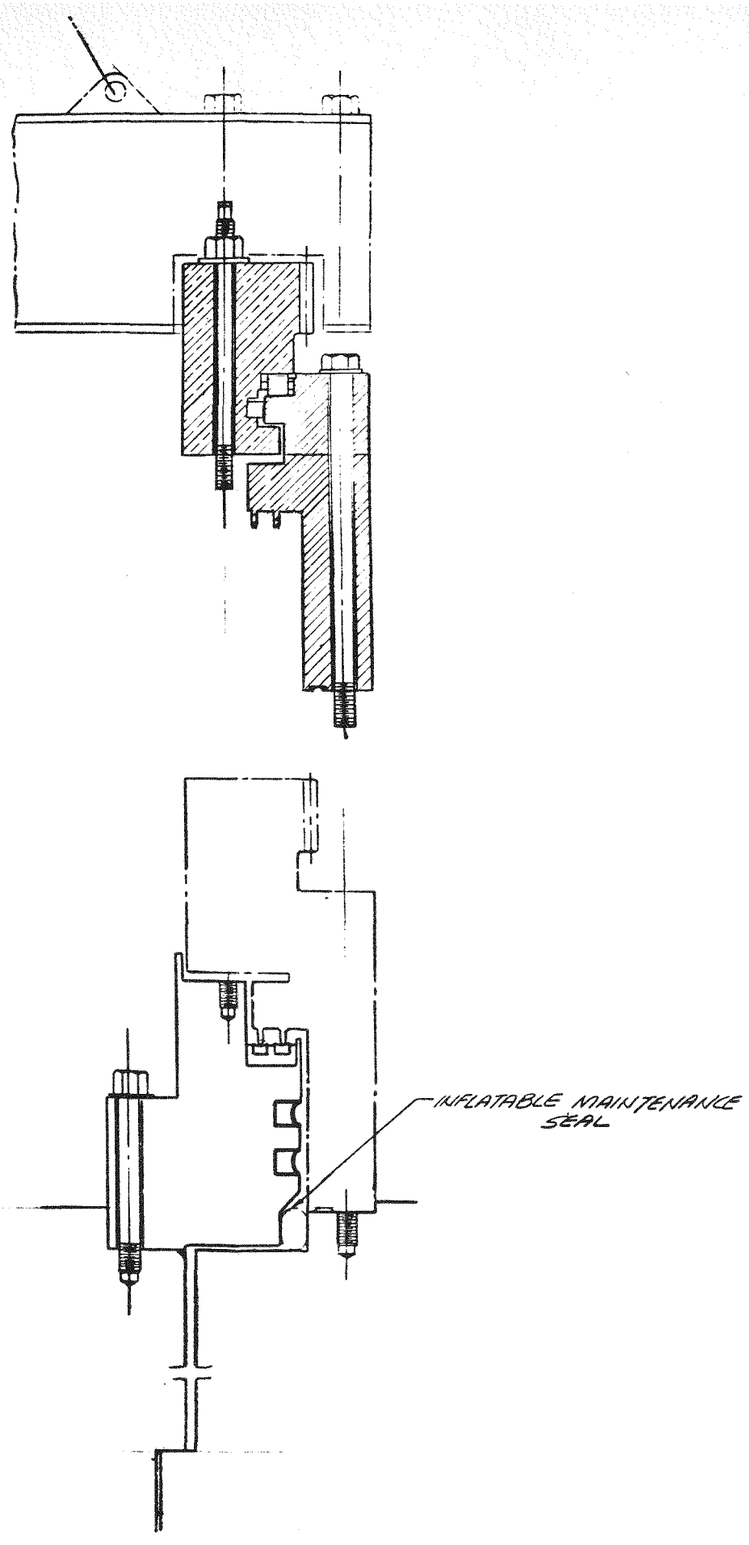

MAINTENANCE MODE

Figure 4-5 Operating Modes

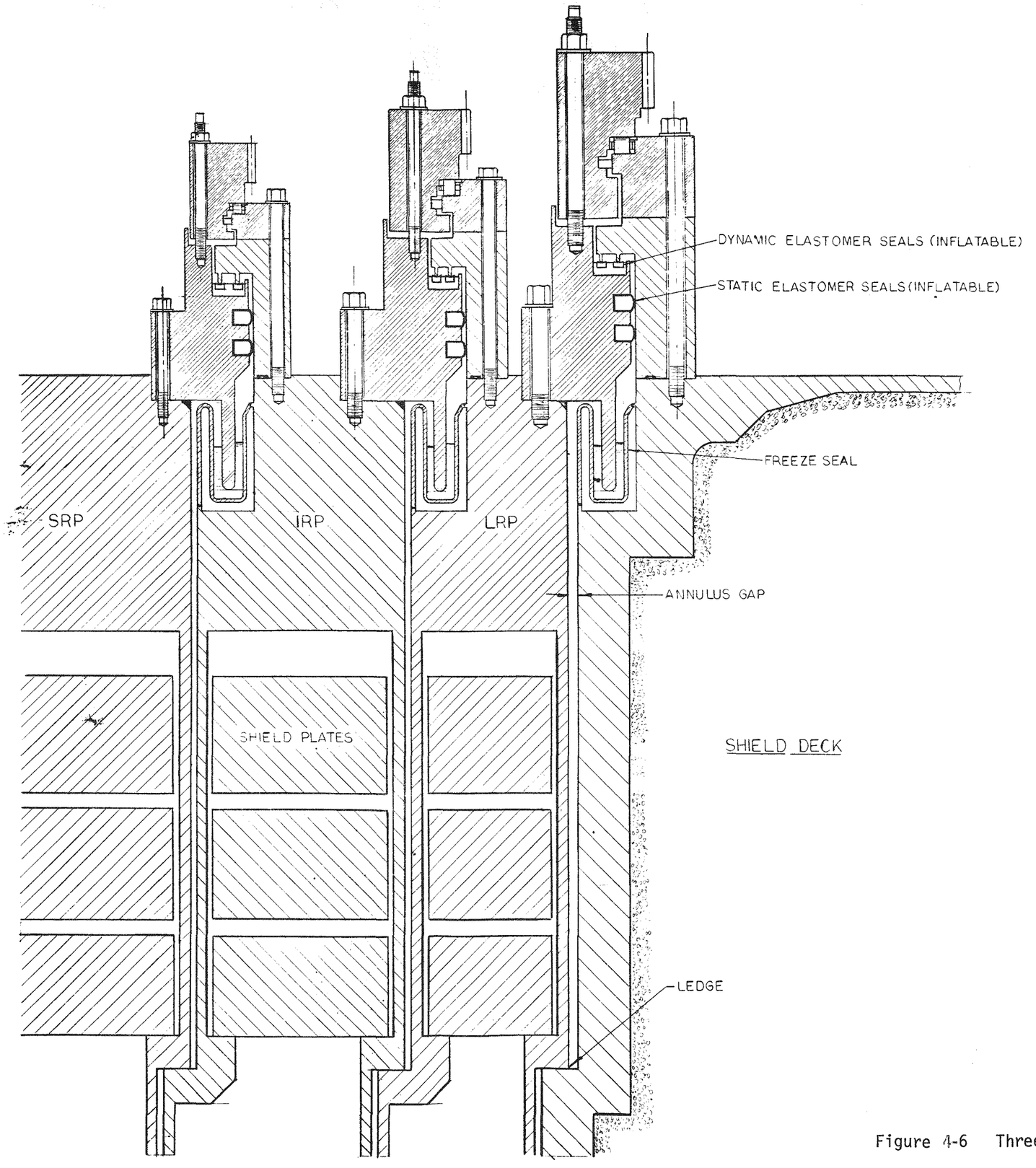

Figure 4-6 Three Flange Assembly - Freeze Seals

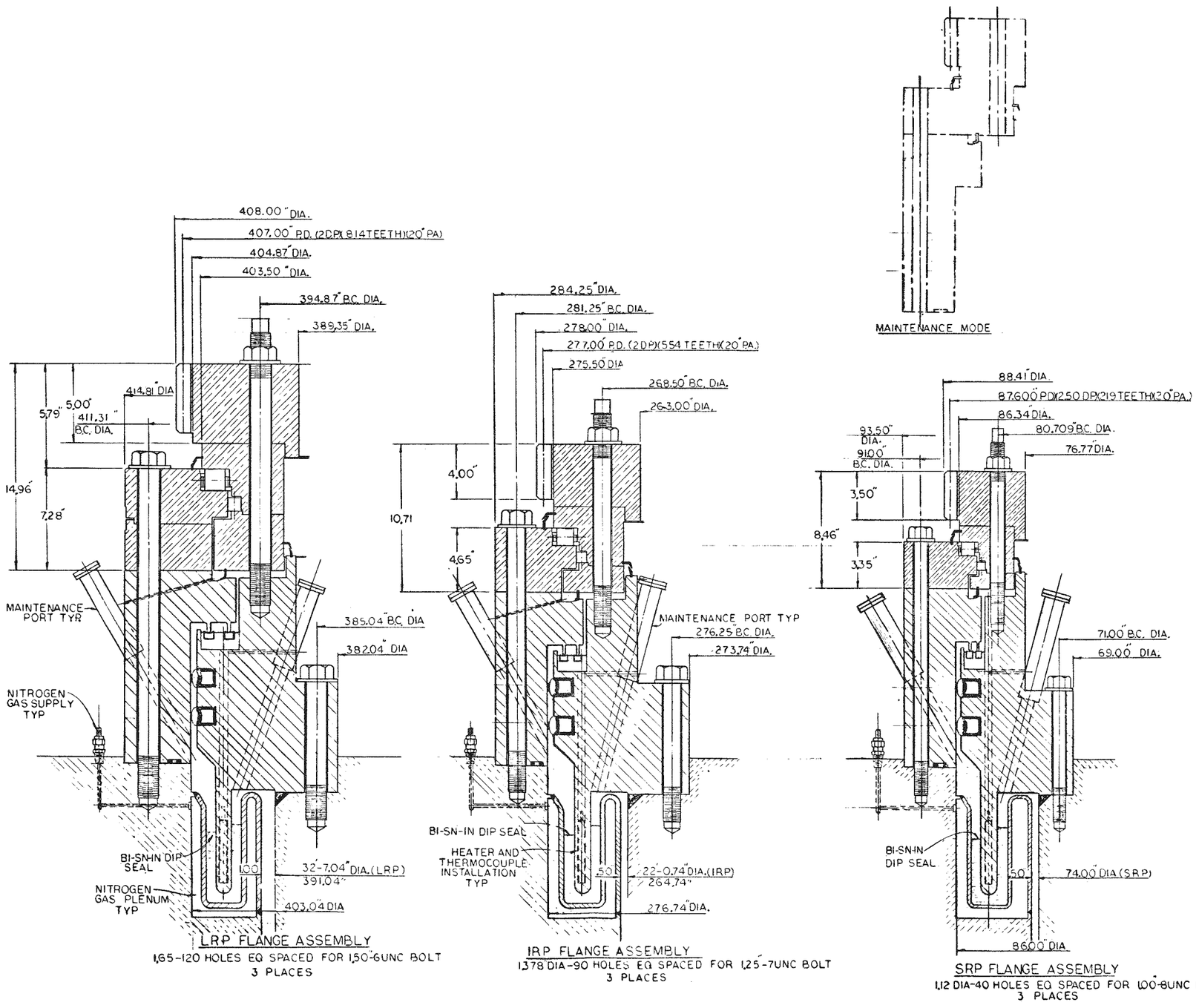

Figure 4-7 Detail of Three-Flange Assembly - Freeze Seals

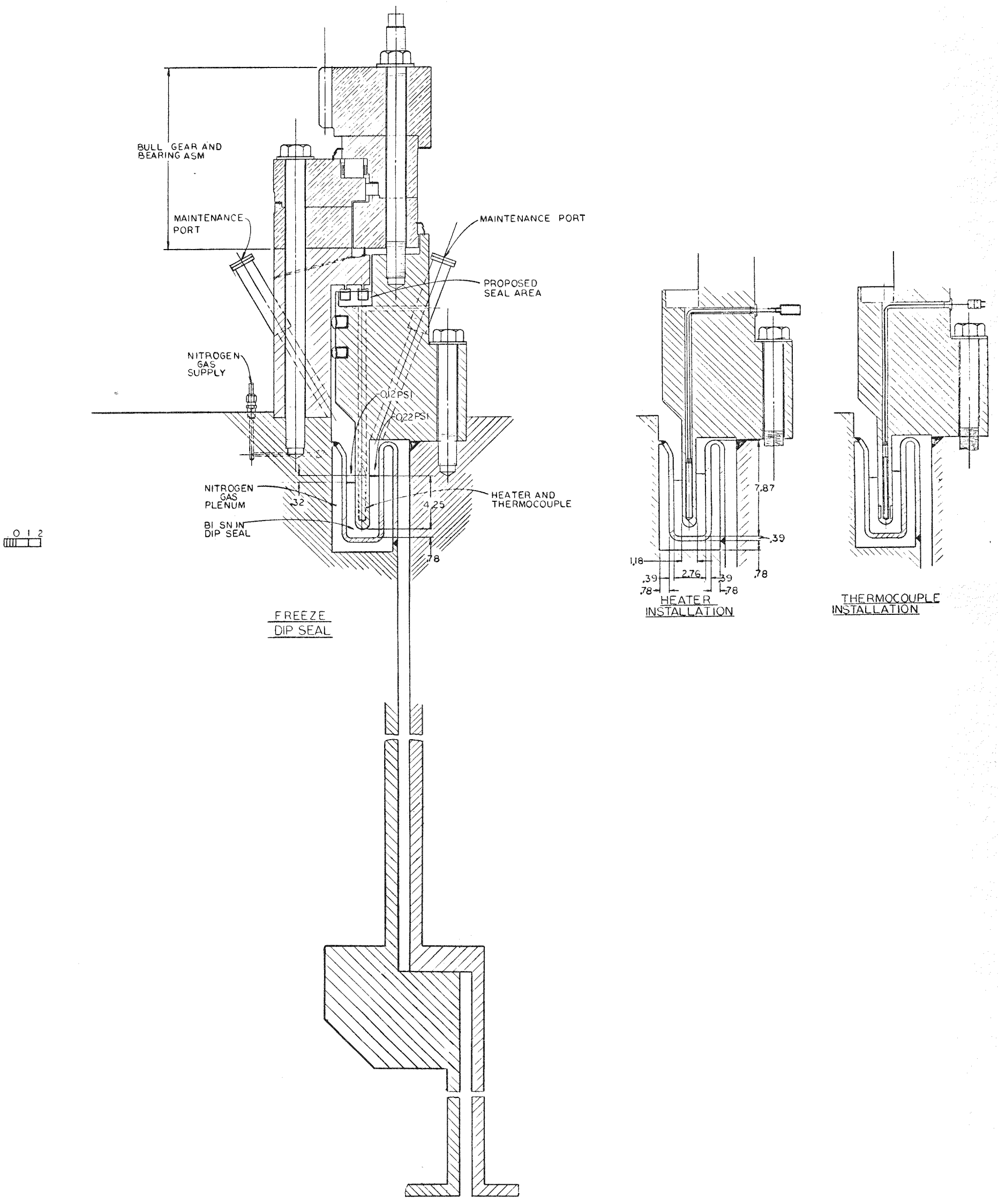

Figure 4-8 Typical Freeze Seal/Flange Arrangement

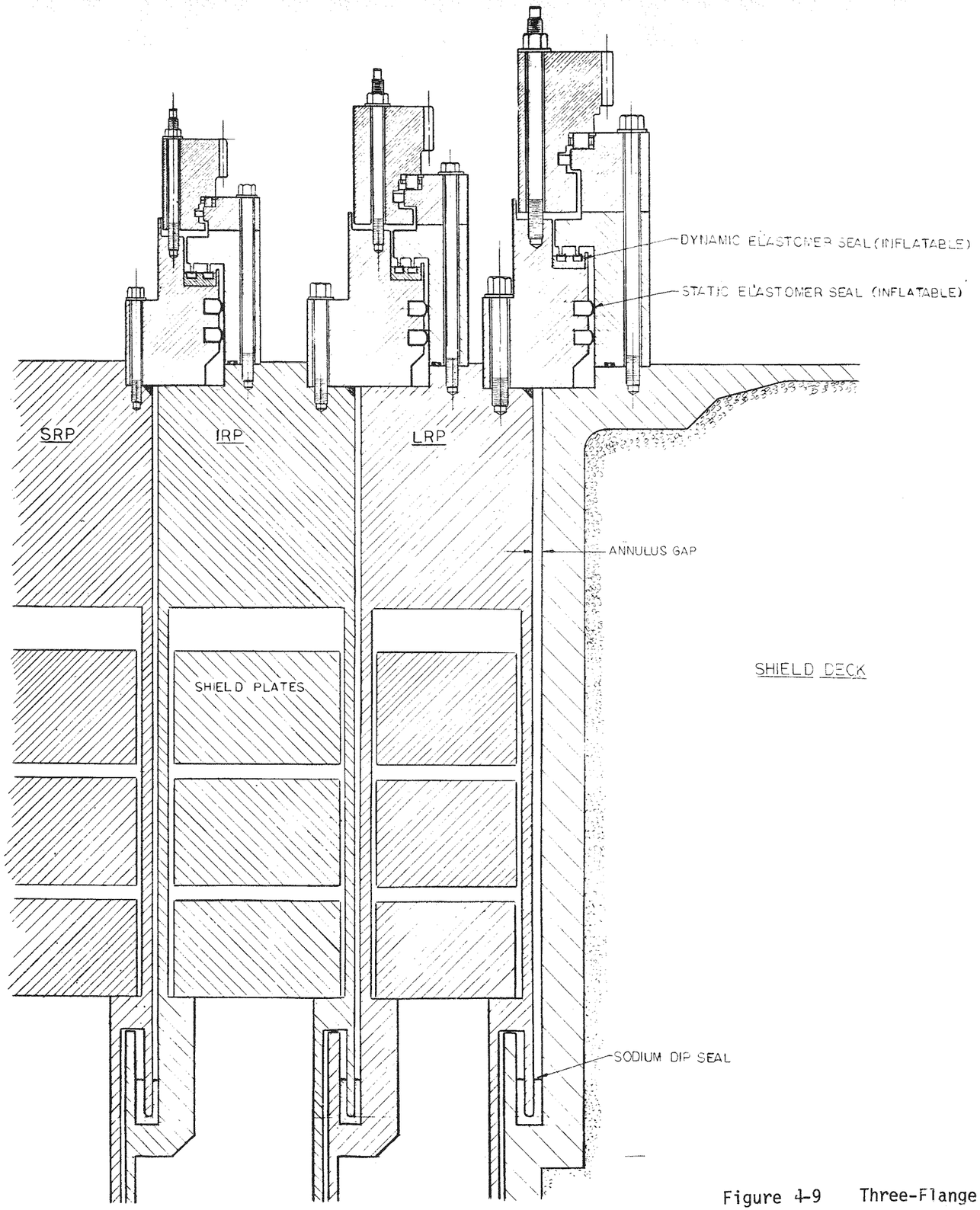

Figure 4-9 Three-Flange Assembly - Small Sodium Seals

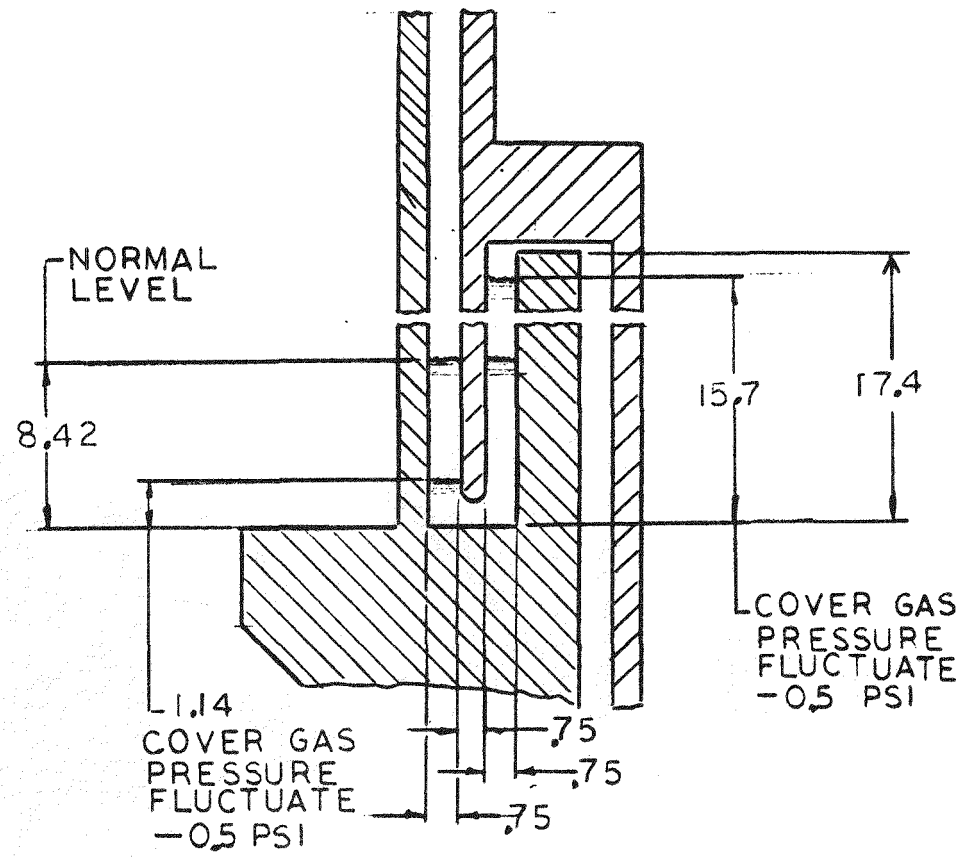

Figure 4-10 Sodium Dip Seal - Small

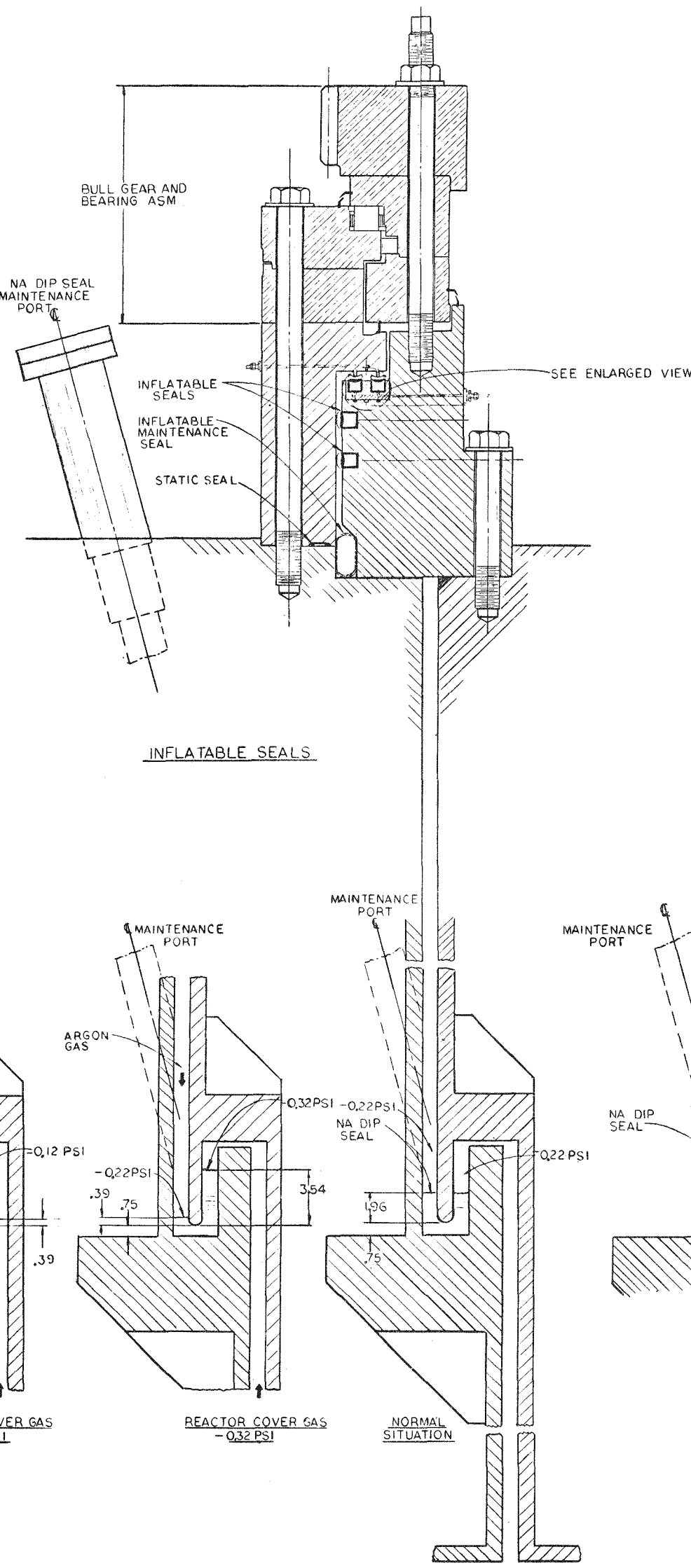

INFLATABLE SEALS

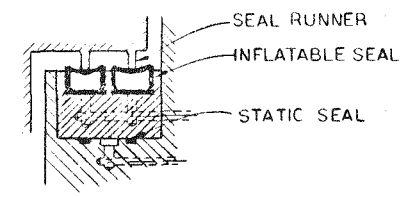

ENLARGED VIEW

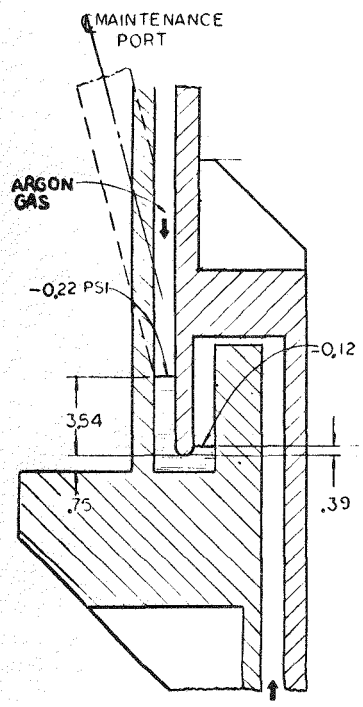

REACTOR COVER GAS -0.12 PSI

REACTOR COVER GAS -0.32 PSI

NORMAL SITUATION

NA DIP SEAL

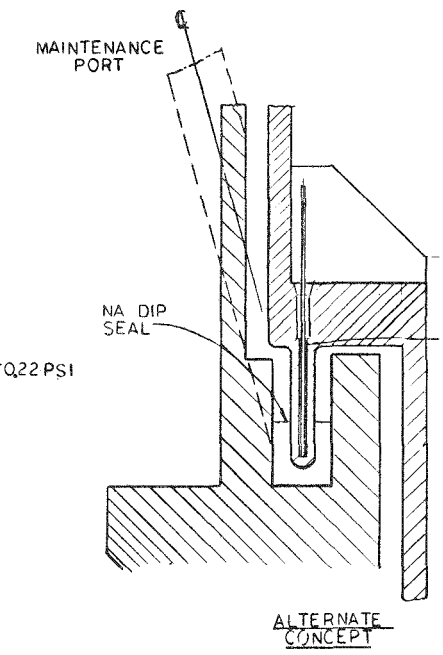

ALTERNATE CONCEPT

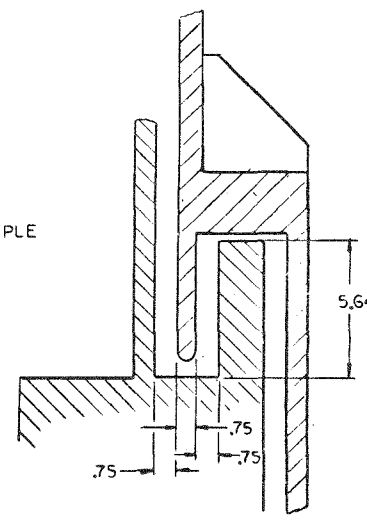

DETAIL

Figure 4-11 Typical Small Sodium Seal/Flange Arrangement

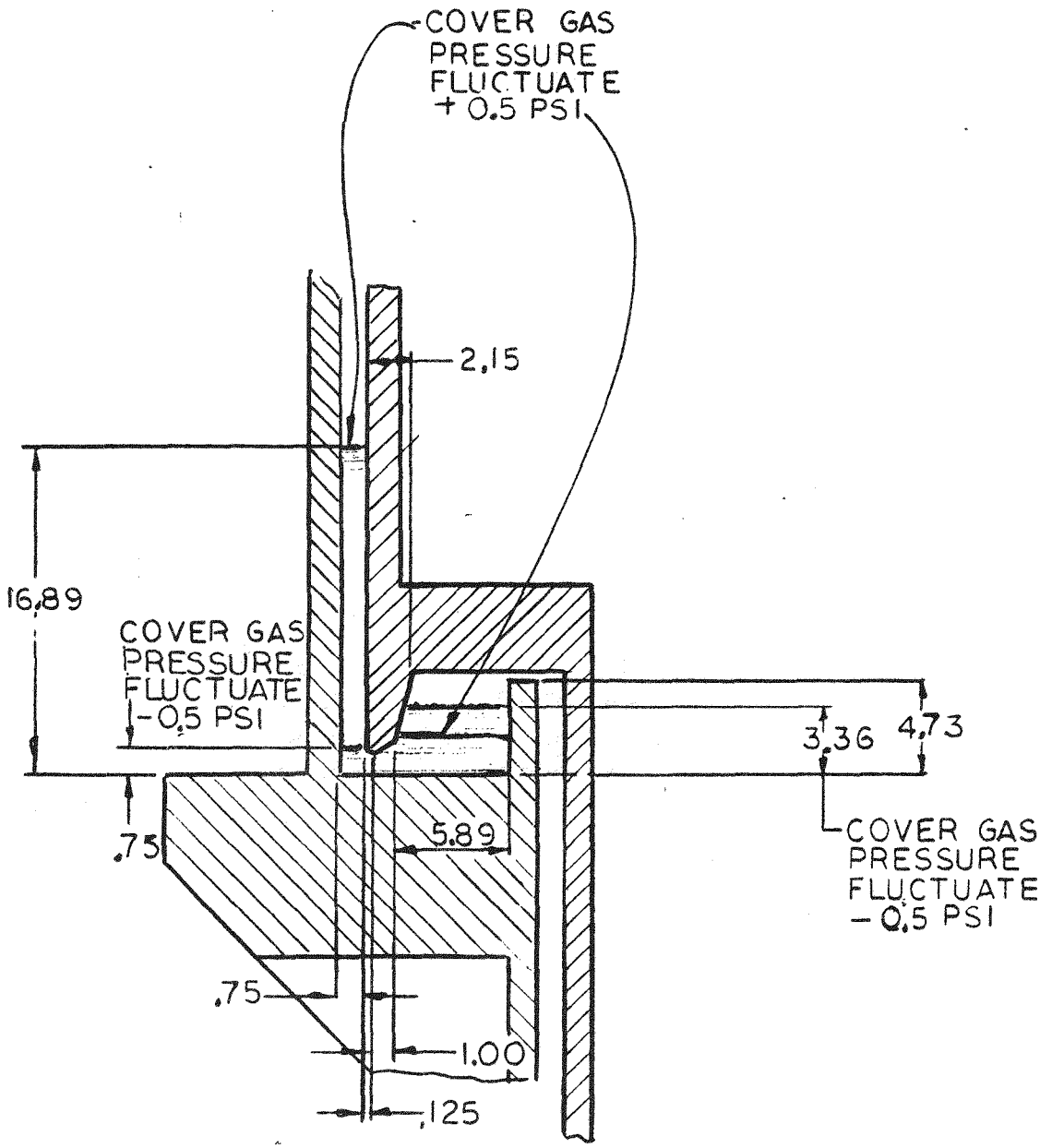

Figure 4-12 Sodium Dip Seal - Large

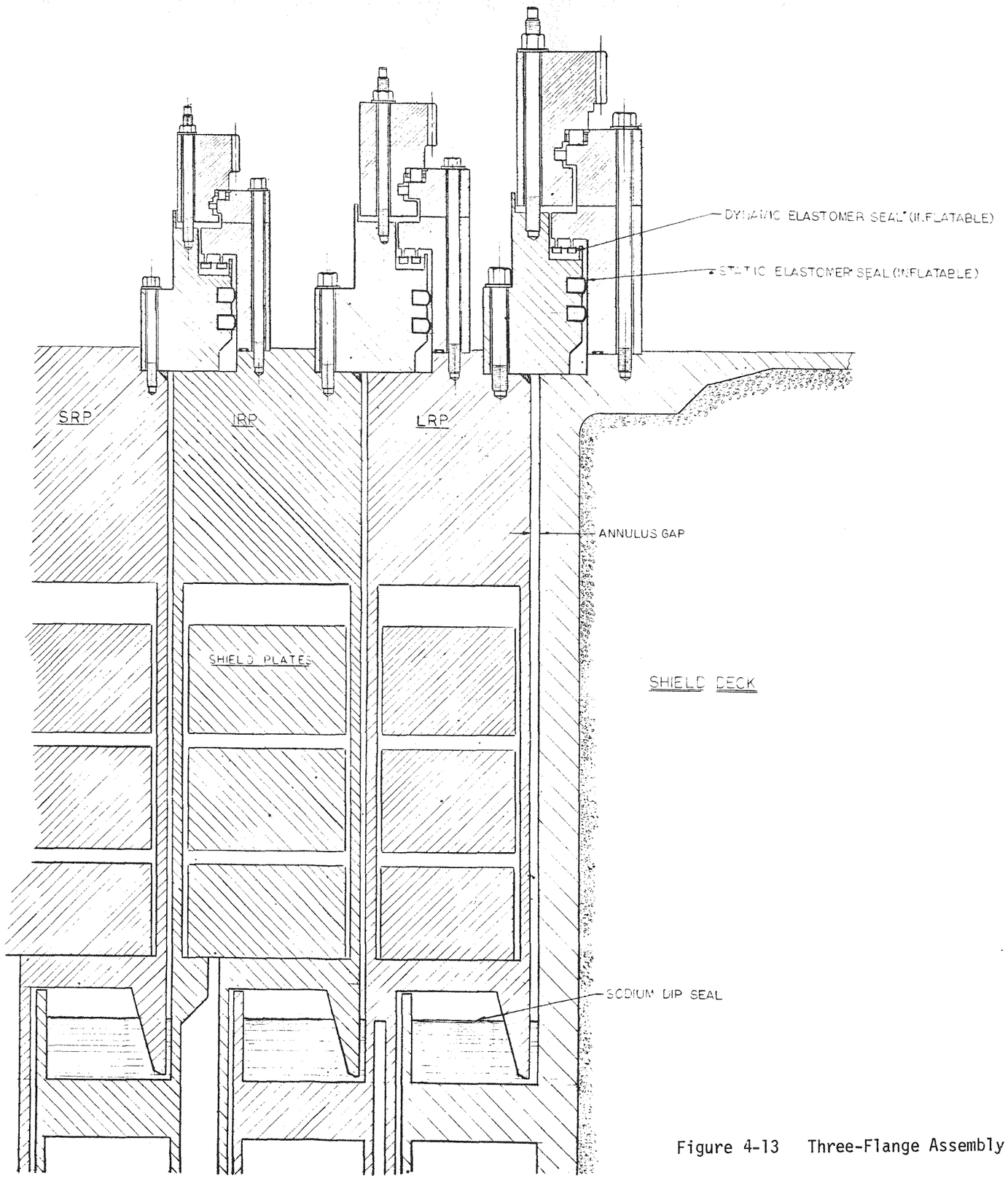

Figure 4-13 Three-Flange Assembly - Large Sodium Seals

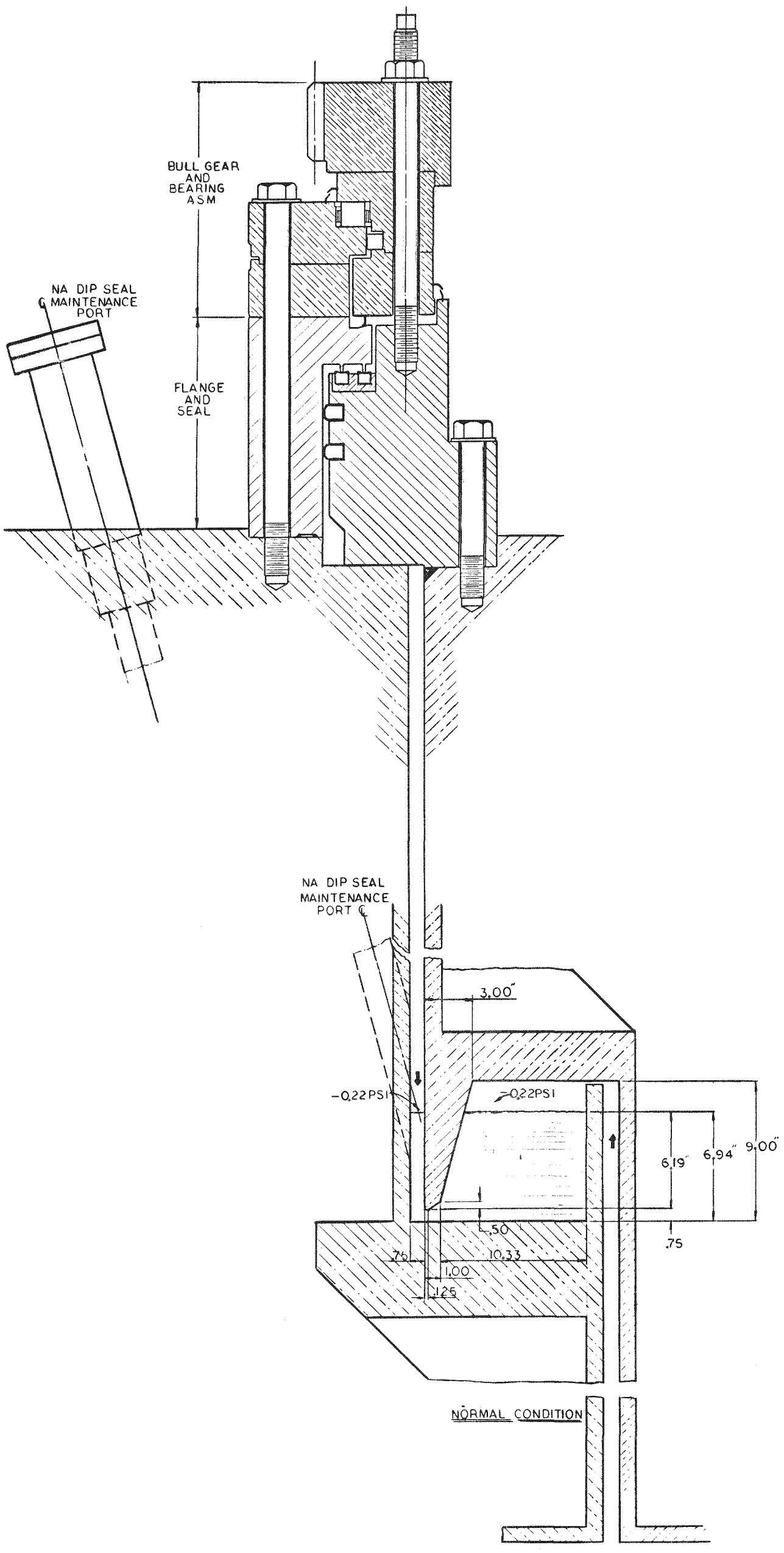

NA DIP SEAL WITH RESERVOIR

Figure 4-14 Typical Large Sodium Seal/Flange Arrangement

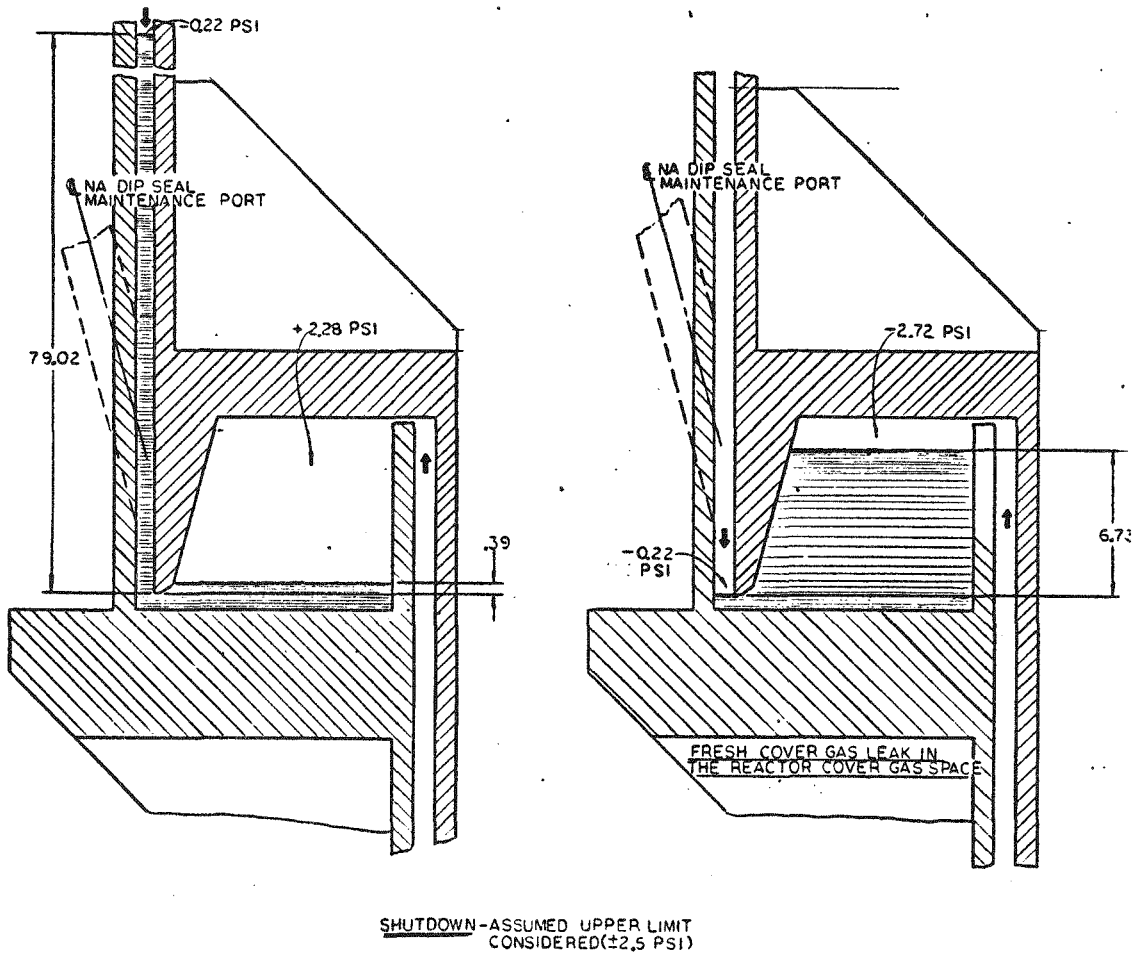

Figure 4-15 Typical Large Sodium Seal - Pressure Fluctuations

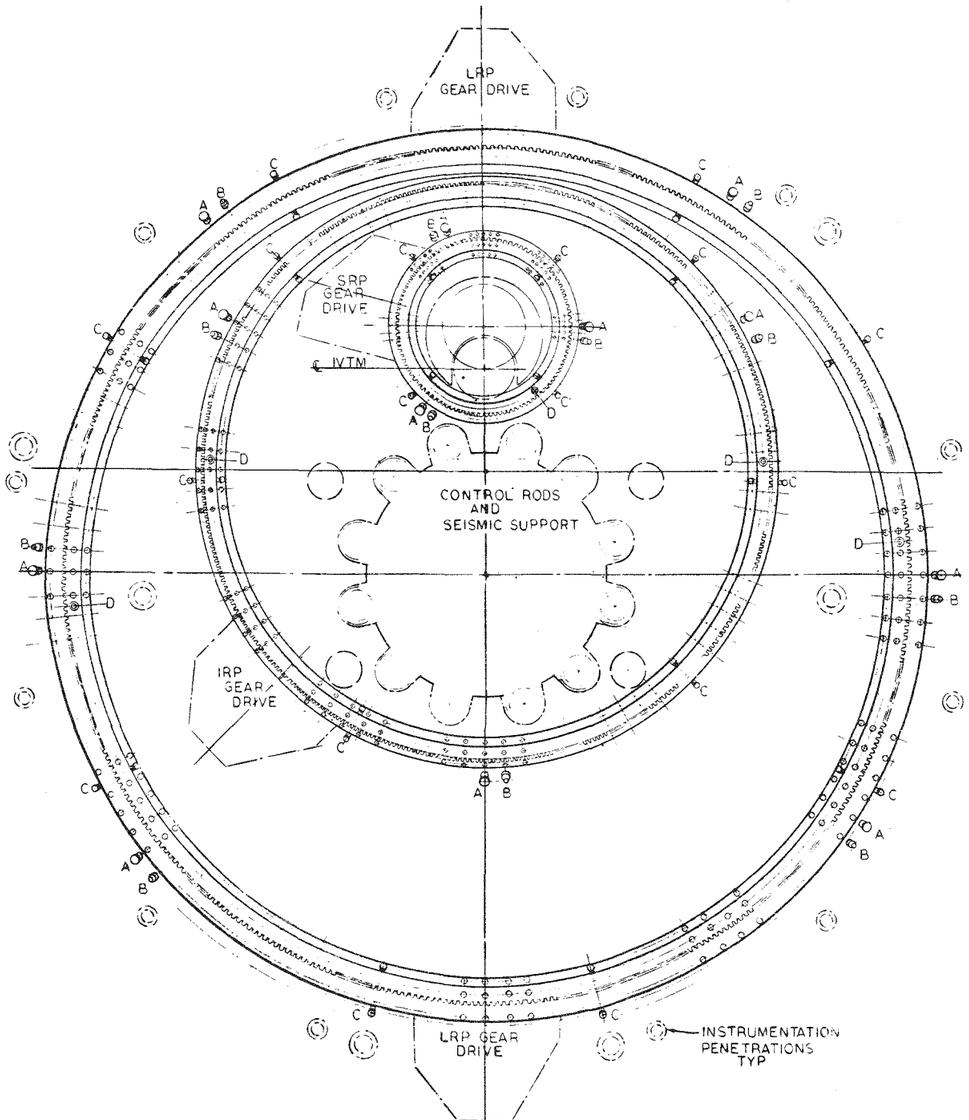

INDEX	PENETRATIONS	QUANITY SRP	IRP	LRP
A	NA MAINTENANCE PORT	3	4	6
B	NA REFILL PORT	3	4	6
C	BI-SN-IN MAINTENANCE PORT	8	12	16
D	INSPECTION PORTS	1	2	2

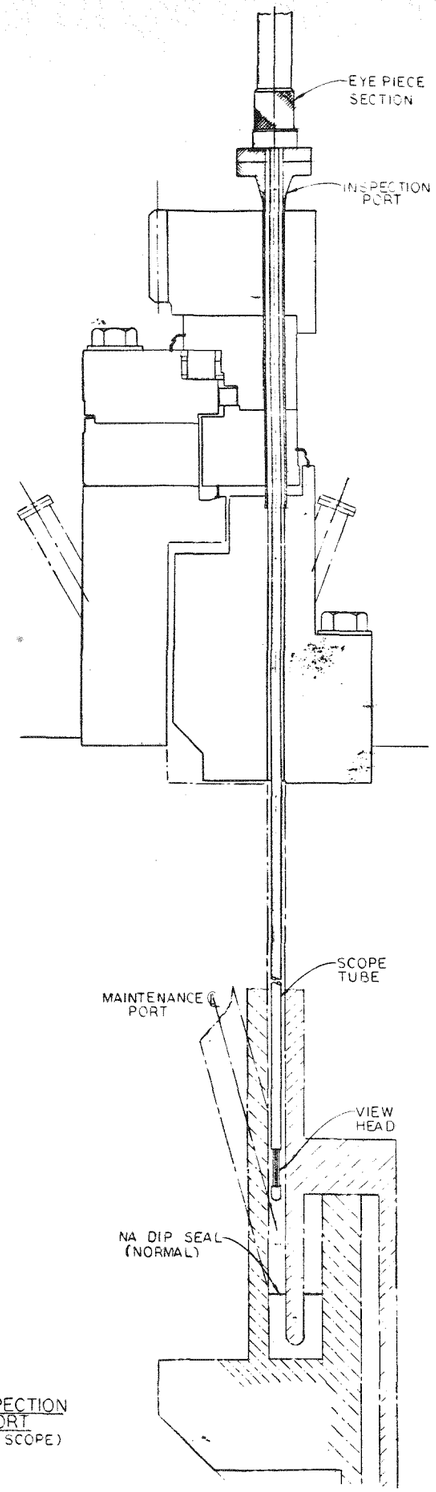

INSPECTION PORT
(BORE SCOPE)

Figure 4-16 Seal Inspection Method

PART II: REACTOR ASSEMBLY - STRUCTURES

APPENDIX IIA: ENGINEERING STUDY OF THE DESIGN, FABRICATION, CONSTRUCTION AND TESTING OF THE MAJOR STRUCTURAL COMPONENTS OF A 1000 MWe POOL-TYPE LMFBR - ALTERNATE VESSEL SUPPORT

CBI Nuclear, Inc.

EDITORS NOTE:

This appendix covers the same general areas as Appendix IVA except that the alternate vessel support is used in construction. Only the sections of Appendix IVA which are different because of this change are in this appendix. For the missing sections, please refer to Appendix IVA.

CONTENTS

		Page
1.	Introduction	IIA-1
2.	Summary	IIA-1
2.7	Construction Summary	IIA-1
2.8	Schedule Summary	IIA-2
4.7	Construction	IIA-2
4.8	Schedule	IIA-7

FIGURES

		Page
4.8	Schedule - Major Components	IIA-7
4.9.2.0	General Arrangement	IIA-11
4.9.2.1	Guard Vessel	IIA-13
4.9.2.2	Primary Vessel	IIA-15
4.9.2.3	Core Support	IIA-17
4.9.2.4	Thermal Barrier	IIA-19
4.9.2.5	Top Deck General Plan	IIA-21
4.9.2.6	Site Plan	IIA-23
4.9.2.7	Lifting Sequence	IIA-25
4.9.2.8	Platform Ringer With Twin Tower Attachment	IIA-27

ENGINEERING STUDY OF THE DESIGN, FABRICATION, CONSTRUCTION AND TESTING OF THE MAJOR STRUCTURAL COMPONETS OF A 1000 MWE POOL TYPE LMFBR - ALTERNATE VESSEL SUPPORT

1. INTRODUCTION

This report is a preliminary engineering study and re-examination of construction methods, sequences, and scheduling of the major structural components of a pool type liquid metal fast breeder reactor. The report was prepared under the direction of the CBI Nuclear Company. Any use of the acronym "GE" in this report refers to the General Electric Company - Advanced Reactor Systems Department, Sunnyvale, California.

The information given in Appendix IVA was prepared in July 1978 and discussed modified construction techniques and lifting equipment to allow the subassembly of major vessel components into single units.

Various primary vessel support schemes have been developed and it is the purpose of this study to re-examine the information given in Appendix IVA applying the support scheme designated "Concept II-B". This concept utilizes an integral cone type support skirt which includes a large section of built-up plates at the junction of reactor vessel wall and support skirt, as indicated on GE Drawing #908A536, Revision E dated 6/20/78.

Many of the elements of Appendix IVA are common to this consideration and will be referenced without general repetition.

2. SUMMARY

The following presentation is a supplemental discussion of construction and scheduling from the previous report.

2.7 CONSTRUCTION SUMMARY

The construction of the vessel will consist of major subassemblies with an additional subassembly consisting of the stiffened cylinder and conical support skirt. Each component will be subassembled in the yard adjacent to the permanent foundation and single lifts range from 185 tons to a maximum of 721 tons. The maximum lift represents the combination of the primary vessel and core support into one subassembly.

The sequence, for erection of components on the foundation, will be the guard vessel, primary vessel/core support assembly, primary vessel thermal barrier, vessel support skirt assembly, top deck, and rotating plugs. The primary vessel/core support structure assembly will be temporarily supported by a structure between the primary and guard vessels. The guard vessel skirt and shell will be analyzed and stiffened as required to carry this additional construction load. The subassemblies of the top deck will be supported by the permanent flange which will eliminate any necessity for temporary props to the core support structure.

Penetrations in the top deck and core support will be installed in position. The rotating plug seat, the penetration spot faces, and the core support seat will be machined in position after final assembly.

2.8 SCHEDULE SUMMARY

The schedule durations will be the same as discussed in Appendix IVA and are as follows:

1) Total contract time is approximately 50 months.
2) Total on site construction time is approximately 30 months.
3) Total time on the foundation is approximately 22 months.

4.7 CONSTRUCTION

4.7.1 GENERAL CONSTRUCTION COMMENTS

Same as Appendix IVA.

4.7.2 OVERALL CONSTRUCTION SEQUENCE FOR MAJOR STRUCTURAL COMPONENTS OF PLBR POOL REACTOR

The following General Construction Sequence is a modification of that which appears in the Appendix IVA and now incorporates the support skirt assembly. Comments on the detailed construction procedures will be confined to the sequences which have changed from Appendix IVA.

4.7.2.1 Completely assemble and erect the guard vessel.

4.7.2.2 Completely assemble the primary vessel and the core support and erect as one section which will be temporarily supported from the core support ring to the guard vessel.

4.7.2.3 Erect the primary vessel thermal barrier assembly.

4.7.2.4 Install support skirt base plate on concrete at elevation (-) 11'5", level, and shim.

4.7.2.5 Install conical support skirt plate assembly and weld cone to base plate.

4.7.2.6 Install top deck without penetrations.

4.7.2.7 Connect the primary vessel to the support skirt.

4.7.2.8 Remove the temporary supports between the primary vessel and the guard vessel in accordance with code requirements.

4.7.2.9 Lay out and install the penetrations in the top deck.

4.7.2.10 Install the top deck shielding.

4.7.2.11 Machine the top deck rotating plug support hub ring and the penetration spot bases.

4.7.2.12 Project down from the top deck and install the core support penetrations.

4.7.2.13 Install and machine the core support "basket".

4.7.2.14 Install the pump thermal barriers.

4.7.2.15 Install the core barrel on the core support.

4.7.2.16 Install the closure plug, installing the outer rotating plug first, the intermediate plug, and then the small plug.

4.7.2.17 Put temporary covers over all penetrations and test* the primary vessel.

4.7.2.18 With the primary vessel full, test* the guard vessel.

4.7.3 GUARD VESSEL CONSTRUCTION SEQUENCE

Same as in Appendix IVA.

4.7.4 PRIMARY VESSEL CONSTRUCTION SEQUENCE

To accommodate the concept II-B support system, the top of the primary vessel 1" shell will now be at elevation (-) 6'3" which is 3'9" higher than the previous configuration. Five shell courses, above the core support skirt, will be maintained with wider plates than previously considered. The erection sequence will be identical to that outlined in Appendix IVA.

*See Appendix IVA.

4.7.5 CORE SUPPORT PLATFORM CONSTRUCTION SEQUENCE

Same as Appendix IVA.

4.7.6 CONSTRUCTION SEQUENCE OF THE PRIMARY VESSEL THERMAL BARRIER

Same as Appendix IVA.

4.7.7 CONSTRUCTION SEQUENCE FOR THE PRIMARY VESSEL STIFFENED RING AND SUPPORT SKIRT

4.7.7.1 Subassemble (fit and weld) the 4" thick cylinder plates and the 2" cylinder using normal plate erection techniques.

4.7.7.2 Fit and weld the 6" thick external stiffening rings and install the 1.5" web plates.

4.7.7.3 While the assembly of the upper stiffened section is proceeding, ground assembly the conical sections erecting the 1.5" thick course first and assembling the 3" thick course to it. Install necessary bracing on the cone section and erect the stiffened ring.

4.7.7.4 Fit and weld the connection of the upper cone section to the lower stiffener.

4.7.7.5 Assemble the base plate components into a complete ring, check the bolt circle and take any corrective action. Erect the complete base plate on the foundation over the anchor bolts.

4.7.7.6 Erect the support skirt assembly on the foundation and fit and weld to the base plate.

4.7.7.7 Fit, weld, and inspect the joint of the primary vessel to the support assembly.

4.7.7.8 Remove the temporary lugs connecting the primary vessel shell to the guard vessel.

4.7.8 CONSTRUCTION SEQUENCE OF THE TOP DECK

As a result of the revised support configuration Concept II-B for the top deck and primary vessel, the outside diameter of this component has been reduced from 78'-0 O.D. to 72'10" O.D. For an "in depth" study a revised top deck design would be required. Since this is unavailable at this time the following assumptions, with reference to Drawing 4.9.2.5, have been made for the construction study.

a) The structural details remain the same as in Appendix IVA inside radius 36' 5" per Section A-A.
b) Between radii 33'6" and 36'5" the structural details will be similar to Section A-A except compressed.
c) The section depth will be a constant 11'0".
d) All penetrations will remain the same except those beyond radius 33'6" will move radially inward as a result of the reduced width of the section.

4.7.8.1 The top deck will be subassembled into two pieces outside the containment vessel in a temporary enclosure generally following the sequence set out in the report "Phase A Appendix IVA. The subassemblies will consist of the center hub with half the outer deck attached and one outer deck assembly. Both of the subassemblies will have the corresponding segments of the support flange welded to them to allow erection of the top deck sections directly on the permanent support ring which will eliminate the necessity for any temporary props to facilitate erection. The two subassemblies will weigh approximately 711 tons (center hub, outer deck, and top flange) and 410 tons (outer deck and top flange). The increased weight due to the attachment of the 6" top flange is offset by the reduced diameter of the top deck.

4.7.8.2 The top flange will be shop fabricated in 12 segments approximately 20' in arc length complete with the stud holes drilled and sections match marked.

4.7.8.3 The top flange sections will be erected on temporary supports, aligned carefully following the shop match marks, and the radial butt joints fit, welded and examined.

4.7.8.4 After the assembly is complete the radial joints will be locally postweld heat treated and bolt circle diameter verification checks will be made.

4.7.8.5 The complete flange ring, weighing approximately 68 tons will be erected on the top deck subassembly, on temporary brackets welded to the exterior of the 1½" thick outer deck skin plates. Concentricity measurements will be made

to center the bolt circle, following which the joint connecting the top deck to the flange will be fit and welded.

4.7.8.6 During assembly of the top flange to the deck two radial joints in the flange, coincident with the field joint in the top deck, will be cut apart and match marked for final assembly.

4.7.8.7 Prior to erection of the top deck assembly construction of the primary vessel is complete, the core structure in place, and the primary vessel thermal barrier installed.

4.7.8.8 After a final check is made of the concentricity of the bolt holes in the upper flange of the support structure, to see they coincide with those of the top deck flange, the levelling shims will be installed in position on the top flange of the support structure.

4.7.8.9 The two top deck sections are now erected and the permanent support bolts installed.

4.7.8.10 Fit and weld the top deck subassemblies together and the radial closure joints in the top flange. During this operation the permanent support studs should have only enough tension to support the construction loads and allow for some movement during fitting and welding of the top deck closure seams.

4.7.8.11 Tension the flange hold down studs to the required torgue following the proper bolting sequence.

4.7.8.12 Install the seismic restraint cylinder and shims, securing it to the support structure with cap screws.

4.7.8.13 Fit and weld the sealing cover segments to the upper support flange and the stiffener of the support structure. Install the seismic stop blocks and shims and final tension the anchor bolts to the skirt base plate.

4.7.8.14 Lay out and install the top deck penetrations.

4.7.8.15 Install the top deck shielding.

4.7.8.16 Machine the center hub to accept the rotating plug closure. Machine the penetration spot faces as required.

4.7.8.17 Install the core support penetration and core support "baske as described in the core support erection sequence.

4.7.8.18 Install the center rotating plugs utilizing the existing lifting equipment.

4.7.8.19 Test the primary vessel.

4.7.8.20 Test the guard vessel.

4.7.8.21 After vessel testing is complete and the test medium has been removed, the primary vessel is available for installation of the pumps, heat exchangers, insulation, core, and other components.

4.8 SCHEDULE

The schedule for assembly of the major components will remain approximately the same as indicated by the bar chart (Figure 4.8). The additional subassembly "Primary Vessel Stiffened Ring and Support Skirt" will add more work to the assembly yard phase however the overall effect will be offset by the reduced amount of fitting, welding and examination involved in the smaller top deck assemblies. The erection of the conical support assembly, on the permanent foundation, will add only a nominal amount of time to the foundation occupancy. Access for the in place connection of the primary vessel to the Concept II-B support 2" plate will be easier than in the Appendix IVA scheme. Overall foundation occupancy will be the same as in Appendix IVA.

CONTRACT AWARD DATE WITH FULL INFORMATION

MOVE ON SITE

DESCRIPTION \ TIME YEARS	-1-	-2-	-3-	-4-	-5-
DESIGN & ORDER MATERIAL					
MATERIAL DELIVERY					
SHOP FABRICATION					
SITE SUBASSEMBLY					
SET GUARD					
SET PRIMARY & CORE SUPPORT					
SET THERMAL BARRIER					
ERECT TOP DECK & SUPPORT SKIRT					
INSTALL TOP DECK & CORE SUPPORT PENETRATIONS					
INSTALL CLOSURE PLUG					
TEST					

▬▬ { MAJOR COMPONENT ASSEMBLY IN THE SITE SUBASSEMBLY YARD

TIME ON FOUND = 22 MONTHS

TIME ON SITE = 30 MONTHS

Indicates revision from previous issue

Revisions	By	Chkd	Date	Remarks
2				REVISED FOR PHASE A EXTENSION - CONCEPT II B
1				REVISED FOR PHASE A EXTENSION

Chicago Bridge & Iron Company CBI

SCHEDULE
PLBR MAJOR COMPONENTS
FIGURE 4.8

Purchaser's No. _____

By _____ Chkd _____ Date _____

Engineering Coordinator

Contract No. 81792

Dwg Rev

THIS DRAWING IS THE PROPERTY OF CHICAGO BRIDGE & IRON COMPANY AND IS TO BE USED ONLY IN CONNECTION WITH PERFORMANCE OF WORK BY THE CHICAGO BRIDGE & IRON COMPANY. REPRODUCTION IN WHOLE OR IN PART FOR ANY OTHER PURPOSE IS EXPRESSLY FORBIDDEN.

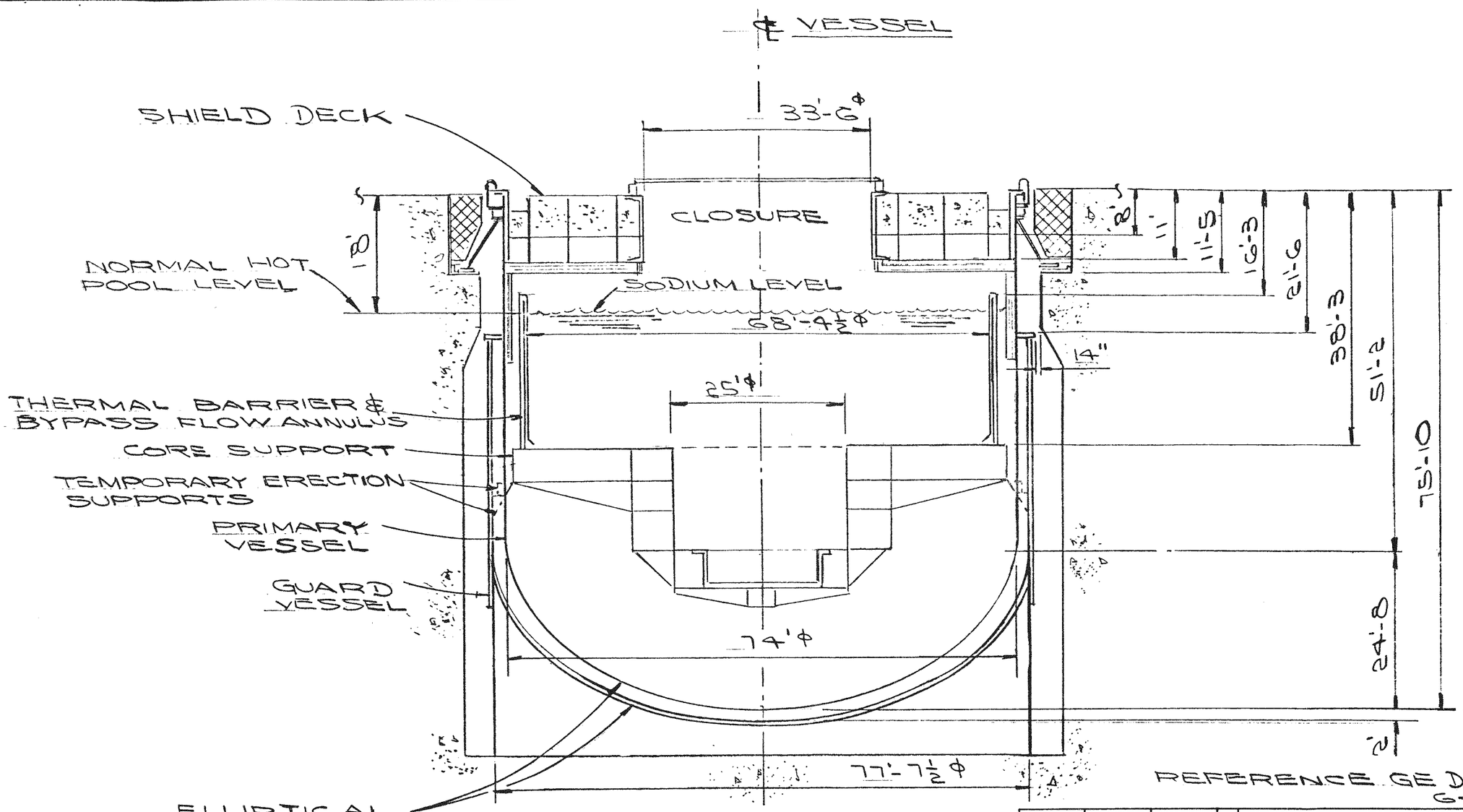

ELEVATION

REFERENCE GE DWG. 908E536
6-20-78 REV. E

Indicates revision from previous issue

Revisions	By	Chkd	Date	Remarks
				REVISED FOR CONCEPT B

Chicago Bridge & Iron Company CBI

GENERAL ARRANGEMENT

FIG. 4.9.2.0

Purchaser's No. _____ Contract No. 81792

By LK Chkd _____ Date 9-22-78

Engineering Coordinator

Dwg Rev

THIS DRAWING IS THE PROPERTY OF CHICAGO BRIDGE & IRON COMPANY AND IS TO BE USED ONLY IN CONNECTION WITH PERFORMANCE OF WORK BY THE CHICAGO BRIDGE & IRON COMPANY. REPRODUCTION IN WHOLE OR IN PART FOR ANY OTHER PURPOSE IS EXPRESSLY FORBIDDEN.

DR 72A REV 11-72

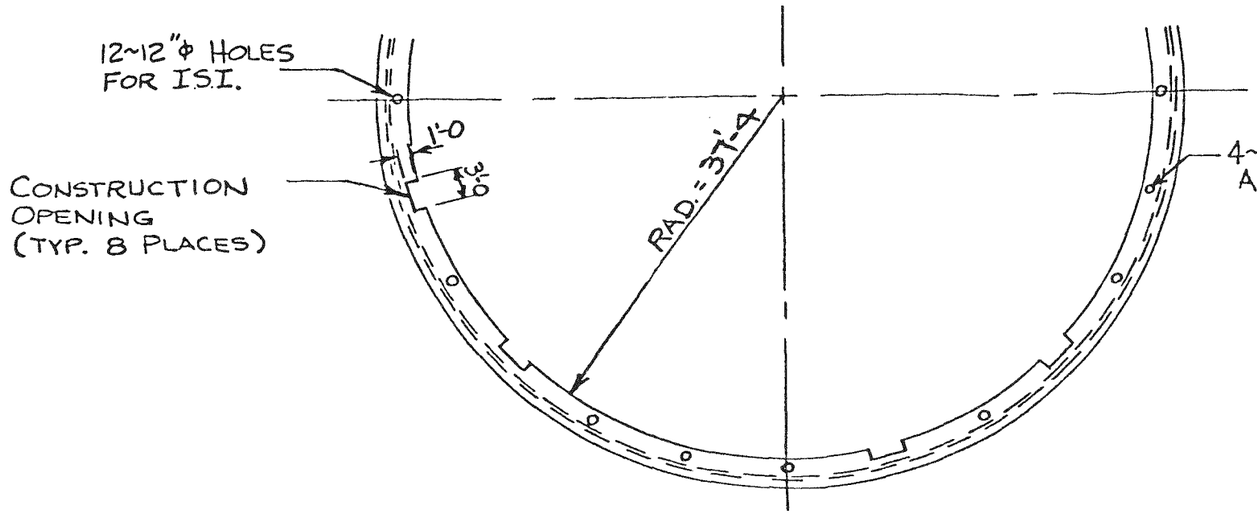

PLAN OF TOP FLANGE

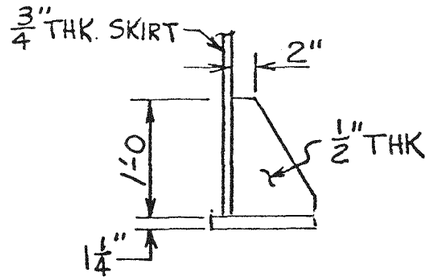

SECTION "B-B"

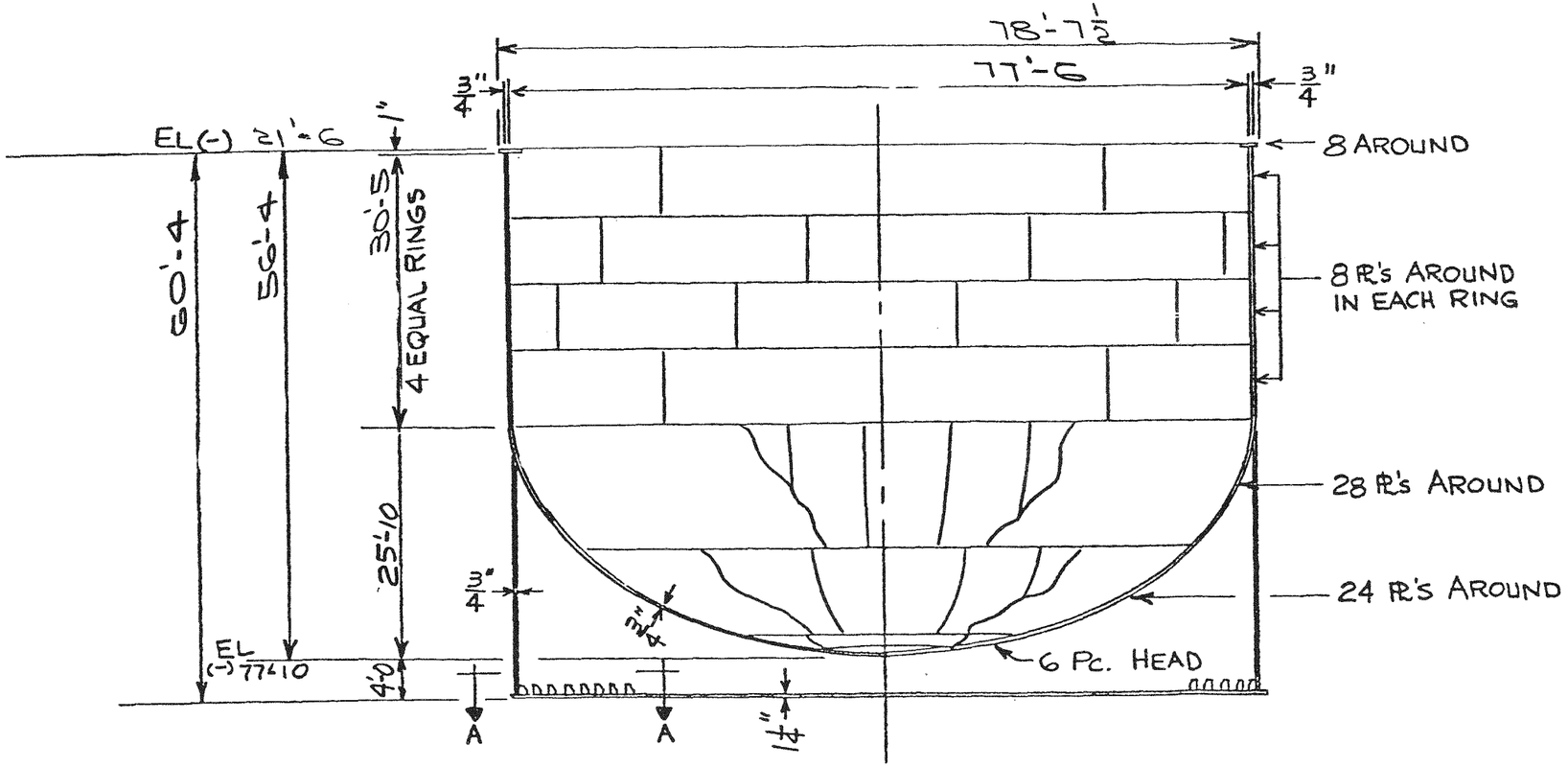

ELEVATION OF GUARD VESSEL

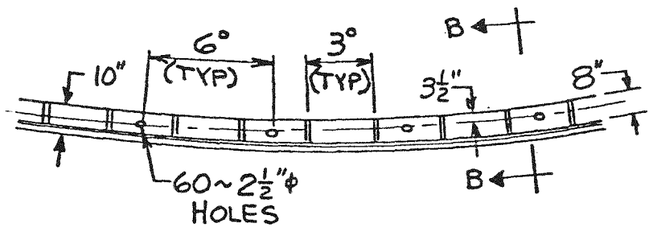

SECTION "A-A"

Revisions	By	Chkd	Date	Remarks
2	LK		9-25-78	CHGED DIMS
1	RBP		6-14-78	REDRAWN @ SUB-ASSY'S A'B REMOVED

Chicago Bridge & Iron Company

GUARD VESSEL
FIG. 4.9.2.1

Purchaser's No. _____ Contract No. 81792

By _____ Chkd _____ Date _____

Engineering Supervisor _____ Dwg Rev. 2

THIS DRAWING IS THE PROPERTY OF CHICAGO BRIDGE & IRON COMPANY AND IS TO BE USED ONLY IN CONNECTION WITH PERFORMANCE OF WORK BY THE CHICAGO BRIDGE & IRON COMPANY. REPRODUCTION IN WHOLE OR IN PART FOR ANY OTHER PURPOSE IS EXPRESSLY FORBIDDEN.

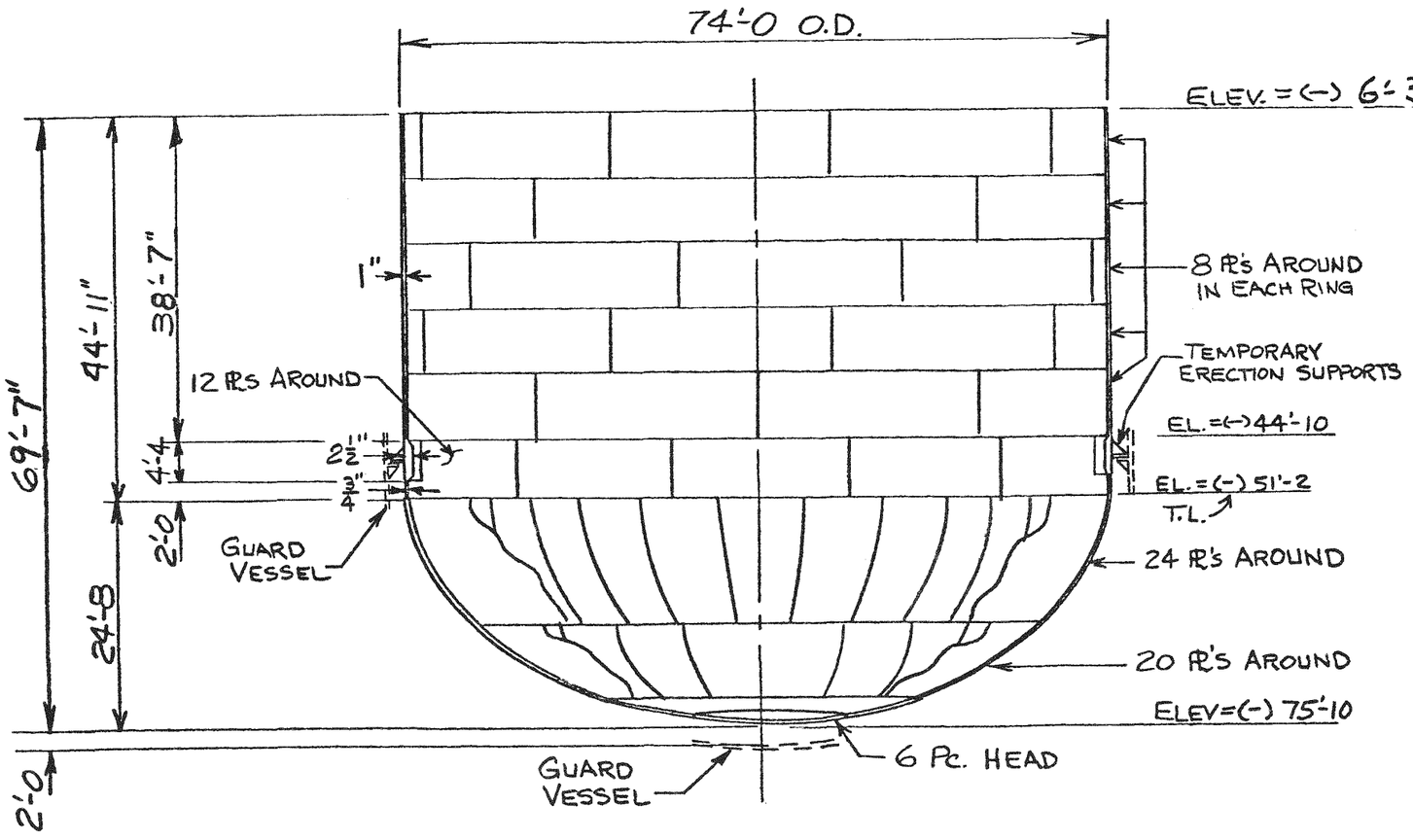

ELEVATION
(ALL MATERIAL 304 SS)

By	Chkd	Date	Revisions	Remarks
			2	REVISED FOR PHASE A EXTENSION CONCEPT III B
RSR		6-14-78	1	REDRAWN @ SUB-ASSY'S A & B REMOVED

Chicago Bridge & Iron Company

PRIMARY VESSEL
FIG. 4.9.2.2

Purchaser's No.

By _____ Chkd _____ Date _____

Engineering Supervisor

Contract No. 81792

Dwg _____ Rev. _____

THIS DRAWING IS THE PROPERTY OF CHICAGO BRIDGE & IRON COMPANY AND IS TO BE USED ONLY IN CONNECTION WITH PERFORMANCE OF WORK BY THE CHICAGO BRIDGE & IRON COMPANY. REPRODUCTION IN WHOLE OR IN PART FOR ANY OTHER PURPOSE IS EXPRESSLY FORBIDDEN.

4'-8½ ϕ PENETRATION (TYP. OF 2)

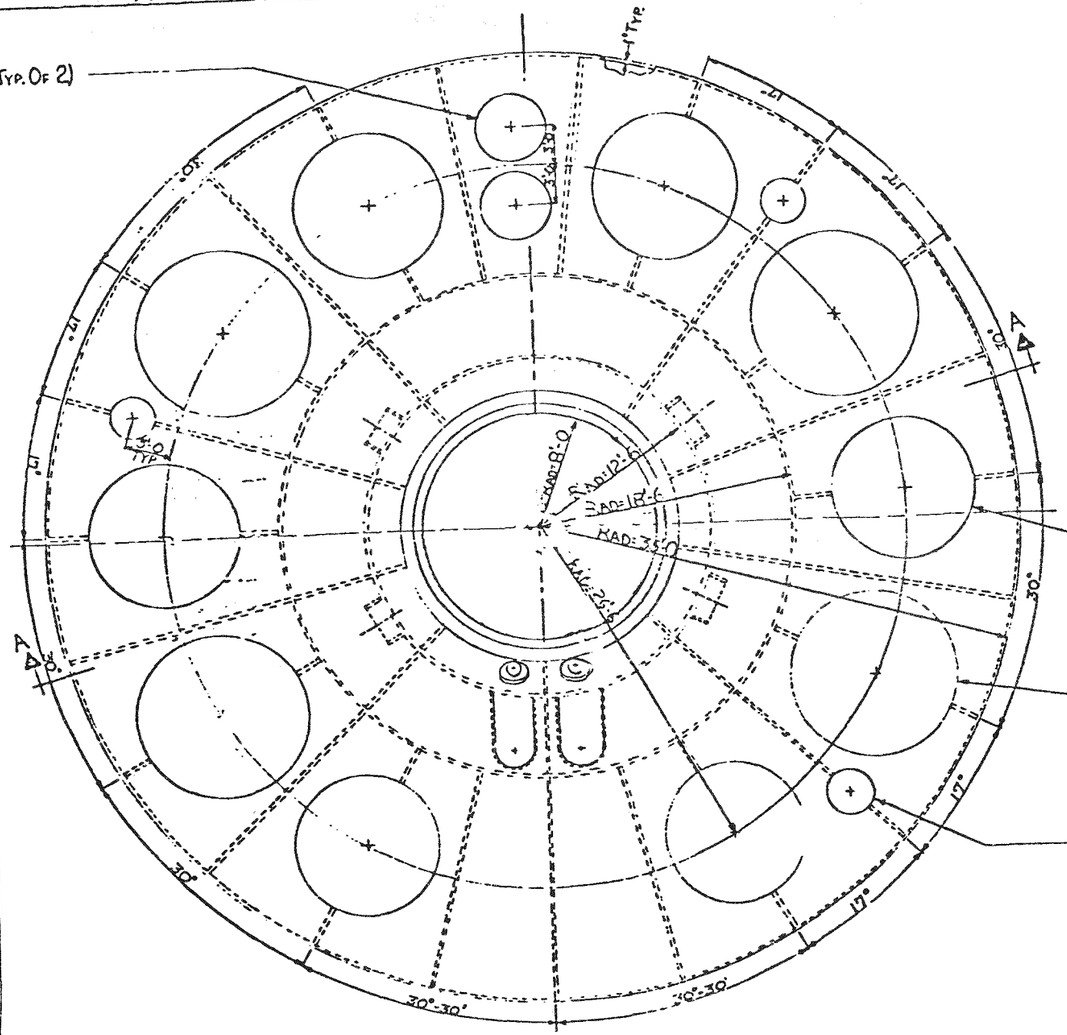

PLAN

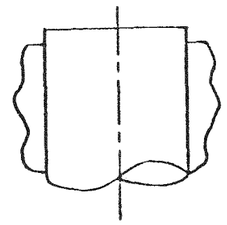

TYPICAL PENETRATION

10'-2½ ϕ PENETRATION (TYP. OF 6)

11'-10½ ϕ PENETRATION (TYP. OF 4)

3'-2½ ϕ PENETRATION (TYP. OF 3)

A/B DASHED LINES ON SECTION INDICATE CONSTRUCTION SUBASSEMBLY DIVISIONS

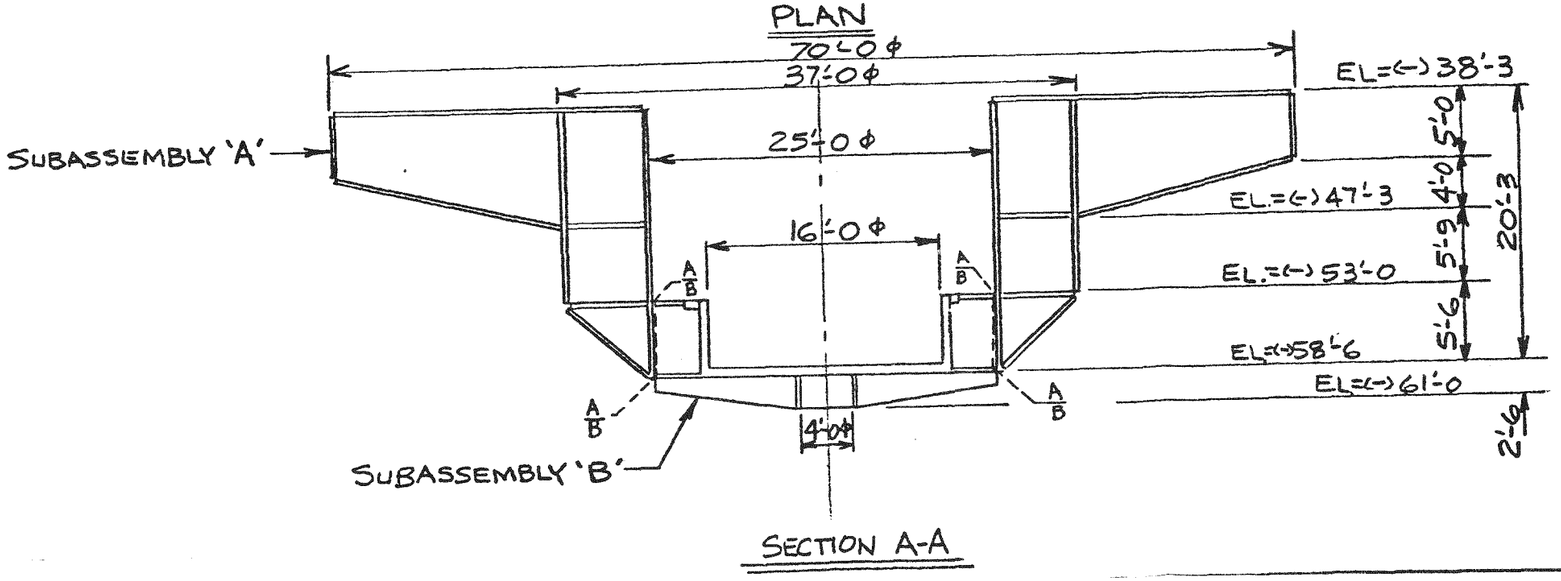

SECTION A-A

By	Chkd	Date	Revisions	Remarks
RBR		6-14-78	REDRAWN, CHANGED SUBASSY'S.	

Chicago Bridge & Iron Company

CORE SUPPORT
FIG. 4.9.2.3

Purchaser's No.

By Chkd Date

Engineering Supervisor

Contract No. 81792

Dwg. Rev.

THIS DRAWING IS THE PROPERTY OF CHICAGO BRIDGE & IRON COMPANY AND IS TO BE USED ONLY IN CONNECTION WITH PERFORMANCE OF WORK BY THE CHICAGO BRIDGE & IRON COMPANY. REPRODUCTION IN WHOLE OR IN PART FOR ANY OTHER PURPOSE IS EXPRESSLY FORBIDDEN.

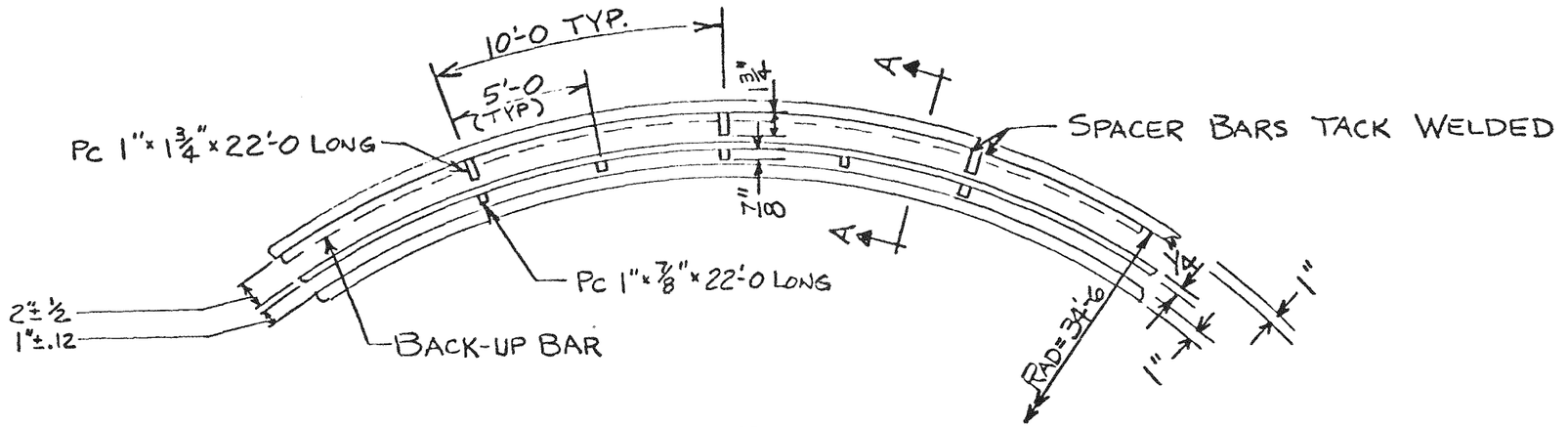

PARTIAL PLAN

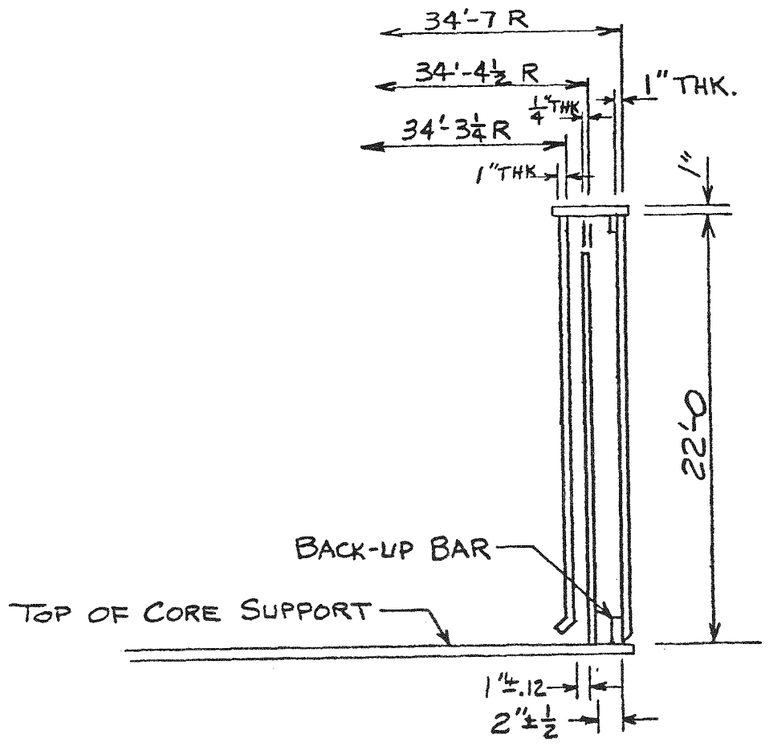

SECTION A-A

By	Chkd	Date	Remarks
			ADDED B-V BAR
RBR		6-14-78	

Chicago Bridge & Iron Company

THERMAL BARRIER

FIG. 4.9.2.4

Purchaser's No. _____

By _____ Chkd _____ Date _____

Engineering Supervisor

Contract No. 81792

Dwg. 7m

THIS DRAWING IS THE PROPERTY OF CHICAGO BRIDGE & IRON COMPANY AND IS TO BE USED ONLY IN CONNECTION WITH PERFORMANCE OF WORK BY THE CHICAGO BRIDGE IRON COMPANY. REPRODUCTION IN WHOLE OR IN PART FOR ANY OTHER PURPOSE IS EXPRESSLY FORBIDDEN.

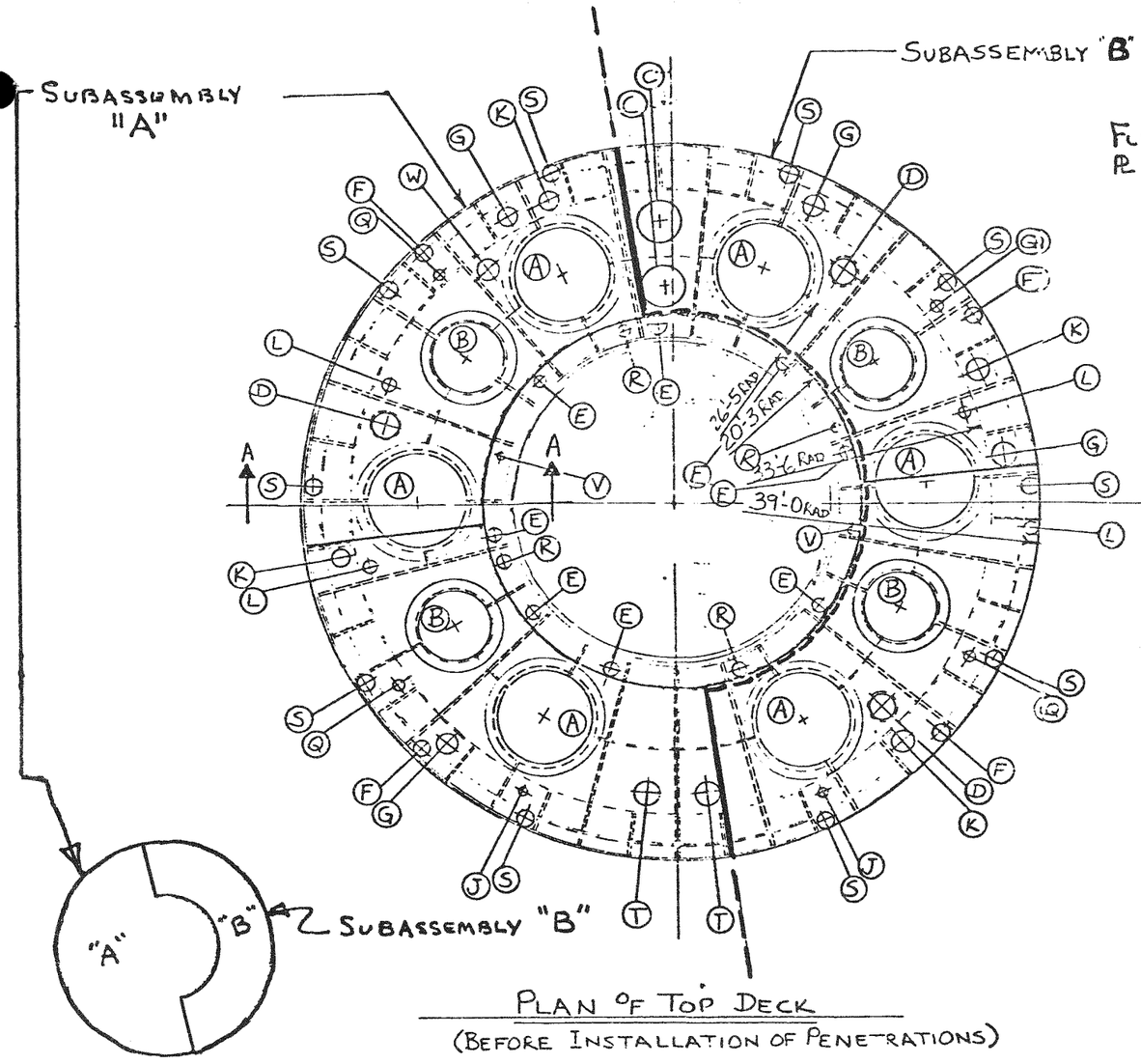

PLAN OF TOP DECK
(BEFORE INSTALLATION OF PENETRATIONS)

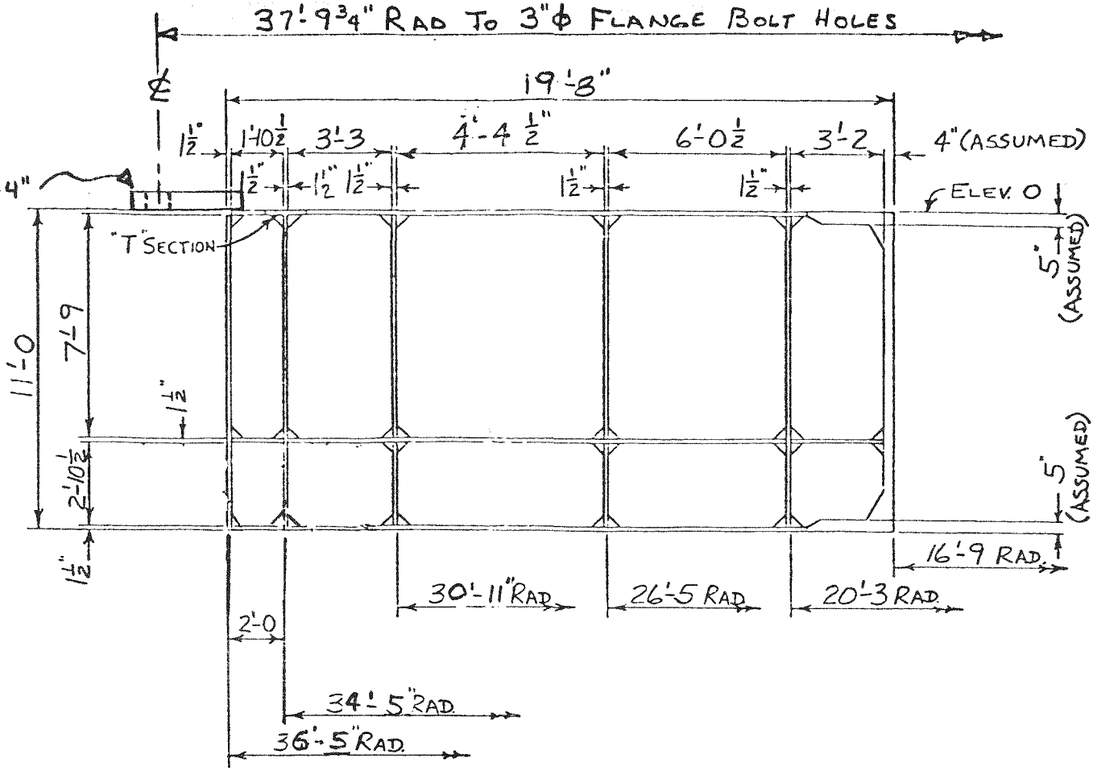

SECTION "A-A"

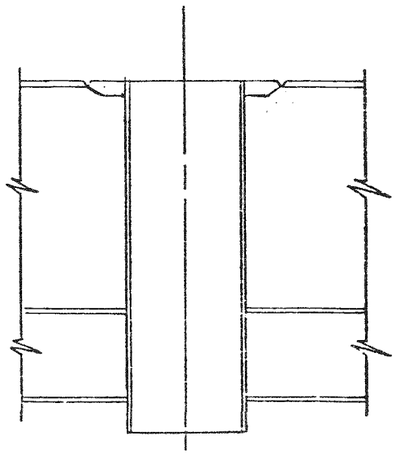

TYP. PENETRATION

GENERAL NOTE:

THE CONNECTION BETWEEN ASSEMBLY "A" & "B" WILL BE MADE AFTER BOTH SECTIONS ARE SET & BOLTED TO PERMANENT SUPPORT

PENETRATION SCHEDULE

	PENETRATION	QTY	FLANGE DIA.	OPENING IN DECK	COMPONENT WT. LBS
A	IHX	6	11 FT - 11.00	10 FT - 2.00 DIA.	420,000
B	PUMP	4	10 FT - 7.00	9 FT - 3.00	[illegible]
C	COLD TRAP	2	----------	4 FT - 6.00	[illegible]
D	AUXILIARY IHX	3	----------	3 FT - 0.00	20,000
E	NUCLEONIC INSTR.	6	14.00	6.00	----------
F	LEAK SPACE T/C & STRAIN GAGE	4	20.00	LATER 6.00	----------
G	T/C & STRAIN GAGE	4	2 FT - 4.00	14.00	----------
J	NA FILL & DRAIN	2	10.00	4.00	----------
K	NA HEATING	4	2 FT - 2.00	14.00	----------
L	NA LEVEL INSTR	4	14.00	6.00	----------
Q	CORE FLOW METER	4	14.00	6.00	----------
R	ARGON COVER GAS	4	2 @ 14.00 & 2 @ 12.00	10.00	----------
S	PRIMARY VESSEL INSPECTION	10	22.00	LATER 10.00	----------
T	FUEL TRANSFER	2	----------	2 FT - 6.00	[illegible]
V	NA SAMPLING	2	8.00	LATER 2.00	----------
W	CARBON METER	1	2 FT - 2.00	LATER 14.00	----------
X	REACTOR CLOSURE		35 FT - 4.17	33 FT - 7.00 DIA.	2,640,000

▷ INDICATES CHANGE FROM PREVIOUS ISSUE

PHASE A EXTENDED CONCEPT IIB
REVISED FOR PHASE A EXTENDED

Chicago Bridge & Iron Company (CBI)

TOP DECK
GENERAL PLAN
FIG. 4.9.2.5

By EMR Chkd. Date 11-11-77
Engineering Coordinator
Contract No. 81792
Dwg. Rev.

THIS DRAWING IS THE PROPERTY OF CHICAGO BRIDGE & IRON COMPANY AND IS TO BE USED ONLY IN CONNECTION WITH PERFORMANCE OF WORK BY THE CHICAGO BRIDGE & IRON COMPANY. REPRODUCTION IN WHOLE OR IN PART FOR ANY OTHER PURPOSE IS EXPRESSLY FORBIDDEN

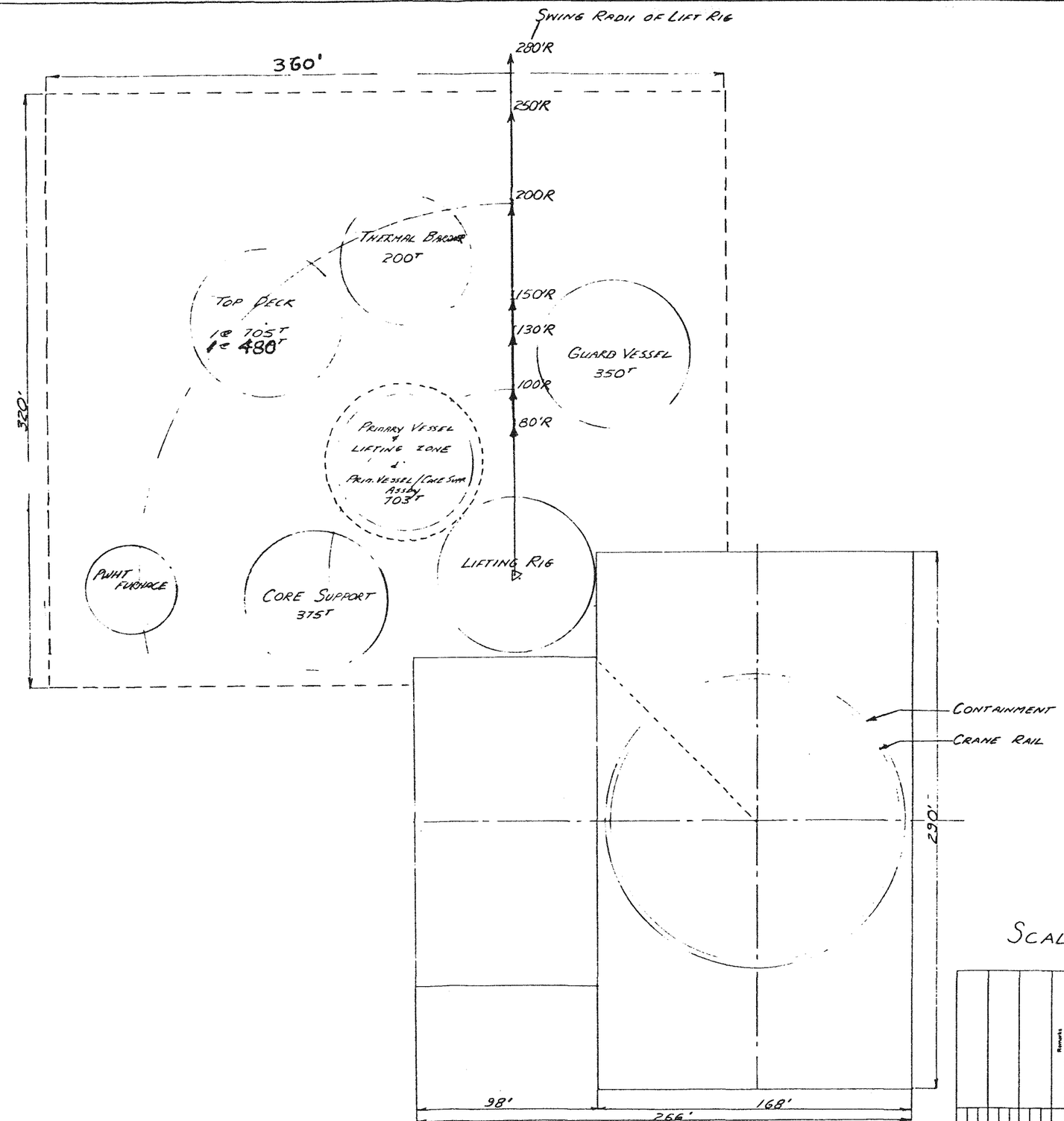

SCALE: 1" = 30'

▶ INDICATES CHANGE FROM PREVIOUS ISSUE

Chicago Bridge & Iron Company CBI

SITE PLAN

FIG. 4.9.2.6

Purchaser's No. | Contract No. 4.9.2.6

By ACP Chkd. Date 6-19-78

Engineering Supervisor | Dwg. | Rev. 1

THIS DRAWING IS THE PROPERTY OF CHICAGO BRIDGE & IRON COMPANY AND IS TO BE USED ONLY IN CONNECTION WITH PERFORMANCE OF WORK BY THE CHICAGO BRIDGE & IRON COMPANY. REPRODUCTION IN WHOLE OR IN PART FOR ANY OTHER PURPOSE IS EXPRESSLY FORBIDDEN.

Revisions | By | Chkd | Date | Remarks

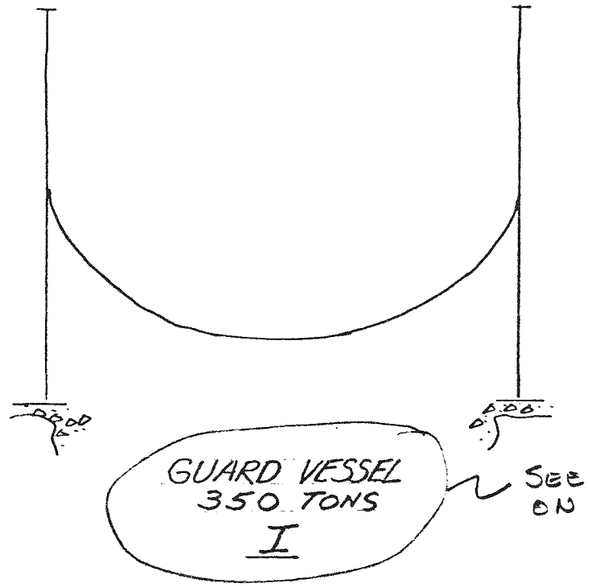

GUARD VESSEL
350 TONS
I

SEE NOTE ON FIG 4.9.20

PRIMARY VESSEL 346 T
CORE SUPPORT 375 T
721 T

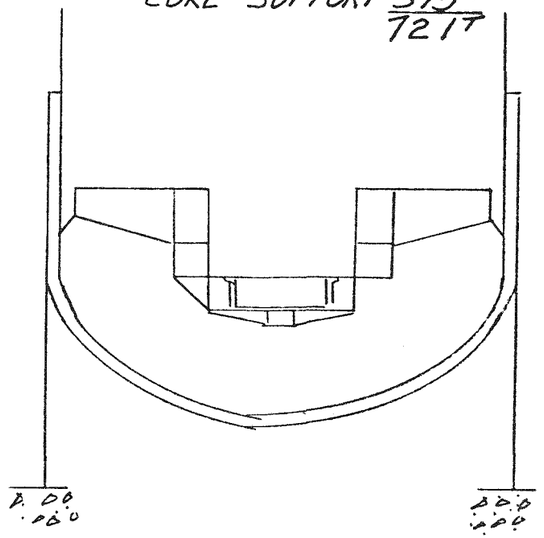

II

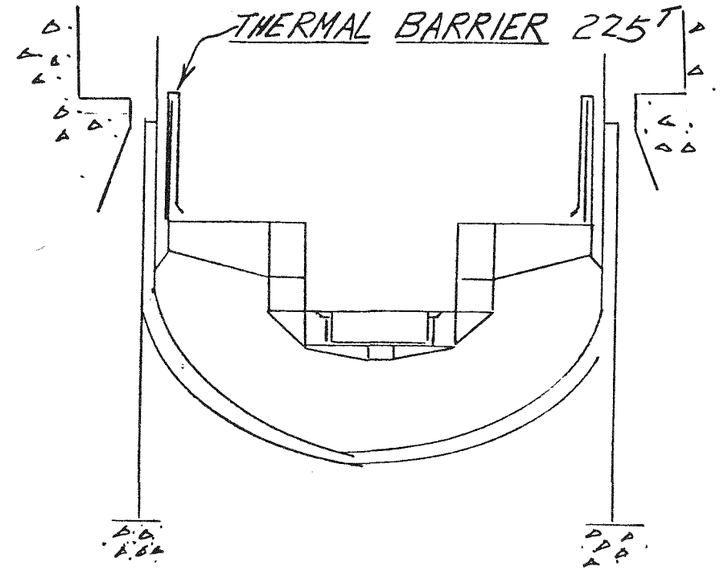

III

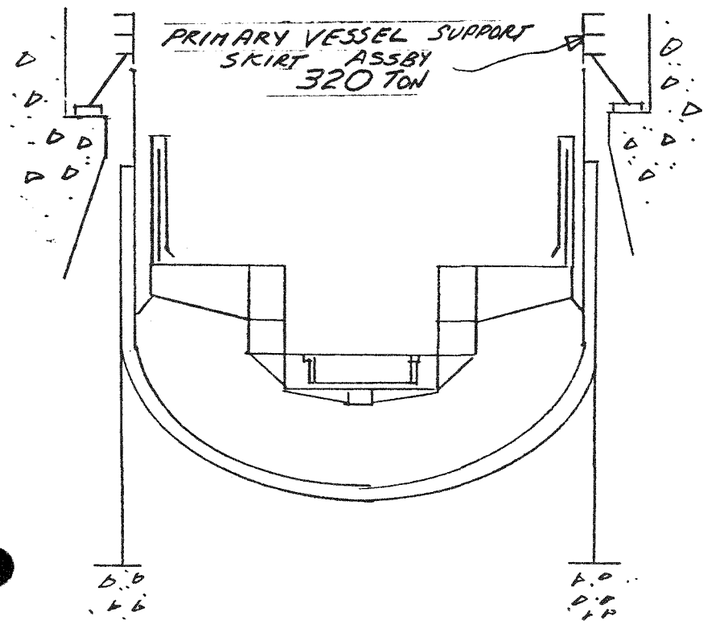

IV

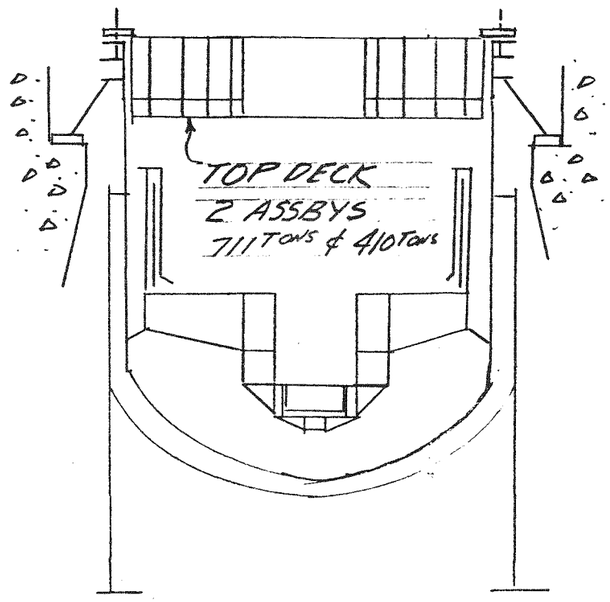

V

▶ Indicates revision from previous issue

By	Chkd	Date	Revisions	Remarks
			1	REVISION FOR PHASE A EXTENSION CONCEPT II 13

Chicago Bridge & Iron Company CBI

LIFTING SEQUENCE

FIGURE 4.9.2.7

Purchaser's No. _____ Contract No. 81792

By ACP Chkd _____ Date 7-24-78

Engineering Coordinator

Dwg Rev

THIS DRAWING IS THE PROPERTY OF CHICAGO BRIDGE & IRON COMPANY AND IS TO BE USED ONLY IN CONNECTION WITH PERFORMANCE OF WORK BY THE CHICAGO BRIDGE & IRON COMPANY. REPRODUCTION IN WHOLE OR IN PART FOR ANY OTHER PURPOSE IS EXPRESSLY FORBIDDEN.

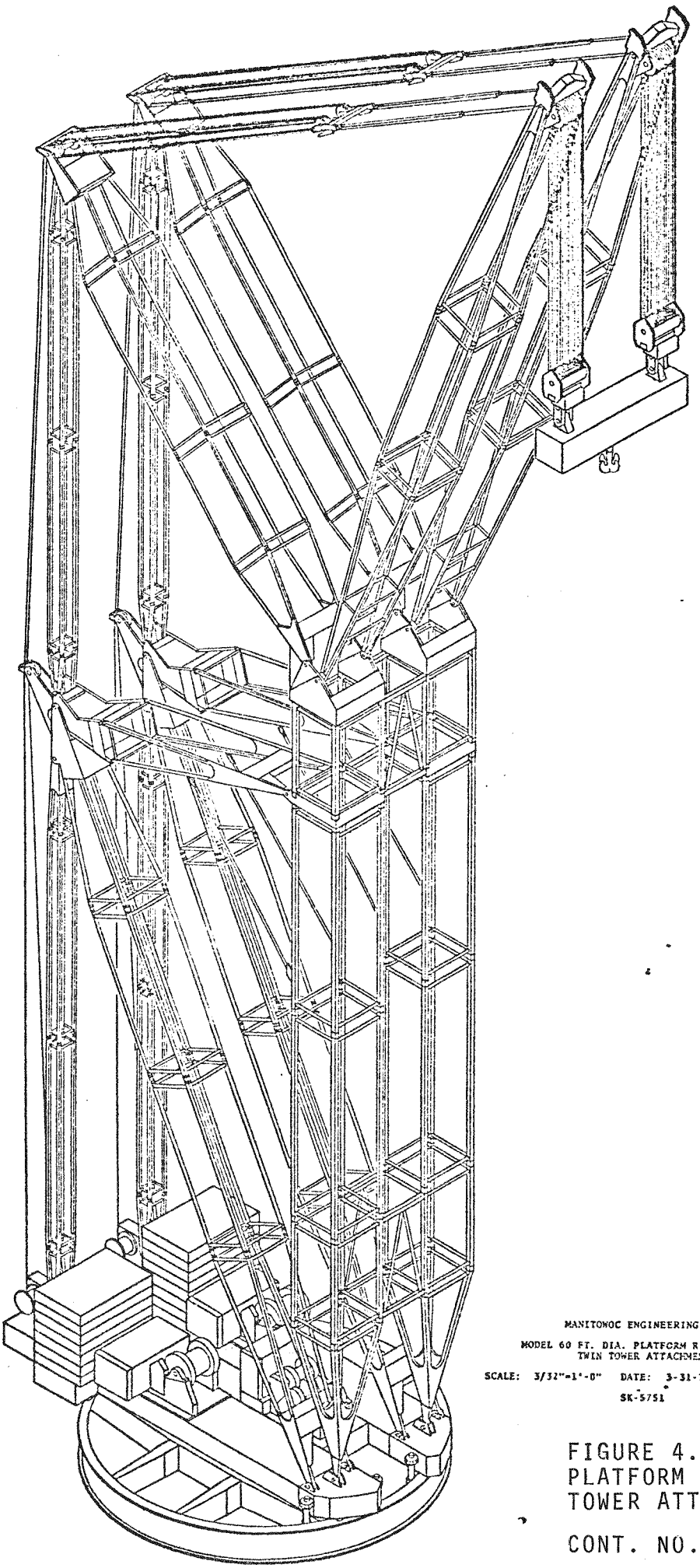

MANITOWOC ENGINEERING CO.

MODEL 60 FT. DIA. PLATFORM RINGER-WITH TWIN TOWER ATTACHMENT

SCALE: 3/32"=1'-0" DATE: 3-31-78 DRAWN: CFS

SK-5751

FIGURE 4.9.2.8
PLATFORM RINGS WITH TWIN TOWER ATTACHMENT

CONT. NO. 81972

POOL-TYPE LMFBR PLANT

1000 MWe PHASE A - EXTENSION 1 DESIGN

Contents

VOLUME 1: Part I: EXECUTIVE SUMMARY

1. Introduction
2. Results and Conclusions
3. Nuclear Steam Supply System
4. Balance of Plant

VOLUME 2: Part II: REACTOR ASSEMBLY - STRUCTURES

1. Introduction and Summary
2. General Arrangement
3. Thermal Barriers
4. Alternate Support for Primary Vessel
5. Seismic Analysis - Alternate Vessel Support
6. Pump-to-Plenum Piping and Seals
7. Upper Internals Structure
8. Internal Shielding
9. Rotating Plug Size Study
10. Rotating Plug Thermal Analysis
11. Rotating Plug Seals

Appendix IIA - Engineering Study of the Design, Fabrication, Construction and Testing of a Pool-Type LMFBR - Alternate Vessel Support

VOLUME 3: Part III: REACTOR ASSEMBLY - DECK

1. Introduction and Summary
2. Design
3. Insulation
4. Penetrations
5. Removable Shielding
6. Inspection
7. Thermal Stress Analysis of Shortened Support Skirt

Appendix IIIA - Design Concepts for Removable Radiation Shielding for the 1000 MWe Pool-Type LMFBR

Appendix IIIB - EPRI Guidelines for LMFBR Pool Design

VOLUME 3: (Cont'd.)

Part IV: REACTOR ASSEMBLY - FABRICATION

1. Introduction and Summary

Appendix IVA - Phase A Extension Engineering Study of the Design, Fabrication, Construction and Testing of a Pool-Type LMFBR - Reference Vessel Support

VOLUME 4:

Part V: HEAT TRANSPORT SYSTEMS COMPONENTS

1. Introduction and Summary
2. Intermediate Heat Exchanger Design
3. IHX Seismic Analysis
4. Primary Pump Valve
5. Primary Pump Seismic Analysis
6. Operation With Components Out Of Service
7. Plant Duty Cycle
8. Plant Transients
9. Reactor Outlet Plenum Thermal Hydraulics

Appendix VA - Preliminary Design of an Alternate Bent-Tube IHX for the 1000 MWe Pool Reactor

VOLUME 5:

Part VI: REACTOR AUXILIARY SYSTEMS

1. Introduction and Summary
2. Primary Sodium Purification and Sampling Systems
3. Auxiliary Cooling Systems
4. Cover Gas Pressure Control

Part VII: INSTRUMENTATION AND CONTROL

1. Introduction and Summary
2. In-Vessel Instrumentation
3. Deck Cabling and Cabinets
4. Failed Fuel Detection
5. Post-Scram Sodium Pump Control
6. Plant Control

VOLUME 6

Part VIII: BALANCE OF PLANT

1. Introduction and Summary
2. Reactor Head Compartment Layout
3. Primary Heat Transport System Component Removal Study
4. Intermediate Heat Transport System Piping Enclosure Study

VOLUME 6:
(Cont'd.)

5. Pool Reactor Assembly Support Interface
6. Decay Heat Removal Systems Layout and Performance Study
7. Cover Gas System
8. Pool Reactor Assembly Erection and Schedule